NATIONAL COOPERATIVE HIGHWAY RESEARCH PROGRAM REPORT **140**

FLEXIBLE PAVEMENT DESIGN AND MANAGEMENT

MATERIALS CHARACTERIZATION

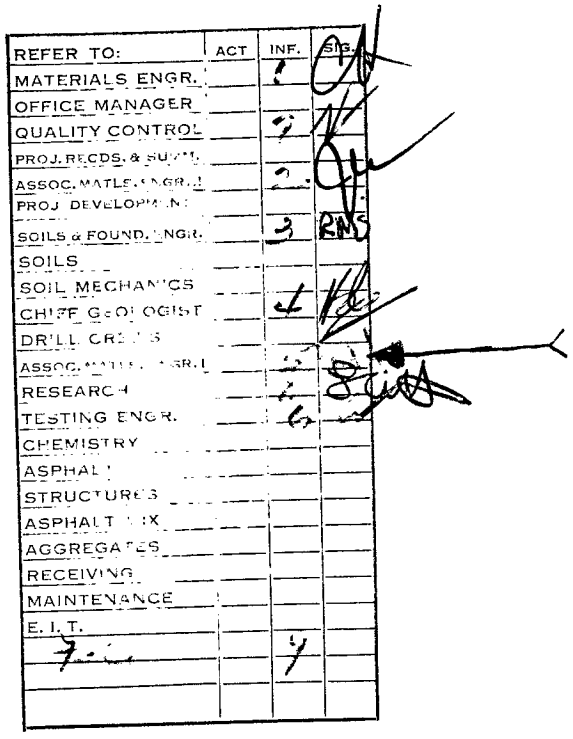

HIGHWAY RESEARCH BOARD
NATIONAL RESEARCH COUNCIL
NATIONAL ACADEMY OF SCIENCES—NATIONAL ACADEMY OF ENGINEERING

NATIONAL COOPERATIVE HIGHWAY RESEARCH PROGRAM
REPORT 140

FLEXIBLE PAVEMENT DESIGN AND MANAGEMENT
MATERIALS CHARACTERIZATION

KESHAVAN NAIR AND C-Y CHANG
MATERIALS RESEARCH AND DEVELOPMENT, INC.
OAKLAND, CALIFORNIA

RESEARCH SPONSORED BY THE AMERICAN ASSOCIATION OF STATE HIGHWAY OFFICIALS IN COOPERATION WITH THE FEDERAL HIGHWAY ADMINISTRATION

AREAS OF INTEREST:
- PAVEMENT DESIGN
- PAVEMENT PERFORMANCE
- BITUMINOUS MATERIALS AND MIXES
- MINERAL AGGREGATES
- SOILS, GEOLOGY AND FOUNDATIONS

HIGHWAY RESEARCH BOARD
DIVISION OF ENGINEERING NATIONAL RESEARCH COUNCIL
NATIONAL ACADEMY OF SCIENCES—NATIONAL ACADEMY OF ENGINEERING 1973

NATIONAL COOPERATIVE HIGHWAY RESEARCH PROGRAM

Systematic, well-designed research provides the most effective approach to the solution of many problems facing highway administrators and engineers. Often, highway problems are of local interest and can best be studied by highway departments individually or in cooperation with their state universities and others. However, the accelerating growth of highway transportation develops increasingly complex problems of wide interest to highway authorities. These problems are best studied through a coordinated program of cooperative research.

In recognition of these needs, the highway administrators of the American Association of State Highway Officials initiated in 1962 an objective national highway research program employing modern scientific techniques. This program is supported on a continuing basis by funds from participating member states of the Association and it receives the full cooperation and support of the Federal Highway Administration, United States Department of Transportation.

The Highway Research Board of the National Academy of Sciences-National Research Council was requested by the Association to administer the research program because of the Board's recognized objectivity and understanding of modern research practices. The Board is uniquely suited for this purpose as: it maintains an extensive committee structure from which authorities on any highway transportation subject may be drawn; it possesses avenues of communications and cooperation with federal, state, and local governmental agencies, universities, and industry; its relationship to its parent organization, the National Academy of Sciences, a private, nonprofit institution, is an insurance of objectivity; it maintains a full-time research correlation staff of specialists in highway transportation matters to bring the findings of research directly to those who are in a position to use them.

The program is developed on the basis of research needs identified by chief administrators of the highway departments and by committees of AASHO. Each year, specific areas of research needs to be included in the program are proposed to the Academy and the Board by the American Association of State Highway Officials. Research projects to fulfill these needs are defined by the Board, and qualified research agencies are selected from those that have submitted proposals. Administration and surveillance of research contracts are responsibilities of the Academy and its Highway Research Board.

The needs for highway research are many, and the National Cooperative Highway Research Program can make significant contributions to the solution of highway transportation problems of mutual concern to many responsible groups. The program, however, is intended to complement rather than to substitute for or duplicate other highway research programs.

NCHRP Report 140

Project 1-10 FY '67 and '69
ISBN 0-309-02128-6
L. C. Catalog Card No. 73-3239

Price $5.60

Notice

The project that is the subject of this report was a part of the National Cooperative Highway Research Program conducted by the Highway Research Board with the approval of the Governing Board of the National Research Council, acting in behalf of the National Academy of Sciences. Such approval reflects the Governing Board's judgment that the program concerned is of national importance and appropriate with respect to both the purposes and resources of the National Research Council.

The members of the advisory committee selected to monitor this project and to review this report were chosen for recognized scholarly competence and with due consideration for the balance of disciplines appropriate to the project. The opinions and conclusions expressed or implied are those of the research agency that performed the research, and, while they have been accepted as appropriate by the advisory committee, they are not necessarily those of the Highway Research Board, the National Research Council, the National Academy of Sciences, or the program sponsors.

Each report is reviewed and processed according to procedures established and monitored by the Report Review Committee of the National Academy of Sciences. Distribution of the report is approved by the President of the Academy upon satisfactory completion of the review process.

Published reports of the

NATIONAL COOPERATIVE HIGHWAY RESEARCH PROGRAM

are available from:

Highway Research Board
National Academy of Sciences
2101 Constitution Avenue
Washington, D.C. 20418

(See last pages for list of published titles and prices)

FOREWORD

By Staff
Highway Research Board

This report and its companion, *NCHRP Report 139,* "Flexible Pavement Design and Management—Systems Formulation," will be of interest and practical value to people of a number of disciplines in highway departments and other agencies. Both reports are the result of research conducted under NCHRP Project 1-10, "Translating AASHO Road Test Findings—Basic Properties of Pavement Components." From the highway administrator's standpoint, there should be considerable interest in the systems engineering concept of pavement management described in *NCHRP Report 139* as a method to provide the desired level of pavement service at the most economical over-all cost. The materials characterization investigation, covered in this report, is considered to be a phase of a longer-range endeavor aimed at more substantial changes in the structural facet of the pavement design process that will lead to more rational procedures for design of the pavement structural subsystem. Greatest interest in the results will be found among pavement designers, researchers, and engineers involved with materials and soils testing.

The structural design of highway pavements involves empirical techniques based to a large extent on long-time experience of highway agencies and augmented by test programs, the most ambitious of which was the AASHO Road Test conducted near Ottawa, Ill., and completed in the fall of 1960. Because a field test program involving the many variables known to affect pavement performance would become unfeasible, the sponsors of the Road Test chose to include only a limited number of variables in the project. As a result, it is generally recognized that the relationships between traffic loadings and pavement performance developed at the Road Test apply only to the conditions at the test site. Applications of these relationships in other areas of the United States must be based on experimental or other evidence of the effects of differences in subgrade soil, paving materials, construction practices, traffic, environment, and maintenance procedures. A number of early NCHRP projects dealt with extrapolation of Road Test findings to conditions other than those at the test site.

NCHRP Project 1-10 was initiated by a research team from Materials Research and Development, Inc., with the objective of using basic properties of pavement component materials to translate AASHO Road Test findings to other conditions and thus ultimately develop more rational pavement design procedures. In the early stages of the study it was determined that measurement of basic properties of materials and components significant to pavement performance was a highly complex problem requiring (a) development of new testing equipment, and (b) considerable laboratory data collection, followed by (c) field experimentation. It was also recognized that the pavement design decision-making processes involve factors other than the structural ability of a section to support predicted traffic loadings (e.g., maintenance strategies, user considerations, and long-term economics). The concept of considering management of a pavement system throughout its operational life during the initial design process was developing. Consequently, project efforts were divided into two separate but coordinated activities—materials

characterization and systems formulation—with each activity under the direction of a separate research team.

An operational pavement systems model (SAMP5), as described in *NCHRP Report 139,* has been formulated that organizes the over-all influencing factors such as materials characteristics, construction techniques, maintenance requirements, and economics within a suitable framework for flexible pavement design and management. A computer program has been prepared using 58 to 100 input variables and the *AASHO Interim Guides for Design of Flexible Pavements* as the structural subsystem. An earlier version of the system is currently being implemented by the Texas Highway Department. The procedure can be applied to flexible pavement design problems now by any agency having the proper input data and using AASHO design guides. However, for the method to be more easily implemented, detailed descriptions for users' guides, input forms, and data feedback and storage systems are needed. These are being prepared and the procedures are being subjected to a sensitivity analysis and pilot testing during an implementation phase of the study under NCHRP Project 1-10A.

Intermediate and long-range prospects for improvements in pavement design within the systems concept may depend largely on the development of more rational approaches to the formulation of the structural subsystem based on properties of the subgrade and paving materials, rather than on the empirical relationships developed during the AASHO Road Test. A procedure, including the necessary laboratory equipment, has been developed for characterization of materials in terms of stress/strain relationships representative of loading and environmental conditions to which they are likely to be subjected as components of a pavement. The methodology is illustrated in this report by its application to the characterization of an asphaltic concrete, a granular base material, and a cohesive subgrade soil. The description of the testing equipment and accumulated materials characterization data should be of considerable interest to pavement design researchers. Research aimed at application of more rational approaches to solutions of structural subsystem problems is scheduled to be initiated within NCHRP in 1973.

The essential findings of this study, aimed at both immediate and long-range improvements in the pavement design and management process, are further summarized under "Systems Formulation" and "Materials Characterization," two separate but coordinated activities responsive to over-all project objectives.

Systems Formulation

Systems engineering in its broad sense is a codified procedure for attacking complex problems in a coordinated fashion to permit realistic decisions that can be justified on the basis of selected decision criteria. A conceptual pavement systems diagram was prepared primarily to illustrate the interrelation of many inputs and subsystems involved in the pavement design and management process. The inputs to the system include a range of load, environmental, structural, construction, and maintenance variables, all of which are stochastic in nature and are interrelated. Although conceptualizing the over-all pavement system was essential to solving the problem, it was necessary from an application standpoint to develop an operational

system. After a review of the efforts of other researchers in the area of applying systems engineering concepts to pavement design, it seemed desirable to modify and extend the efforts of Scrivner, McFarland, and Carey,* who had developed the first known computer-oriented operational system for the design of flexible pavement, rather than expend time and effort on an entirely new system. Thus, the working method developed on this project, Systems Analysis Model for Pavements (SAMP), is an extension of the algorithms initially conceived by Scrivner et al. In the particular version (SAMP5) described in *NCHRP Report 139,* there are seven classes of input variables, as follows: (1) material properties, (2) environment and serviceability, (3) load and traffic, (4) constraints, (5) traffic delay, (6) maintenance, and (7) program control and miscellaneous. An example problem using the operational model is included. A limited sensitivity analysis and evaluation of the program was conducted, and the feasibility of revising the structural subsystem to permit the use of more rational concepts—such as elastic layered theory—was demonstrated.

The major conclusions and recommendations of this portion of the research are as follows:

1. An uncoordinated attack on the structural design of pavements will not be successful in solving the problem. A systems engineering approach is required that can be used to describe the over-all behavior and performance of the pavement system, as well as the functions of its component parts, during its entire life as a portion of the highway transportation network.
2. A conceptual pavement systems model has been formulated to show the relationships between the many groups of input variables that must be considered.
3. An operational flexible pavement systems model (SAMP5) has been developed, including a computer program using 58 to 100 input variables.
4. Possible improvements to SAMP5 are illustrated, including the use of elastic layered theory and the most recent materials characterization information to provide a more rational structural subsystem.
5. Efforts should be made to: (a) implement the present operational system in several states, (b) modify and improve each of the subsystems, and (c) ultimately upgrade the model toward a true "pavement management system" capable of evaluating the adequacy of the pavement, in terms of providing the intended service over its operational life.

Materials Characterization

Use of the systems approach to pavement design and management requires the description and solution of the various subsystems, one of which is the structural (primary response) subsystem. In theoretical or rational approaches to structural subsystem solutions it is assumed that the primary response of the pavement structure can be defined by its mechanical state. In conventional terms, determining the primary response involves the formulation and solution of appropriate boundary value problems to determine the stress/strain relationships (mechanical state) of each component in a pavement due to applied loads under a variety of environmental conditions. The results obtained from solution of specific boundary value problems are then evaluated in the light of established performance criteria to determine the capability of the pavement system to sustain the input. It is important to recognize the complexity of this task and the iterative nature of the procedure.

---

* Scrivner, F. H., McFarland, W. F., and Carey, G. R., "A Systems Approach to the Flexible Pavement Design Problem." *Res Rep. 32-11* Texas Transportation Institute (1968).

For the purpose of determining the mechanical state through the formulation and solution of boundary value problems, materials are currently described by simplified mathematical models. To determine the likelihood of distress, it is necessary to establish performance criteria for the various materials comprising the pavement system. These performance criteria are related to limiting values of stress and strain that can be permitted to occur in the material, the numerical magnitude of the material, the environment, and the loading conditions.

Characterization of materials, as defined for this project, is the selection of constitutive equations to adequately model the response of paving materials to the loading and environmental conditions to which they are likely to be subjected as components of a pavement. In the preliminary model selected for this study, no attempt was made to include environmental factors (e.g., temperature and moisture). However, the effects of these factors on material behavior were taken into account by testing over a range of temperatures and moisture contents likely to exist in actual pavements systems.

No equipment for characterizing materials was found to be capable of fulfilling the desired project requirements, necessitating the design and fabrication of suitable laboratory testing equipment. Essentially, this consisted of modification of conventional triaxial testing apparatus to provide for independent control of axial and radial stresses. Using the modified triaxial equipment, repeated load tests were conducted on two paving materials—an asphaltic concrete and a cohesive subgrade soil. Similar data for a granular base material were available from a previous study. The tests were conducted on the assumption that the materials were elastic, though not necessarily linear; and, hence, the resilient deformations were measured. The data were analyzed on the basis of an incremental formulation of a physically nonlinear elastic constitutive law. In recognition that solution techniques currently available are for linear and "ad hoc" nonlinear problems, the results are presented (in this report) in terms of an approximate modulus of elasticity and Poisson's ratio. The variations of these parameters with temperature and stress level have been indicated.

The following findings are considered significant with regard to the response of the particular material tested under the loading conditions of the investigation:

Asphaltic Concrete

1. The temperature is the most significant factor in determining the response of asphaltic concrete. This suggests that the characteristics of the asphalt cement are of major significance.

2. At any particular temperature the stress level influences the response of the asphaltic concrete. The asphaltic concrete is less resistant to deformation at higher temperatures. For a constant stress level the deformation increased with increasing temperature.

3. A nonlinear elastic model can provide a suitable representation of the response of asphaltic concrete below temperatures of 55F for the loading conditions of the study—a repeated load of short duration applied to the material after an initial period of conditioning under repeated load. Above this temperature the time-dependent effects are too significant to neglect; hence, consideration should be given to a viscoelastic model.

4. The data indicate that the asphaltic concrete might initially be isotropic and that anisotropy was induced as a function of the stress state and temperature.

Granular Material

1. The response of granular materials is, for all practical purposes, time-independent and completely recoverable.

2. The influence of stress level on the resistance to deformation is considerable and is indicated by the dependence of the response under load on the first stress invariant. The resistance to deformation increases with an increase in the value of the first stress invariant.

3. A nonlinear elastic constitutive law is a reasonable representation of the response of a granular material.

Cohesive Soil

1. Water content exerts a significant influence on the response of the subgrade soil. An increase in water content causes a decrease in resistance to deformation of the soil.

2. There is a large influence of stress level on the response of the cohesive subgrade soil. In general, an increase in the axial stress or radial stress caused a decrease in the resistance to deformation. The effect is greatest at stress levels below 3 psi, and appears important for stress levels up to 6 psi. These stress levels are typical of those that exist in the subgrade of a well-designed pavement.

3. For this particular soil and within the range of water content at which it was tested, a nonlinear elastic constitutive law is a satisfactory representation.

4. An evaluation of the data indicates that the effects of stress-induced anisotropy may be significant. However, the data are inadequate at this time to be definitive as to the importance of these effects.

CONTENTS

ACKNOWLEDGMENTS

The research reported herein was performed under NCHRP Project 1-10 by Materials Research & Development, Inc. B. A. Vallerga, President of MR&D acted as principal investigator, with Dr. Keshavan Nair, Vice-President of MR&D as co-principal investigator in materials characterization and Dr. W. R. Hudson, Director of Research, Council for Advanced Transportation Studies, University of Texas at Austin, as co-principal investigator in systems formulation. F. N. Finn, Senior Research Engineer, MR&D, served as a co-principal investigator during the first phase of the work. Dr. B. F. McCullough, Assistant Professor of Civil Engineering, University of Texas at Austin, assisted in the systems formulation study; Dr. C-Y. Chang, Project Research Engineer, MR&D, conducted the laboratory testing and assisted in the data analysis in the materials characterization study.

Consultants to the project who provided technical guidance in all phases of the work were Professor C. L. Monismith and Dr. K. S. Pister, both of the University of California at Berkeley, the latter being the first to point out the necessity for utilizing systems engineering concepts and techniques in the total pavement design problem. Their valuable contributions are greatly appreciated.

Special acknowledgment is made to Dr. R. G. Hicks for permission to utilize data developed for his Ph.D. dissertation, titled "Factors Influencing the Resilient Properties of Granular Materials" and to James F. Shook, The Asphalt Institute, B. E. Colley, Portland Cement Association, and the late Bonner S. Coffman, Ohio State University, all of whom participated in the initial project planning conference.

Grateful acknowledgment is also extended to James H. Wilson, Laboratory Supervisor, and his staff for assistance in designing and calibrating the cyclic triaxial equipment and in helping conduct the laboratory test program.

During the course of the study, contacts were maintained with the Federal Highway Administration and other federal and state agencies and individual researchers too numerous to list here. Their cooperation and advice assisted in the development of the concepts utilized in this project.

FLEXIBLE PAVEMENT DESIGN AND MANAGEMENT
MATERIALS CHARACTERIZATION

CHAPTER ONE

INTRODUCTION AND RESEARCH APPROACH

Pavements are extremely complicated physical systems involving the interaction of a number of complex and interrelated factors. Therefore, a systematic and logical approach must be used in the development of a rational and generally applicable method of pavement design. To develop such a design method a systems approach has been proposed. This is discussed in detail in *NCHRP Report 139*. An essential step in this approach is the formulation of a diagram (Fig. 1) that shows the relationship between the various factors in a pavement system and identifies the various subsystems that comprise the total system.

The development of the design method requires the completion of the various subsystems. An important subsystem is that which has as its objective the determination of the primary response. All existing "theoretical" methods for the structural design of pavements fit within this subsystem. It is assumed that the primary response of the pavement structure can be defined by its mechanical state. The concept that the determination of the mechanical state, as defined by the matrices of stress and strain, is necessary to the design of pavements is fundamental to this discussion. It is recognized that mechanical state is not the only state that has to be determined; e.g., the chemical state might be important. However, this report considers only those factors necessary for the determination and evaluation of the mechanical state in a pavement system.

In more conventional terms, determining the primary response involves the formulation and solution of appropriate boundary value problems to determine the stress and strain * (mechanical state) in a pavement as a result of loads applied under a variety of environmental conditions. The results obtained from the solution of specific boundary value problems are then evaluated in the light of established performance criteria in order to determine the capability of the pavement system to sustain the input.

Figure 2 shows the procedure involved in the development of methods for determining the primary response. It is important to recognize the complexity of this task and the iterative nature of the development procedure.

* Definitions of stress and strain appear in Appendix A.

The problem of determining the mechanical state falls within the discipline of solid mechanics. The starting point of solid mechanics is the basic laws of classical physics,** expressed in mathematical form. These laws include the laws of thermodynamics, the laws of momentum and force (Euler's generalization of Newton's laws), and the laws embodying the principles of conservation.

If, in addition to this, one could formulate a complete mathematical description of the physical properties of the materials and the input variables (e.g., load, temperature), one could obtain the solution to any problem in solid mechanics from a general system of governing equations within the limitations of existing mathematical methods for the solution of these equations. At present, the lack of a general description of material properties and input variables in mathematical form and the limitations in solution techniques do not permit such a general approach. The approach used now is to formulate and solve boundary value problems that are based on an idealization of the real physical situation through the construction of various simplified mathematical models for the materials, the input, the geometry of the problem, and various other factors.

For the purpose of determining the mechanical state through the formulation and solution of boundary value problems, the materials are described mathematically in the form of constitutive equations. To evaluate the primary response (mechanical state) to determine the likelihood of distress, it is necessary to establish performance criteria for the various materials comprising the pavement system. These performance criteria are related to limiting values of the mechanical state (stress and strain) that can be permitted to occur in a material. In conventional terms these limiting values are strength parameters that are formulated in terms of the failure theories being used. Their numerical magnitude depends on the material and the environmental and loading conditions.

Therefore, in addition to the characteristics of the material represented by a constitutive equation, the limiting

** Particulate (discrete) mechanics which has been used primarily for the study of granular media is not considered in this study.

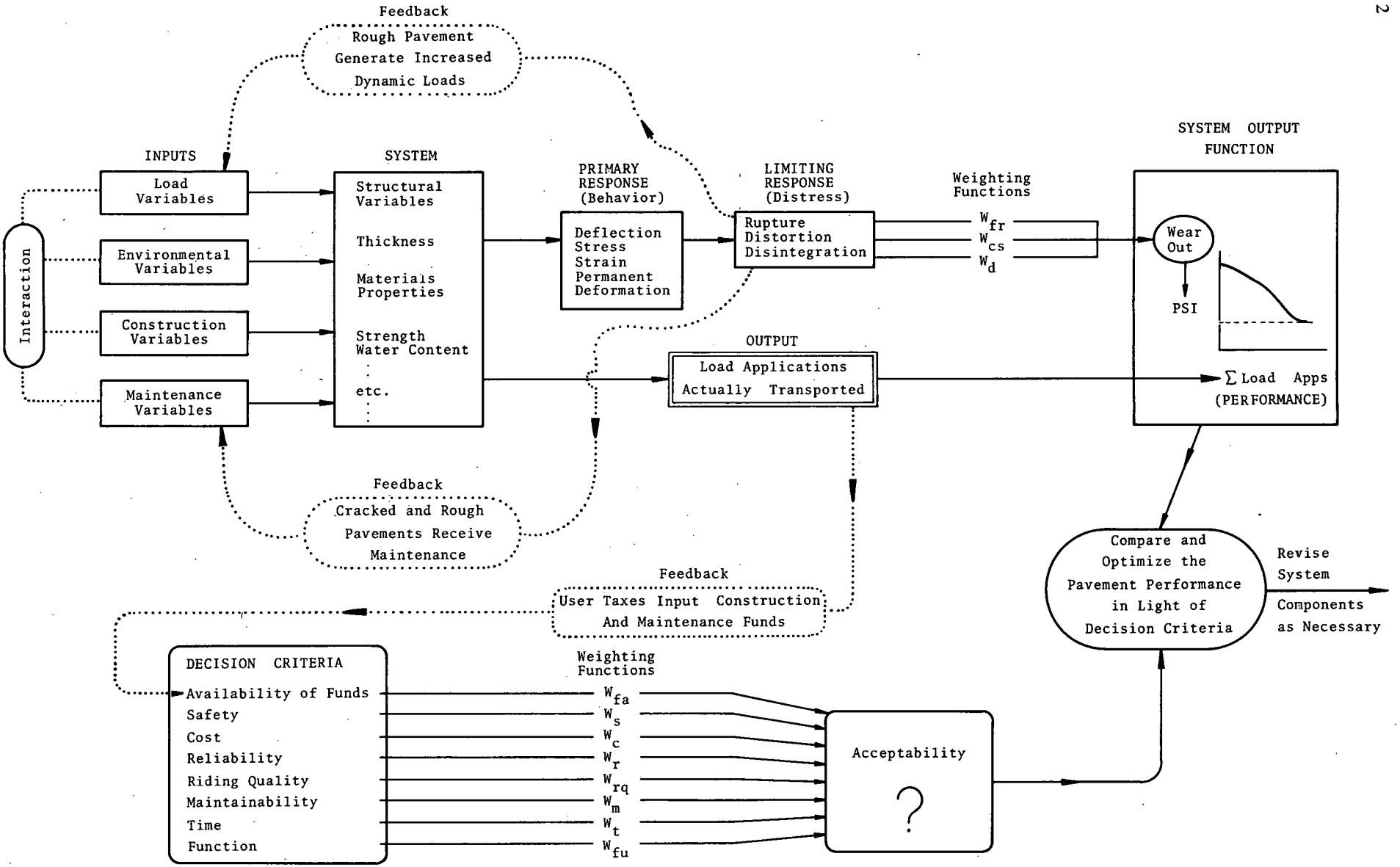

Figure 1. Block diagram of the pavement system.

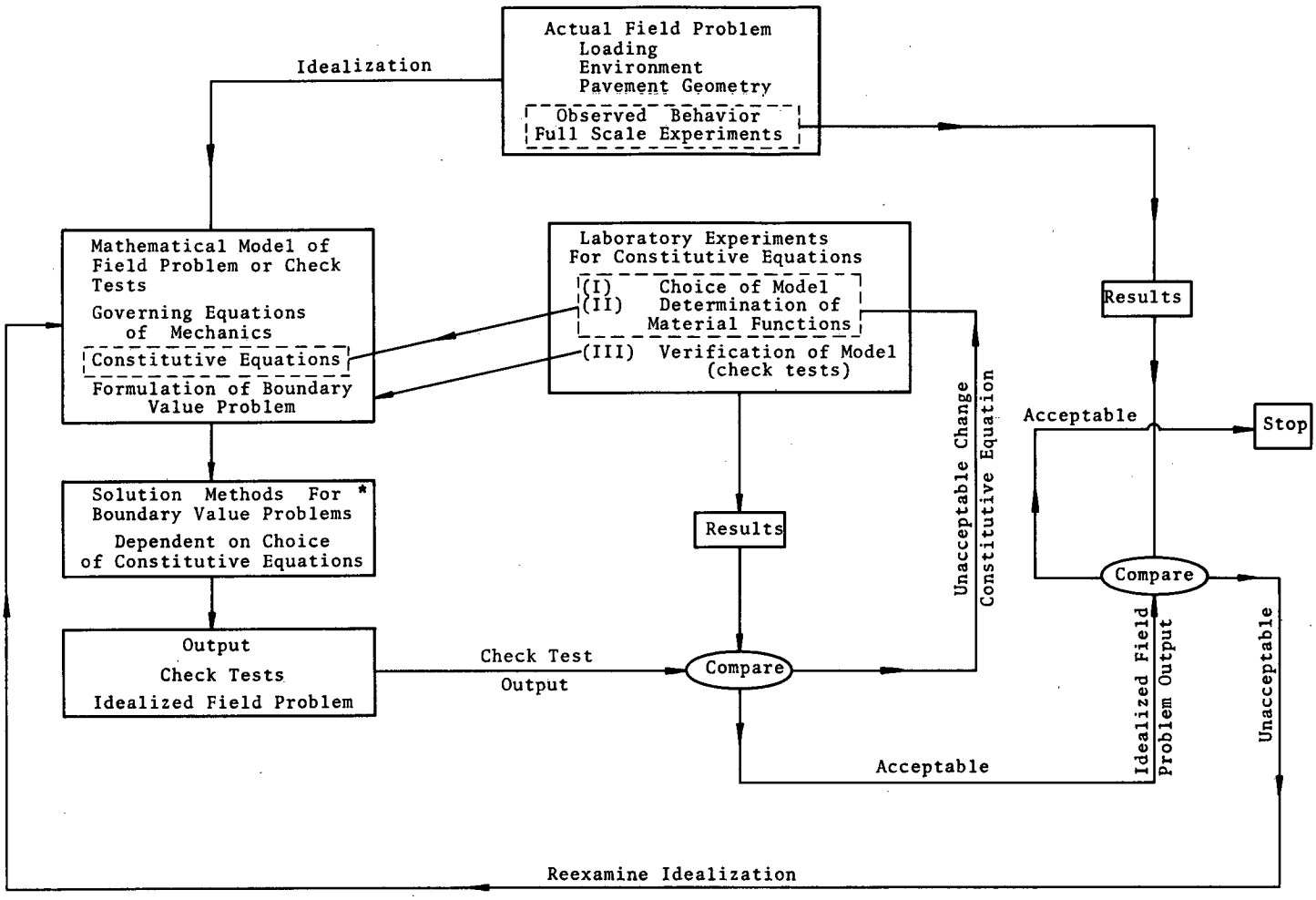

*The Solution Methods Involve Iterative Techniques For Nonlinear Constitutive Equations

Figure 2. Development of a model for determining primary response.

stress and strains (strength parameters) are material properties that are essential to the structural design of a pavement system. Recognition of this leads to the following definition of basic material properties as applied to the structural design of pavement systems.

Basic material properties are defined as the functions necessary to quantify the constitutive equations and the failure theories developed to predict material response and to evaluate possible failure, respectively.

For example, modulus of elasticity and Poisson's ratio are basic properties for a linear isotropic elastic constitutive equation, and the shear strength is a basic property for use with the maximum shear stress failure theory.

Significant basic material properties are those basic properties that are necessary for the determination of, and have a significant effect on, the response and performance of the system.

The selection of the significant basic properties from the list of basic properties depends on the problem under consideration and the method of analysis. For example, Poisson's ratio is a "basic" property to linear elastic theory; yet, when one is analyzing a beam composed of linear elastic material by conventional beam theory, Poisson's ratio does not enter into the computation. Hence, it cannot be considered significant under these conditions. However, the accurate prediction of the stresses and deflections in layered elastic systems is dependent on Poisson's ratio. Thus, in this case Poisson's ratio is a significant basic property.

For this project, material characterization * is defined as the selection or formulation of constitutive equations to represent the behavior of the various materials that form part of the pavement system. These constitutive equations are really degenerate forms of general equations and include only (for the particular problem, or aspect of a problem) those phenomena that are of importance. For example, such a simplified model is the theory of elasticity; further simplifications for various special problems result in the theories of shells, plates, and beams. It should be

* Other definitions of characterization, which are more concerned with assisting in the development of new materials, are also used in the material science literature. Furthermore, material properties associated with performance criteria are not considered in this definition of material characterization.

emphasized that a simple model containing the important physical aspects of a problem is superior to a model of considerable generality that is deficient in its representation of the physical behavior of the particular material for the specific problem under consideration.

The development of numerical techniques in conjunction with the availability of digital computers has increased the available capability for obtaining solutions to realistic boundary value problems. It is therefore appropriate to increase the level of precision in characterizing materials. In selecting a mathematical model suitable for use in a specific problem one must obtain the advice of those people who understand the physical nature of the real field problem. If the models available are not adequate for representing the materials, the physical behavior must be described to the research worker in mechanics so that an appropriate mathematical model may be developed. It is the blending of theory and physical reality that is the key to the development of improved methods of material characterization necessary for the development of improved methods for the structural design of pavements.

METHODOLOGY FOR MATERIAL CHARACTERIZATION

A constitutive equation (mathematical model) to describe a material is selected through a study of experimental and field data on the performance of the material. Experimental observation is always limited in scope; observations into a mathematical law should be reduced through scientific reasoning (logic) and in accordance with sound theoretical principles.

It was considered essential to the development of improved material characterization techniques that a step by step procedure for characterizing materials be outlined. Such a procedure is shown in Figure 3. It is an amplification of one aspect of the primary response subsystem shown in Figure 2. It is important to recognize the complexity of the task and the iterative nature of the characterization process. The following briefly explains the steps shown in Figure 3.

Theoretical Background

To choose a mathematical model to represent the behavior of a material, one must clearly understand the assumptions and idealizations involved in the development of the various models. Mathematical models are based on idealized concepts of material behavior; they cannot represent every facet of the behavior of a real material. Accordingly, one must recognize their capabilities and limitations. For example, an elastic model, by definition, cannot account for time effects. Further specialization of this model to the linear case requires that the components of stress and strain be linearly related. This study is not concerned directly with the development of new mathematical models. Therefore, the choice of a model to represent a material is limited to those existing in the field of mechanics.

As Figures 2 and 3 show, constitutive equations are used in formulating boundary value problems that are repre-

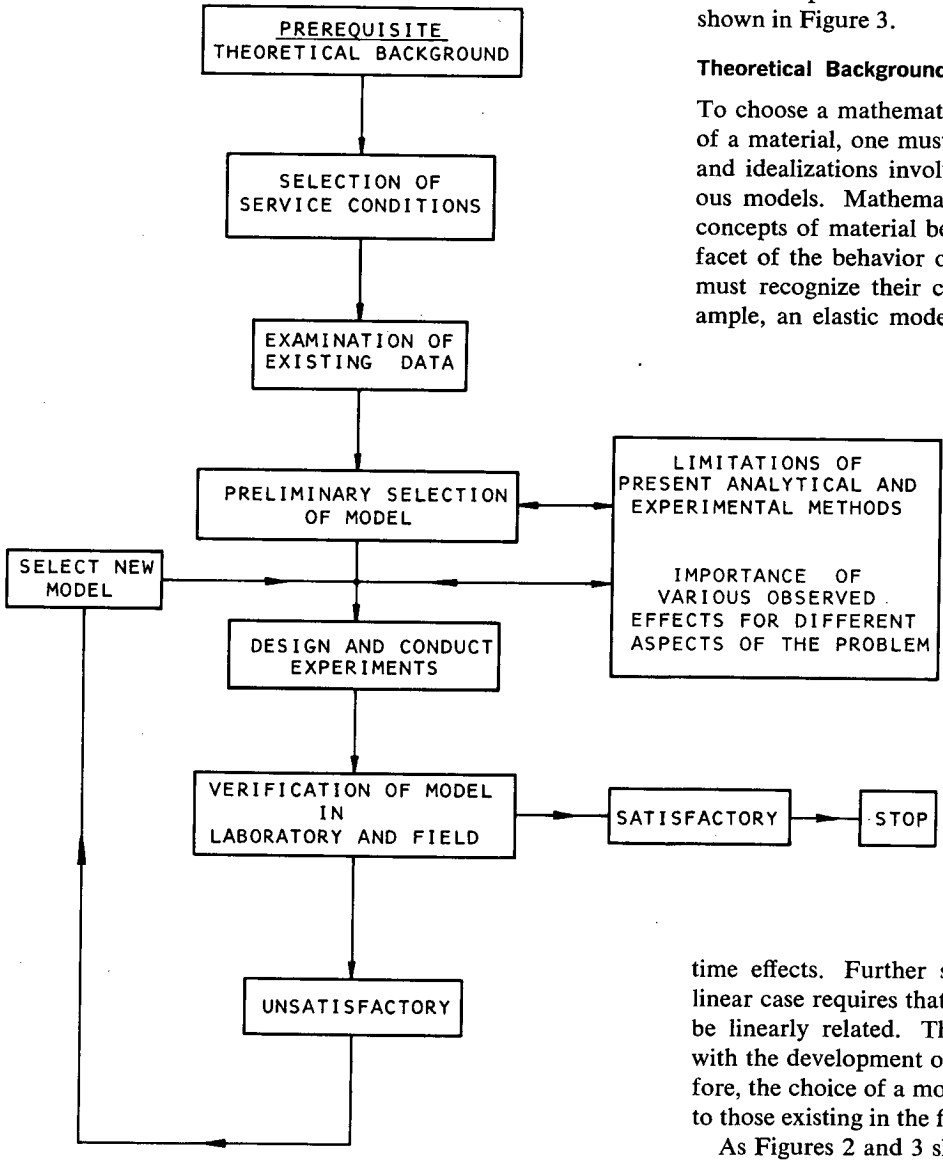

Figure 3. Steps in material characterization.

sentative of laboratory and field problems. The results obtained from the solution of a boundary value problem are used to predict the observed behavior in the laboratory and in the field. The accuracy of the prediction is used as a basis for deciding on the adequacy of the constitutive equation to represent a material.

Therefore, a laboratory test that is to be used to characterize a material must be analyzable as a boundary value problem using the constitutive equation that is supposed to represent the material being tested. This concept is fundamental. Hence, the theoretical framework for characterizing materials includes the formulation and methods of solution for the appropriate boundary value problems.

Selection of Service Conditions

Because it is not possible to perform a completely general characterization for a material that will be valid under all conditions, it is necessary to specify the conditions under which the characterization should be performed. These conditions should be representative of those to which the materials are subject in service. The conditions under which materials comprising a pavement system are expected to perform are called "service conditions." These can be grouped under the three following headings:

1. *Loading Conditions.*—Because all real materials exhibit some nonlinear effects, it is essential to decide on the stress and strain levels at which tests should be performed. This is an iterative process because it requires the determination of the stresses and strains in the system before a model can be selected on the basis of experiments. A simplified assumption, such as linear elasticity, can be used to make the initial determinations.

In the field, materials are subject to three-dimensional states of stress; hence, characterization tests must be under multiaxial stress conditions. Therefore, tests in which the material is subject to a uniaxial state of stress (e.g., unconfined compression or tension tests) generally are inadequate for material characterization. The dynamic nature of the load, the duration of the load, and the number and frequency of repetitions also should be considered.

2. *Environmental Conditions.*—The two principal environmental factors are moisture and temperature. It is generally assumed that the effects of load, temperature, and moisture can be considered separately (decoupled) and the effects superimposed. The distribution of stress due to load and the distribution of temperature and moisture can be obtained from the solution of independent boundary value problems.

The effects of temperature and moisture can be grouped into two categories:

a. Thermal and hygrostresses that may be introduced in the pavement system due to the existence of temperature or moisture differential in the system. This requires the use of a mathematical model to represent the material and is therefore an iterative process.
b. The temperature and moisture in the system may affect the material properties. The range of temperature and moisture used in testing the materials must reflect the values likely to occur in service.

3. *Construction Conditions.*—Construction techniques can exert a significant influence on the material. Laboratory-prepared specimens should attempt to duplicate construction methods. In addition to their influence on the state and the formation of the various materials, various methods of construction might result in significant residual stresses existing in the pavement system. It is necessary to incorporate these stresses into the determination of the stress state in the pavement system.

Examination of Existing Data

If there were no information on the behavior of the materials that comprise a pavement system, the first step would be to conduct experiments to get a preliminary idea of material response. However, there is a large body of laboratory and field data on the response of paving materials under simulated service conditions. Considerable benefit can be obtained by examining these data.

Existing data can be studied to obtain the necessary information to perform a preliminary selection of a suitable mathematical model. This may be considered as the first iteration (Fig. 3) in arriving at a final selection. The idealizations and the assumptions involved in the development of the various mathematical models must be recognized when one is studying the experimental data with a view to selecting a particular model. It is also important to examine carefully the test procedures used in obtaining the data.

Preliminary Selection of a Model

From an examination of available data, the important aspects of material response are identified. The next step is to determine which of the available constitutive relationships is suitable for modeling the observed material behavior. In general, it will not be possible to model all the observed effects with a single constitutive law. Therefore, it might be necessary to divide the general problem in order to reduce the number of significant material characteristics that have to be modeled at one time. How to divide the general problem is significant in the choice of a satisfactory model, and this decision must be based primarily on the knowledge of those with first-hand field and laboratory experience in the behavior and performance of pavements and materials. Based on these decisions, it might be necessary to use more than one model to represent a single material; i.e., a material might have to be characterized by different models for different aspects of the problem.

Once a model has been chosen, one must determine if meaningful stress analyses can be performed for the types of boundary value problems that are pertinent to the structural design of pavement systems. If they cannot, a further simplification must be made, and a model must be selected for which experimental techniques and methods of stress analyses are adequately developed.

The influence of available methods of stress analysis and existing experimental techniques is shown in Figure 3.

The concept of dividing the problem and selecting a model subject to the influence of available analytical and experimental techniques is shown in Figure 4.

Once the preliminary selection of various models is made

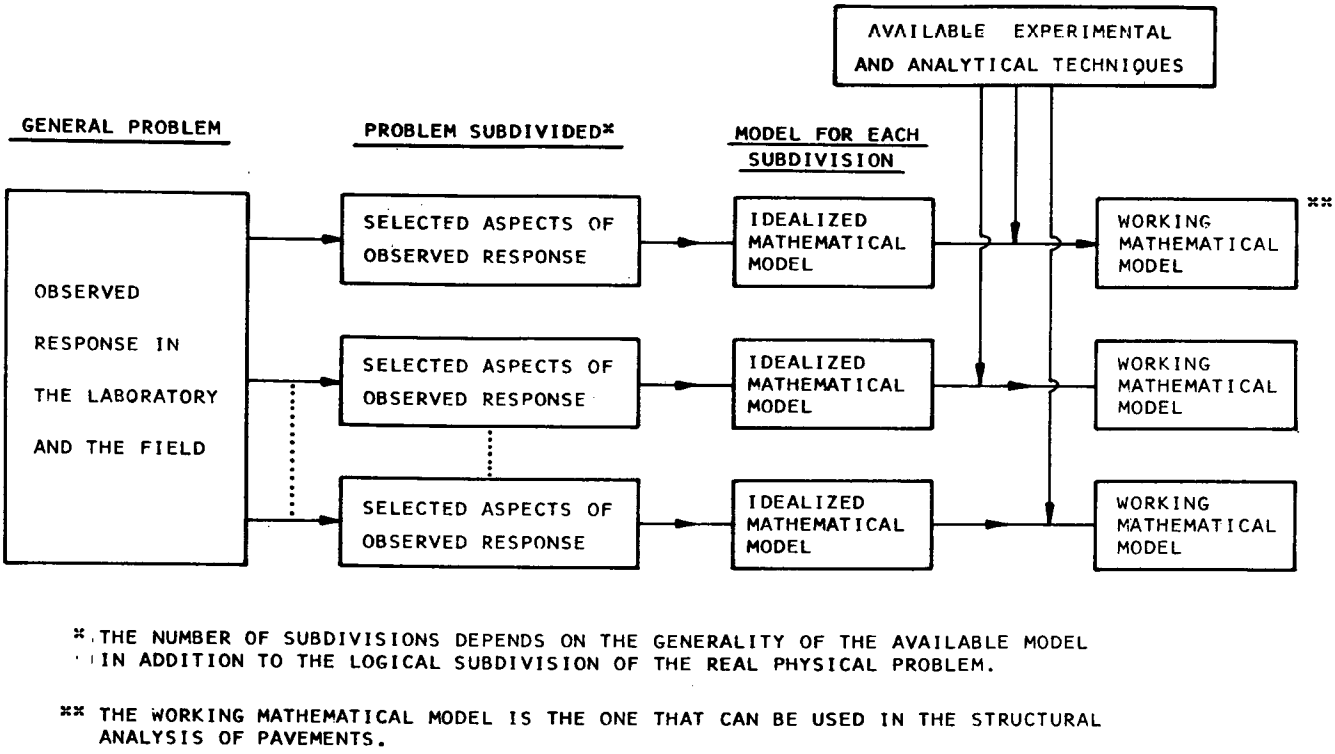

Figure 4. Subdividing a problem and selecting a mathematical model for use in analysis of pavements.

in the manner described, the next step is to design and conduct experiments to determine constants and verify the choice of the models.

Designing and Conducting Experiments

The principles involved in the design of experimental procedures are contained in the theoretical basis for the various constitutive equations. Two steps must be recognized in material characterization: (1) proving that a constitutive equation is a satisfactory representation of the material; and (2) quantifying the constitutive equation. In accordance with the foregoing concept, materials testing falls into two categories:

1. Tests that are necessary and sufficient to prove that a material can be represented by a particular constitutive law. Such tests are sometimes referred to as critical experiments.
2. Tests that measure appropriate material functions to quantitatively define the selected constitutive equation.

The tests under the first category can also quantify the constitutive equation; however, the tests in the second category are usually much simpler to perform. For example, a uniaxial unconfined compression test cannot establish if a material is linear, homogeneous, isotropic, and elastic; but if this already has been established only the uniaxial test is needed to determine the constants (E, ν) that are necessary to quantify the constitutive equation.

In general, to design experiments that are necessary and sufficient to prove the validity of a model, one must be able to vary the principal stresses independently and impose shear stresses in the presence of arbitrary normal stresses. (The availability of equipment to conduct such tests is discussed later herein.) Furthermore, except for linear homogeneous isotropic materials, these tests are also necessary for quantifying the model. Designing and conducting such experiments is a complex and difficult task.

Because the characterization of materials under completely general conditions is not possible, all tests must be conducted under the appropriate service conditions. An important aspect of this is incorporation into the test procedures of the temperature and moisture conditions under which the materials are likely to perform.

Various other factors, such as the definition of the input variables and limitations in the instrumentation capabilities, could cause differences between predicted and measured values. If, after due consideration, it is believed that the model is inadequate, then one must reexamine the assumptions and select a new model with improved predictive capabilities (Figs. 2 and 3).

Summary

The characterization of paving materials is a complex task that must be performed through the logical and systematic study of observed material response in the laboratory and the field. It is unlikely that any one constitutive equation will be able to model, with sufficient accuracy, all the significant observed aspects of the response of paving materials. Mathematical models must be tailored to suit particular problems; hence, the stress analysis and the material

characterization are closely intertwined. It is not difficult to foresee that, in the future, the appropriate stress and strain conditions for performing characterization tests will be communicated directly to a testing machine from results of a stress analysis. The results of such tests will then be incorporated into the analysis. This kind of iterative process may have to be repeated many times before the final solution is obtained.

The correct characterization of materials is a painstaking and slow process and does not appear to have the glamour that accompanies a solution to a hypothetical boundary value problem. However, without correct characterization, solutions to boundary value problems cannot be used with confidence in predicting pavement response. Hence, improved methods in material characterization are essential to advances in pavement design.

Material characterization is, in general, an iterative process. As one reads the subsequent discussions on various specific materials, the emphasis should be on the logic of the approach rather than on detail. Once such an approach is established, the treatment of various detailed aspects of the problem improves with each successive iteration.

CHAPTER TWO

DEVELOPMENT AND CONDUCT OF EXPERIMENTAL PROGRAM

SELECTION OF SERVICE CONDITIONS

The inability to characterize materials under completely general loading and environmental conditions makes it necessary to specify the conditions under which the material is expected to perform in service. Because the asphaltic concrete, granular material, and cohesive subgrade soil are functioning in one system (i.e., the pavement system), much of the discussion on service conditions is common to the three classes of materials. Thus, the discussion on service conditions for all the materials is combined. The San Diego Test Road has been used as the basis for selecting the service conditions. However, because the pavement section consists of asphaltic concrete laid directly on a cohesive subgrade, the service conditions determined are for these two materials only. Furthermore, no direct testing of granular material was undertaken during this project.* It should be noted that the nature of the loading for granular materials is the same as for the asphaltic concrete and cohesive subgrade; however, the range of stresses is different. It is the method of selecting the service conditions and the recognition of the importance of various factors that is significant. For a problem as general as pavements, specific values are of little significance, as they depend on the particular problem.

Loading Conditions

Determination of loading conditions involves determination of the stress states to which the material is subjected in the field. To calculate the stress states, it is necessary to formulate and solve appropriate boundary value problems. This requires representing the various materials comprising the pavement system by suitable mathematical models. Therefore, it is necessary to make an initial assumption for the mathematical models so that a range of stress levels under which the material is expected to perform in the field can be determined. These stress levels must be checked after the material is characterized and the appropriate boundary value problem is solved.

The boundary value problems analyzed for determining the loading conditions use two significant approximations with regard to the nature of the load: (1) the load is treated as a static load; and (2) the distribution of the loads is taken to be axisymmetric.

Dynamic problems generally are more difficult to solve than static problems, and Pister and Westmann (1962) and Avramesco (1967) have shown that, at conventional traffic speeds, the influence of the dynamic (inertial and impact) effects on the stress levels can be neglected. The assumption of an axisymmetric distribution results from the inability, at present, to account for nonaxisymmetric loads of the type represented by the wheel-load configurations of a vehicle.

Although the stress level may be computed for static assumptions, traffic loads generally are of short duration and are repetitive. The time distribution of traffic loads is random; however, for testing purposes it is necessary to decide on a frequency and duration of loading. There are situations where the loads may be static and of long duration; under such circumstances creep or relaxation tests must be conducted.

To determine the range of stress states likely to exist under service conditions so that they may be incorporated in test programs, boundary value problems for Section 2 at the San Diego Test Road Site (MR&D, 1966) were solved by finite element techniques. A finite element mesh configuration and boundary conditions are shown in Figure 5. The section consists mainly of two layers: 8.8-in.

* However, the data obtained from certain granular materials recently tested by Hicks (1970) are analyzed and presented in Chapter Three.

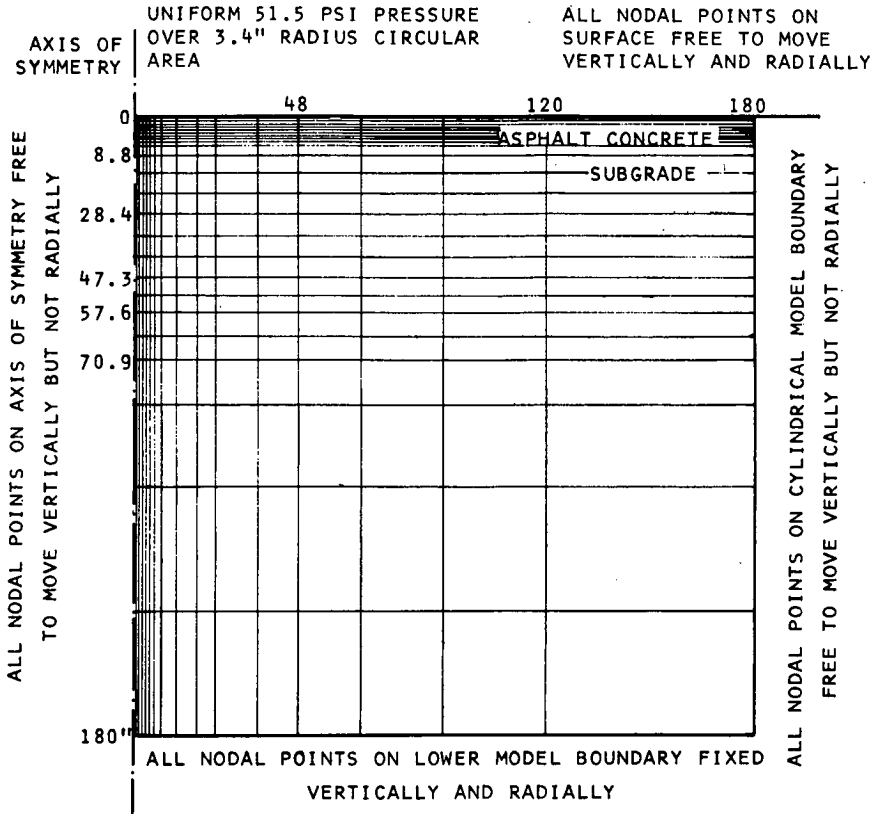

RADII TO COLUMNS OF NODAL POINTS (INCHES):

0,0.5,1,2,3,3.4,3.8,4.8,6,8,12,18,24,36,48,66,90,120,180

DEPTHS TO ROWS OF NODAL POINTS (INCHES):

0,0.8,1.7,2.6,3.5,4.4,5.3,6.2,7.1,7.95,8.8,11.8,16.4,22.4,
28.4,34.7,41,47.3,52.4,57.6,64.2,70.9,84,108,144,180

Figure 5. Finite element mesh configuration and boundary conditions for Section 2, San Diego Test Road Site.

asphaltic concrete on top of subgrade soils. A uniform pressure of 51.5 psi was applied over a 3.4-in.-radius circular area to simulate traffic loading. Two cases were analyzed: one with a stiff subgrade for which the resilient modulus varied with depth as shown in Figure 6 (Dehlen, 1969); the other with a soft subgrade for which the modulus was assumed to be 5,000 psi, as determined from preliminary tests. For both cases, the modulus for the asphaltic concrete was assumed to be the same and its value was assumed to vary with temperature (213,000 psi at 70°F, and 39,000 psi at 92°F). Temperatures in the asphaltic concrete during road tests, as reported by Dehlen (1969), varied from 92°F near the surface to 70°F at the bottom. The values of the modulus were interpolated for the corresponding temperature between the moduli at 70°F and 92°F. Results of the analyses are shown in Figures 7 and 8. Figure 7 shows the variation of vertical and radial stresses with depth in the subgrade beneath the center of the load area. Note that the traffic-induced stresses decrease rapidly with depth. The maximum traffic-induced compressive stresses occurred near the bottom of the asphaltic concrete layer. The magnitudes of the maximum traffic-induced vertical stress varied from 9 to 3 psi, depending on the modulus of the subgrade. The higher stress is associated with the stiff subgrade; the lower stress, with the soft subgrade. For both stiff and soft subgrade soils, traffic-induced radial stresses were less than 1 psi. The magnitude of stresses in the subgrade will depend on the tire pressure and the properties of the asphaltic concrete and the subgrade comprising the pavement system.

Stresses in the asphaltic concrete layer vary widely from compressive to tensile stresses, depending on the properties of underlying supporting materials, as shown in Figure 8 for Section 2 at the San Diego Test Road site. Vertical stress is always compressive and decreases from the magnitude which is the same as the tire pressure at the surface to a small value at the bottom. Radial stress, however, varies from high compressive stresses at the surface to tensile stresses at the bottom. The magnitude of the tensile stress depends largely on the modulus of the subgrade. The soft subgrade causes a large tensile stress to occur at the bottom of the asphaltic concrete layer.

The stresses determined from the foregoing analysis provide a basis for selecting stress levels at which to test the

various materials. For a different set of loading and environmental conditions the stress conditions may be quite different.

From a study of the results of the analyses shown in Figures 7 and 8, the following conclusions can be drawn:

For asphaltic concrete:

1. Multiaxial stress conditions exist. There are wide variations in the magnitude of both the horizontal and vertical stresses with location.
2. Both tensile and compressive stresses exist. The magnitude and location depend on the relative moduli of the layers comprising the pavement system.

For subgrade soil:

1. Multiaxial stress conditions exist. However, unlike the stress conditions for the asphaltic concrete, the lateral pressure varies between narrow limits. The variation in stress is primarily in the vertical direction.
2. There are no tensile stresses in the subgrade. All stresses are compressive.

The magnitude of the stress levels and the nature of the stresses to be used in the testing should be representative of the conditions likely to exist in the pavement system. In the experimental data, the information obtained for asphaltic concrete in the stress range of 80 psi compression to 80 psi tension and in multiaxial stress states is of primary interest. For subgrade soils, however, the information obtained in the lower stress level less than 10 psi is of primary interest. The specific states of stress and their numerical magnitudes used in the testing program are discussed later under "Experimentation."

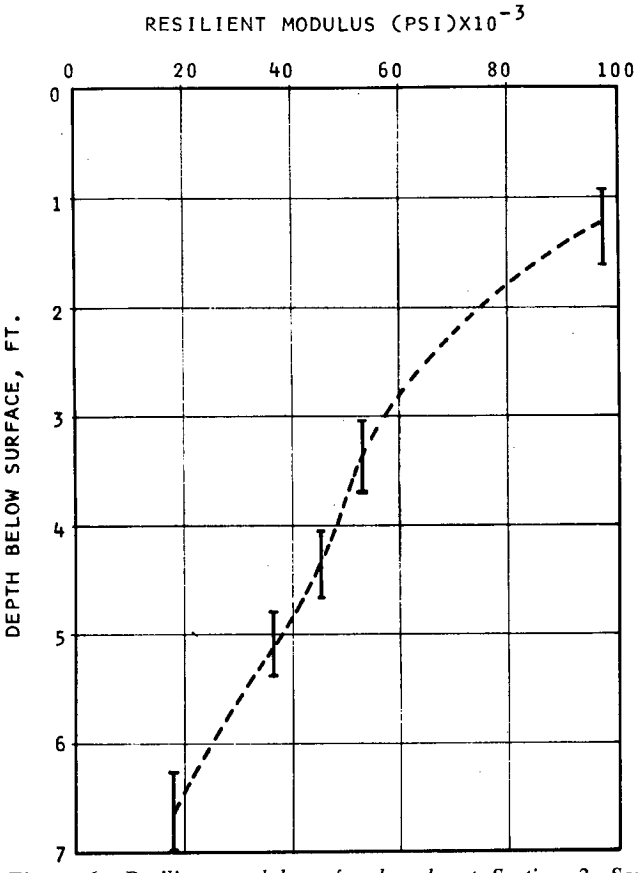

Figure 6. Resilient modulus of subgrade at Section 2, San Diego Test Road site (Dehlen, 1969).

Environmental Conditions

Moisture Conditions

Moisture conditions are defined by the water content. Soil suction [see Richards (1966)] also has been used as a parameter to define the moisture condition. Sauer and Monismith (1968) have studied the influence of soil suction on the resilient response of a glacial till.

1. *Subgrade Soil.*—The subgrade soil at the San Diego Test Road is a compacted cohesive soil. The effect of moisture on the behavior of a similar subgrade soil has been summarized by Seed et al. (1967), and is discussed briefly later. The primary effect of moisture is a change in material properties; e.g., reduced resistance to deformation with increased moisture content. It is assumed that the distribution of moisture in the soil does not cause any stress in the soil. In some soils, changes in moisture content may result in significant changes in volume, causing distortion and stresses to develop in the surface layers. Only very limited measurements on variation of moisture content with time of year and depth have been performed at the San Diego Test Road site. The moisture contents in the subgrade were primarily in the range of 15 to 19 percent.

When the researchers examined the experimental data and selected the moisture contents at which the compacted cohesive subgrade soil was to be tested in this study, a range of moisture contents that encompassed the foregoing values was considered. For a complete characterization that would be valid under a variety of conditions, it would be necessary to obtain information on moisture conditions as a function of space and time.

2. *Asphaltic Concrete.*—It is assumed that the variation in moisture content caused no change in properties. It is further assumed that moisture differential does not cause any stresses in the asphaltic concrete. The possibility of stresses in the asphaltic concrete due to volume changes in the subgrade should be recognized. This effect is not considered in this study.

Temperature Conditions

1. *Subgrade Soil.*—For the range of temperatures likely to occur at the San Diego Test Road, it is assumed that temperature has no influence on the properties of the subgrade soil. However, a change in the stress state in the surface layer due to temperature may influence the stress conditions in the subgrade. This is not considered in this study.

2. *Asphaltic Concrete.*—The response of asphaltic concrete is significantly influenced by its temperature. It is necessary to examine the available data and conduct experiments over a range of temperatures that are likely to

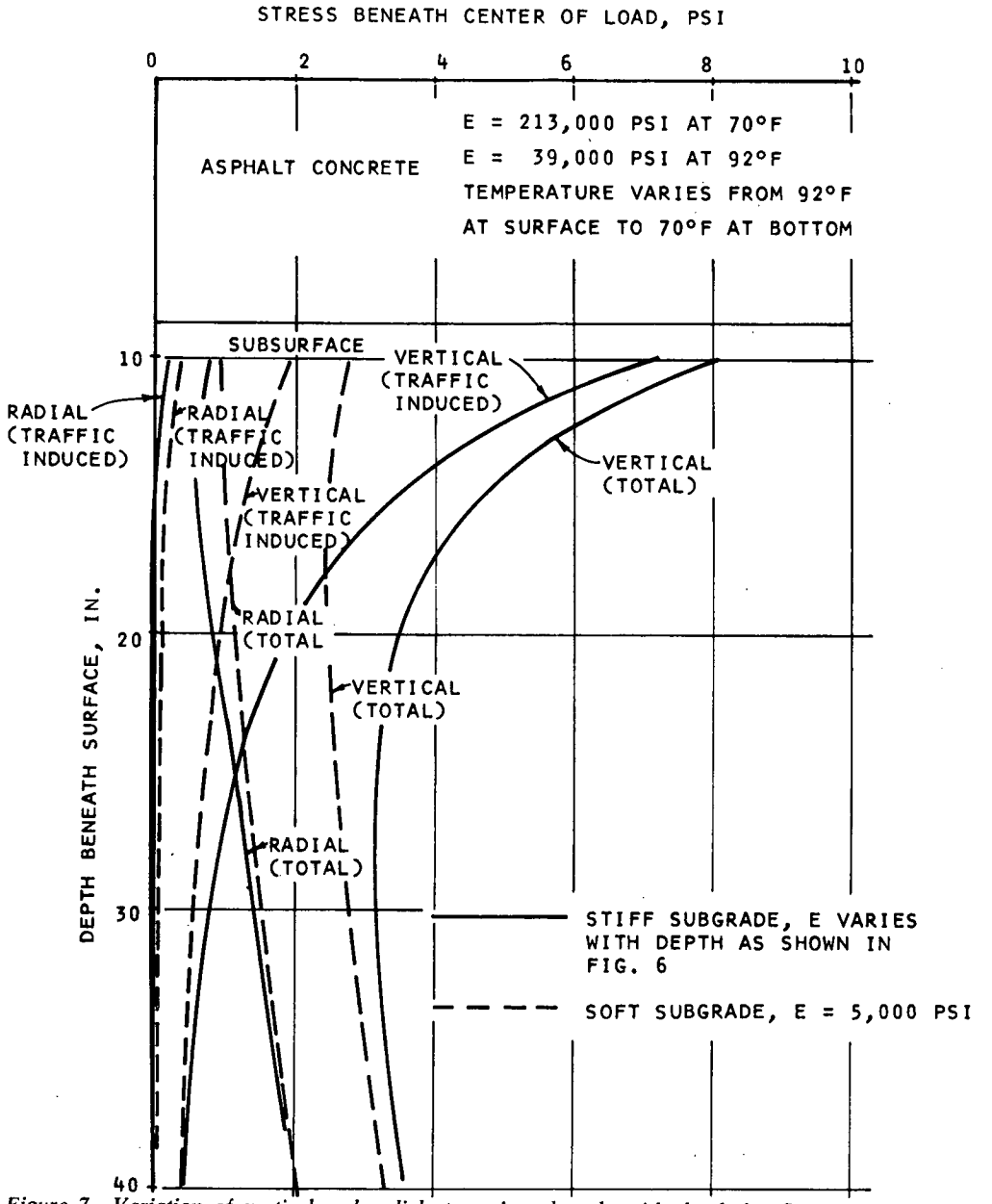

Figure 7. Variation of vertical and radial stress in subgrade with depth for Section 2, San Diego Test Road site.

occur in the field. A temperature range of 40°F to 140°F was selected; this is expected to be representative for most areas in the U.S. where freezing temperatures do not occur.

Construction Effects

Construction may result in nonhomogeneity and anisotropy. Another possible effect of construction is the "residual stress," sometimes referred to as the "prestress," that may be introduced in the soil as a result of the compactive effort. Although there are suggested methods of determining the magnitude of this stress (e.g., K_o test), evidence appears insufficient to justify the validity of such procedures. Accordingly, residual stress is neglected in this study. Conceptually, there is no difficulty in taking a residual stress into account, its effect being to change the stress level existing in the pavement system and thus to alter the stress level at which testing should be performed. However, at present, there is no method for evaluating the effects of construction in terms of residual stress. The use of field core samples is an attempt to include the effect of construction techniques in the laboratory. For laboratory-prepared samples, it is necessary to reproduce field conditions. Seed et al. (1967) believe that "using an appropriate method of sample preparation and conditioning, it is now possible to simulate closely in the laboratory any desired field condition of a soil." Although this statement appears

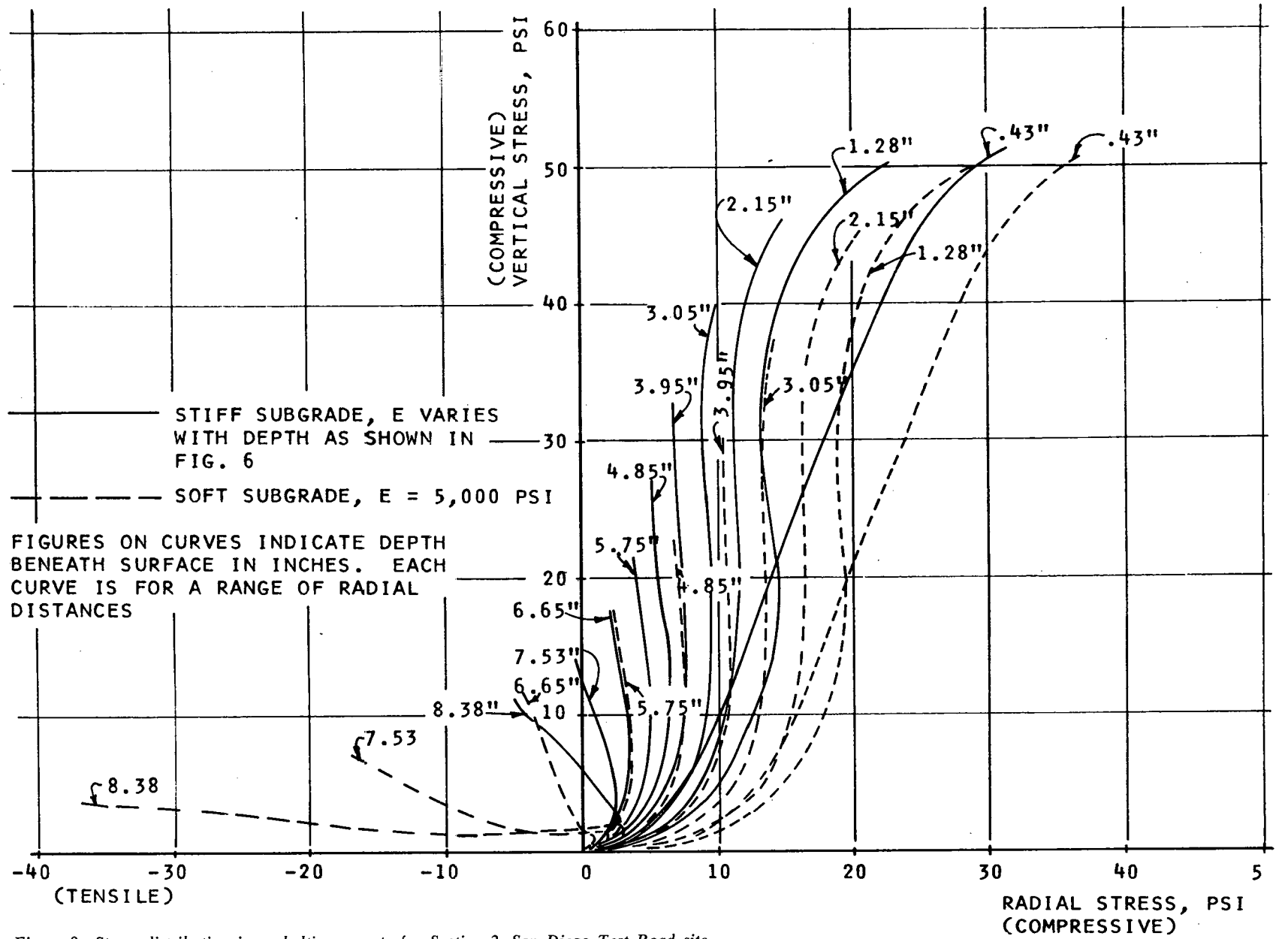

Figure 8. Stress distribution in asphaltic concrete for Section 2, San Diego Test Road site.

somewhat optimistic, the ability to duplicate field conditions unquestionably has improved considerably in recent years.

The significance of the various service conditions has been pointed out. The stress conditions, temperature, and moisture conditions appear to be the most significant. The nature of the stress conditions, and a range in magnitude of stress, temperature, and moisture have been selected. The next step is to examine available data in this context.

SELECTION OF PRELIMINARY MODEL

Selection of a preliminary model is made on the basis of existing data. The model selected is used to plan the subsequent experimental program. In examining the experimental information, attention is focused on data that established general trends rather than on data that elaborated detail. For simplicity, the selection of a preliminary model is divided into two stages. In the first stage, significant aspects of material response are identified. These are then restated in a format that is commonly used to describe the characteristics of various constitutive equations.

Asphaltic Concrete

The experimental data reviewed here are primarily from three research centers active in the study of asphaltic concrete: the University of California at Berkeley; the Massachusetts Institute of Technology; and the Ohio State University. Many other institutions in the U.S. and elsewhere have contributed significant information on the response of asphaltic concrete. However, for this investigation, the information obtained through the research conducted at the three centers is considered representative of existing information.

In recent years, testing of asphaltic concrete for use in pavement design research has been confined almost exclusively to (1) repeated load tests in flexure and compression, and (2) uniaxial creep and relaxation tests.

From an examination of the data, the following general conclusions can be drawn with regard to the response of asphaltic concrete under loading and environmental conditions representative of those that will occur in service. The significant characteristics of the response of asphaltic concrete are illustrated through the use of typical experimental information.

1. Under the application of constant load, there is an instantaneous deflection and a deflection that increases with time (Figs. 9, 10, 11).

2. On removal of the load, a portion of the deformation is recovered instantaneously. This instantaneous recovery is not necessarily equal to the instantaneous deformation that occurred on application of the load. With increase in time, more deformation is recovered; however, some permanent deformation remains (Fig. 9).

3. For uniaxial compression creep tests at low axial strains (<0.1 percent), the relation between axial stress and strain appears linear. However, temperature has a

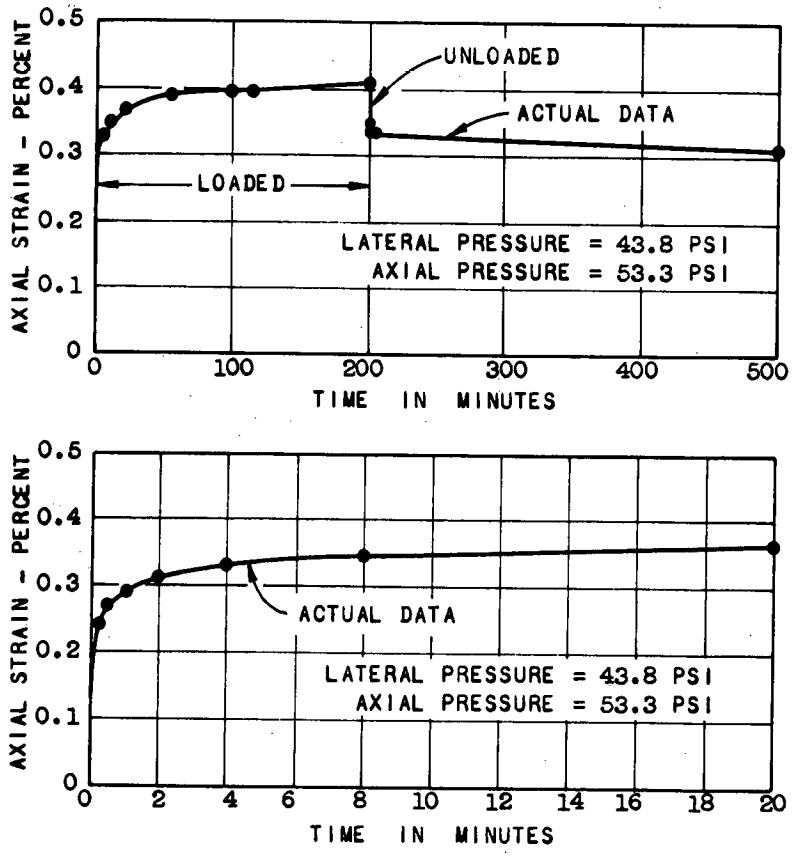

Figure 9. Uniaxial tests on asphaltic concrete.

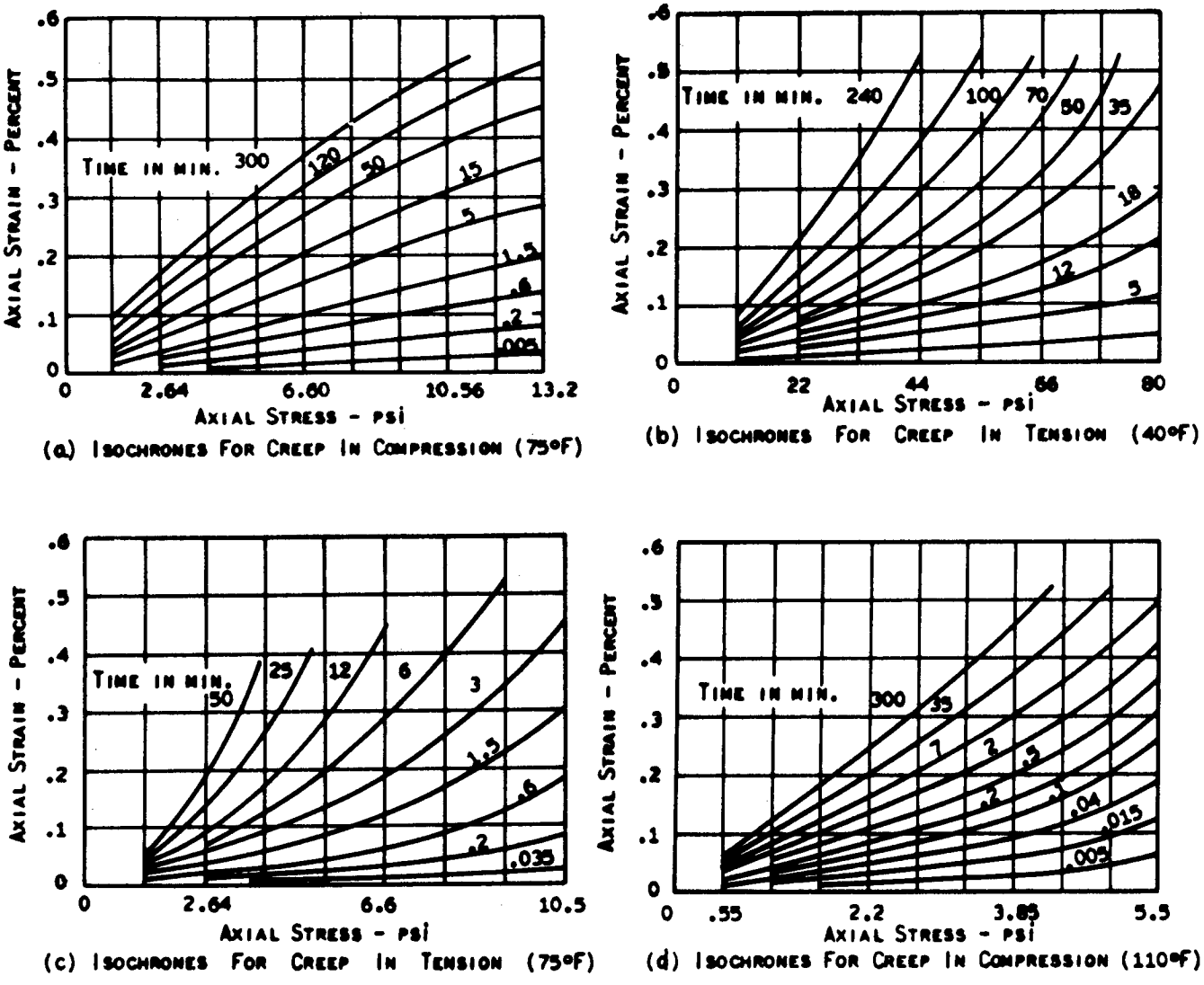

Figure 10. Data from creep tests on asphaltic concrete. (After Monismith, Alexander, and Secor, 1966.)

significant effect on the stress levels for which linearity is valid (Fig. 10).

4. For uniaxial tension creep tests, deviations from linearity in the relationships between axial stress and axial strain are greater than for the compression creep tests. There is a significant difference in the response under tensile and compressive loads (Fig. 10).

5. The data from constant rate of compression tests indicate nonlinear behavior (Figs. 12, 13, 14). Figure 12 shows the nonlinear effect as the influence of confining pressure on the relationship between axial stress and strain.

6. Under repeated loading tests, both residual and recoverable deformation occur. The amount of residual strain that occurs under a single application of load is very small compared to resilient strain (Fig. 15).

7. The stress level has considerable influence on the modulus of resilience (defined as the ratio of repeated stress to resilient strain); this is true in repeated flexural and compression tests (Fig. 16). This influence appears to be greatest for values of $(\sigma_1 - \sigma_3)$ less than 10 psi. Between 20 and 40 psi, the effect appears minor at the particular temperature shown in Figure 16. At higher temperatures (>100°F) the influence of stress level is much greater.

8. Under uniaxial stress conditions for tests where the temperature is maintained constant, it appears possible to combine the results of tests at different temperatures over a limited time range to obtain the response of the asphaltic concrete at a single temperature over an extended time span. This indicates that the effect of temperature on the variation with time of the material response can be represented by a shift of the material response on the time scale without a change in shape; i.e., the material is said to exhibit thermorheologically simple behavior (Figs. 17, 18).

9. The frequency of load application in a repeated load test influences the material response; the influence is greater at the higher temperature (Fig. 19).*

* Figure 19 reproduced with permission of the Conference Executive Committee, Second International Conference on the Structural Design of Asphalt Pavements.

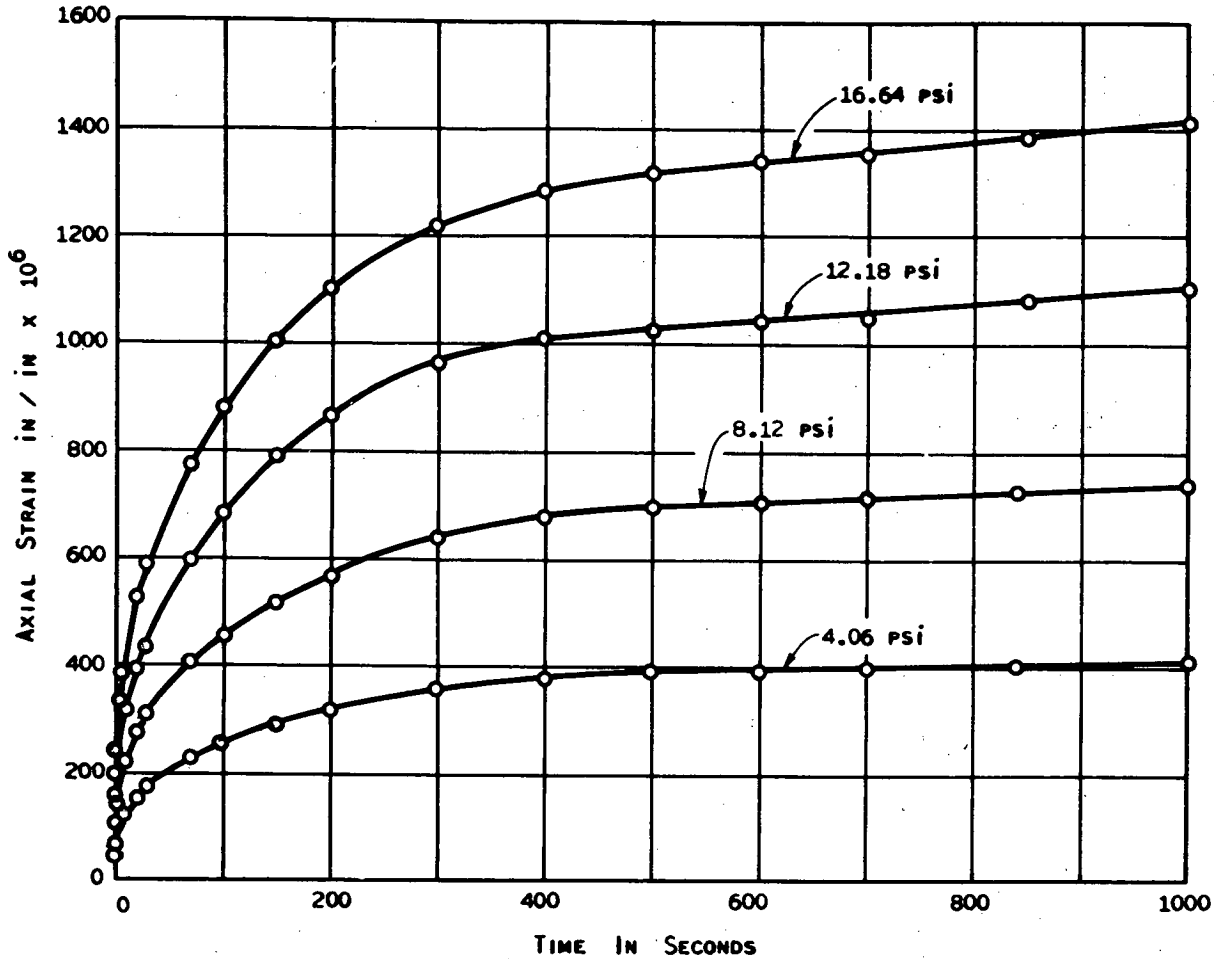

Figure 11. Data from uniaxial creep tests on asphaltic concrete. (After Pagen, 1953.)

A mathematical model was selected on the basis of the foregoing conclusions, which were arrived at after examining available experimental data. To make this selection it was convenient to rephrase and group together various observed effects, using terminology associated with the response of various mathematical models:

1. Linear and Nonlinear Behavior. There is considerable evidence of nonlinear behavior, as indicated by the influence of stress level on the material response and the difference in behavior under tensile and compressive loads. Nonlinear behavior exists over extended time intervals (Conclusions 3, 4, 5, 7, and 8).

2. Time-Dependent Behavior. The response of asphaltic concrete has both time-dependent and instantaneous components (Conclusions 1 and 2). The relative importance of these components depends on the nature of the applied load. For loads of long duration, the time-dependent response is the most significant (Conclusions 1, 2, and 6). The nature of time-dependent response has not been clearly established.

3. Permanent Deformation. The permanent deformation occurring has time-dependent and independent components (Conclusions 1, 2, and 6). After an initial conditioning effect the amount of permanent deformation occurring under each application of a load of short duration is small compared to the recoverable deformation and decreases with number of applications.

4. Time-Independent Behavior. For rapidly applied loads of short duration, the time-independent behavior predominates. The time-independent component of the deflection is not completely recoverable (Conclusions 2 and 6).

5. Temperature Effects. Temperature has considerable influence on the response of asphaltic concrete. Based on the data available, a preliminary assumption of thermorheological simplicity appears justified.

6. Stress History Effects. The nature of the time dependence of asphaltic concrete indicates that stress history must have an effect on its behavior. Such effects are not necessarily linear. No significant investigations of stress history effects have been reported.

Because of the inability to develop a general constitutive law to model all aspects of observed behavior, it is necessary to divide the problem of determining the mechanical state in a pavement (this concept is discussed in Figure 4). If these divisions are considered individually, the number

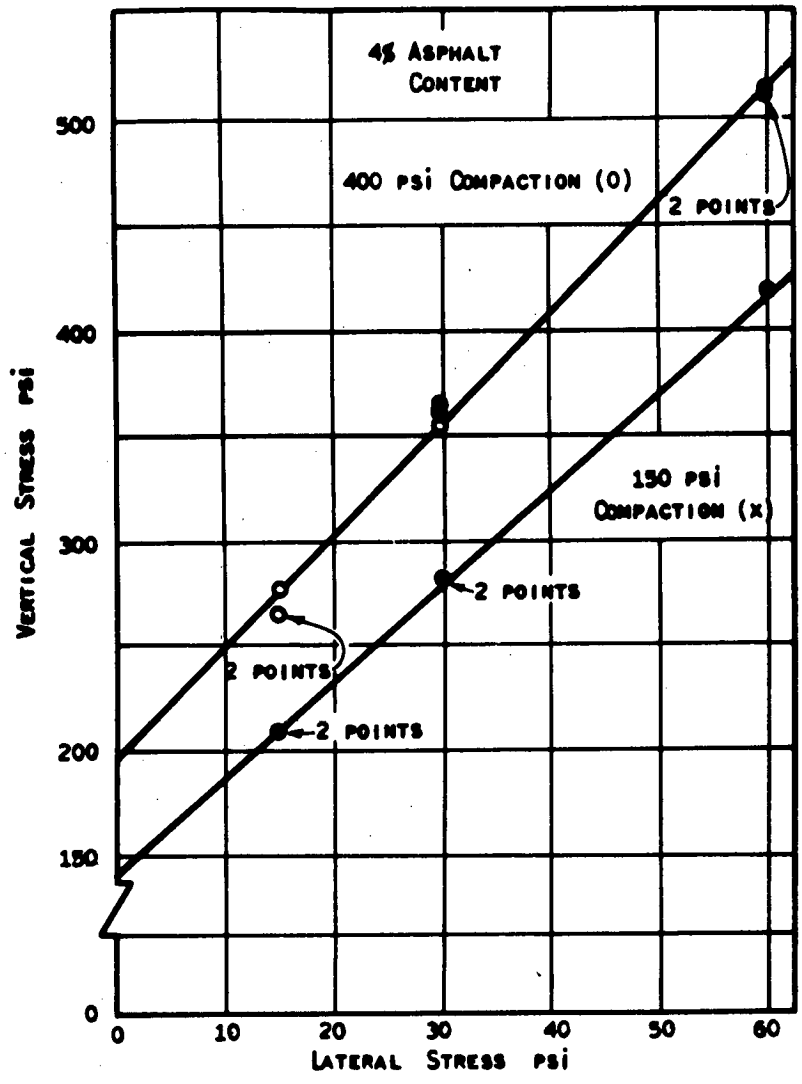

VERTICAL STRESS VS LATERAL STRESS AT 2 PERCENT STRAIN

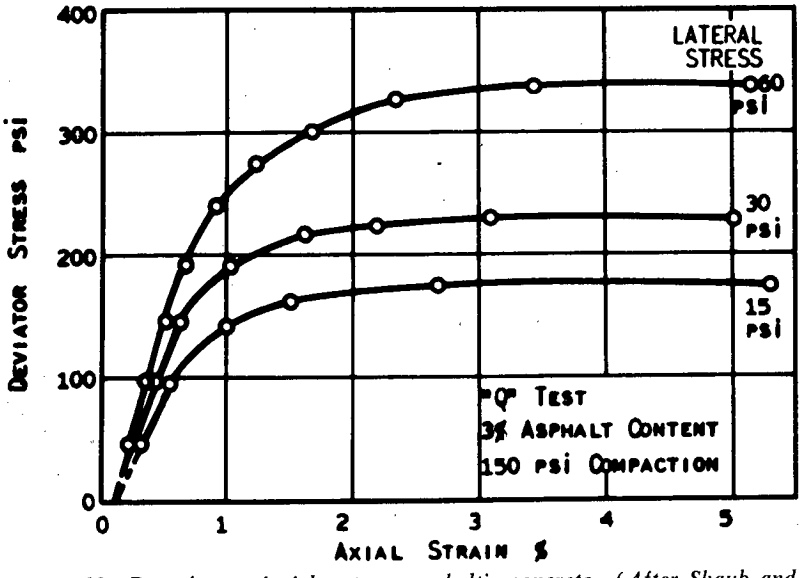

Figure 12. Data from triaxial tests on asphaltic concrete. (After Shaub and Goetz, 1961.)

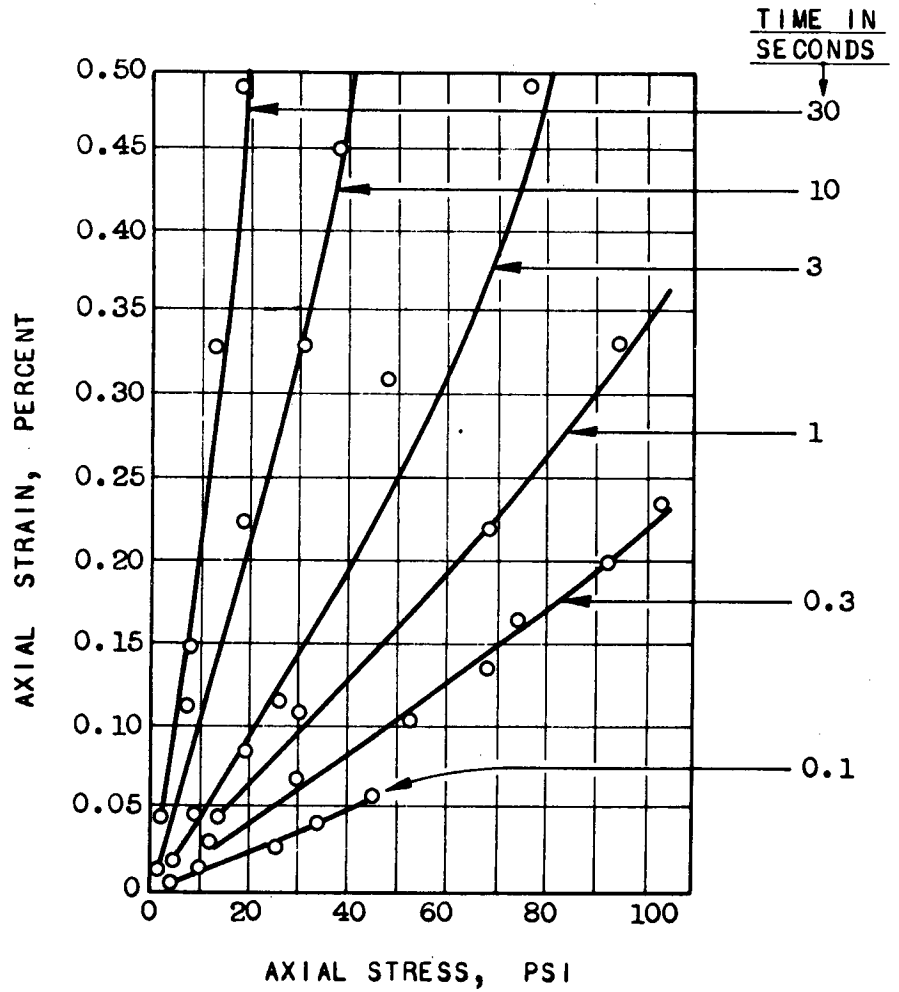

Figure 13. Isochrones for constant rate of strain in tension at 75°F for asphaltic concrete. (After Monismith, Alexander, and Secor, 1966.)

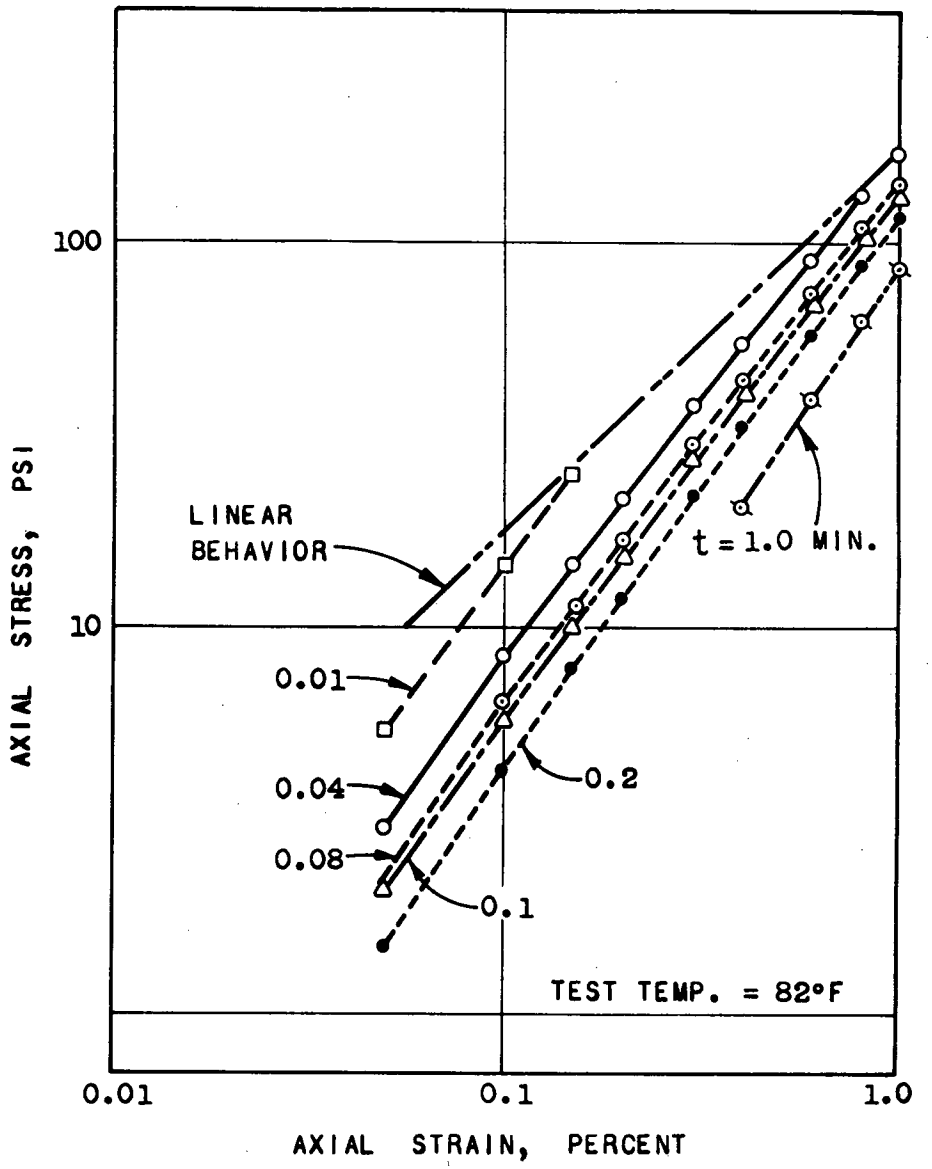

Figure 14. Constant rate of compression test on asphaltic concrete—stress strain data. (After Krokosky et al., 1963.)

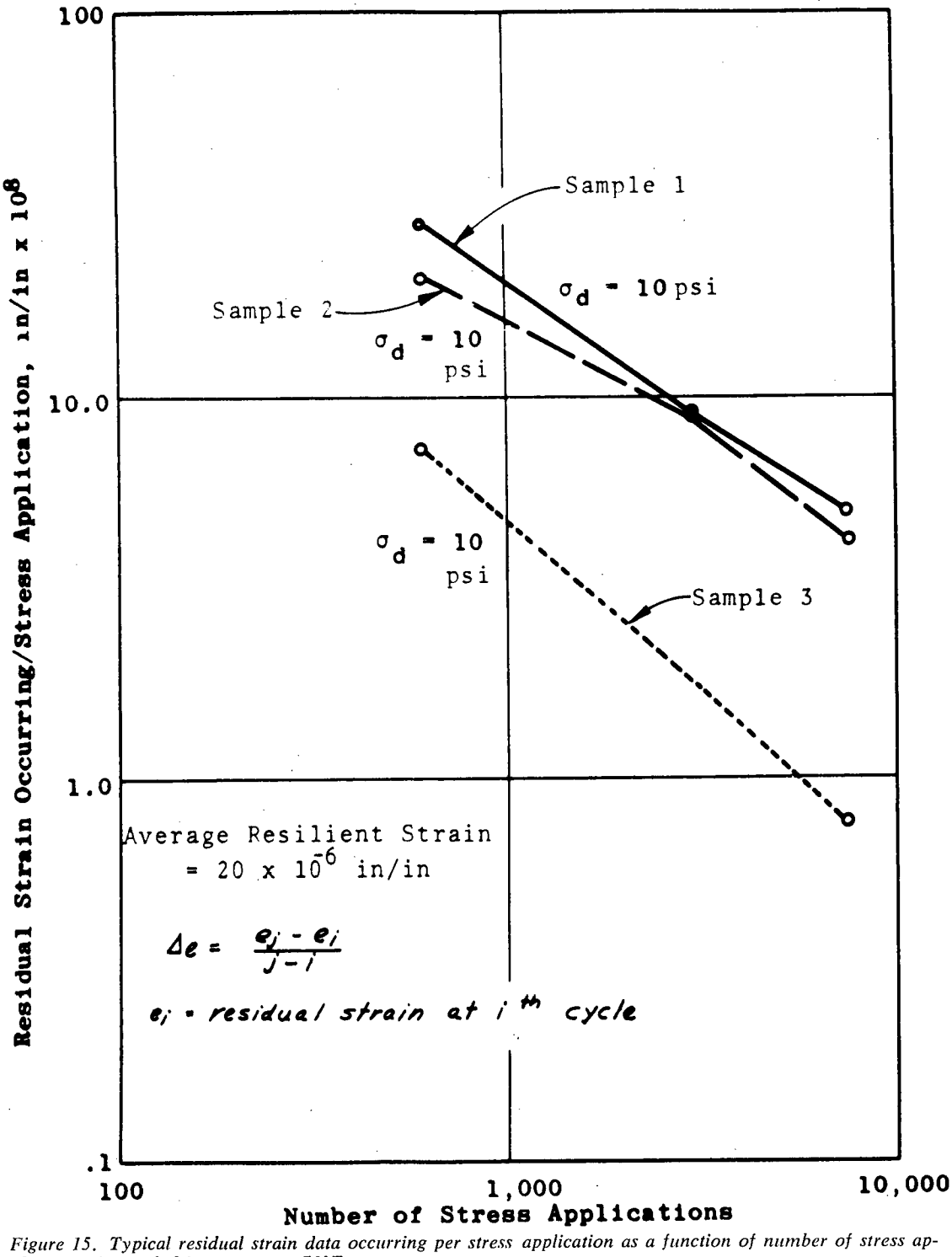

Figure 15. Typical residual strain data occurring per stress application as a function of number of stress applications for asphaltic concrete at 70°F.

of effects that have to be modeled at any one time is reduced. Regarding the response of asphaltic concrete, it appears reasonable to consider the following three subdivisions of the general problem of determining the mechanical state in a pavement system.

1. Determination of stresses and strains introduced in a pavement system by the single application of a wheel load acting for a short duration. For this aspect of the problem the following characteristics of material response are significant and should be accounted for:

   a. The data from repeated load tests and observed pavement performance indicate that, after an initial pe-

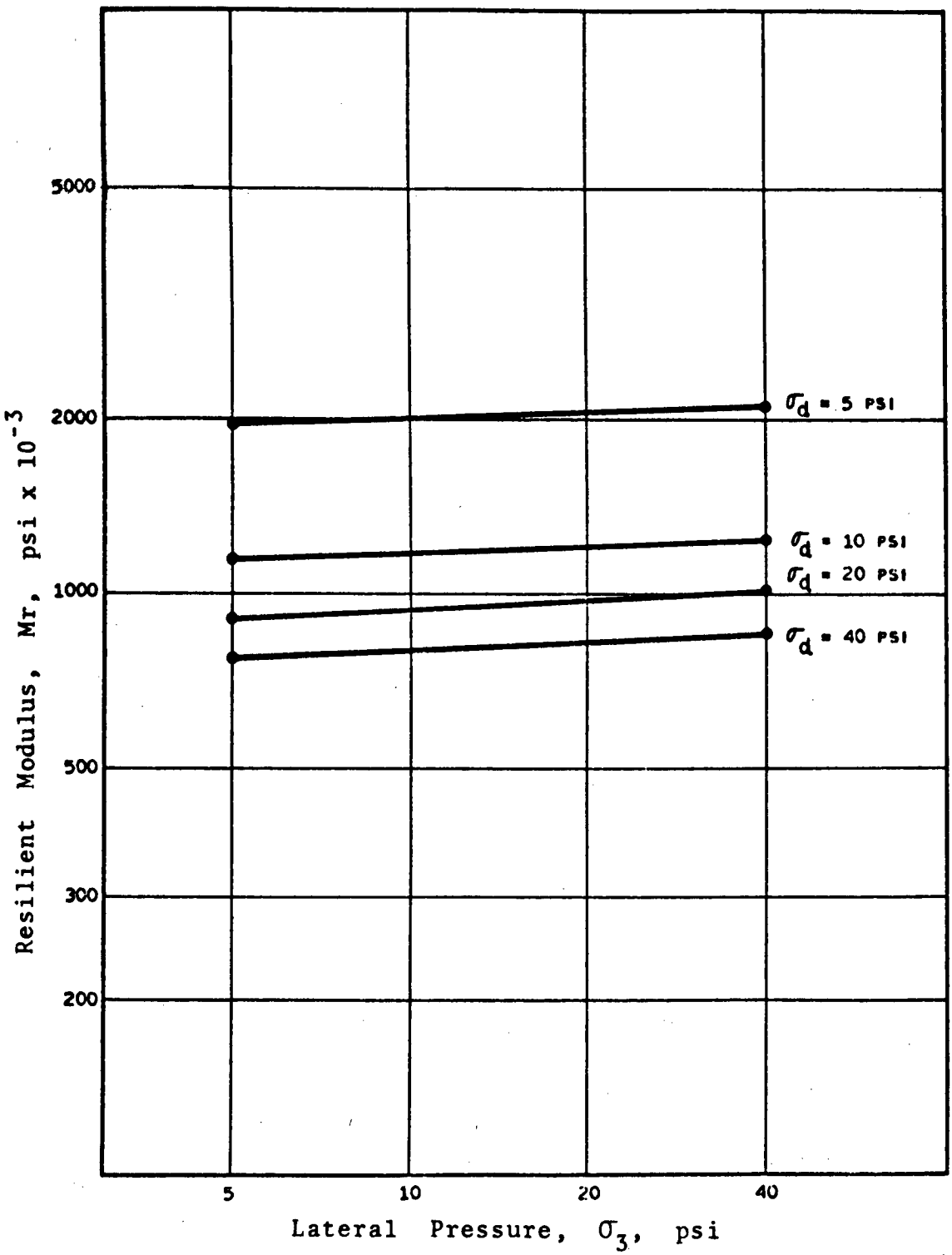

Figure 16. Resilient modulus vs lateral pressure for laboratory-prepared specimens of asphaltic concrete base tested at 68°F. (After Terrel, 1967.)

riod of conditioning, the predominant response under a load of short duration is elastic. This is particularly true at temperatures below 100°F. The magnitude of the temperature effect is known to be influenced by the characteristics of the asphalt cement.

b. Nonlinear effects are present to a significant degree under loads of short duration.
c. Time effects are not significant for loads of short duration except at high temperatures (e.g., 100°F) which are dependent on the characteristics of asphalt cement.

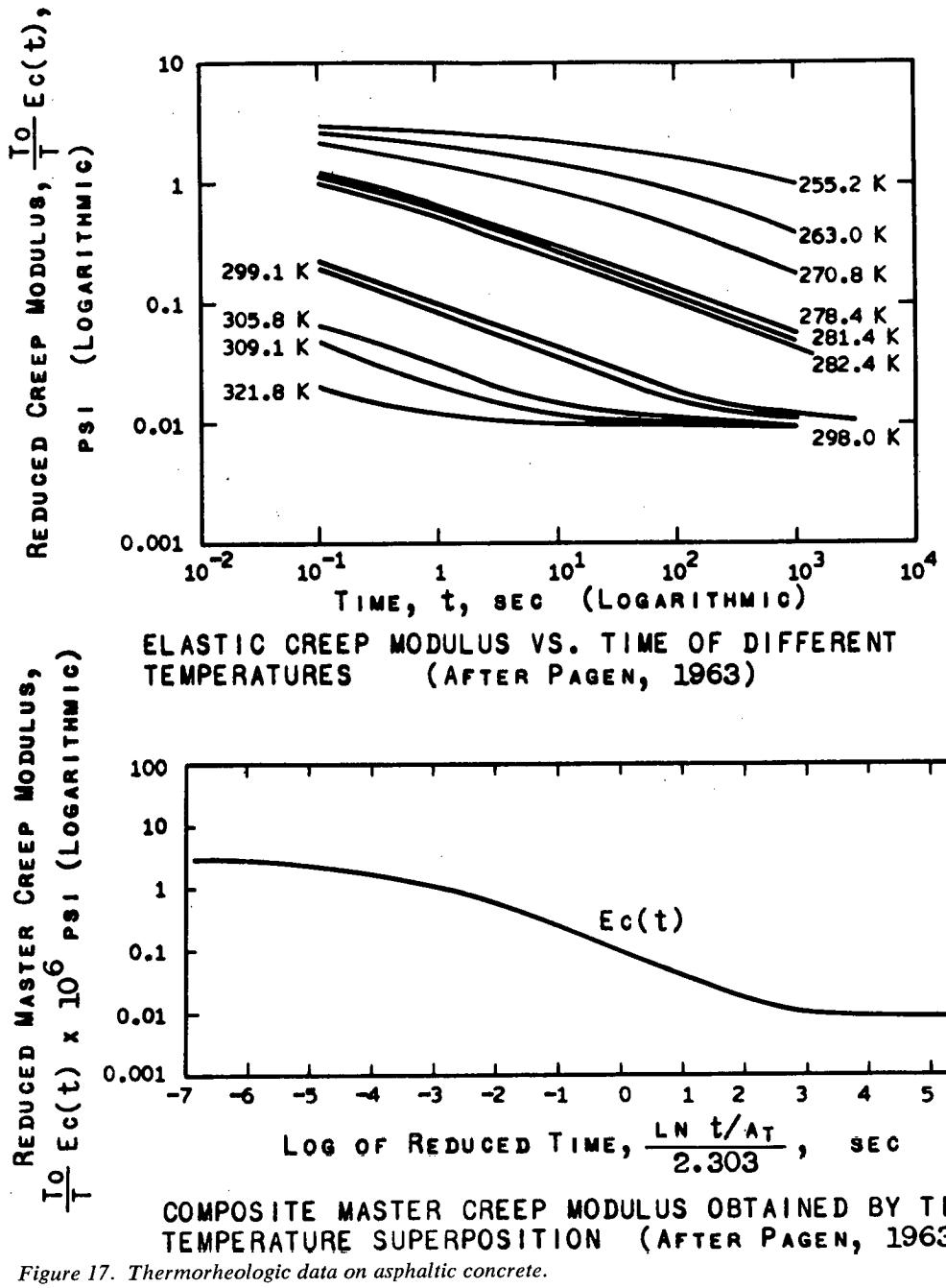

Figure 17. Thermorheologic data on asphaltic concrete.

d. The temperature of the asphaltic concrete at the time of load application will significantly influence the response.
e. The frequency and rate of load application can have a significant influence on the response of asphaltic concrete.

Considering these effects, it appears that nonlinear effects are important and that as a first approximation the residual deformation in any one application can be neglected. For a general model, time-dependent effects would also have to be included. Experimental procedures and solution techniques for boundary value problems using nonlinear time-dependent constitutive laws (e.g., nonlinear viscoelasticity) are not well developed. Consequently, one must decide whether to include nonlinear or time-dependent effects. The choice is not critical at the first iteration. The most appropriate choice becomes evident in successive iterations.

Based on the foregoing considerations, it was decided to try to model the nonlinear aspects of the response in this iteration. Therefore, the constitutive law chosen to represent asphaltic concrete for this aspect of the problem is physical nonlinear elasticity. (Because of the small deformations that occur under a load of short duration only physical nonlinearity is considered. In all further refer-

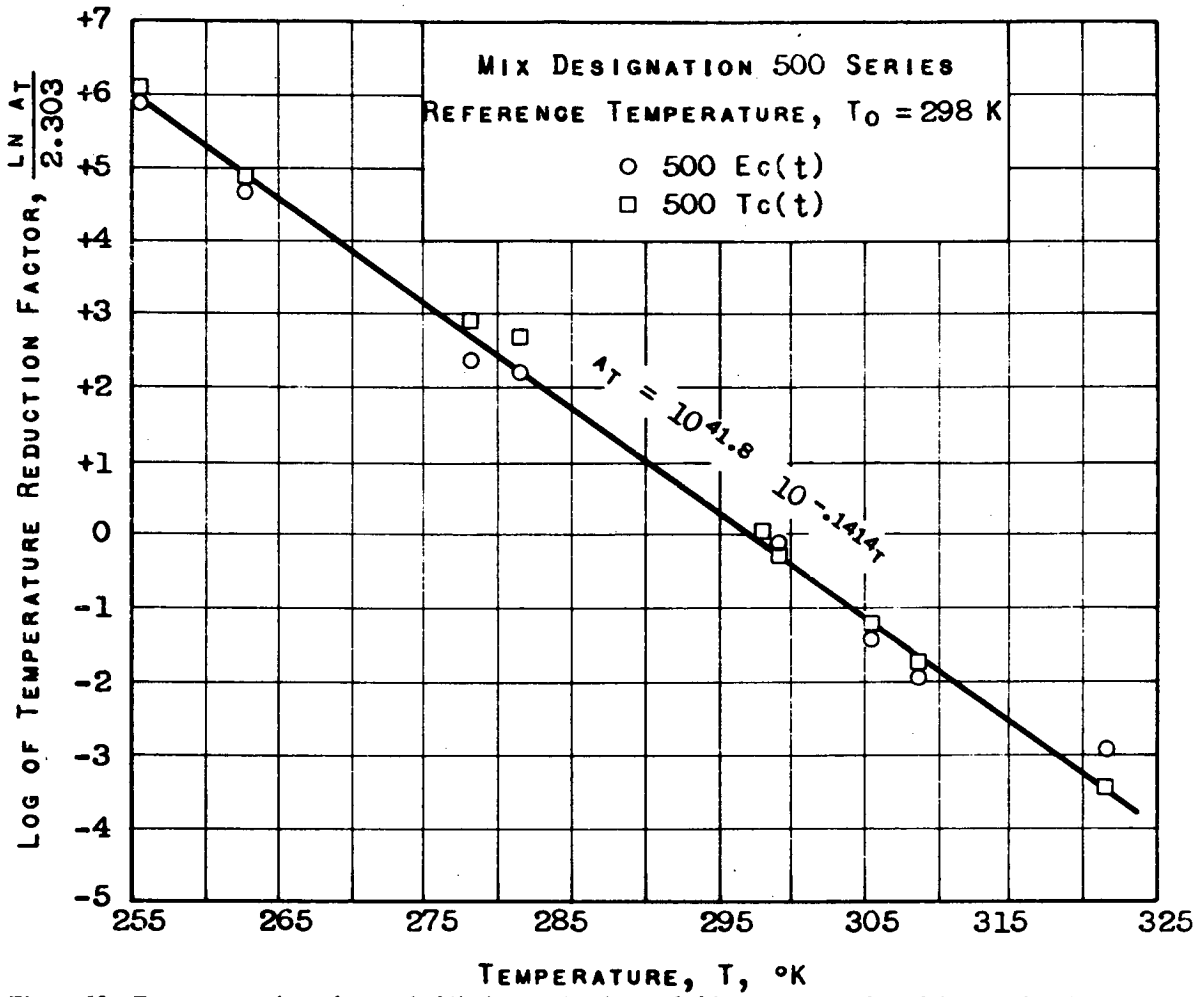

Figure 18. Temperature dependence of shift factor A_T, for asphaltic concrete evaluated from reduced elastic and transverse creep moduli. (After Pagen, 1963.)

ences to nonlinear elasticity, only physical nonlinearity is implied.) This is only a first iteration in the selection of a mathematical model.

2. Determination of the stresses and strains and the residual deformation that occurs under each application of a load of short duration in order to compute the cumulative permanent deformation that might occur over the life of the pavement. For this aspect of the problem, the following effects appear significant:

a. Under repeated loads there is a time-dependent and a time-independent component of the deformation.
b. All the deformation is not recovered on removal of the load. Some of the deformation is recovered gradually; some remains as permanent deformation. The mechanism of the permanent deformation is not well defined.
c. Temperature and stress level influence the nature and magnitude of the deformation. With an increase in temperatures and stress levels the percentage of the total deformation that is time-dependent or permanent increases.

In this aspect of the problem, in addition to the nonlinear and time-dependent effects, the influence of temperature is significant. Because one objective of this aspect of the problem is to determine permanent deformation, elastic constitutive laws are not considered. Because the nonlinear effects with regard to the time-dependent and permanent deformation are not well defined with respect to repeated loads, and experimental procedures and solution techniques for nonlinear time-dependent constitutive laws are not sufficiently developed, it is suggested that the nonlinear effects be neglected in the first iteration.

On the basis of the foregoing considerations it is recommended that linear viscoelasticity be used to model the response of asphaltic concrete for this aspect of the problem. The use of linear viscoelasticity permits the incorporation of temperature effects if the material can be assumed to be thermorheologically simple.

3. Determination of the time-dependent deformation under a load that is maintained for a long time (e.g., a standing load). For this aspect of the problem, the following effects appear significant:

a. Under a constant load, the deformation of asphaltic

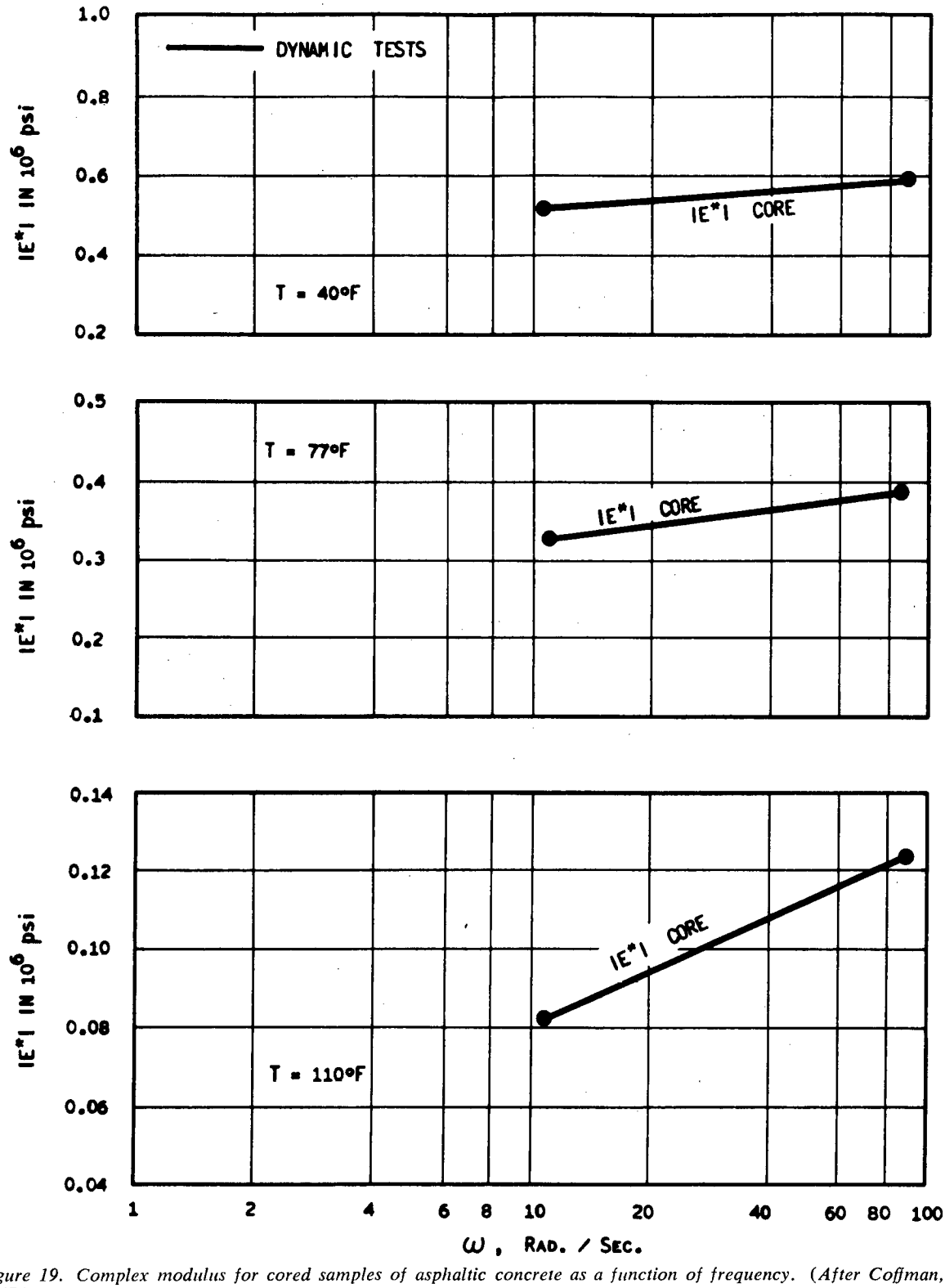

Figure 19. Complex modulus for cored samples of asphaltic concrete as a function of frequency. (After Coffman, 1967.)

concrete has two components: an instantaneous component, and a time-dependent component. With time, the deformation increases.

b. The variation of temperature during the period of loading has considerable influence on the response.

c. The stress level has a significant influence on the deformation.

Because the loading conditions give rise to creep deformation, it is possible to consider nonlinear stress-strain-

time relations that can be used in the analysis of boundary value problems. Nonlinear creep laws are often used in stress analysis problems concerned with metals at elevated temperatures. Based on creep test data, an appropriate creep law could be formulated. The approach used in the analysis is similar to that used in incremental plasticity, the creep strain being calculated over small time intervals. If the nonlinear effects are not considered significant, it would be possible to use linear viscoelasticity.

Cohesive Subgrade Soil

An examination of the service conditions leads to the conclusion that the maximum stress in the subgrade is generally less than 10 psi. The maximum stress occurs in the vertical direction. Considering the nature of the loading applied to pavements, the testing of subgrade soils for pavement design research has been confined primarily to repeated load tests. Some creep testing also has been reported. Information from other tests also is used to illustrate specific aspects of material behavior. Seed et al. (1967) have summarized the available information on the behavior of compacted cohesive soils under repeated loads. The importance of construction conditions on the behavior of cohesive subgrade soils under loads was demonstrated by the influence of the following factors on the response of laboratory specimens.

1. Age at initial loading (thixotropy). The resilient and total strain obtained in the first few stress applications is greatly influenced by the time interval between compaction and testing of those soils that have a high degree of saturation. It was observed that after a few repetitions the influence of thixotropy is reduced and the resilient deformation appears to be independent of the age of the specimen. The effect of thixotropy on the total deformation appears to continue to the maximum number of repetitions applied in the laboratory, which is still a small percentage of what the soil will be subjected to in service.

2. Method of compaction. Those methods that tend to produce dispersed structures * in soils also produce increased resilient deformation.

3. Compaction density and water content. The influence of these quantities on the resilient characteristics of fine-grained subgrade soils is summarized by Seed, Chan, and Lee (1962). For a constant dry density, an increase in water content causes an increase in deformation; for a constant water content, an increase in density causes a decrease in the resilient strain. These effects also will result from a change in water content and compaction after placement.

The factors listed here indicate the importance of determining and duplicating the appropriate service conditions in the laboratory. Ideally, it would be desirable to incorporate the effects of moisture, density, and age directly into the mathematical model. However, the development of such a general model does not appear possible at present. It is therefore necessary to duplicate the service conditions. The characterization is then valid only for the conditions under which the test was conducted.

From an examination of the data, the following significant characteristics of the behavior of compacted cohesive subgrade soils under representative loading and environmental conditions can be identified. Typical experimental data are presented for illustration:

1. The deformation obtained under a constant load consists of an instantaneous deformation and a time-dependent deformation, the total deformation increasing with time (Fig. 20).
2. On removal of the load in a creep test, a portion of the deformation is recovered instantaneously, some is recovered with time, and there is some permanent deformation. The deformation recovered instantaneously is not necessarily equal to that obtained on application of the load (Figs. 20 and 21).*
3. The deformation that occurs in a fine-grained subgrade soil under repeated loads consists of a permanent and recoverable component (Fig. 22).
4. The number of stress applications influences the resilient strain and the resilient modulus (Fig. 22).
5. The magnitude of the "deviator" stress ($\sigma_1 - \sigma_3$) has considerable influence on the modulus of resilience, especially at low stress levels, less than 10 to 15 psi, which is generally the range of stress that exists within a subgrade (Fig. 23).
6. After a few cycles, the permanent deformation that occurs in each cycle of loading is extremely small as compared to the resilient deformation (Fig. 24).
7. The effect of lateral pressure has not been documented for repeated loading tests. However, data from triaxial tests do indicate that change in lateral pressure influences the stress-strain character of the material.
8. Data on complex modulus tests indicate that frequency of load application in a repeated load test influences the material response.

To select a mathematical model to represent the observed material behavior it is convenient, as was done for asphaltic concrete, to regroup the conclusions in a manner suitable for making such a selection.

1. Linear and Nonlinear Behavior. There is considerable evidence of nonlinear behavior, as shown by the influence of stress level on the response of the material to repeated loads. This nonlinear behavior is most apparent at the stress levels likely to exist in a subgrade and extends over a long time. Difference in behavior in tension and compression is another expression of nonlinear behavior.
2. Time-Dependent Behavior. Relaxation and creep tests (loads of long duration) indicate that the response of the material has a significant time-dependent component. The nature of the time-dependent component has not been clearly established. As pointed out under (1), there is evidence of nonlinear time-dependent behavior.
3. Permanent Deformation. The permanent deformation occurring has a time-dependent and a time-independent

* A dispersed structure is one where the clay particles are arrayed in a relatively parallel position.

* Figure 21 reproduced with permission of the Conference Executive Committee, First International Conference on the Structural Design of Asphalt Pavements.

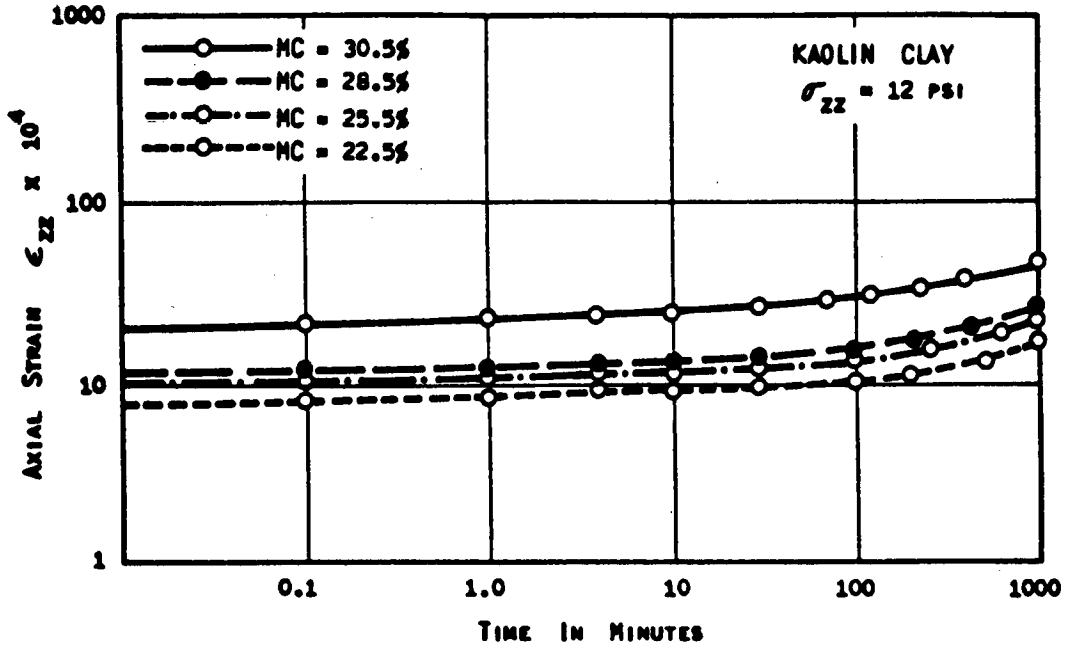

(a) AXIAL STRAIN vs TIME IN A CREEP TEST

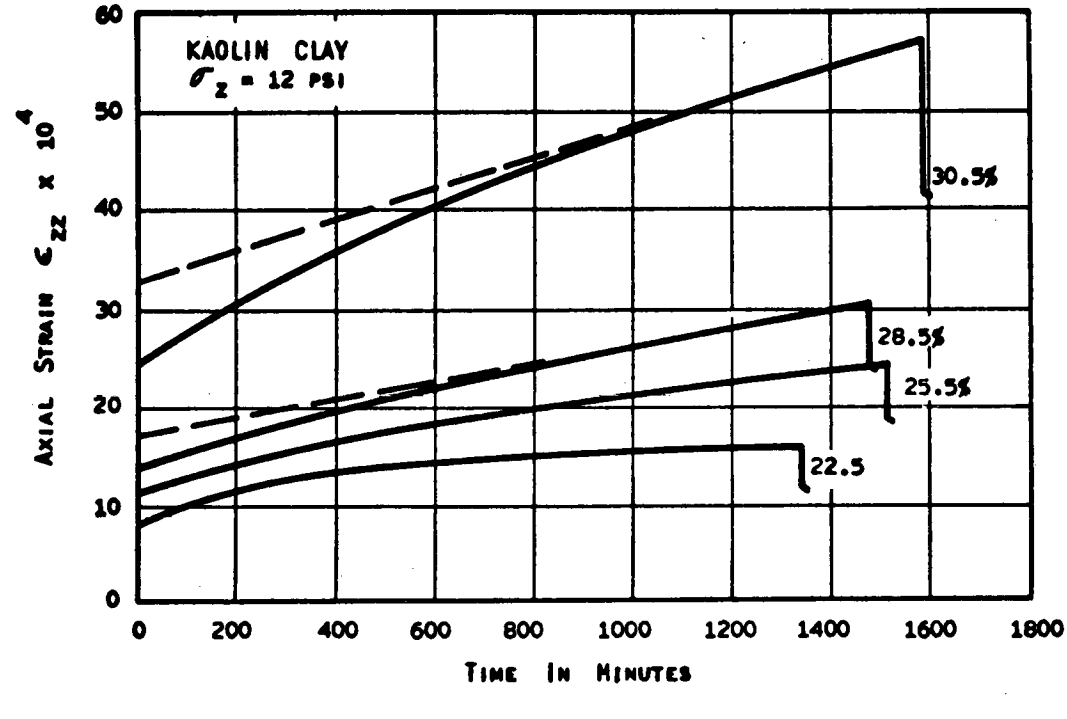

(b) AXIAL STRAIN vs TIME

Figure 20. Uniaxial creep test on clay.

component. After an "initial conditioning" the amount of permanent deformation occurring under each application of a load of short duration decreases with the number of applications and is very small when compared to the recoverable deformation.

4. Time-Independent Behavior. For rapidly applied

loads of short duration, the time-independent effects predominate. The time-independent deformation that occurs on the application of a load is not completely recoverable on removal of the load. As pointed out under (1), the time-independent behavior is significantly influenced by the stress level; i.e., nonlinear effects are present.

5. Moisture Effects. Moisture content has considerable influence on the response of the material to load. In this study, no attempt was made to incorporate these effects directly into the model. Moisture effects may be incorporated into the behavior by testing at different moisture contents.

6. Stress History Effects. As pointed out in (2), the response of the material is time-dependent. The nature of the time-dependent behavior indicates that the stress history has an effect on the response. Furthermore, the history

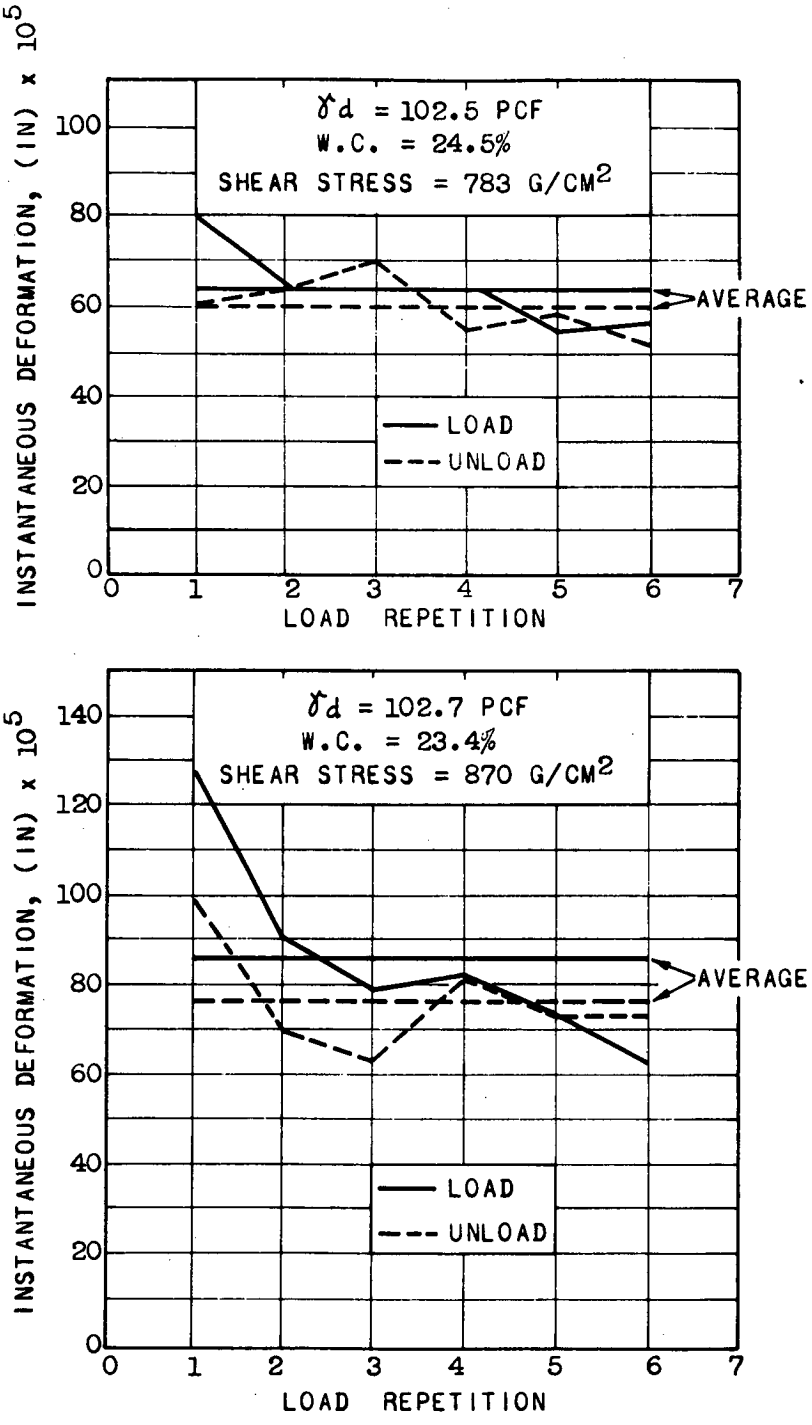

Figure 21. Effect of load repetition on instantaneous deformation, torsion shear test. (After Lara-Thomas, 1962.)

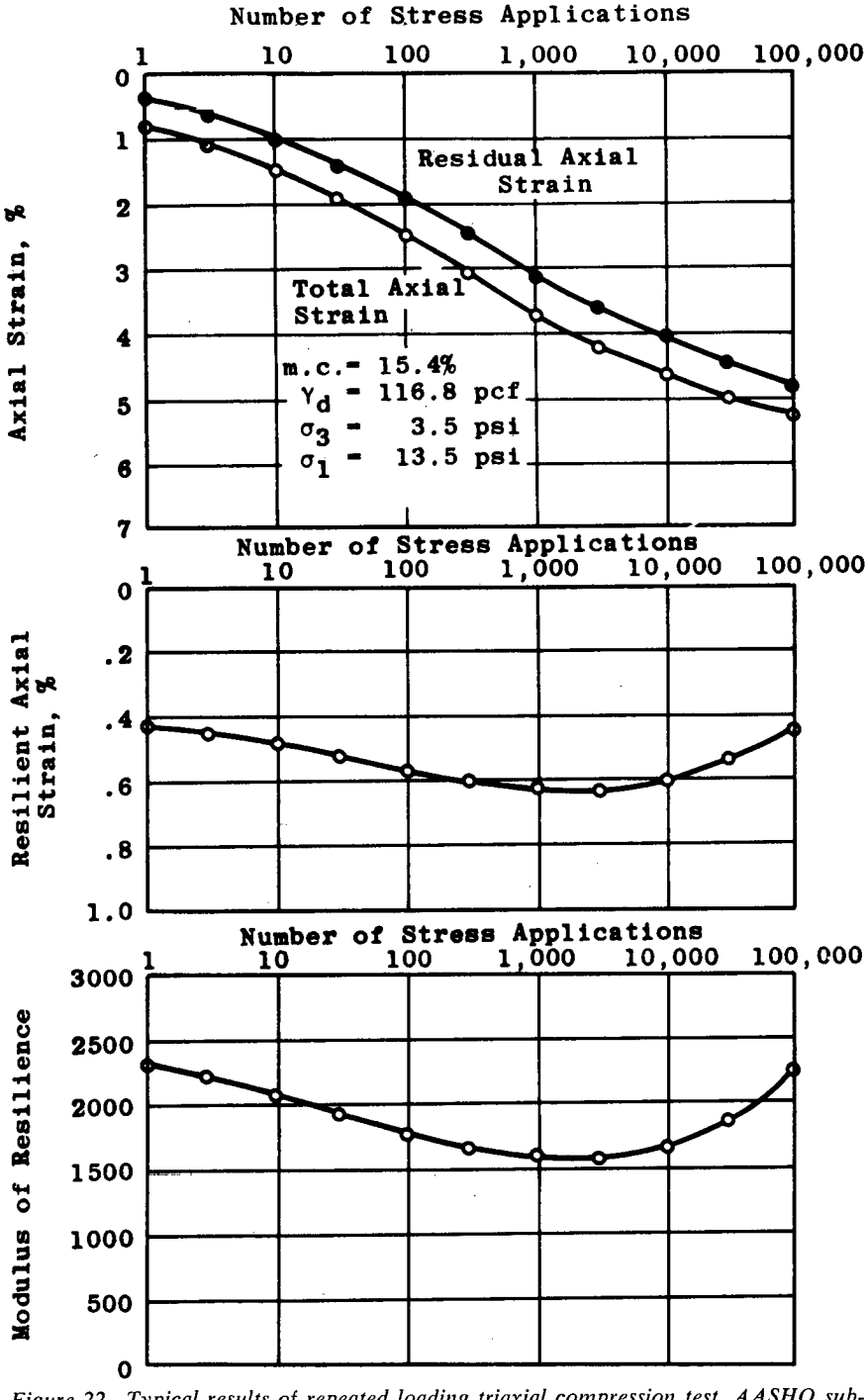

Figure 22. Typical results of repeated loading triaxial compression test, AASHO subgrade soil. Frequency of stress applications=20/min. (After Seed et al., 1967.)

effects are not necessarily linear. The influence of the number of repetitions on the recoverable deformation in a repeated load test is an illustration of a history effect.

7. Temperature Effects. For the range of temperatures considered, temperature effects are not considered significant in the response of cohesive subgrade soils.

Because of the inability to develop a constitutive law to model all the observed response characteristics, it is necessary (as was the case for asphaltic concrete) that the problem of determining the mechanical state in a pavement system be subdivided to reduce the number of effects to be modeled at any one time. As in the case of asphaltic concrete, it appears appropriate to consider separately the following three distinct aspects of the problem of the determination of the mechanical state in a pavement system.

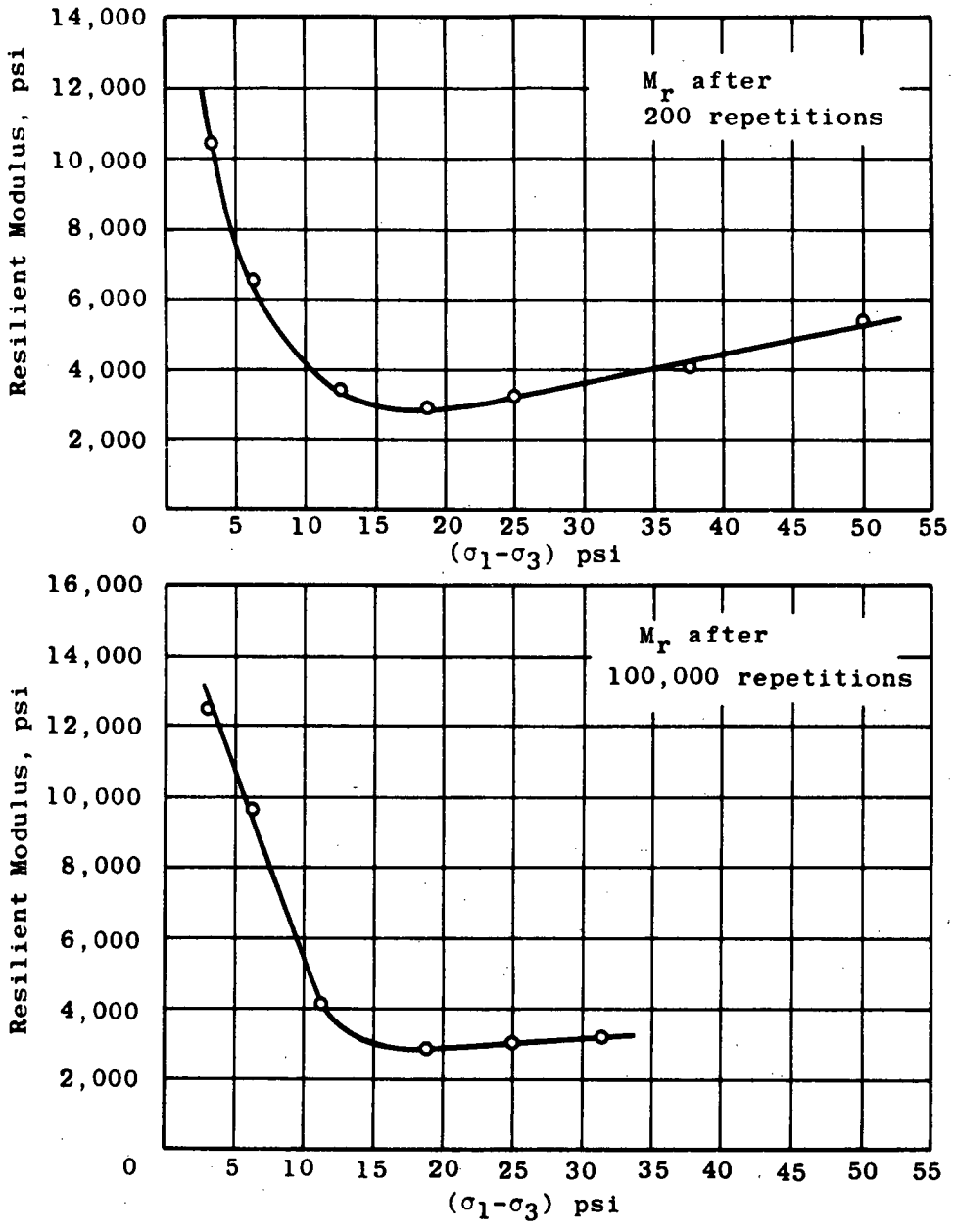

Figure 23. Modulus of resilience as a function of $(\sigma_1-\sigma_3)$, *AASHO subgrade soil. (After Seed et al., 1967.)*

1. Determination of stresses and strains introduced in the pavement system by the single application of a wheel load acting for a short duration. For this aspect of the problem, the following characteristics of material response are significant and should be accounted for:

a. The data from repeated load tests and observed pavement performance indicate that, after an initial period of conditioning, the predominant response under a load of short duration is elastic. The residual deformation that occurs under each application of load is very small when compared to resilient (elastic) deformation.
b. Nonlinear effects are present to a significant extent under loads of short duration.
c. Time effects are not significant for loads of short duration except for frequency effects, as listed below.
d. The moisture content and density of the soil at the time of load application will significantly influence the response.
e. Frequency and rate of load application can significantly influence the response of a cohesive subgrade soil.

Considering these effects, it appears that nonlinear effects are important and that as a first approximation the residual

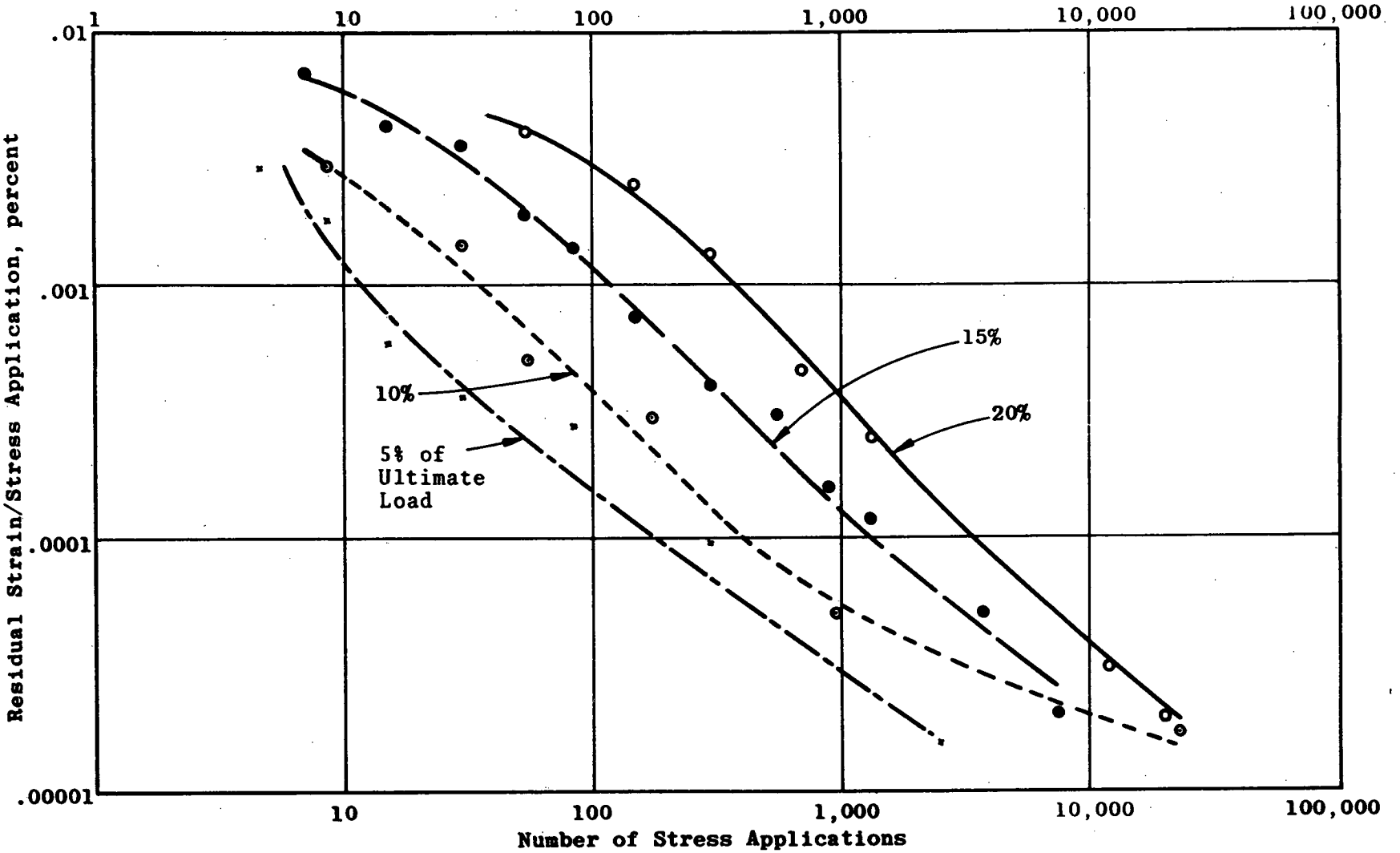

Figure 24. Residual strain as a function of number of stress applications for subgrade soil.

deformation in any one application can be neglected. For this first iteration, it is suggested that frequency and rate effects be neglected.

Based on the foregoing considerations, the constitutive law chosen to represent a compacted cohesive subgrade soil for this phase of the problem is nonlinear elasticity. This is only a first iteration in the selection of a mathematical model.

To account for moisture effects it is necessary to test the subgrade soil at different moisture contents and determine the appropriate material functions that are valid for the particular moisture content.

2. Determination of the stress and strain and the permanent deformation that occurs under each application of a load of short duration so that the cumulative permanent deformation that might occur over the life of the pavement can be computed. For this aspect of the problem, the following effects appear significant:

a. Under repeated loads, after an initial conditioning period, the additional permanent deformation that occurs with each application of load is small compared to the recoverable deformation. Nonlinear effects also are present, but their influence on the permanent deformation has not been defined.
b. All deformation is not recovered on removal of the load. Some of the deformation is recovered with time. There is some permanent deformation.
c. Water content has an influence on the permanent deformation. The permanent deformation is found to increase with increased water content.

Because determination of the permanent deformation is an objective of this aspect of the problem, elastic constitutive laws cannot be considered. Because the development of a solution technique has not reached a level that permits the use of nonlinear laws in boundary value problems of the complexity of layered systems, it is suggested that linear viscoelasticity be used to model the cohesive subgrade soil as a first approximation.

3. The determination of the stress and strain in a pavement system under a load that is maintained for a long time; i.e., a standing load. For this aspect of the problem, the following effects appear significant:

a. Under a constant load, the deformation of a cohesive subgrade soil has two components: an instantaneous component, and a time-dependent component. With time, the deformation increases.
b. Moisture variations that occur while the load is acting will have considerable influence on the response.
c. Nonlinear effects are present in their influence on the time-dependent deformation.

Under a stationary constant load the subgrade soil may creep. Stress-strain-time relation that includes nonlinear effects similar to those used in the structural analysis of metals at elevated temperatures can be used to represent the subgrade soil (see Appendix A). These relationships are developed on the basis of generalizing one-dimensional relationships and are therefore approximate in their representation of stress-strain relations under multiaxial conditions. Methods of stress analysis using these kinds of stress-strain-time relations have been developed.

If the nonlinear effects are not significant, then linear viscoelasticity which has a sounder theoretical basis can be used.

Granular Materials

Under the types of loadings to which pavements are subjected, the most significant difference between the behavior of granular base course materials and the asphaltic concrete and cohesive subgrade soil components is that the granular materials do not exhibit time-dependent effects. Because of the fewer effects that have to be considered, it is convenient to proceed directly to a discussion of material response in terms that are appropriate to the selection of a suitable constitutive equation.

Moisture content, density, and the gradation of the material are factors that significantly influence the response of a granular material. For this investigation, these factors were accounted for in the preparation and selection of the samples for testing. They are not directly included in the constitutive equation. Under the foregoing stated assumption the dominant aspect of the response of granular material is its nonlinear character. Because the deformation of granular soils was essentially independent of the deviator stress, Brown and Pell (1967) deduced a variation of modulus with confining pressure based on measurements of stress and strain in prototype pavements. Holden (1967) varied the axial and radial stress simultaneously to represent the stress conditions that exist at various depths in homogeneous sand areas below a circular load. He found that the stress-strain character of the sand as expressed by the tangent modulus can be expressed as a function of the octahedral normal and shear stress.

In the limiting case of no confining pressure, a granular material is assumed to have no strength. An important aspect of granular materials is their inability to withstand tensile stress. This is another manifestation of nonlinear behavior.

The modulus of resilience as determined in a repeated load triaxial test is dependent on the confining pressure. Biarez (1962), Trollope et al. (1962), and Morgan (1966) have all reported a significant increase in the modulus of resilience of sand with an increase in confining pressure. This dependence on confining pressure can be directly expressed as a function of the radial stress or as a function of the sum of the three principal stresses, as follows: $M_r = K_1(I_1)^{K_2}$. The latter is more convenient for incorporating in methods of stress analysis. Typical results obtained by Seed et al. (1967) are shown in Figure 25. The form of the expression for the modulus of resilience shown in Figure 25 applies to gravel also. Shifley (1967) found that an expression similar to that in Figure 25 was valid with an insignificant change in coefficients for dry and near-saturated conditions.

In a conventional triaxial test it has been observed that at constant lateral stress the stress-strain curves are approximately linear at stress levels below 50 percent of the failure stress. Because time-dependent phenomena can be

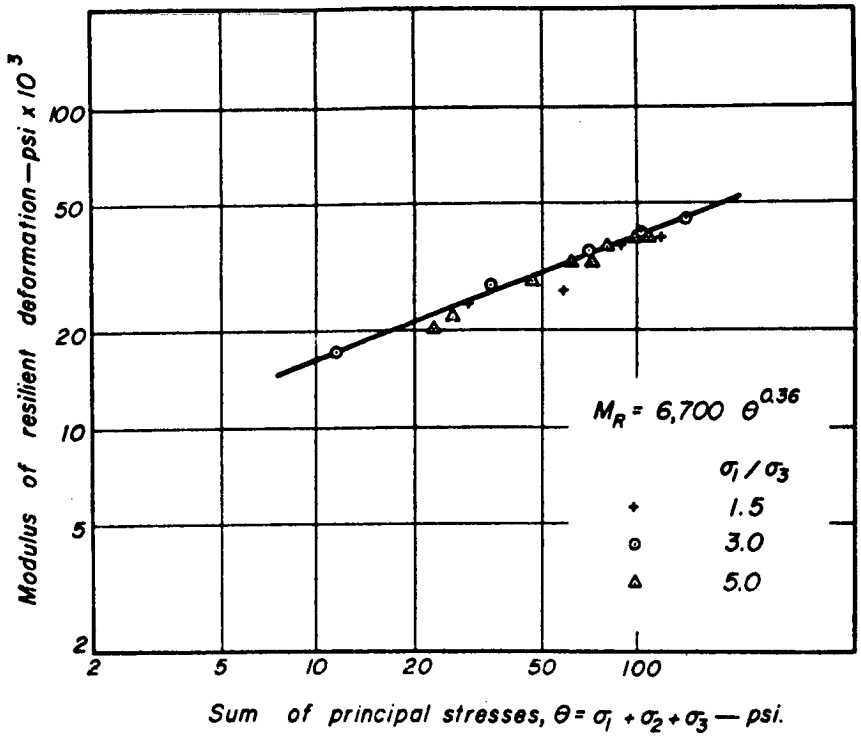

a. Sand

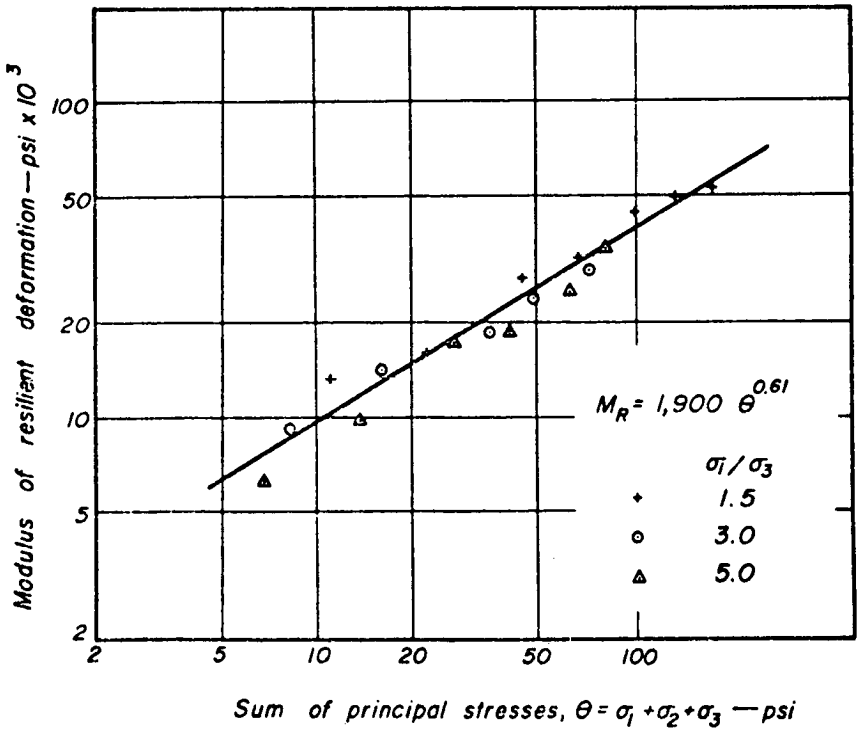

b. Dry Gravel

Figure 25. Effect of the sum of principal stresses on the resilient moduli of sand and gravel measured in repetitive-load triaxial tests. (Seed et al., 1967.)

neglected and the stress levels are sufficiently low to exclude the possibility of plastic flow, only an elastic constitutive law need be considered. Because of the relatively few aspects of material behavior that have to be modeled, it is not necessary to subdivide the problem of determining the mechanical state in a pavement system.

Experimental evidence indicates that a nonlinear elastic constitutive relation would be a suitable representation of the response of granular material to loading conditions representative of that which might occur in pavement systems. If it is desired to further simplify the representation for the first iteration, an equivalent modulus which is a function of the first stress invariant or the confining pressure can be used with a provision to include a reduced modulus under a tensile stress.

Summary

A study of available information indicated that the response of asphaltic concrete and cohesive subgrade soil was sufficiently complex to prevent all the significant factors from being modeled by one constitutive equation. Therefore, the problem of determining the mechanical state in a pavement system was divided into three problems to reduce the number of significant factors that had to be modeled at one time. From this division it was found that nonlinear elasticity and linear viscoelasticity represented suitable approximations of the real behavior of these materials. For this investigation, only one aspect of the total problem was considered—the determination of the stresses and strains induced in a pavement system under a single application of load. For this aspect of the problem, nonlinear elasticity is chosen as the constitutive equation for modeling the response of asphaltic concrete and cohesive subgrade soils. A study of the information on granular materials indicated that nonlinear elasticity also was suitable for modeling the response of granular materials.

The experimental program discussed next is based on the premise that nonlinear elasticity is a suitable first approximation for representing the response of the various materials to be tested.

EXPERIMENTATION

The experimental program depends on the selection of the preliminary model. In designing an experimental program it is first necessary to concede the result. In other words, the response of the material has to be assumed. The more general the assumed response (constitutive relation), the more complicated the experimental program. If the experimental program is designed on the basis of a general constitutive relation, it would be possible to obtain from the data the necessary information for characterizing the material in accordance with a specialized case of the general constitutive equation. For example, if the experimental program is designed on the basis of a nonlinear elastic constitutive relationship, the data obtained should also permit characterization according to a linear relationship.

As indicated in Chapter One, an examination of the existing data led to the conclusion that a nonlinear elastic constitutive equation was a suitable first approximation for representing the response of the asphaltic concrete, the cohesive subgrade soil, and the granular material under certain loading and environmental conditions. The experimental program was designed on the basis of the material having a nonlinear elastic response under repeated loads acting for a short duration under a variety of temperature and moisture conditions.

The experimentation can be divided into three sections: the first is concerned with the design of the equipment; the second is concerned with establishing test procedures; and the third details the actual test program. However, these three facets depend on the theoretical considerations underlying this investigation.

Theoretical Considerations

The development of a nonlinear elastic constitutive equation is shown in Appendix A. Before proceeding to a discussion of the experimental methods, it is appropriate to review briefly the salient features of the nonlinear theory, with an emphasis on the methods for determining the material functions.

The incremental constitutive law as derived in Appendix A is:

$$\epsilon_{ij} + \epsilon_{ij}' = G_{ij}(\sigma_{mn}) + B_{ijkl}\,\sigma_{kl}' \tag{1}$$

in which ϵ_{ij}' and σ_{kl}' are small increments in strain and stress, respectively, applied at the reference state ϵ_{ij}, σ_{mn}; B_{ijkl} is a coefficient matrix (incremental modulus tensor) that depends on the reference stress-strain state; G_{ij} is a coefficient matrix relating the reference state of strain and stress.

Under triaxial test conditions the relation between the incremental stresses and strains can be represented as:

$$\begin{Bmatrix} \epsilon_{rr}' \\ \epsilon_{\theta\theta}' \\ \epsilon_{zz}' \end{Bmatrix} = \begin{bmatrix} B_{11} & B_{12} & B_{13} \\ B_{21} & B_{22} & B_{23} \\ B_{31} & B_{32} & B_{33} \end{bmatrix} \begin{Bmatrix} \sigma_{rr}' \\ \sigma_{\theta\theta}' \\ \sigma_{zz}' \end{Bmatrix} \tag{2}$$

In a triaxial test $\sigma_{rr}' = \sigma_{\theta\theta}'$, and under conditions of isotropy or transverse isotropy $\epsilon_{rr}' = \epsilon_{\theta\theta}'$. Therefore, under the special stress conditions of a triaxial test

$$\begin{Bmatrix} \epsilon_{rr}' \\ \epsilon_{zz}' \end{Bmatrix} = \begin{bmatrix} B_{11} + B_{12} & B_{13} \\ B_{31} + B_{32} & B_{33} \end{bmatrix} \begin{Bmatrix} \sigma_{rr}' \\ \sigma_{zz}' \end{Bmatrix} \tag{3}$$

It is not possible to represent graphically the variation of strain with stress for the general axisymmetric stress-strain state. However, for the triaxial test where two of the principal stresses are equal, it is possible to plot the variation of one principal strain as a function of the stress state. Figure 26 shows a schematic representation of the axial strain as a function of the stress state in a triaxial test. Note that the variation of one component of strain with the stress state is represented by a surface. When a test is conducted at a constant lateral pressure, the stress-strain surface is intersected by a plane perpendicular to the $\sigma_{zz} - \sigma_{rr}$ plane and parallel to the σ_{zz} axis. The resulting line of intersection as represented by I'I' is the two-dimensional stress-strain plot generally used to represent stress-strain data. A similar curve J'J' is obtained for the test at constant axial stress. The restrictive nature of this plot, in that it repre-

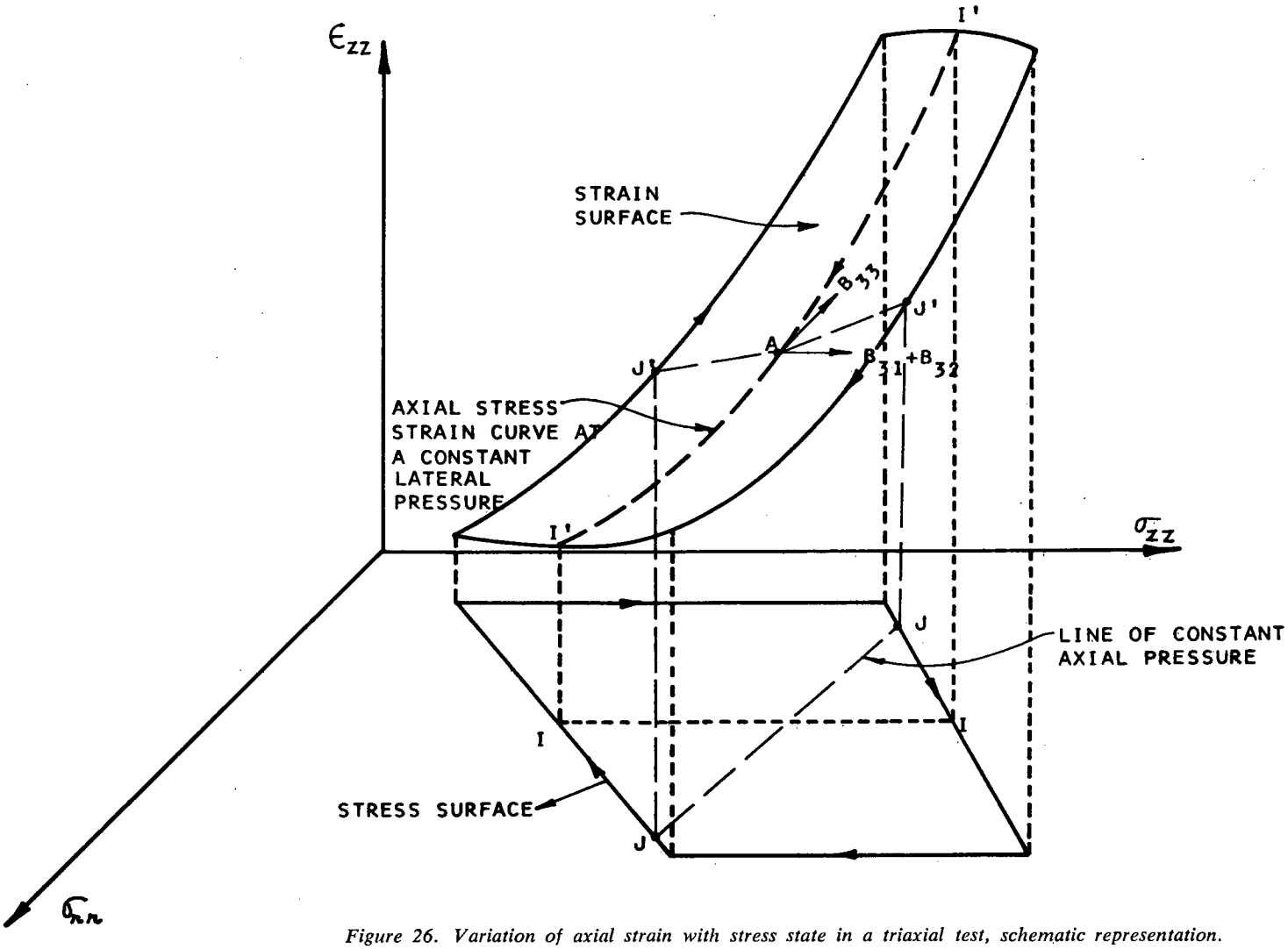

Figure 26. Variation of axial strain with stress state in a triaxial test, schematic representation.

sents only one aspect of the stress-strain variation, is evident from this discussion.

For each reference stress state, there is a corresponding reference axial strain; these are various points (e.g., Point A) on the surface in Figure 26. The coefficient B_{33} represents the slope of the surface in the direction that represents a variation in σ_{zz}; $(B_{31} + B_{32})$ represents the slope of the surface in the direction of a variation in σ_{rr}. These slopes vary with location on the surface; this is the graphical meaning of the incremental coefficients depending on the reference stress state.

A figure analogous to Figure 26 would represent a surface for ϵ_{rr} or $\epsilon_{\theta\theta}$ as a function of the stress state; the geometrical interpretation of $(B_{11} + B_{12})$ and B_{13} is similar to that given for B_{33} and $(B_{31} + B_{32})$. If one uses a two-dimensional plot, the data from a triaxial test can be represented by sets of four curves. Two of the curves represent the variation of axial strain (e.g., I'I' and J'J') and two the variation of radial strain.

A number of approaches may be taken to determine the incremental coefficients, which implies determining the slope of surface at various points. One approach is to apply increments of stress that can be considered small enough to determine the slope with sufficient accuracy. The method of computing the coefficients follows. If an incremental stress σ_{zz}' is applied with σ_{rr} constant (i.e., $\sigma_{rr}' = 0$) and ϵ_{rr}' and ϵ_{zz}' measured, the incremental stress-strain relations can be written:

$$\epsilon_{rr}' = B_{13}\,\sigma_{zz}' \tag{4}$$

$$\epsilon_{zz}' = B_{33}\,\sigma_{zz}' \tag{5}$$

From these B_{13} and B_{33} can be determined. Under the special conditions of a triaxial test $B_{13} = B_{23}$; and, from symmetry considerations, B_{31} and B_{32} would also be known.

If an incremental stress σ_{rr}' is applied with $\sigma_{zz}' = 0$ and ϵ_{rr}' and ϵ_{zz}' measured, the incremental stress-strain relations can be written:

$$\epsilon_{rr}' = B_{11}\,\sigma_{rr}' + B_{12}\,\sigma_{rr}' = (B_{11} + B_{12})\,\sigma_{rr}' \tag{6}$$

$$\epsilon_{zz}' = B_{31}\,\sigma_{rr}' + B_{32}\,\sigma_{rr}' = (B_{31} + B_{32})\,\sigma_{rr}' \tag{7}$$

The smaller the size of the increment, the more accurate the incremental coefficients at a particular reference state. However, this would require characterization at a larger number of reference states.

An alternate approach is to use a larger stress increment

at each reference state, fit the stress-strain data by a suitable analytical expression (e.g., a polynomial), and determine the slope of the curve (incremental coefficients) at various points by differentiation.

Another approach is suggested by the nature of the loading in the problem under consideration. In the subgrade there is initial stress that depends on the weight of material above it. Owing to traffic, an additional stress that is of the same order of magnitude is applied. Therefore, one can consider the reference stress state and an excursion of stress about this state as discussed in the approach outlined previously. However, for the asphaltic concrete the initial stresses are negligible compared to the stresses induced due to the traffic. Furthermore, applying a sustained stress to represent a reference state results in creep deformation that complicates the response under a repeated load. Note that this continuing deformation under a sustained load is not occurring in the field for the phase of the problem that is being modeled in this study. This suggests that in the triaxial test the axial and the radial stress should be cycled simultaneously from an initially unstressed condition. To determine the incremental coefficients, the level of one of the cycled stresses would be kept constant when the other is varied. For example, if the axial stress were kept constant this would give various points along the curve J'J', whereas if the radial stresses were kept constant various points on the curve I'I' would be obtained. In this procedure the reference state is obtained at various points on the stress-strain surface. If enough of these points are obtained, the stress-strain data can be fitted by analytical expressions and differentiated to determine the incremental coefficients at various points.

It is important to recognize that instead of the incremental formulation, suitable polynomial representations of the stress-strain data can be used (see Appendix A). The choice of the actual nonlinear representation is determined by experimental data and the solution techniques for nonlinear problems.

The experimental data show that temperature significantly influences the response of asphaltic concrete. Consequently, the ability to test the asphaltic concrete is a requirement in the design of the equipment. For the subgrade soil it is necessary to test the soil over a variety of moisture contents.

Because the nonlinear constitutive equation is suggested as a model to predict the response of the asphaltic concrete and subgrade soil in a pavement system under a single application of load after an initial "conditioning" period, it is necessary to incorporate into the test procedure a conditioning sequence of loads. The loading history that the pavement is subject to in the field is random. To account for the conditioning, it was decided to use a small number (about 1,000) of repetitions of a stress level that approximated the maximum stress level under service conditions. It was believed that in any conditioning process the effect of the maximum stress would predominate. The number of repetitions for conditioning was governed by the requirement that the resilient response of the sample remain unaltered with further repetitions. Therefore, the equipment and the test procedures must include methods for applying repeated axial and radial stresses and have techniques for measuring the axial and radial strain. In addition, it is necessary to prepare subgrade samples at representative moisture and density conditions and to provide temperature control facilities for testing the asphaltic concrete.

Equipment Design

In developing laboratory equipment for characterizing materials, the governing requirement is the desirability of testing the material to loading and environmental conditions that accurately represent the conditions that exist in a pavement system. In addition, there should be provisions for measuring those aspects of material response that are necessary for characterizing the material in accordance with the assumed mathematical model.

If it is assumed that moisture effects are taken into account in the preparation of the sample, then the two factors that must be considered in the design of the equipment are the loading and temperature conditions. In general, an element in a pavement system can be subject to an arbitrary combination of normal and shear stresses. Depending on the nature of the traffic, these stresses may vary with time. An apparatus designed to include general stress conditions should have the capability of applying arbitrary normal stresses * and also permit the application of shear stresses in the presence of these normal stresses. Furthermore, it should be possible to vary these stresses with time. When this project was begun (1969), there was no equipment capable of fulfilling all these requirements. In formulating the requirements for the apparatus it was necessary to consider the limitations imposed by the state of the art in experimental techniques, the importance of the various factors from a design standpoint, and available project time and funds. A first approximation was to limit the loading conditions to a periodic variation with a single waveform. Furthermore, because a triaxial cell was used it was not possible to consider independent control of the principal stresses or the application of shear stresses. In spite of these limitations, modifications were made in the conventional triaxial testing apparatus which represent a significant improvement over currently used testing techniques in characterizing pavement materials. (The apparatus is shown in Figs. 27 and 28.) These modifications and other features of the triaxial apparatus used in this program are discussed in the following.

Loading Conditions

Independent Control of Axial and Radial Stresses

The triaxial apparatus used in this study differs from the conventional apparatus in that the axial and radial stresses may be applied independently to the specimen. Effects of the cell pressure on the axial stress were eliminated by making the effective area of the axial loading plunger the same as that of the specimen, and attaching the cap at the other end of the specimen rigidly to the cell. The sets of double-acting pistons of different sizes were used to permit the application of a wide range of both tensile and com-

* This implies independent control of the three normal stresses.

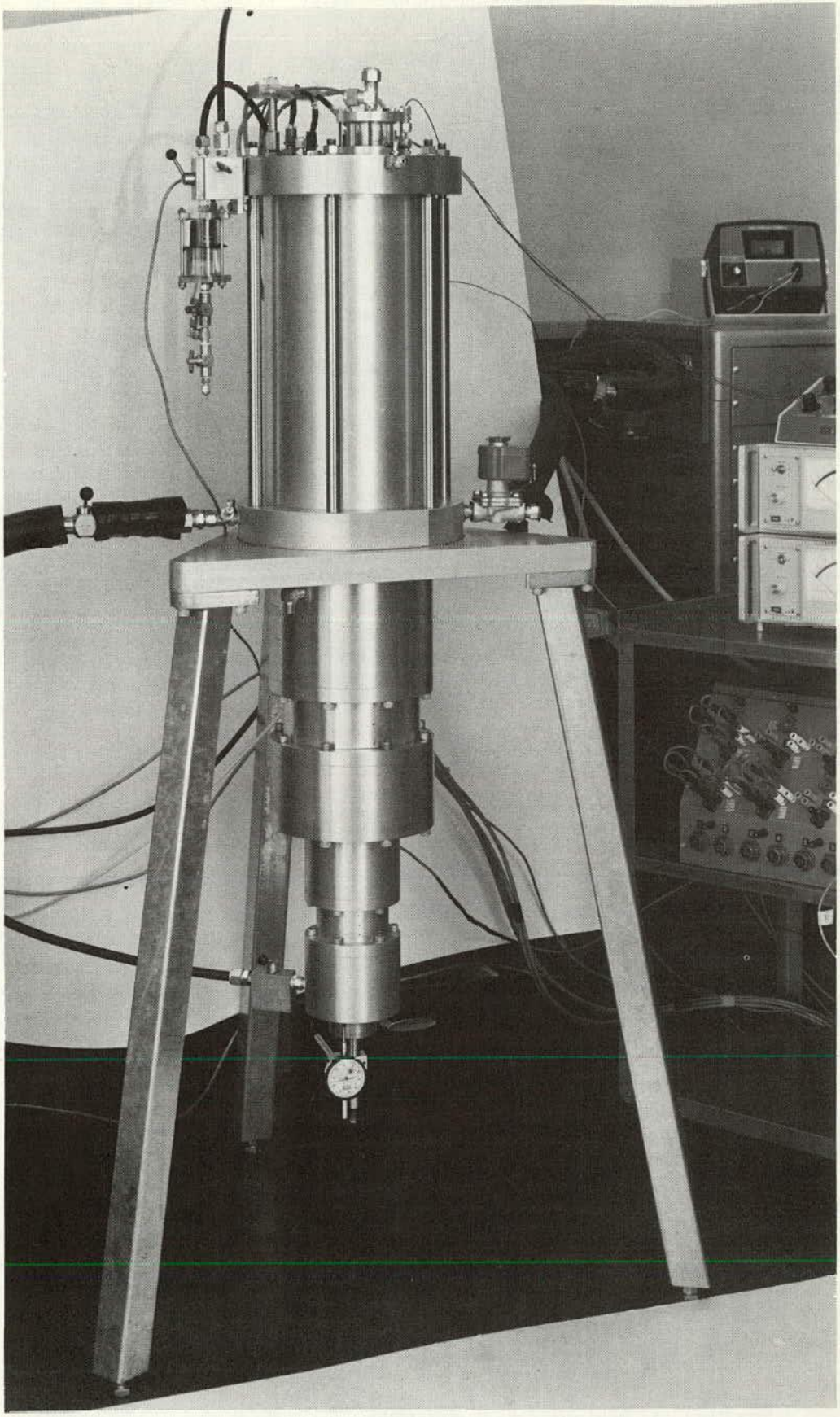

Figure 27. Triaxial apparatus permitting independent variation of axial and radial stresses.

pressive axial stresses to the specimen. These pistons were combined with the cell and located beneath the cell for convenience. A load cell attached to the top of the specimen and fastened to the cell was used to monitor the axial load applied to the specimen.

To apply axial tensile stresses, asphaltic concrete specimens were bonded to the end caps with an epoxy resin (Minnesota Mining and Manufacturing Co. 2158B/A). Because the top end cap had to be screwed to the load cell and the bottom end cap had to be screwed to the loading plunger, it was necessary that the end caps attached to the specimen be parallel to each other. A special device (Figs. 29 and 30) was used for this purpose. In order to apply and release the radial stresses as rapidly as the axial stresses, it was necessary to fill the cell with relatively incompressible fluid. Dow Corning 200 electronic fluid, which has good dielectric properties, a low viscosity (5 centistokes at 25°C), and no effect on the linear variable differential transformers (LVDT) immersed in it, was suitable for this purpose. The air pressure was applied to the oil through a bellofram (Fig. 28) to avoid splashing when the pressure was applied rapidly.

In terms of principal stresses, the domain of the stress conditions that can occur in a pavement system is the three-dimensional space defined by the principal stresses, as shown in Figure 31A. To test over this entire range of stress conditions, it would be necessary to control the three principal stresses independently. In a triaxial test the radial and circumferential stresses are equal; therefore, the possible stress states are confined to the two-dimensional space shown in Figure 31B. In the conventional triaxial test all the stresses are compressive, and axial stress is always greater than or equal to the radial stress. The range of stress states that can be applied to a specimen is shown in Figure 31C. Because of the independent control of radial and axial stress and the ability to apply axial tensile stresses, the range of stress conditions that can be studied with the apparatus used in this study is shown in Figure 31D. A

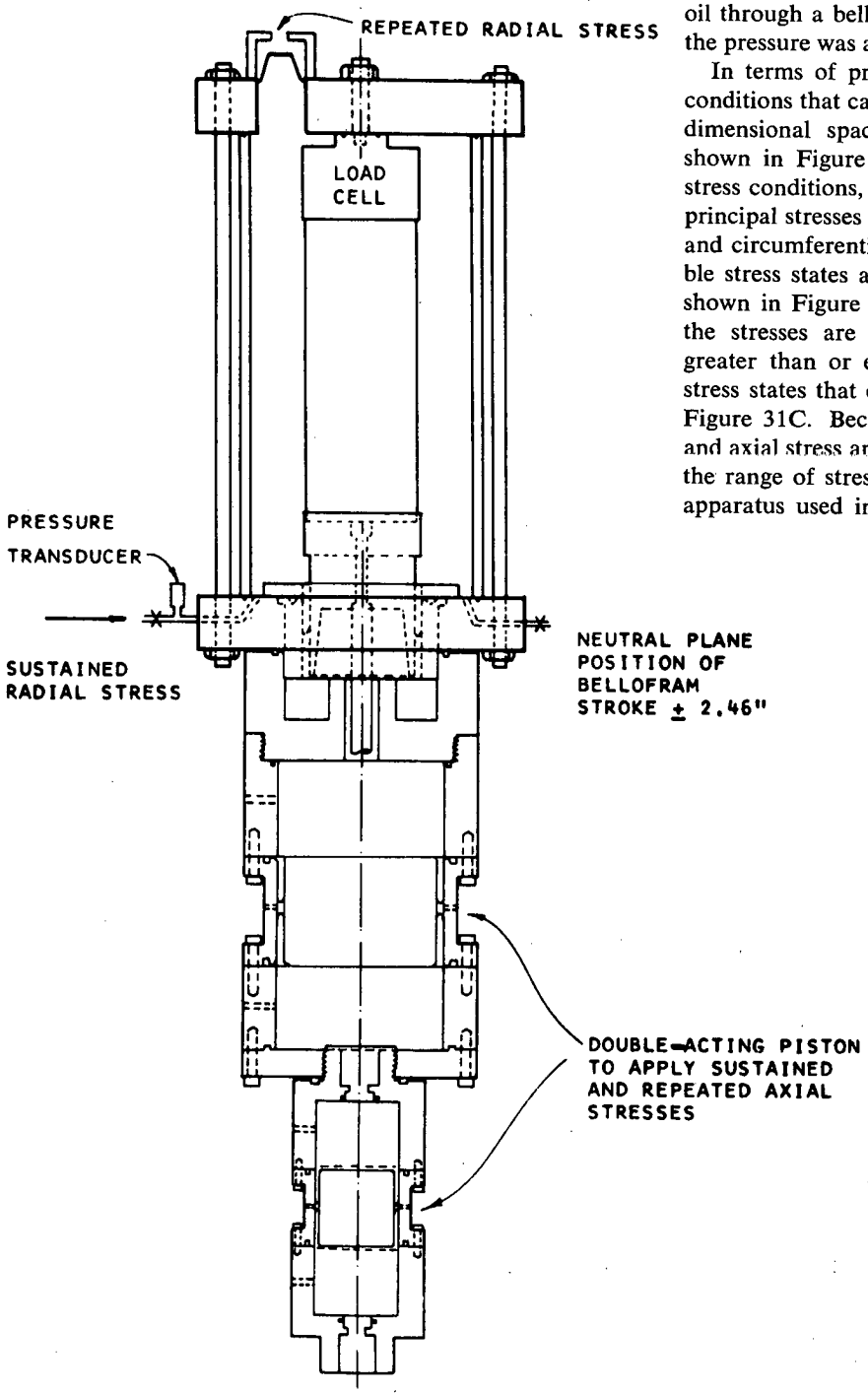

Figure 28. Triaxial apparatus permitting independent variation of axial and radial stresses.

comparison of Figures 31C and 31D shows that a significant increase in the stress states can be obtained with the apparatus developed for this study. A comparison of Figures 31A and 31D indicates the necessity of developing general three-dimensional testing techniques.

Pneumatic Repeated Stress Application System

The pneumatic system for applying the repeated stresses is similar in principle to that developed by Seed and Fead (1959). A sustained axial stress can be applied to the specimen by one of the loading pistons. The other piston was used to apply the pulsating stress. For this piston, a three-way normally open solenoid (WABCO super spool) was connected in the air line and actuated by a microswitch for 0.1 sec at 3-sec intervals. The air pressure in the air line was adjusted by pressure regulators to apply a specified load to the specimen. The magnitudes of the sustained and pulsating pressures were monitored and adjusted using the load cell. A reservoir tank was placed in the lines between the regulator and the solenoid valve to allow a rapid build-up of the pulsating stress on the specimen. It was necessary to place the solenoid valve as close as possible to the loading piston to obtain a nearly rectangular stress-time waveform. A duplicate system was used to apply the pulsating pressure on the cell oil to induce the repeated radial stress. Because it was necessary to circulate the cell fluid to keep the specimen temperature constant and at the same time keep the cell fluid confined in the cell while the pulsating stress was applied, a check valve was placed in the line leading to the cell and a two-way normally open solenoid valve was placed in the line leaving the cell (Fig. 32). Figure 33 shows the typical pulsating stress-time waves for both axial and radial stresses applied to the specimen using this load system as measured by the load cell and the pressure transducer.

Temperature Control System

To test asphaltic concrete specimens at constant temperatures ranging from 40°F to 140°F, a temperature control system (Fig. 32) was designed. The major units of the system were a mixing chamber, a heating unit, a refrigeration unit, and a turbine pump. The refrigeration unit circulated the refrigerated coolant at constant temperature through a series of coils installed in the mixing chamber. The heater immersed in the mixing chamber was connected to a temperature-power controller (Thermac Series 6000, Model 6-5), by which a desired fluid temperature was adjusted and maintained automatically. The fluid in the mixing chamber was thoroughly mixed by an air motor to obtain uniform temperature; then it was pumped to circulate around the specimen in the triaxial cell by the turbine pump. Because of the heat loss or gain during the circulation of the fluid through the triaxial cell, the fluid temperature in the triaxial cell may not be the same as that in the mixing chamber. Therefore, the temperature in the cell was monitored by a thermocouple that was connected to a digital thermometer. The temperature was adjusted through the temperature-power controller. It was found that the fluid temperature in the triaxial cell could be maintained within ±0.5°F of the desired temperature during testing.

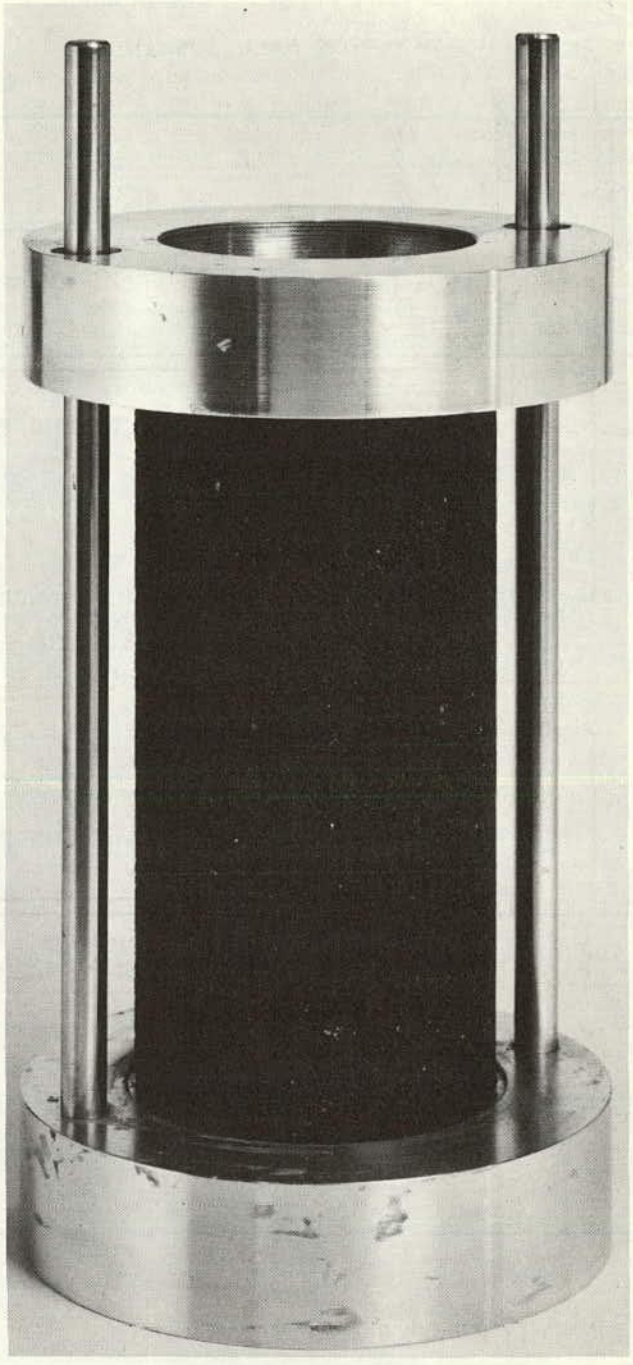

Figure 29. Device to ensure end caps are parallel.

Because it was the fluid temperature that was being monitored, it was necessary that the sample be at the same temperature as the surrounding fluid. Consequently, the sample had to be at the desired temperature prior to testing. The time required for a 4-in.-diameter asphaltic concrete specimen surrounded by a 0.013-in.-thick membrane to reach a desired temperature was investigated; the results are shown in Figures 34 and 35. Two thermocouples were inserted in the specimen—one near the surface and the

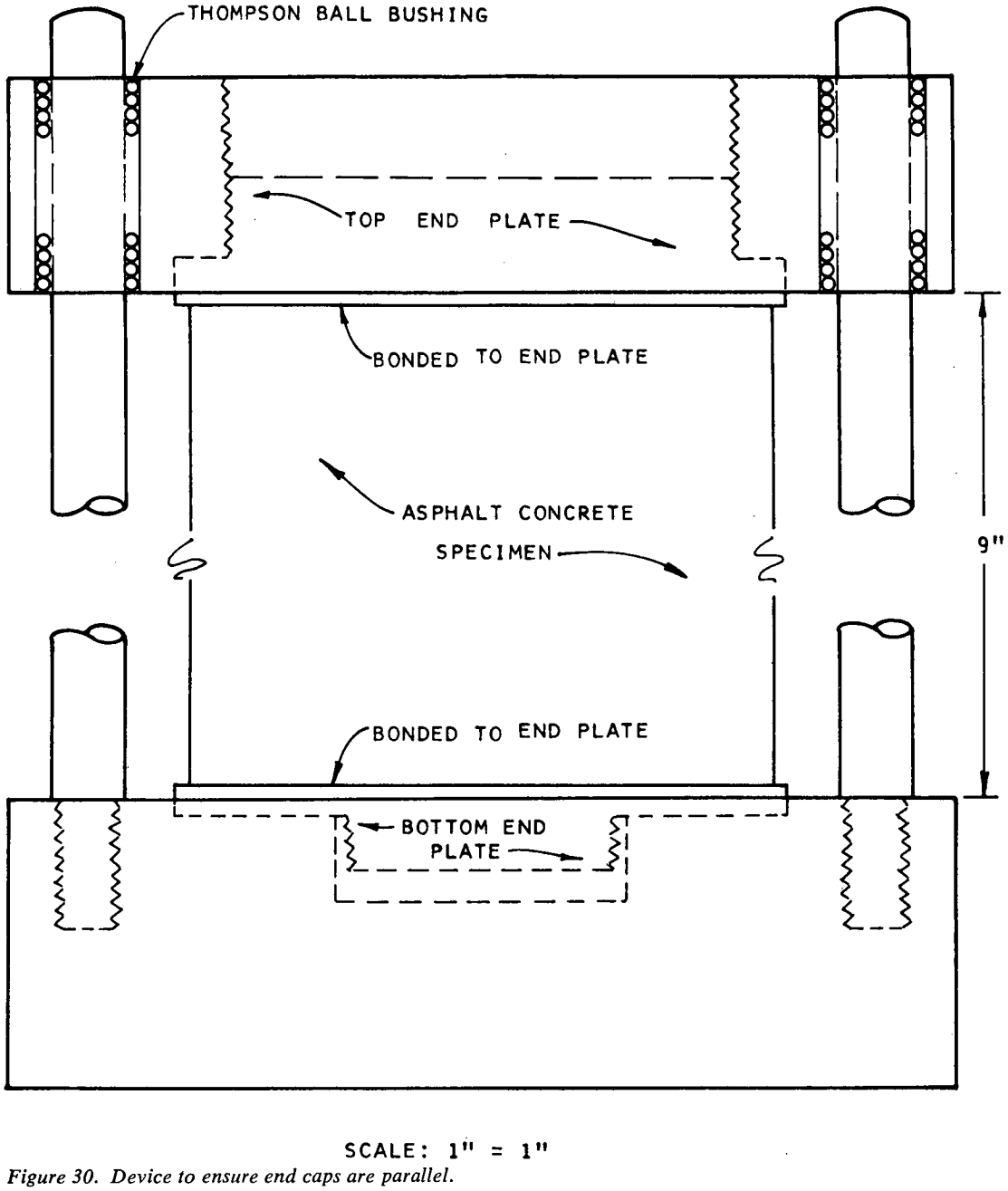

Figure 30. Device to ensure end caps are parallel.

other at the center of the specimen. The test results indicate that about 150 min were required for the specimen to reach 140°F, and about 210 min were required for the specimen to reach 40°F. For convenience, all the asphaltic concrete specimens tested were kept overnight, surrounded by circulating cell fluid at the specified temperatures, before being tested.

Measurement Techniques

Axial strain in the asphaltic concrete specimens was measured with a pair of A-9-4 wire resistance strain gauges bonded to the specimen near midheight with EPY 150 cement. This technique has been used with success by others (Terrel, 1967; and Dehlen, 1969). These gauges have an active length of 2½ in. and were selected so as to be long enough to indicate accurately the mean strain in the mixture (maximum size of aggregate ½ in.), but not so long as to be influenced by the decreased strains near the specimen ends resulting from the rigid bonding to the end caps. Dehlen (1969) indicated that in 6- or 8-in.-high specimens the underestimate of resilient strain due to the bonded end caps probably would not exceed 2 percent. Two dummy strain gauges were used to complete the wheatstone bridge. The potential difference in the bridge occurring due to straining during testing was amplified by a transducer amplifier (Daytronic 300D) and recorded

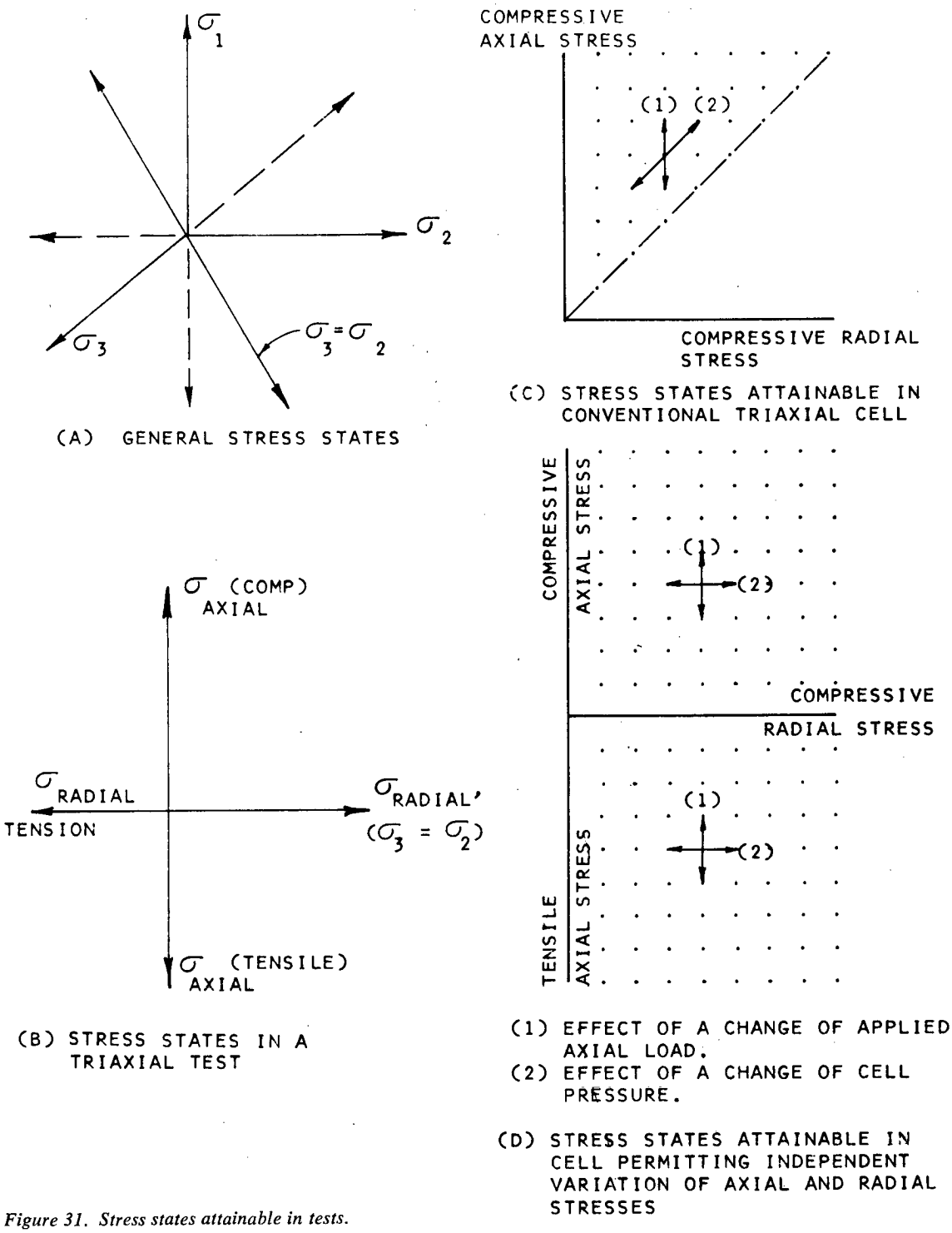

Figure 31. Stress states attainable in tests.

using 18-channel recorder (CEC Oscillograph), as were the outputs from the LVDT's, load cell, and pressure transducer described elsewhere. Strains of less than 10 μin./in. were difficult to measure using this type of recorder. Smaller strains may be measured with less-sensitive galvanometers or other types of recorders.

In the case of unbound or weakly bound materials (such as cohesive subgrade, granular materials, and lime-stabilized soils), bonded strain gauges cannot be used, and axial strains may be computed from measurements of the relative displacements of the loading plates, or, more specifically, from the movement of the loading plunger relative to the cell top. This procedure may be acceptable in the case of soft materials. In measuring the resilient properties

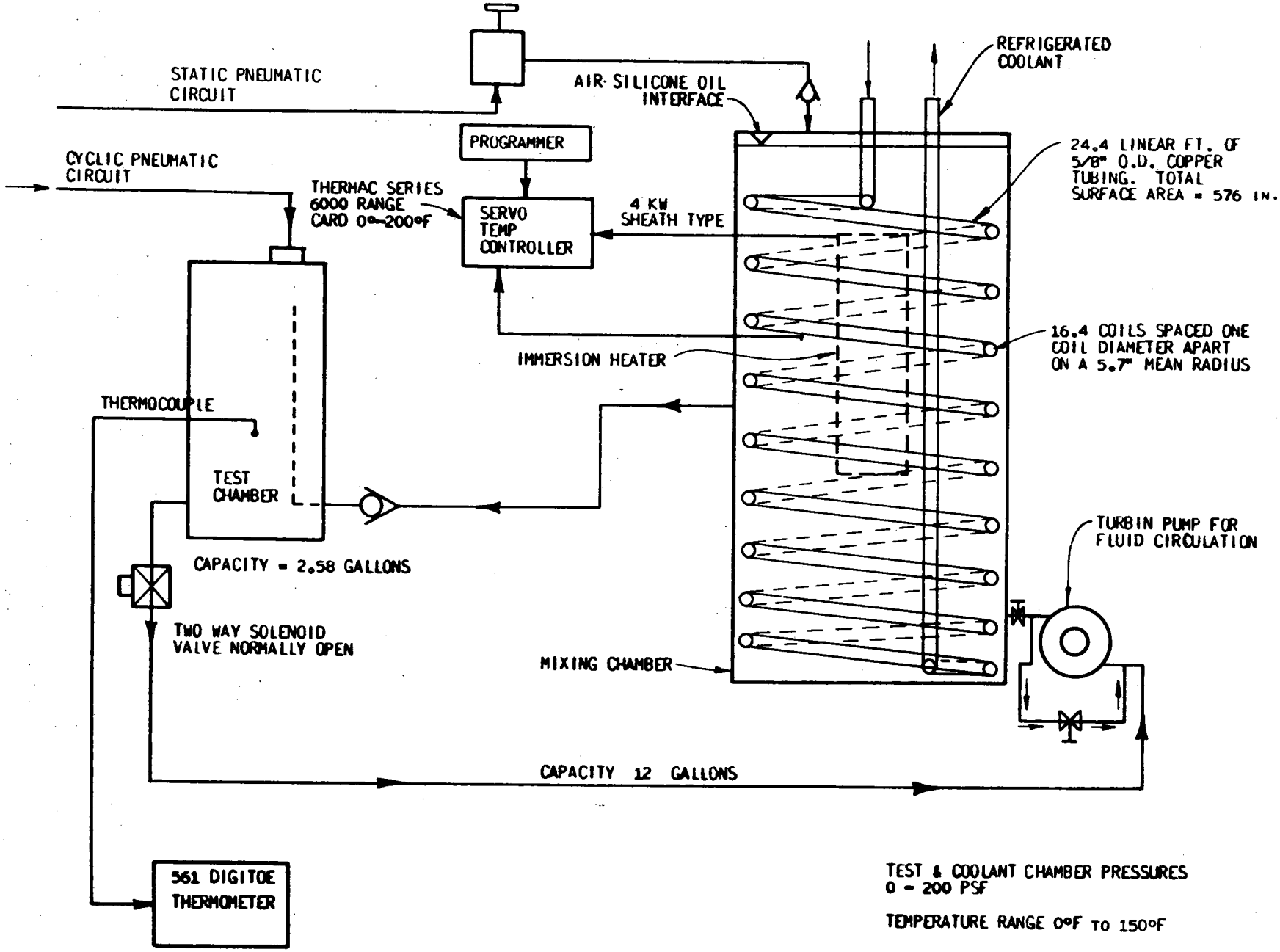

Figure 32. Temperature control system for testing asphaltic concrete specimens.

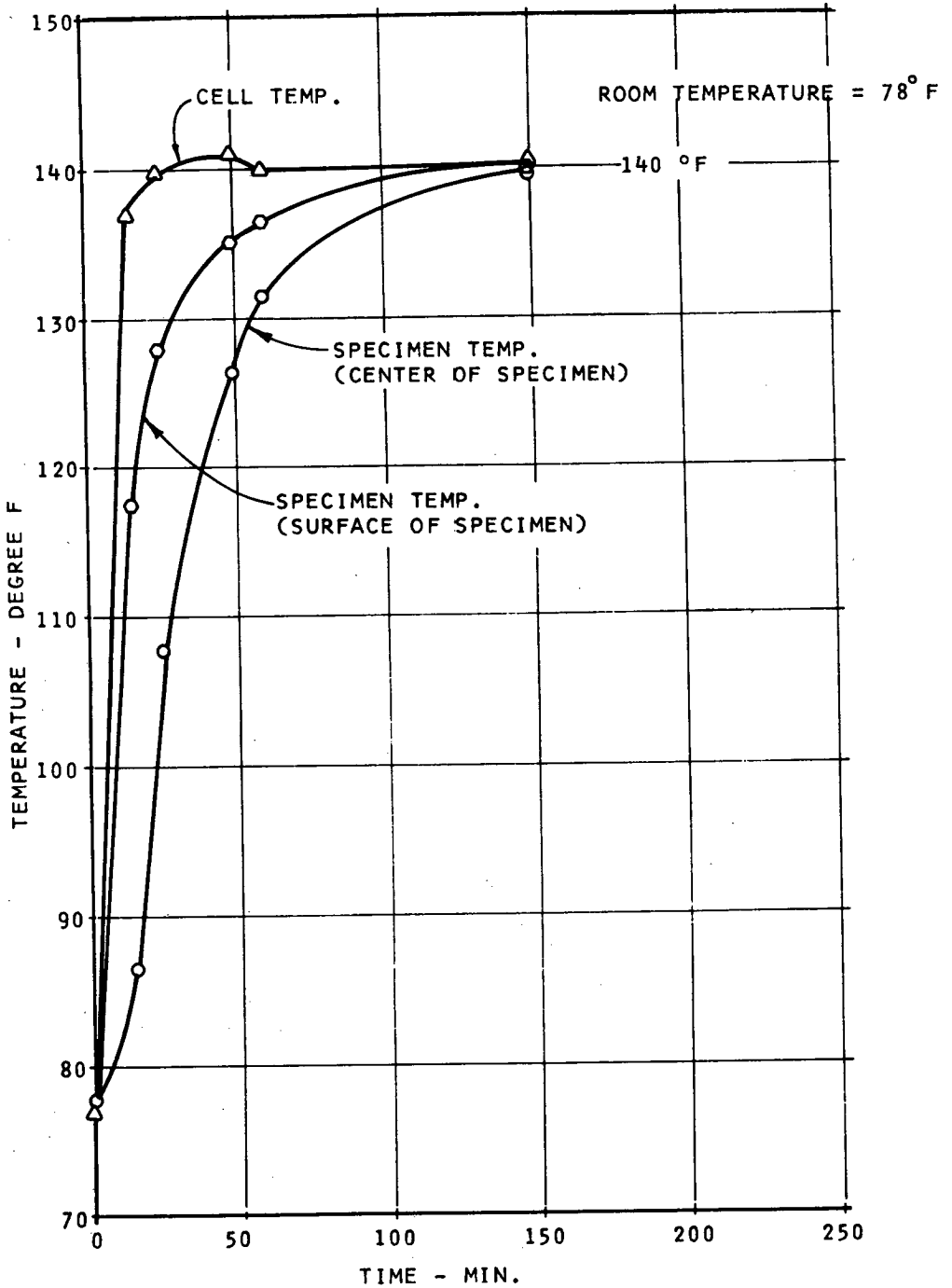

Figure 34. Variation of specimen temperature and cell temperature with time for 4-in.-diameter specimen of asphaltic concrete with one 0.013-in.-thick membrane (desired temperature, 140°F).

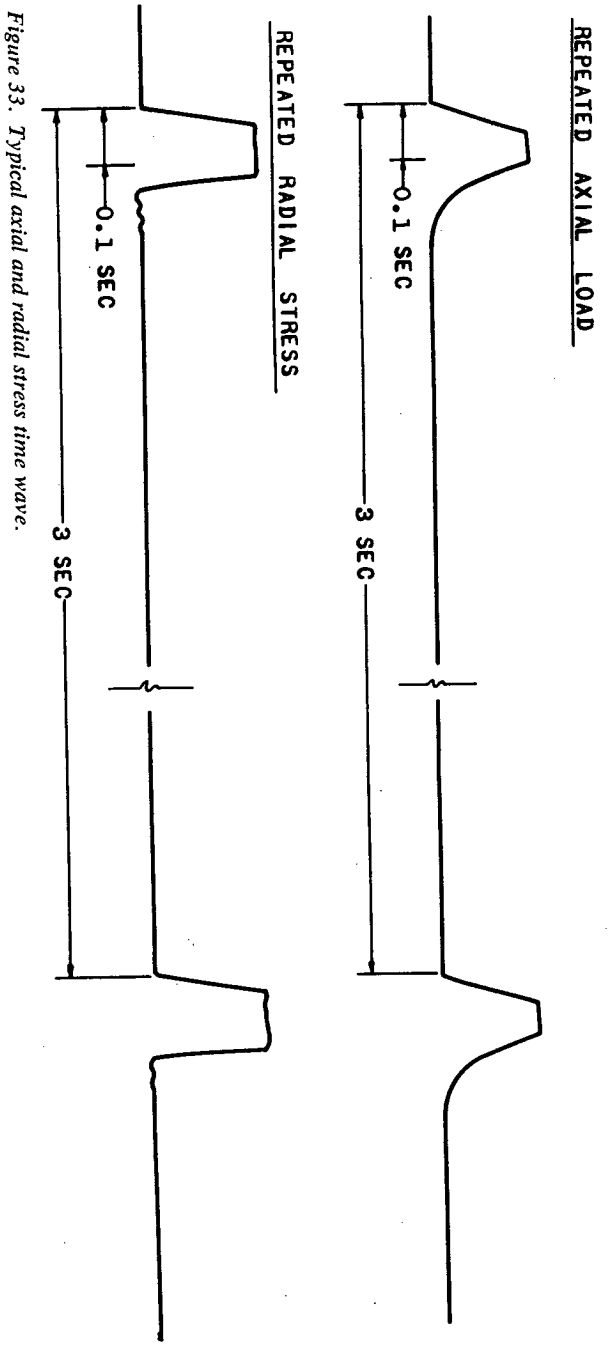

Figure 33. Typical axial and radial stress time wave.

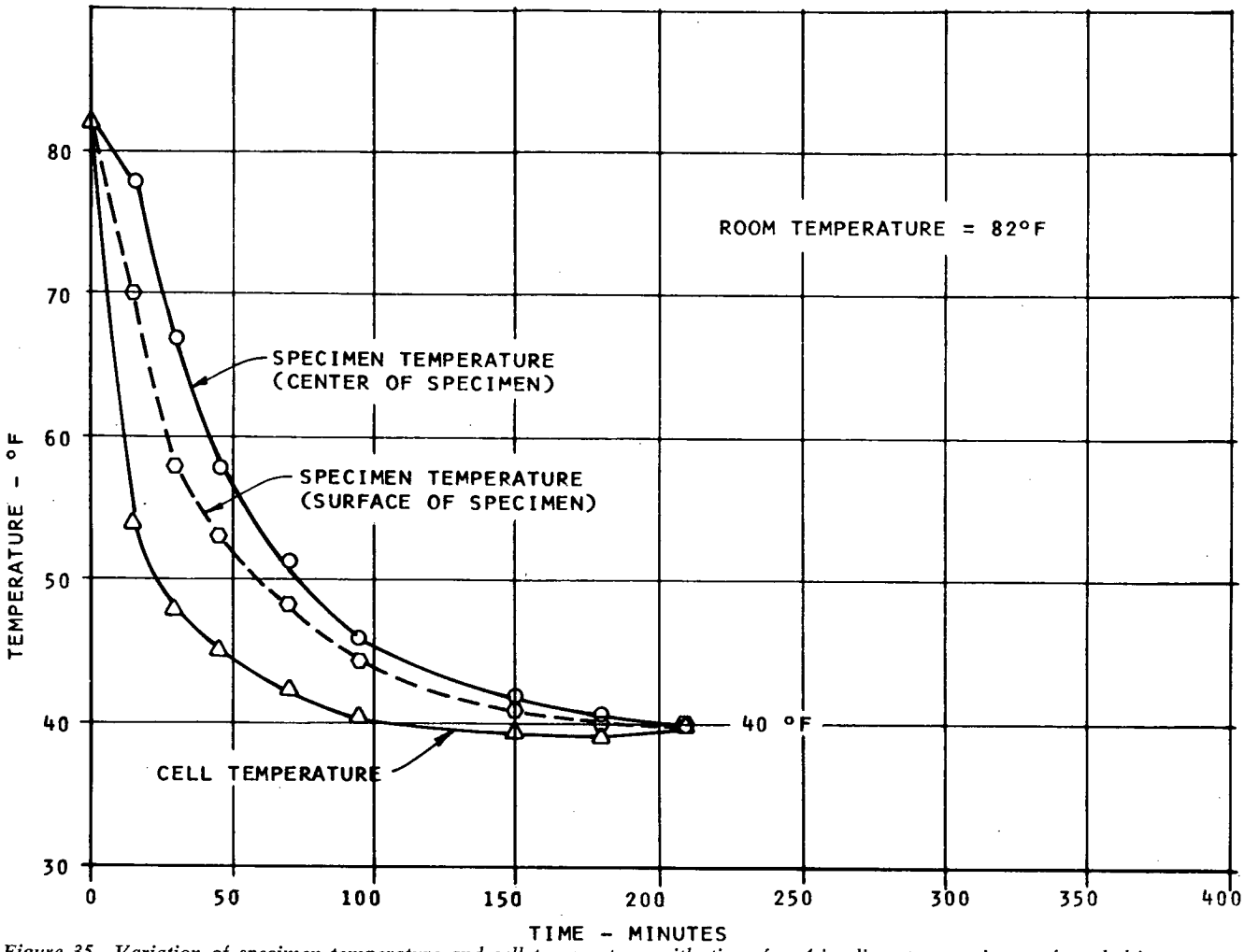

Figure 35. Variation of specimen temperature and cell temperature with time for 4-in.-diameter specimen of asphaltic concrete with one 0.013-in.-thick membrane (desired temperature, 40°F).

of stiffer materials, however, errors due to poor contacts between the loading plunger and the sample cap, and between the sample and the end caps can be of the same order as the strains occurring in the sample. To eliminate this source of error the following system was used. Two circular clamps were placed around the specimen, equidistant from the ends and 3.3 in. apart. Their relative displacements were measured by a pair of small matched LVDT's (Daytronic 103C-200) and the axial strains were computed as a ratio of the relative displacement to the 3.3-in. gauge length. To permit lateral strain to occur, the clamps were held to the sample by light springs.

It may be assumed that the radial strains equal the circumferential strains under cylindrical states of stress (this condition is satisfied under the more restrictive assumption of isotropy). The circumferential strains in the asphaltic concrete specimens were measured with a pair of A-9-4 strain gauges bonded to the specimen at midheight, with their long sides horizontal.

Measurement of radial strains in clay and granular materials is difficult. In this investigation, diametric strain was measured by adding horizontal LVDT's to the sprung extensometer clamps. This technique did not prove entirely satisfactory for the measurement of radial strains of soft materials at low stresses. When the applied stresses are low, the springs used to hold the clamps onto the specimen would apply some pressures that, in turn, prevented the specimen from moving out laterally; i.e., the radial strain is underestimated in tension. Dehlen (1969) pointed out that inaccuracies could result from compression in the rubber membrane when testing stiffer cohesive subgrade specimens. A more accurate technique should be developed to measure radial strains for soils.

Test Procedures

The importance of simulating service conditions such as the nature and type of loading, and environmental and construction variables, in the characterization of paving materials is pointed out elsewhere. In the preliminary model selected for this study no attempt was made to include the environmental factors (e.g., temperature and moisture) in the constitutive equation. However, the effects of these factors on material behavior are taken into account by testing over a range of temperatures and moisture contents

likely to exist in the actual pavement system. The basis for establishing the test procedures is the theoretical considerations discussed earlier and the capabilities of the equipment.

Asphaltic Concrete

A certain initial "conditioning" is necessary to bring the sample to a state that is representative of the state in which it is likely to be in situ.

After conditioning, a limited number of repeated axial and radial stresses must be applied to the specimen to represent the traffic-induced stresses. Because the gravity stresses in the asphaltic concrete surfacing are very small compared to the traffic-induced stresses, they are neglected and cycled from zero stresses (Fig. 36). Both axial and radial stresses were cycled simultaneously because creep prohibited the application of sustained stresses to asphaltic concrete. The resilient axial and radial strains were recorded for 50 repetitions. The waveform duration and magnitude of each stress represent the stress that will be induced in the asphaltic concrete on the passage of a moving wheel load. This process was continued until all desired combinations of stress to cover the range of stress states and stress levels expected in the field had been applied. The testing procedures necessary to characterize an asphaltic concrete are:

1. Select the range of temperature likely to exist in the pavement.
2. With appropriate resilient properties of the materials in the pavement system, conduct a preliminary structural analysis of the pavement under designed traffic loads to determine the range of the stress states and the stress levels likely to occur in the asphaltic concrete layer at various temperatures. To do this it may be necessary to conduct some preliminary tests to estimate the properties of the materials.
3. Compact specimens at the desired air voids, type, and gradation of aggregate, type of asphalt cement, and asphalt content expected to be used in the actual pavement, or obtain undisturbed samples from the in-service pavement.
4. Design a series of possible combinations of vertical and radial stresses in accordance with the calculated range of stress states and stress levels.
5. Condition the specimen under 1,000 applications of the maximum vertical and radial stresses to which it is likely to be subject in service.
6. Based on step (4), subject the specimen to a combination of repeated axial and radial stresses. The resilient axial and radial strains should be recorded for 50 repetitions. This process is continued until all combinations of axial and radial stresses are applied.
7. Repeat steps (5) and (6) at various temperatures.

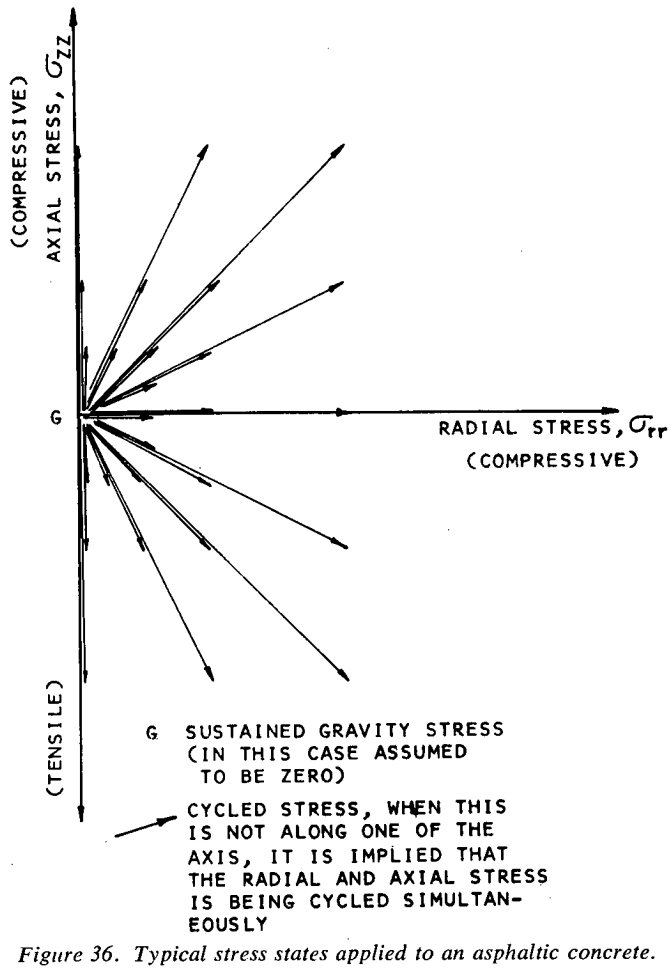

Figure 36. Typical stress states applied to an asphaltic concrete.

Cohesive Subgrade Soils

Effects of temperatures in nonfrost areas on resilient properties of cohesive subgrade soils are not considered significant. However, moisture content is believed to have considerable influence on the behavior of the cohesive subgrade soils. Therefore, it is necessary to determine the range of moisture contents that may exist in the subgrade under expected service conditions. The resilient properties of compacted clays as reported by Seed et al. (1962) may change drastically during initial loading as a result of thixotropic effects. However, these effects will diminish at a large number of stress applications. To represent the in-service conditions, a number of repetitions of the maximum stress the sample would have been subjected to by traffic should be applied to the specimen so that the relatively rapid changes in resilient response occurring during initial loadings may be avoided. Studies made by Dehlen (1969) suggested that, provided the material conditions and stresses are representative of those that would be found in a well-designed pavement, for cohesive subgrade soils the resilient response determined after 50 or 100 repetitions will be a reasonable indication of that for a material subjected to the complex stress history pertaining to a pavement. Dehlen also found that the responses to stresses of different intensities can be measured on a single sample in any sequence, provided only 50 or 100 repetitions are applied at each stress level. The testing procedures for characterizing a cohesive subgrade soil are:

1. Estimate the range of moisture contents and densities likely to exist in the subgrade under the expected service conditions.

2. Determine the range of stress states and stress levels likely to occur in the subgrade due to traffic loads from a preliminary structural analysis of the pavement system. To conduct the preliminary analysis, it is necessary to obtain various material properties. A few preliminary tests may have to be conducted to obtain this information.

3. Based on the results of the analysis, a range of stress states and stress levels is selected for testing.

4. Compact specimens at various moisture contents and densities with an appropriate compaction method to simulate field compaction, or obtain undisturbed samples for the in-service pavement for evaluation purposes.

5. Condition the specimen under 1,000 applications of the maximum vertical and radial stresses to which it would have been subjected under traffic loads. The repeated traffic stresses are applied in addition to the sustained gravity stresses.

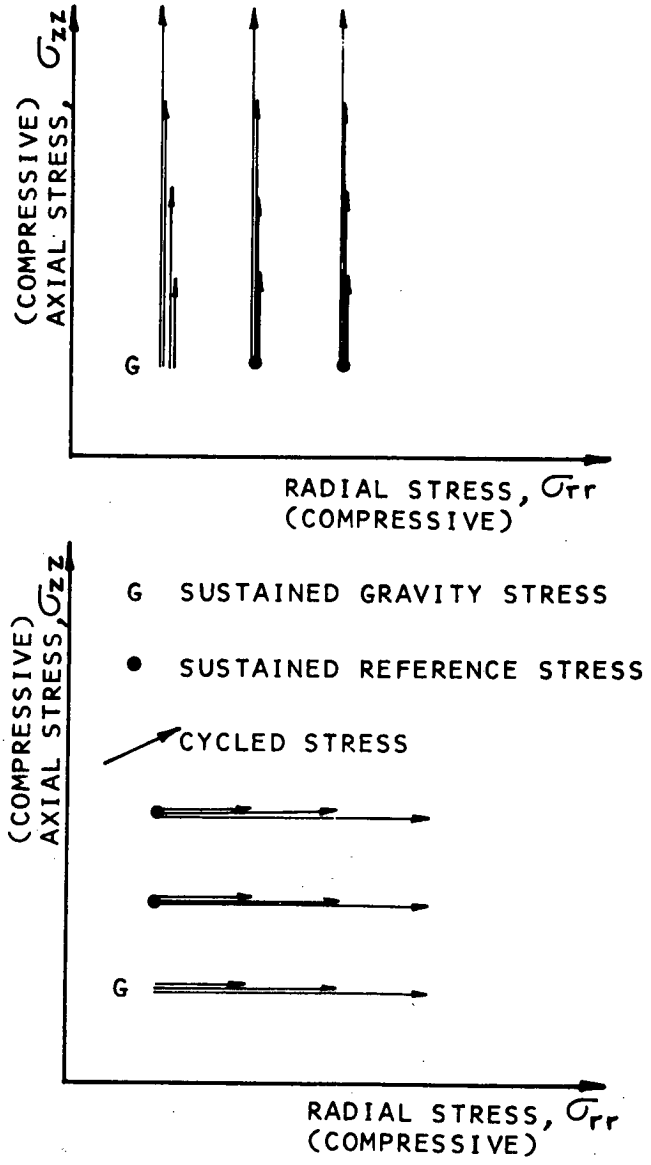

Figure 37. Typical stress states applied to a cohesive subgrade soil.

6. A sustained radial stress corresponding to one of the traffic plus gravity stress levels selected and an axial stress corresponding to the gravity stress are applied, and the axial stress is cycled between the gravity stress and one of the axial traffic stress levels. The resilient axial and radial strains are recorded for 50 cycles. The procedure is then reversed; a sustained axial stress is applied, and the radial stress is cycled between the gravity and one of the radial stress levels. The stress paths described are shown in Figure 37. This process is continued until all combinations of stress have been applied.

7. Repeat steps (5) and (6) for specimens compacted at various moisture contents.

Experimental Program

The primary purpose of the experimental program was to indicate how paving materials may be characterized in accordance with nonlinear constitutive laws. An important aspect of this is that the test program should provide information on the significance of the nonlinear effects and thus help evaluate the necessity of using nonlinear constitutive equations for characterizing paving materials. It should be noted that with nonlinear materials the characterization is dependent on the stress level; therefore, extrapolation to other stress levels generally is not possible.

Asphaltic Concrete

Aggregates and Asphalt Cement.—The aggregates used in this study are Watsonville granite from the Logan Quarry in California. This type of aggregate was selected because of its extensive use in asphaltic concrete research studies during the past 20 years. An average of two types of gradings was selected—namely, the middle of the band of the State of California ½-in. maximum-medium grading and that of ⅜-in. maximum grading, with 100 percent passing ⅜ in. (Fig. 38). An 85-100 penetration asphalt was used. An asphalt content of 6 percent was selected, on the basis of the State of California design criteria. Table 1 is a report of laboratory tests on the penetration asphalt.

Specimen Preparation.—Aggregates used in the mix were separated into the following size fractions: * ⅜ in. × #4, #4 × #8, #8 × #16, #16 × #30, #30 × #50, #50 × #100, <#100; then they were recombined to meet the desired grading specification. Mixing and compaction procedures used in preparing specimens were similar to those described by Epps (1968). The mix was compacted using a kneading compactor in a cylindrical split mold 9.5 in. long and 4 in. in diameter. All specimens were 8.5 in. long and were compacted in seven layers with 35 tamps per layer at 330 psi tamping foot pressure, followed by a leveling load of the same pressure applied at a rate of 0.25 in./min. The specimen obtained by such a pressure was fairly uniform along its length. Air void contents of the specimens compacted ranged from 3.7 to 4.5 percent, with an average of 4.1 percent. The density of the specimens was about 156 lb/cu ft.

* ⅜ in. × #4 implies size fractions between ⅜ in. and No. 4 sieve.

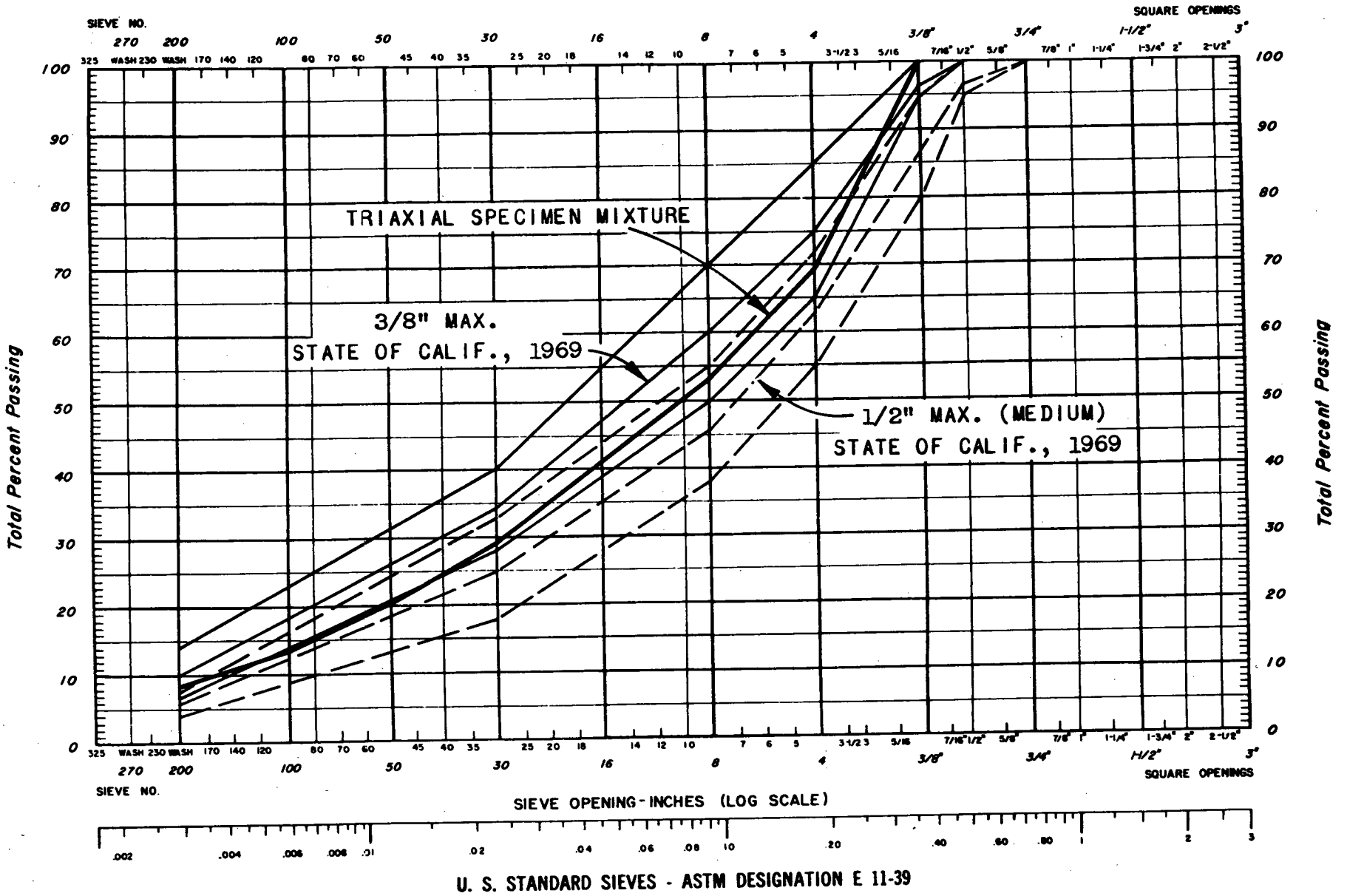

Figure 38. Grading curve, Watsonville aggregate.

TABLE 1

REPORT OF LABORATORY TESTS ON 85-100 PENETRATION ASPHALT (SUPPLIED BY CHEVRON ASPHALT CO.)

TEST	METHOD	MEASURED
Penetration at 77°F, 100g, 5 sec (dmm)	ASTM D5	92
Flash point (°F)	ASTM D93	455
Viscosity at 77°F:	Calif. 348A	
At 0.05/sec (megapoise)		0.90
At 0.001/sec (megapoise)		1.30
Viscosity at 140°F (P)	ASTM D2171	1308
Viscosity at 275°F (cs)	ASTM D2170	261
Chemical composition:	Rostler-White (*Proc. AAPT*, Vol. 31, pp. 72–79).	
Asphaltenes (%)		18.4
Nitrogen bases (%)		38.0
First acidaffins (%)		14.7
Second acidaffins (%)		11.1
$(N+A_1)/(P+A_2)$		1.82
Durability rating	*Proc. Highway Conf. on Research and Development of Quality Control and Acceptance Specifications*, U.S. BPR (Apr. 1965) p. 146; or Hoiberg, A.J., *Bituminous Materials: Asphalts, Tars, and Pitches*, Vol. II, Part One, p. 207.	V
Pellet abrasion:	*ASTM Spec. Tech. Publ. 277*, pp. 64–88; and *Proc. AAPT*, Vol. 35, pp. 123–126.	
Unaged (% loss)		18
Aged 7 days (% loss)		98
Average (0+7)/(2)(% loss)		58
Rolling thin film oven test:	Calif. 346A	
Test on residue:		
Viscosity at 140°F (P)	ASTM D2171	2529
Viscosity at 275°F (cs)	ASTM D2170	356
California durability test:	Calif. 347A	
Tests on residue:	Calif. 348A	
Viscosity at 77°F:		
At 0.05/sec (megapoise)		68
At 0.001/sec (megapoise)		175
Microductility (mm)	Calif. 349A	8

Test Temperature.—A range of test temperatures from 40°F to 140°F was selected to be typical in California. Tests were conducted at five different temperatures: 40°F, 55°F, 70°F, 100°F, and 140°F.

Stress State and Stress Level.—The stress states employed in testing the asphaltic concrete were chosen to represent a typical pavement under wheel loads with a tire pressure of 70 psi. Ranges of stress states and stress levels were selected for each test temperature to cover a range of stress levels expected under this tire pressure. The combinations of these stress states and stress levels for each test temperature have been tabulated (see Appendix D).

The conditioning stresses (the magnitudes of both vertical and radial stresses the same) were selected as 80, 60, 40, 20, and 10 psi for the test temperature of 40°F, 55°F, 70°F, 100°F, and 140°F, respectively. The repeated axial stresses selected ranged from 70 psi in compression to 70 psi in tension at both 40°F and 55°F; from 70 psi in compression to 40 psi in tension at both 70°F and 100°F; and from zero to 30 psi in compression at 140°F. The repeated radial stresses ranged from zero to 70 psi in compression at 40°F, 55°F, 70°F, and 100°F, and from zero to 30 psi in compression at 140°F.

Cohesive Subgrade Soils

The tests were conducted on laboratory-compacted specimens of a cohesive subgrade soil obtained from the San Diego Test Road site. Undisturbed samples of the same material were tested by Dehlen (1969). Moisture contents of the samples tested by Dehlen ranged from 14 to 21 percent; dry densities ranged from 121 to 107 lb/cu ft. Tests performed in this study to investigate the resilient properties of the laboratory-prepared specimens were compacted at a higher moisture content (approx. 23 percent) and lower dry densities (approx. 100 lb/cu ft). These specimens were compacted by a kneading compactor. The properties of some of these undisturbed and laboratory-prepared samples have been tabulated (see Appendix D). The results

of all these tests would provide information on the nonlinear characteristics of the cohesive subgrade soil over a wide range of moisture and density conditions.

Stress State and Stress Level.—A preliminary structural analysis was performed to determine the state of stress to which material at that depth would have been subjected by highway traffic using finite element techniques with average moduli determined in the preliminary tests. The conditioning stresses as well as a series of stress states applied to each sample have been tabulated (see Appendix D). Each sample was subjected to different stress states because the samples were taken at different depths.

CHAPTER THREE

FINDINGS

The purpose of the experimental program was to determine the coefficients in the incremental formulation of the nonlinear elastic constitutive equation. Data obtained from the tests can be used to develop other representations of a nonlinear elastic model. As in previous discussions, the results from each test are first presented as the variation of one component of the strain with one component of stress. Therefore, for each test there are four sets of curves. From these data the incremental coefficients are determined at various stress states.

It is appropriate to review briefly the incremental stress-strain relation indicating which coefficients were determined. Using a cylindrical coordinate system, the incremental stress-strain relation may be written as

$$\begin{Bmatrix} \epsilon_{rr}' \\ \epsilon_{\theta\theta}' \\ \epsilon_{zz}' \end{Bmatrix} = \begin{bmatrix} B_{11} & B_{12} & B_{13} \\ B_{21} & B_{22} & B_{23} \\ B_{31} & B_{32} & B_{33} \end{bmatrix} \begin{Bmatrix} \sigma_{rr}' \\ \sigma_{\theta\theta}' \\ \sigma_{zz}' \end{Bmatrix} \tag{8}$$

in which σ_{rr}' and ϵ_{rr}' are increments of radial stress and strain; $\sigma_{\theta\theta}'$ and $\epsilon_{\theta\theta}'$ are increments of tangential stress and strain; σ_{zz}' and ϵ_{zz}' are increments of axial stress and strain.

In addition, because a triaxial sample is subjected to an axisymmetric stress and strain state, it may further be assumed that $\epsilon_{rr}' = \epsilon_{\theta\theta}'$, and thus $\sigma_{rr}' = \sigma_{\theta\theta}'$. Eq. 8 becomes

$$\begin{Bmatrix} \epsilon_{rr}' \\ \epsilon_{zz}' \end{Bmatrix} = \begin{bmatrix} B_{11} + B_{12} & B_{13} \\ B_{31} + B_{32} & B_{33} \end{bmatrix} \begin{Bmatrix} \sigma_{rr}' \\ \sigma_{zz}' \end{Bmatrix} \tag{9}$$

Several investigators (Barden, 1963; Gerrard and Mulholland, 1966; Busching, Goetz, and Harr, 1967; and Dehlen, 1969) have suggested that highway materials as they exist in pavement structures may exhibit a simple form of anisotropy—namely, transverse isotropy, with an axis of elastic symmetry coinciding with the vertical coordinate axis. If this form of anisotropy occurs in the incremental modulus tensor, the incremental coefficients may be interrelated; $B_{11} = B_{22}$, $B_{12} = B_{21}$, $B_{31} = B_{32}$, and $B_{13} = B_{23}$. (In general, even though the material may be initially isotropic, the incremental modulus tensor is anisotropic because it depends on the reference stress state.) In a triaxial test only four quantities—namely, $(B_{11} + B_{12})$, B_{13}, $(B_{31} + B_{32})$, and B_{33}, as shown in Eq. 9—can be determined. The determination of the specific quantities B_{11}, B_{12}, B_{31}, and B_{32} depends on the assumption of symmetry or transverse isotropy. The experimental data are reduced to give these incremental coefficients and combinations of incremental coefficients.

ASPHALTIC CONCRETE

A series of repeated loading triaxial tests were performed on asphaltic concrete specimens at various temperatures ranging from 40°F to 140°F.

The major emphasis in the following discussion is on the variations of the incremental coefficients with the stress state, the stress level, and the temperature. However, it is first appropriate to comment on the observed response of the asphaltic concrete under a single application of load and on the nature of the stress-strain curves.

Response Under a Single Application of the Load

Figures 39 to 41 show typical examples of the response of the asphaltic concrete under a single load application at different temperatures. There are two important points to consider with regard to the applied stress when one is evaluating the response: (1) the form of the stress wave is not exactly square; there is a finite rise time for the load; (2) the stress waves for the axial and radial stresses are not identical; the reasons for this are discussed in Chapter Two.

When only one component of the stress is applied, the shape of the strain-time curve should be geometrically similar to the stress-time curve if the material were perfectly elastic. The results indicate that asphaltic concrete is not ideally elastic. In examining the degree of approximation involved in assuming elastic behavior it is appropriate to consider two aspects of the response: (1) the permanent deformation, and (2) the time-dependent deformation.

Not all the deformation is recovered instantaneously on removal of the load. However, very little permanent deformation remains when the next repetition of load is

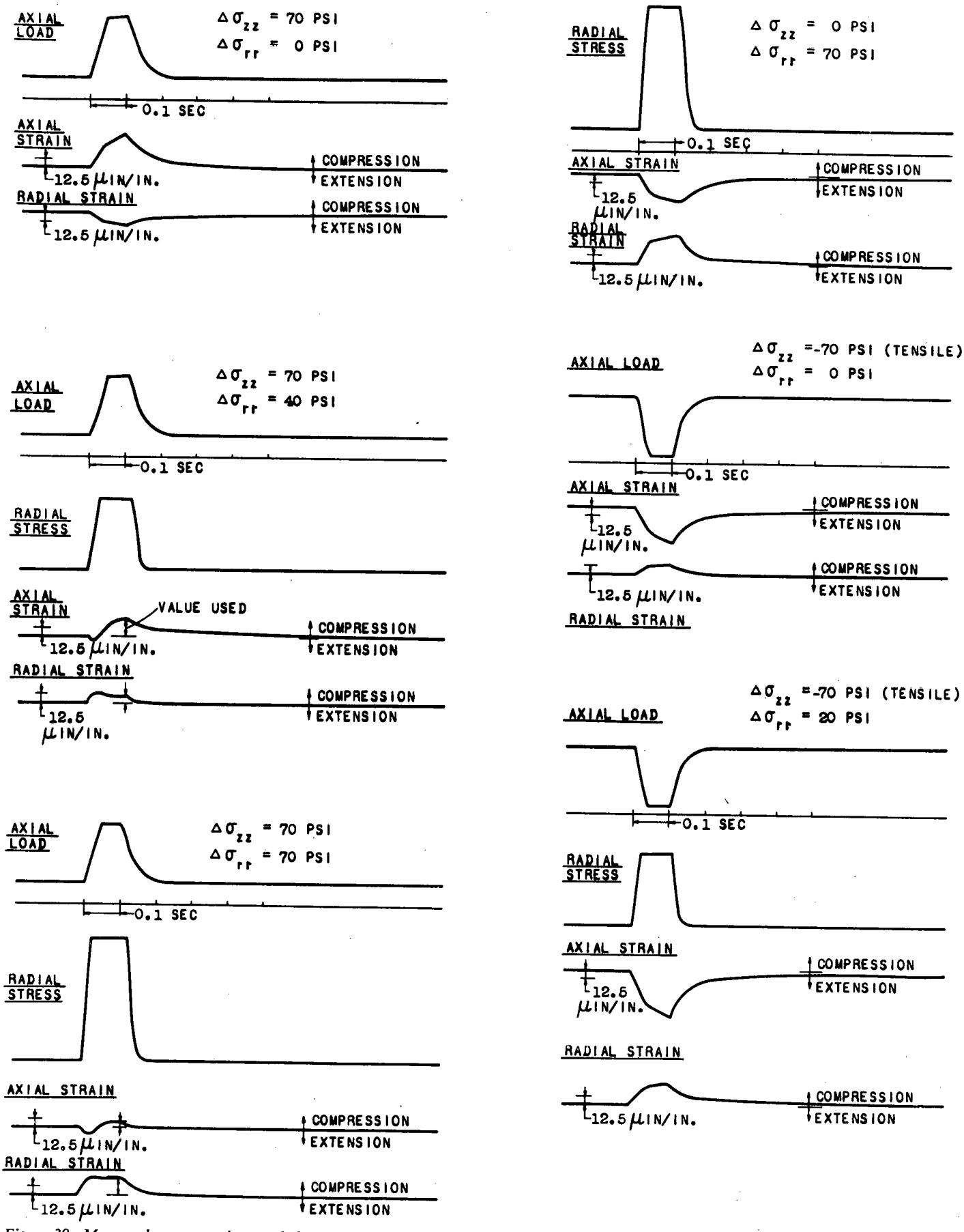

Figure 39. Measured response of an asphaltic concrete at 55°F during a repeated loading test.

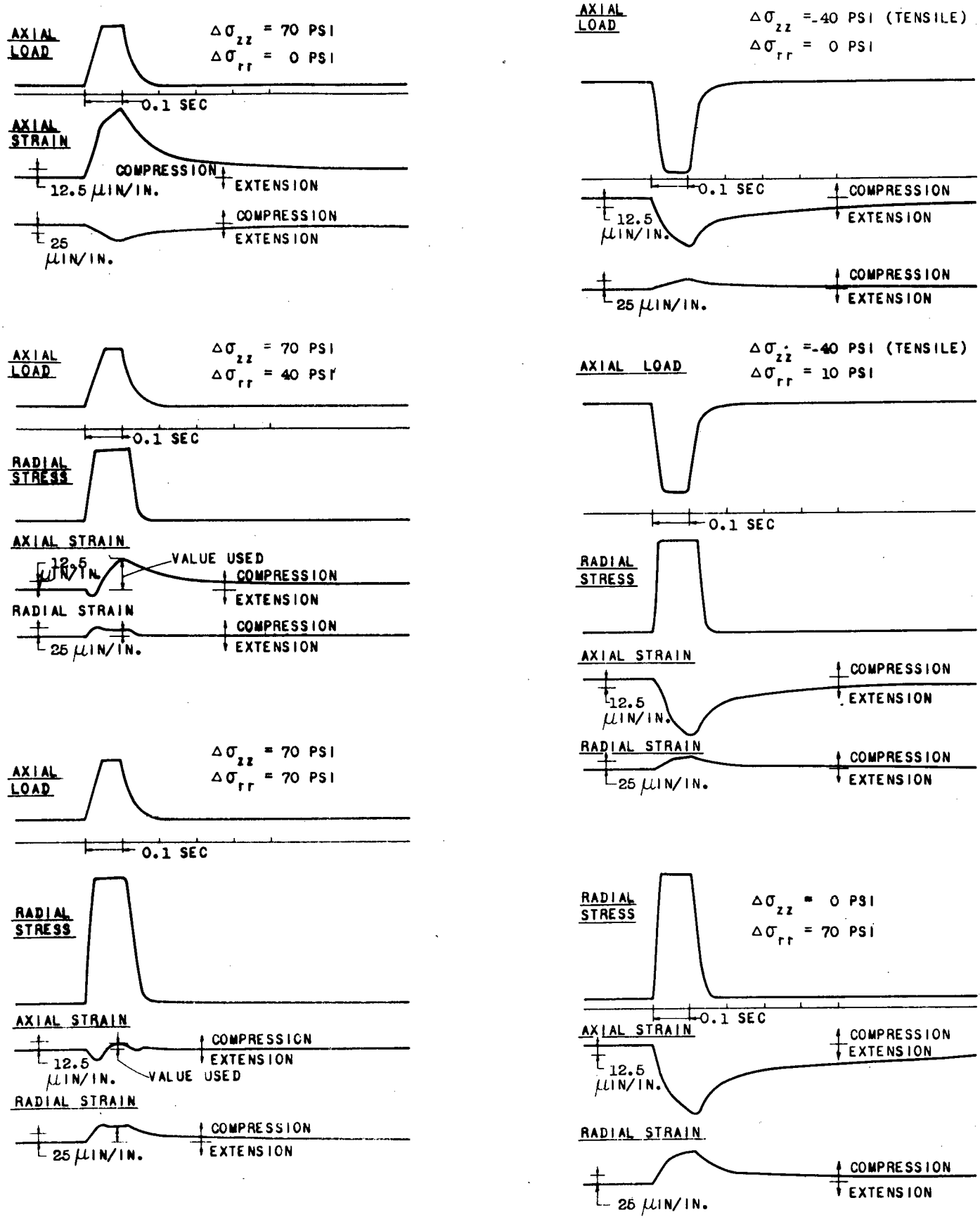

Figure 40. Measured response of an asphaltic concrete at 70°F during a repeated loading test.

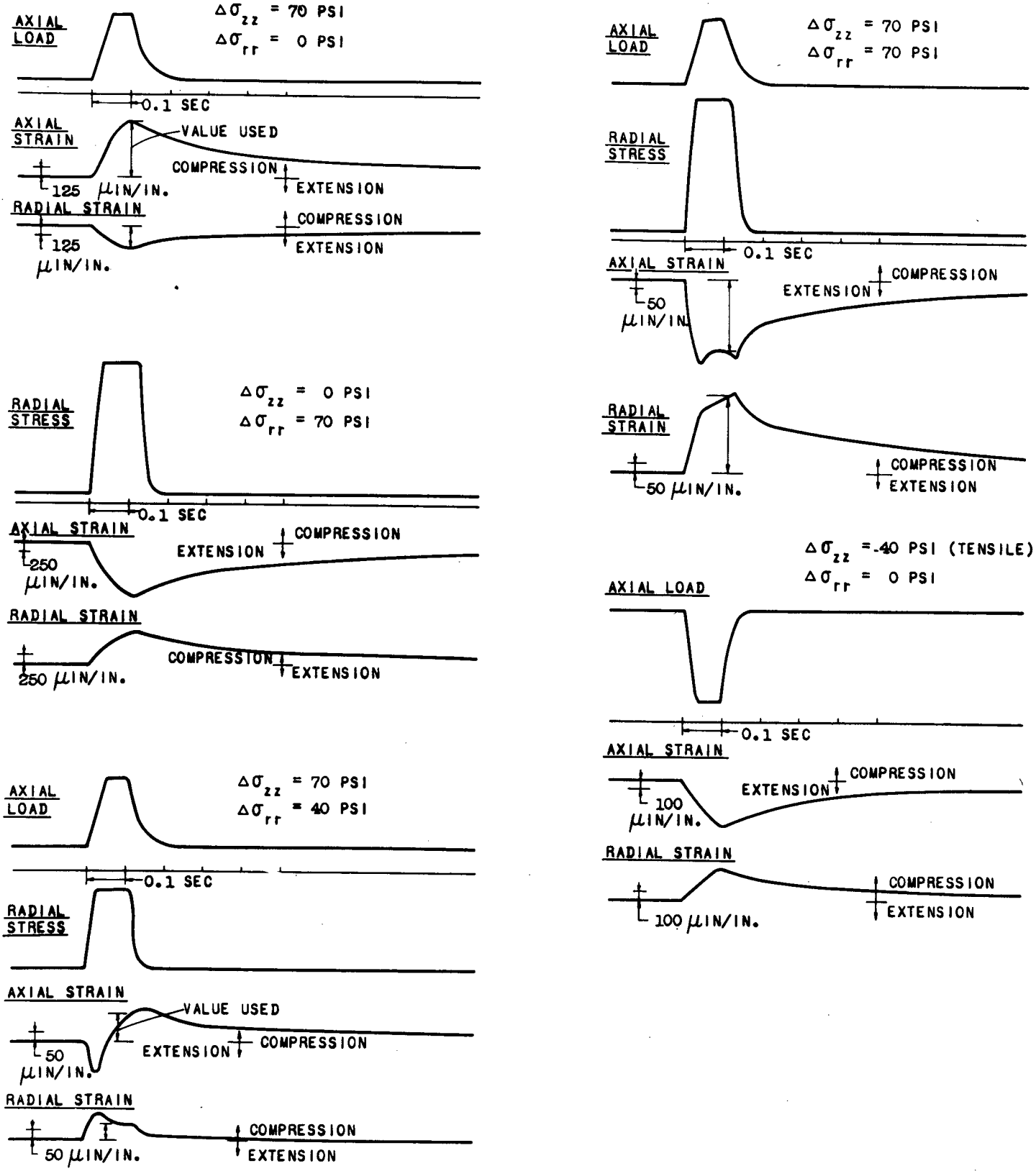

Figure 41. Measured response of an asphaltic concrete at 100°F during a repeated loading test.

applied. Even under the most unfavorable conditions, the deformation is almost completely recovered in a period of 1 sec after removal of the load. Therefore, the assumption of no permanent deformation, which is implicit in using an elastic representation of the material, appears to be satisfactory for analyzing the response of asphaltic concrete under a single load application.

The dominant characteristic of the response which is at variance with the elastic assumption is the time-dependent deformation. This is evident in three aspects of the strain-time history. The first is the difference in rate of increase in strain as compared to the rate of increase of load. The second is the deformation that occurs during the time (0.1 sec) the load is approximately constant. The third is the gradual recovery of the deformation on removal of the load.

In studying the first two of these effects it is appropriate to consider the stress and strain conditions when only one component of the stress is applied. This is because of the difference in rate of application of the radial and axial stresses.

The difference in the initial rate of strain and the rate of stress application does not appear significant for temperatures below 100°F. For temperatures equal to or greater than 100°F, the time-dependent deformation appears to be significant from the beginning of load application.

An examination of the deformation during the interval (0.1 sec) that the load is approximately constant shows that there is a certain amount of time-dependent deformation. This deformation is greatest for the higher temperatures. During the short interval of loading there do not appear to be any significant differences between the response under the action of compressive or tensile stresses. Treating the material as elastic for this short interval using the maximum strain value is conservative. The error involved does not appear to be significant with regard to the computation of the maximum strain.

On the release of the stress, the strain decreases at a rate that is considerably slower than the decrease in stress. However, the majority of the strain has been recovered within 1 sec of the removal of the load for temperatures below 100°F.

An important factor in the stress and strain histories in Figures 39 to 41 is the very short time intervals that are involved. It should be recognized that using an elastic representation of response based on the maximum value of strain is a conservative model for the particular loading conditions. However, this might not be true for other loading conditions. The data indicate that for temperatures greater than 100°F the response of the asphaltic concrete under the loading conditions used is significantly time-dependent.

Stress-Strain Curves

Figures 42 through 45 show a typical set of the stress-strain curves obtained from the repeated loading tests on the asphaltic concrete. These results are obtained at a temperature of 40°F. For stress-strain data obtained at other temperatures (55°F, 70°F, 100°F, and 140°F), see Appendix D. One component of strain can be plotted as a function of the axial and radial stress generating a stress-strain surface. However, for convenience, one strain component is plotted as a function of one stress component. Therefore, there are four curves for each test. For illustration, one component of the strain is plotted as a function of the stress state in the form of a stress-strain surface in Figure 46.

The results of the test at 40°F in which the sample was subjected to axial stresses ranging from 70 psi (compressive) to −70 psi (tension), and radial stresses ranging from zero to 70 psi (compression), indicate that axial stress-axial strain curves are of the stiffening * type in compressive stress range and of the softening ** type in tensile stress range.

The radial stress-axial strain curves are of the softening type. The nonlinearity of the response was less pronounced when the strains were plotted against radial stress. Similar results were obtained for tests at 55°F and 70°F, with magnitude of strain and degree of nonlinearity increasing with an increase in temperature. The test results at 100°F indicate that the axial stress-axial strain curves are of the softening type under tensile stresses and of the stiffening type under compressive stresses up to 40 psi, and change to the softening type when the compressive axial stress is greater than 40 psi. The radial stress-axial strain, and the radial stress-radial strain curves are of the softening type. The sample tested at 140°F was subjected to a range of both compressive axial and radial stresses from 0 to 30 psi. No tensile stress was applied to the sample because of the likelihood of failure. The results obtained indicate that the axial stress-axial strain curves are of the softening type. The stress-strain data indicated a greater scatter than those obtained from the tests at the lower temperatures.

Two samples were tested at more than one temperature. Sample WGAC-14 was tested at three different temperatures, in the following order: 55°F, 70°F, and 100°F. Sample WGAC-10 was tested at two different temperatures, in the following order: 50°F and 140°F. The stress-strain data obtained for these two samples were similar to those tested at only one specific temperature, indicating that over the range of stress states employed, temperature history has little effect on the response of the asphaltic concrete tested in this investigation.

Incremental Coefficients

The determination of the incremental coefficients $(B_{11} + B_{12})$, B_{13}, $(B_{31} + B_{32})$, and B_{33} from the results obtained from a repeated load triaxial test is discussed in Chapter Two, together with the geometrical significance of these coefficients in terms of the slope of the stress-strain surface.

To obtain the incremental coefficients, two approaches may be followed. The first approach considers the stress-strain surface (e.g., Fig. 46) and obtains an approximate analytical expression (e.g., a polynomial) for the surface based on the data. The analytical expression can then be differentiated with respect to the radial and axial stress to

* The rate of increase in strain with stress decreases with increasing stress.

** The rate of increase in strain with stress increases with increasing stress.

determine the value of the coefficients at the various reference stress states. Two of the coefficients can be determined from a plot such as shown in Figure 46. There are two such representations per test. The second approach considers the stress-strain curves as shown in Figures 42 to 45. These are two-dimensional plots, and an analyti-

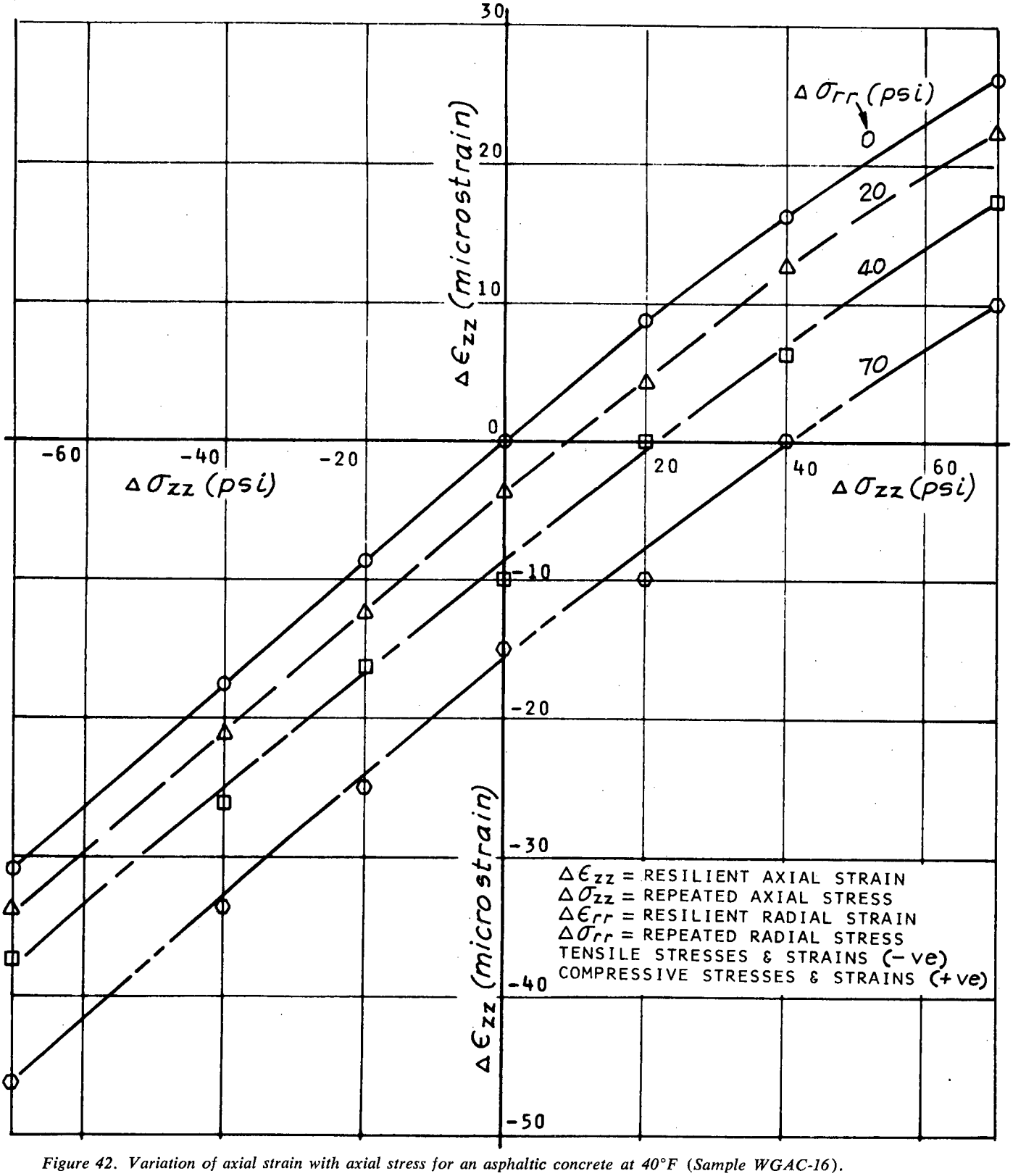

Figure 42. Variation of axial strain with axial stress for an asphaltic concrete at 40°F (Sample WGAC-16).

cal expression (a polynomial) can be chosen to approximate the stress-strain curve. From one curve only one of the coefficients can be determined. There are four such curves per test. The second approach was used in this investigation.

The following technique was adopted to calculate the

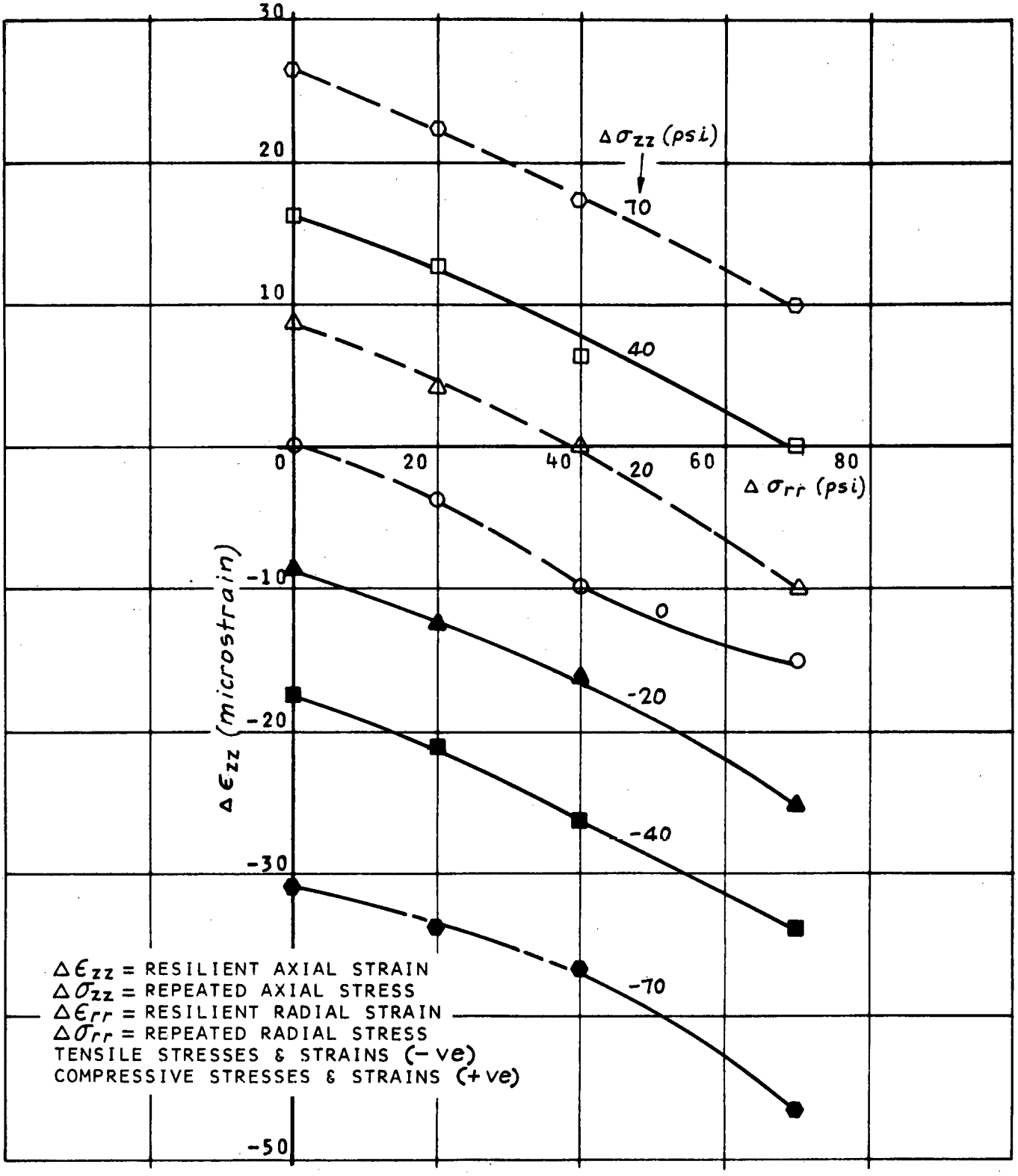

Figure 43. Variation of axial strain with radial stress for an asphaltic concrete at 40°F (Sample WGAC-16).

values of the coefficients from the test data. Using the least squares method, polynomial curves were fitted to the axial and radial strain for various axial (radial) stresses at given radial (axial) stress. The tangents were obtained at various stress levels by differentiation, and the coefficients for Eq. 9 were evaluated. The basis of the method is discussed in Appendix A. These calculations were carried out automatically by a computer program.

The values of the incremental coefficients thus determined were found to be very sensitive to the order of the

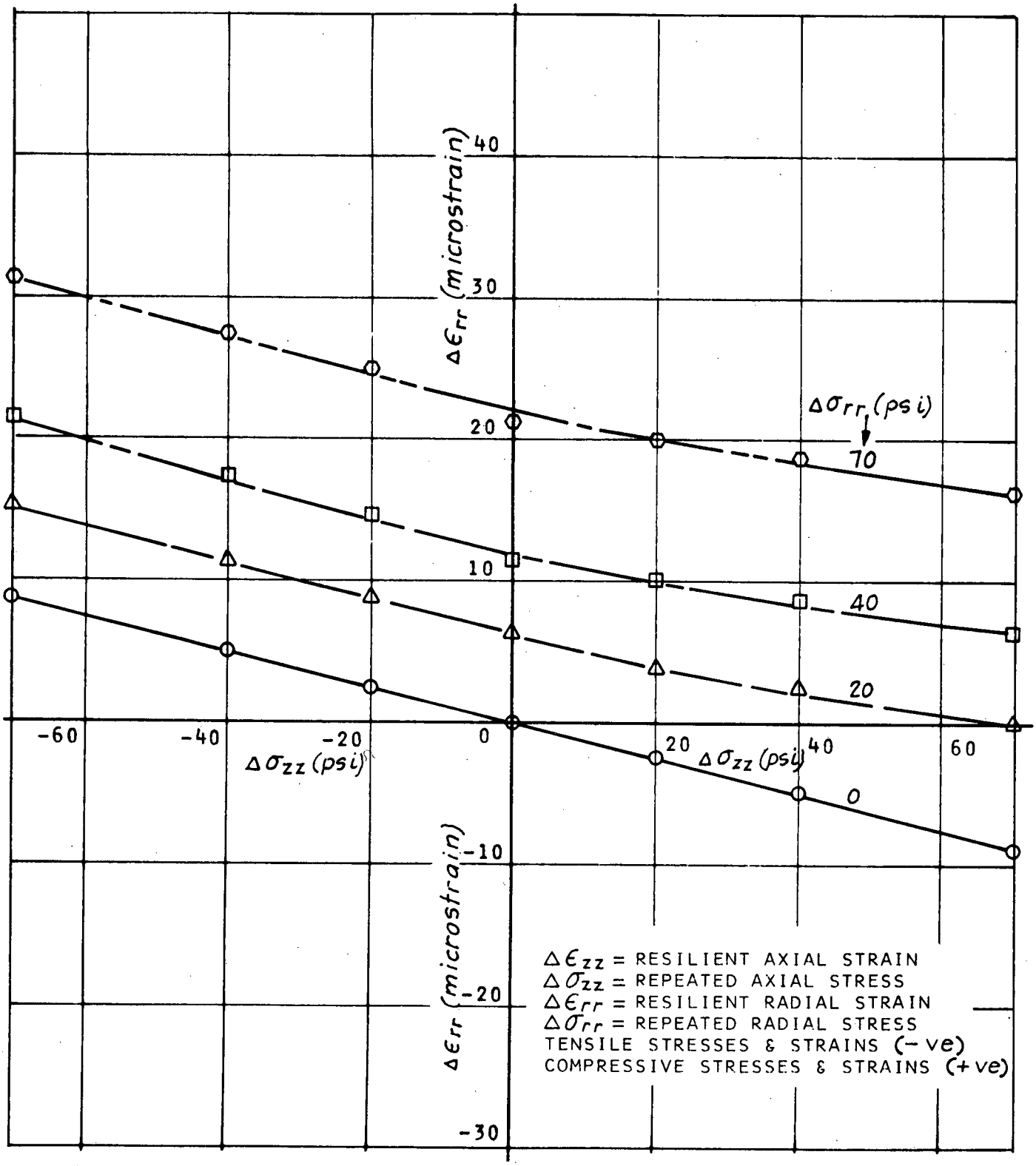

Figure 44. Variation of radial strain with axial stress for an asphaltic concrete at 40°F (Sample WGAC-16).

polynomial equation used to fit the data points. In selecting the degree of the polynomial the data must be examined to evaluate the extent of the nonlinearity. Higher order polynomials can lead to unrealistic values of the incremental coefficients. The lower order polynomials of second and third degree, depending on the number of stress-strain pairs on the curve, were found to fit the data points and eliminate unrealistic oscillations of the coefficients. The incremental coefficients for the asphaltic concrete tested at 40°F, 55°F, 70°F, 100°F, and 140°F were calculated according to the foregoing procedure, and were plotted against reference axial and radial stress (see Appendix D).

The data at 40°F and 55°F indicate that the stress state exerts a different influence on each of the coefficients. In general, the stress state exerts the greatest influence on the value of $(B_{32} + B_{31})$. There did not appear to be a consistent pattern from which to draw any significant conclusions on the variation of $(B_{32} + B_{31})$ with the stress level. However, there appears to be a significant difference in the character of the variation as a function of the radial stress for 55°F as compared to 40°F. The variation with radial stress follows a more regular pattern than that with the

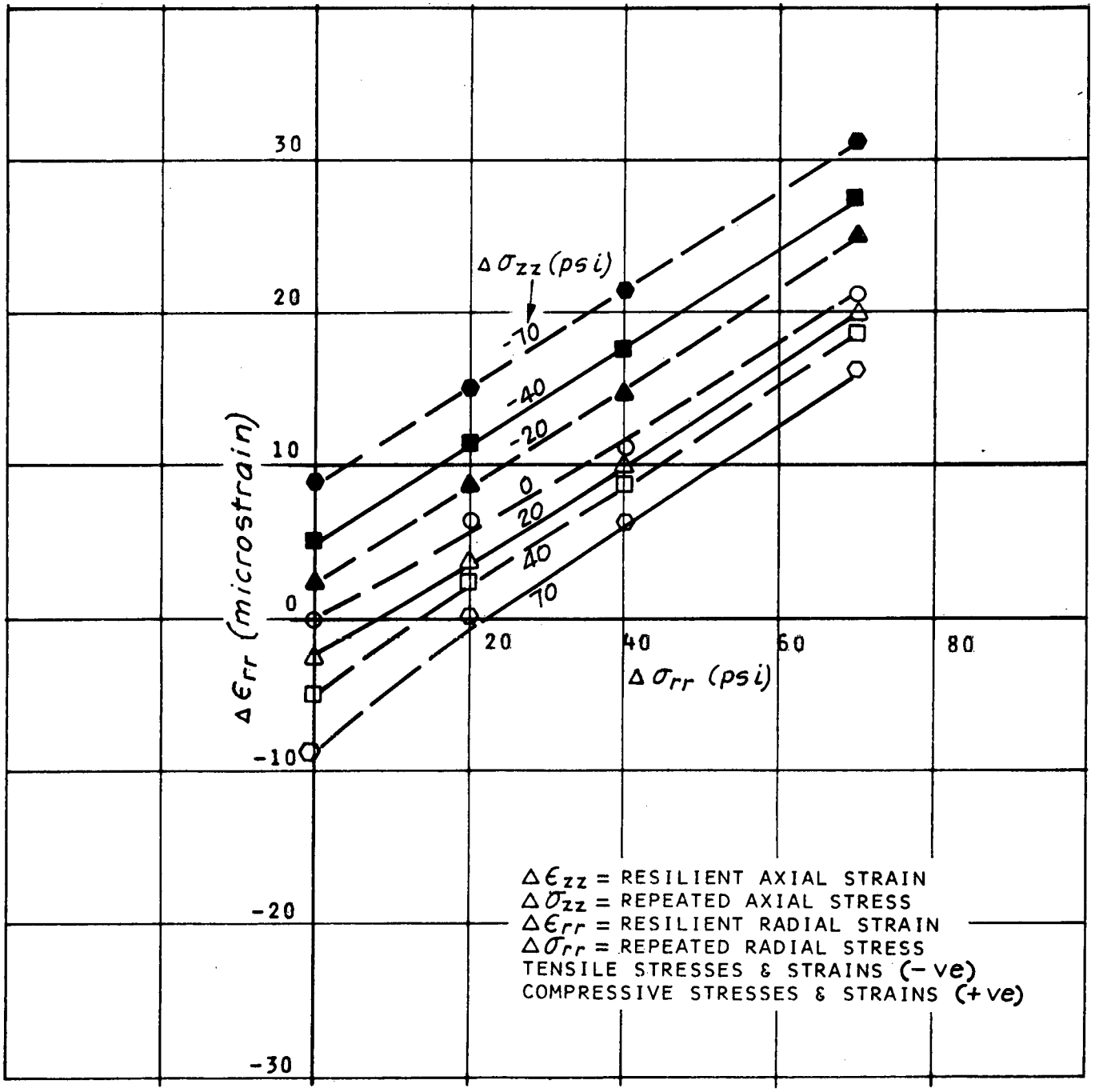

Figure 45. Variation of radial strain with radial stress for an asphaltic concrete at 40°F (Sample WGAC-16).

axial stress. The absolute values of B_{33} and B_{13} decreased with increasing compressive axial stress, and increased with increasing tensile axial stress. The radial stress appears to have little effect on the value of B_{33}. The influence of the stress state on the value of $(B_{12} + B_{11})$ does not appear to be significant.

There is a significant change in the magnitude of the coefficients obtained at 70°F as compared to those obtained at temperatures of 40°F and 55°F. The stress state has the greatest influence on B_{33}. The value of B_{33} decreased as the axial stress varied from −40 psi (tensile) to +40 psi (compressive). However, it increased as the axial stress increased from +40 psi to +70 psi (compressive). Comparatively, the radial stress appears to have little effect on the value of B_{33}. The values of the other coefficients also vary with the stress state; however, to a lesser degree.

At 100°F the stress state has a pronounced effect on all the coefficients. In general, the absolute values of $(B_{12} + B_{11})$ and $(B_{32} + B_{31})$ increased with increasing radial stress and decreased as the axial stress varied from tension to compression. The absolute values of B_{13} and B_{33} decreased as the axial stress varied from −40 psi (tensile) to +40 psi (compressive), and then increased or decreased at the axial stress of +70 psi, depending on the reference radial stress. These values increased as the radial stress increased.

At 100°F the loading history and other time-dependent effects greatly influenced the stress-strain response of the asphaltic concrete. This is reflected in the scatter of the

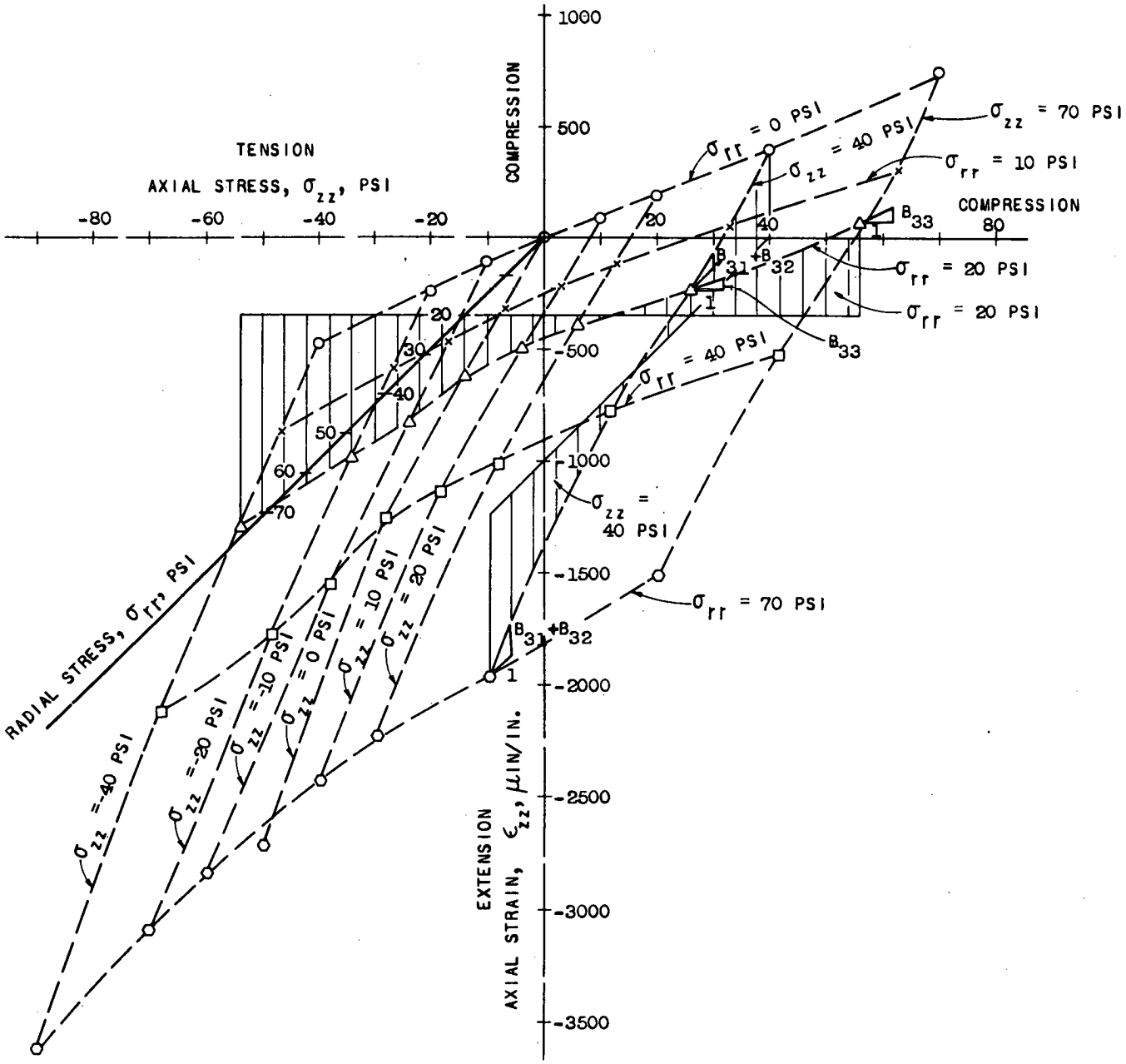

Figure 46. Three-dimensional strain-stress surface variation of axial strain with stress states for an asphaltic concrete at 100°F.

stress-strain data and in the variation of the incremental coefficients with stress. However, the data indicate that the absolute values of B_{13} and B_{33} decreased with an increase in the reference axial stress.

Certain characteristics of the material can be studied by considering the variation of the ratios of various coefficients with the stress state. If the coefficient matrix is symmetric and the material is transversely isotropic,* $2B_{13}$ would be equal to $(B_{31} + B_{32})$. This ratio examines the relative influence of the axial stress on the radial strain and the radial stress on the axial strain. For variations of the coefficient ratio $2B_{13}/(B_{31} + B_{32})$ with the reference stress state for the asphaltic concrete tested at 40°F, 55°F, 70°F, 100°F, and 140°F, see Appendix D. In general, the ratio ranged between 0.5 and 1.5, depending on the stress state and temperature; however, at 140°F, the ratio varied between 1.2 and 0.05. This indicates that the material tested might not be transversely isotropic and/or the coefficient matrix might not be symmetric at certain stress states. If symmetry is assumed, this indicates that the nature of the anisotropy is influenced by the stress state and the temperature—the major influence being temperature.

The ratio B_{11}/B_{33} also would give an indication of the degree of anisotropy of the asphaltic concrete. For isotropic materials B_{11} would equal B_{33}. However, it is not possible to calculate B_{33} independently in a triaxial test configuration. The ratio $(B_{11} + B_{12})/(B_{33} + B_{13})$ also would be unity if the material remained isotropic. The variation of this ratio would provide some indication of isotropy of the material at various reference stress states. In general, this ratio varied between 1.5 and 0.7, depending on the stress state for those specimens tested at temperatures below 70°F. Larger variations of this ratio were observed for the specimens tested at temperatures above 100°F. This provides additional evidence that the degree of anisotropy of the asphaltic concrete depends on temperature and stress state.

Approximate Modulus of Elasticity and Poisson's Ratio

Because of limitations of the triaxial equipment developed for this study it is not possible to determine all the incremental coefficients required in the constitutive equation. Four quantities involving the incremental coefficients [i.e., $(B_{11} + B_{12})$, $(B_{31} + B_{32})$, B_{13}, and B_{33}] may be calculated from test results. These four quantities involve six coefficients; thus, it was not possible to isolate B_{11}, B_{12}, B_{31}, and B_{32}. The incorporation of a nonlinear model into a design procedure requires use of the nonlinear constitutive law in solving various boundary value problems. Solution techniques for nonlinear problems must be developed in order to use nonlinear material characterization in the structural design of pavements. Commonly available solution techniques can only include linear constitutive laws; however, certain numerical procedures are capable of incorporating various ad hoc nonlinear modifications.

Therefore, it was considered appropriate to develop an approximate modulus of elasticity and a Poisson's ratio to use with linear elastic constitutive law (approximate modulus and Poisson's ratio described here are based on incremental values rather than secant values). To use the coefficients obtained from the incremental nonlinear constitutive law in the determination of an approximate linear relationship, the following procedure was used.

Eq. 9 may be written as

$$\begin{Bmatrix} \epsilon_{rr}' \\ \epsilon_{zz}' \end{Bmatrix} = \begin{bmatrix} \frac{1}{E_r}(1 - \nu_{r\theta}) & -\frac{\nu_{rz}}{E_z} \\ -\frac{(\nu_{zr} + \nu_{z\theta})}{E_r} & \frac{1}{E_z} \end{bmatrix} \begin{Bmatrix} \sigma_{rr}' \\ \sigma_{zz}' \end{Bmatrix} \tag{10}$$

in which E_r and E_z are the moduli of elasticity in the radial and axial direction, respectively; $\nu_{r\theta}$ and ν_{rz} are the ratio of circumferential and axial strain to radial strain due to a stress increment in the radial direction; ν_{zr} and $\nu_{z\theta}$ are the ratio of radial and circumferential strain to axial strain due to a stress increment in the axial direction. For an isotropic material, Eq. 10 may be expressed as

$$\begin{Bmatrix} \epsilon_{rr}' \\ \epsilon_{zz}' \end{Bmatrix} = \begin{bmatrix} \frac{1}{E}(1 - \nu) & \frac{-\nu}{E} \\ \frac{-2\nu}{E} & \frac{1}{E} \end{bmatrix} \begin{Bmatrix} \sigma_{rr}' \\ \sigma_{zz}' \end{Bmatrix} \tag{11}$$

Comparing the off-diagonal coefficients in Eqs. 9 and 11, the following expression was used to calculate an approximate value of ν/E:

$$\nu/E = -\tfrac{1}{3}(B_{13} + B_{31} + B_{32}) \tag{12}$$

If it is assumed that B_{12} is equal to $-\nu/E$, B_{11} can be determined because $(B_{11} + B_{12})$ is known. The approximate elastic modulus, E, can then be computed from Eq. 13.

$$\frac{1}{E} = \tfrac{1}{2}[B_{11} + B_{12} + B_{33} - \tfrac{1}{3}(B_{13} + B_{31} + B_{32})] \tag{13}$$

If the approximate modulus is known, Poisson's ratio can be determined because ν/E already has been evaluated.

Values of the approximate modulus and the Poisson's ratio were calculated for the asphaltic concrete tested at 40°F, 55°F, 70°F, 100°F, and 140°F. The results were plotted as a function of the axial and radial reference stresses (see Appendix D). At 40°F and 55°F, values of the approximate modulus increase with increasing axial compressive stress and decreases with increasing axial tensile stress. The radial stress has little effect on the modulus. Values of Poisson's ratio vary between 0.22 and 0.35 at 40°F, and between 0.31 and 0.41 at 55°F. For the asphaltic concrete tested at 70°F, the modulus decreases with increasing axial tensile stress, and increases with increasing axial compressive stress up to 40 psi. The increase in axial compressive stress from 40 to 70 psi causes the value of the modulus to decrease. The increase in radial stress generally causes the modulus to decrease. The value of Poisson's ratio varies between 0.33 and 0.45. The value decreases with increasing axial tensile stress and increases with increasing axial compressive stress. The radial stress has little effect on the value of Poisson's ratio. At 100°F, the value of the modulus decreases with increasing axial tensile stress, and increases with increasing axial compressive stress up to

* This implies that the material remains transversely isotropic irrespective of the stress state.

40 psi. A further increase in axial compressive stress causes decrease or increase in modulus, depending on the magnitude of the radial stress. The modulus decreases if the radial stress is less than 40 psi and increases if it is greater than 40 psi. The value of the modulus decreases with increasing radial stress. The value of Poisson's ratio varies between 0.41 and 0.56. A value of Poisson's ratio greater than 0.5 is an indication that the assumption of isotropy for the asphaltic concrete is not valid. At 140°F, both the modulus and Poisson's ratio increase slightly with the axial compressive stress, and decrease with the radial stress. The value of Poisson's ratio ranges between 0.39 and 0.57.

Table 2 summarizes the range of values of the incremental coefficients, approximate modulus of elasticity, and Poisson's ratio, determined over the range of stress states, at temperatures varying from 40°F to 140°F. Figures 47 and 48 show the variations of the range of values of the approximate modulus of elasticity and Poisson's ratio with temperature. The approximate modulus decreases with increasing temperature. Its average value decreases from 2.3×10^6 psi at 40°F, to 7.0×10^4 psi at 100°F, and 8.6×10^3 psi at 140°F. The value of Poisson's ratio as shown in Figure 48 increases gradually with increasing temperature. Its average value increases from 0.27 at 40°F, to 0.4 at 70°F, and 0.49 at 140°F. Nonlinear effects on the approximate modulus of elasticity, as shown by the range of values in Figure 47, are very small at temperatures below 55°F. The nonlinearity, however, increases with increasing temperature. At 140°F the nonlinear effect becomes smaller again. This is because time-dependent response of the asphaltic concrete becomes important at higher temperature and the elastic assumption implies a greater approximation. The range in modulus values superimposed on the temperature effects (as shown in Fig. 47) indicates that the influence of temperature can be of far greater significance than the influence of the level of stress.

Summary

The response of the asphaltic concrete to repeated stress applications consists of recoverable as well as permanent strains. The recoverable strains had both time-dependent and time-independent components. At the lower temperatures (below 70°F), the time-independent component represented the major portion of the total strain. The time-dependent strains became significant with increasing temperatures. Permanent strains due to a single stress application at the end of 50 cycles were very small at the lower temperatures. They became significant at temperatures higher than 100°F.

The response of the asphaltic concrete is a function of the stress state and the temperature. The nonlinearity in the stress-strain response was more pronounced with axial stress than with radial stress. The nature of the nonlinearity was dependent on the temperature and the stress state.

The incremental coefficients, B_{33}, B_{13}, $(B_{11} + B_{12})$, and $(B_{31} + B_{32})$, calculated from the test results indicated that these quantities were a function of the reference stress state, and the degree of variation increased with increasing temperature.

The approximate modulus of elasticity and Poisson's ratio that may be used in a linear or "ad hoc" nonlinear stress analysis of a pavement system vary with stress state and temperature. The degree of nonlinearity increased with an increase in temperature. In general, the modulus decreased with increasing axial tensile stress. An increase in

TABLE 2

SUMMARY OF RANGE OF INCREMENTAL COEFFICIENTS, APPROXIMATE MODULUS, AND POISSON'S RATIO FOR AN ASPHALTIC CONCRETE

TEST TEMP. (°F)	INCREMENTAL COEFFICIENTS [a] $(1/\text{PSI}) \times 10^6$				APPROX. MODULUS OF ELASTICITY [a] (PSI $\times 10^{-3}$)	POISSON'S RATIO [a]
	$B_{11}+B_{12}$	$B_{31}+B_{32}$	B_{13}	B_{33}		
40	0.28	−0.10	−0.17	0.34	2100	0.18
	to	to	to	to	to	to
	0.43	−0.35	−0.44	0.48	2600	0.35
55	0.38	−0.39	−0.13	0.52	1200	0.28
	to	to	to	to	to	to
	0.70	−0.71	−0.25	0.77	1680	0.43
70	0.77	−0.95	−0.30	0.97	470	0.32
	to	to	to	to	to	to
	1.46	−1.53	−0.84	2.33	790	0.44
100	5.5	−9	−3	7	30	0.40
	to	to	to	to	to	to
	23.5	−35	−18	33	150	0.56
140	53	−82	−1	16	6	0.39
	to	to	to	to	to	to
	132	−128	−64	155	12	0.57

[a] Range in values indicates the influence of stress levels.

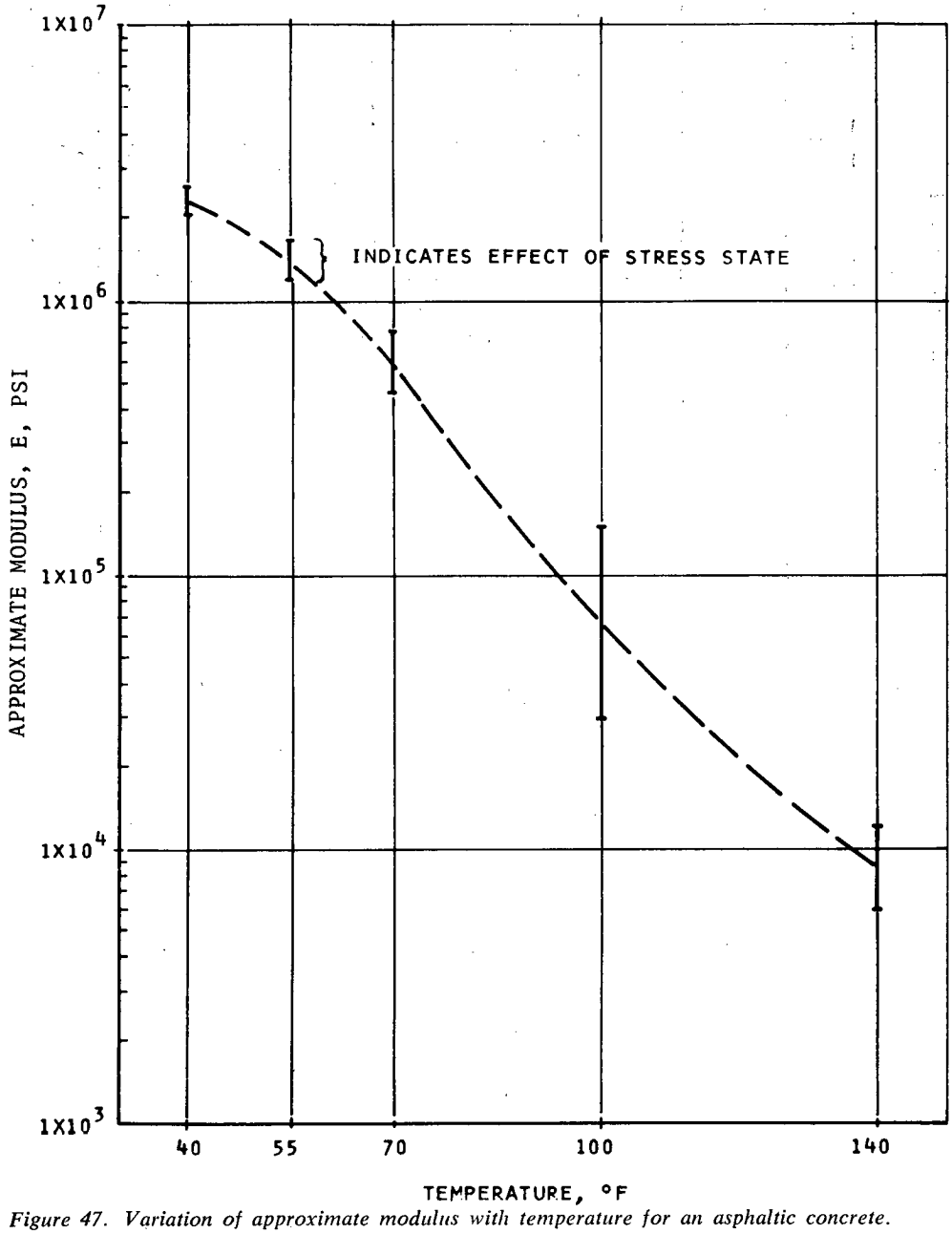

Figure 47. Variation of approximate modulus with temperature for an asphaltic concrete.

the axial compressive stress up to a certain level, this level depending on the temperature, results in an increase in the modulus. Beyond this stress level, an increase in axial compressive stress results in a decrease in modulus.

The influence of radial stress (from 0 to 70 psi) on the approximate modulus did not appear to be significant. The Poisson's ratio varied with stress state. Generally, its value increased slightly with increasing axial compressive stress, and decreased with increasing axial tensile stress. The effect of the radial stress on Poisson's ratio was not significant.

Temperature exerts a major influence on the response of asphaltic concrete. For the short loading duration of 0.1 sec used in this study, the average value of the approximate modulus decreased from 2.3×10^6 psi at 40°F, to 6.8×10^4 psi at 100°F, and to 8.5×10^3 psi at 140°F. It appears, therefore, that temperature has a greater influence on the properties of asphaltic concrete than stress level.

COHESIVE SUBGRADE SOILS

Cohesive subgrade soils from the San Diego Test Road have been tested under repeated load tests by Materials Research and Development (1968) and Dehlen (1969), with the object of characterizing the soil as a nonlinear elastic material. The triaxial apparatus used in conducting the tests reported by MR&D (1968) did not permit the independent control of the axial and radial stress. The tests by Dehlen (1969) were conducted with independent con-

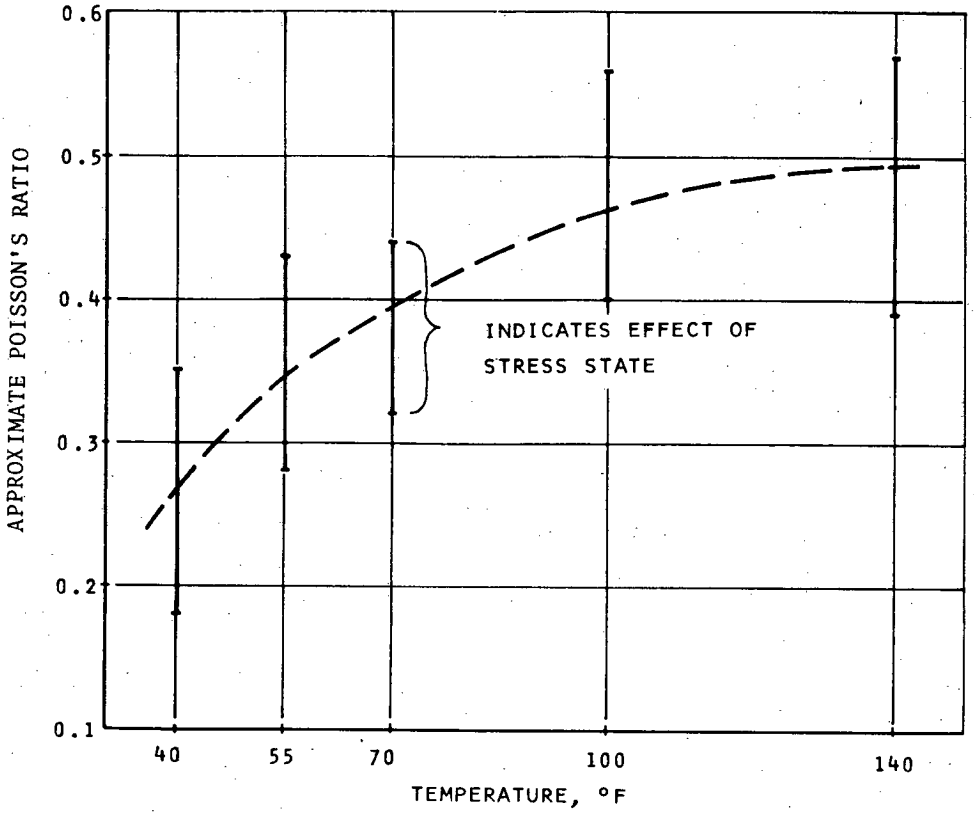

Figure 48. Variation of approximate Poisson's ratio with temperature for an asphaltic concrete.

trol of the radial and axial stress. Dehlen used undisturbed samples from the Test Road. In general, these samples were at a low water content and had a high dry density. To supplement the information already obtained and get a more complete picture regarding the response of the soil it was decided to investigate the response of the cohesive subgrade soil under representative stress levels at a higher water content and a lower dry density. The work by Dehlen and the results of this investigation are combined here for completeness. The testing procedures used for the characterization of subgrade soils are described in Chapter Two.

Response Under a Single Load Application

Figure 49 shows typical axial and radial deformations measured by the dual LVDT's during testing. At the stress levels considered representative of service conditions it may be observed that the response of the strain is essentially time-independent, and that there is no significant permanent strain. This indicates that it is valid to assume that the soil responds elastically to a single application of load. The results shown in Figure 49 are from testing of a laboratory-compacted specimen at a relatively high water content. It can therefore be assumed that the elastic assumption would be valid for the stiffer materials.

Stress-Strain Data

The results of the repeated loading tests on both undisturbed and laboratory-compacted San Diego subgrade samples were obtained in the form of stress-strain curves. Typical results are shown in Figures 50 and 51. (More complete data are described in Appendix D.) Variations of axial and radial strain as a function of either repeated axial or radial stress are shown. The nonlinear character of the response is apparent in all cases. The close coincidence of the curves for various sustained stresses indicates that the repeated stress exerts the major influence on the response. The test results also indicate that the stress-strain curves are of the softening type. Nonlinearity was most apparent at lower stress levels between 0 and 3 psi. The degree of nonlinearity increased as the moisture content of the subgrade soil increased.

Incremental Coefficients

As in the case of asphaltic concrete, values of the incremental coefficients, $(B_{11} + B_{12})$, $(B_{31} + B_{32})$, B_{13}, and B_{33}, may be determined from the stress-strain pairs. The incremental coefficients were obtained by the same method described for the asphaltic concrete. Polynomial curves were fitted to the axial and radial strain for various axial (radial) stresses at given radial (axial) stress, using the method of least squares. The tangents were obtained at various stress levels by differentiation, and the coefficients were evaluated. The incremental coefficients thus obtained for the undisturbed and laboratory-compacted San Diego subgrade samples are plotted against reference axial and radial stress (see Appendix D). In all cases, the values of

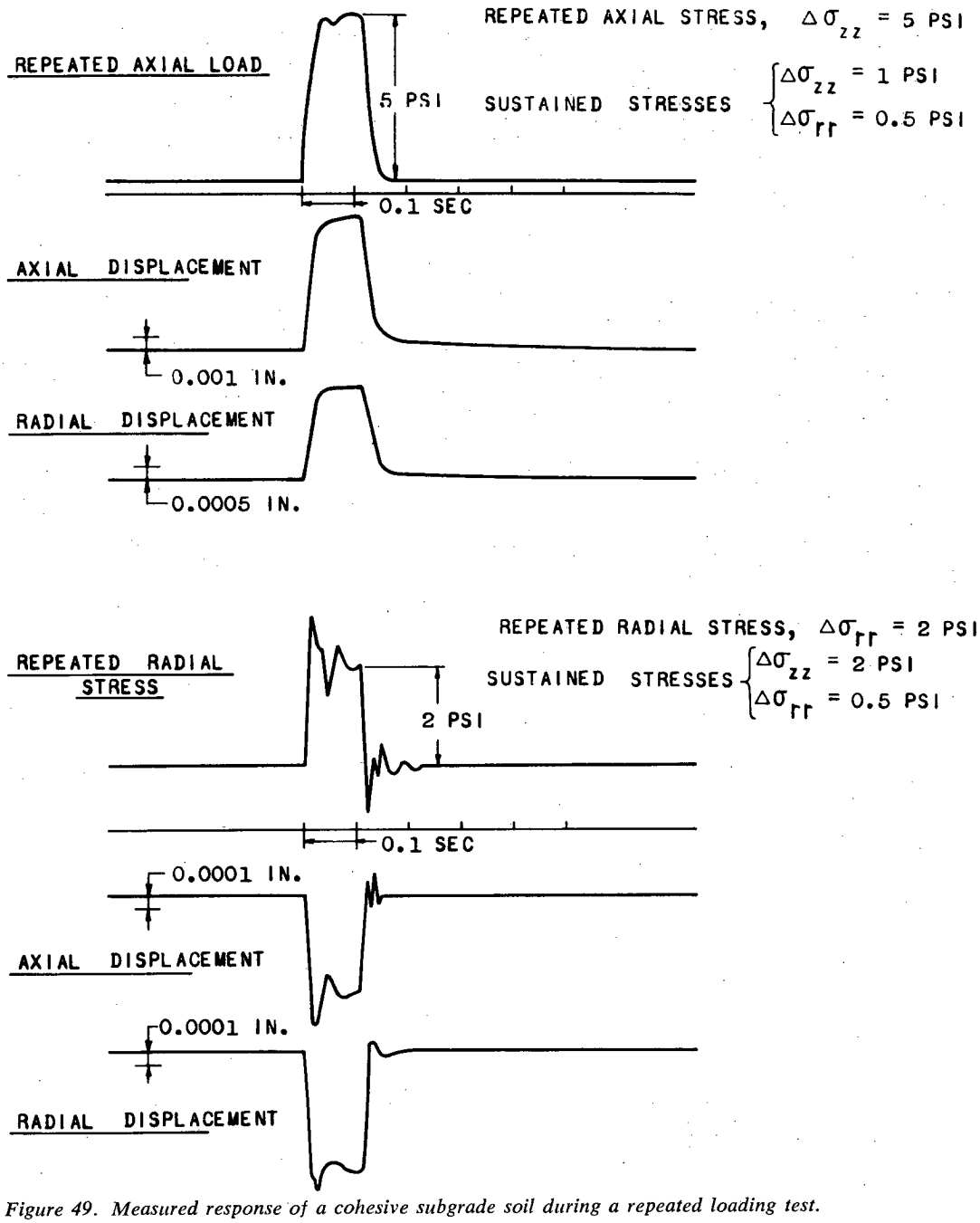

Figure 49. Measured response of a cohesive subgrade soil during a repeated loading test.

the incremental coefficients, B_{33} and B_{13}, increase with increasing axial stress level, indicating nonlinear stress-strain behavior. However, reference radial stress levels have no or little effect on the values of these coefficients. This is to be expected, because B_{33} and B_{13} were determined from the variation of axial and radial strain with repeated axial stress, and these resilient strains were little affected by the magnitude of the reference radial stress. Similarly, the values of the incremental coefficients, $(B_{11} + B_{12})$ and $(B_{31} + B_{32})$, increase with increasing repeated radial stress levels, and are little affected by the magnitude of the reference axial stress.

As with asphaltic concrete, if the soil is transversely isotropic and the coefficient matrix is symmetric, $2B_{13}$ would be equal to $(B_{31} + B_{32})$. The coefficient ratio $2B_{13}/(B_{31} + B_{32})$ increased with increasing axial reference stress, and decreased with increasing radial reference stress. The ratio $2B_{13}/(B_{31} + B_{32})$ was close to unity for hydrostatic reference stress states. This indicates that the anisotropy in the specimen is introduced by the stress state. For variation of the ratio with stress state, see Appendix D.

The coefficient ratio $(B_{11} + B_{12})/(B_{33} + B_{13})$ would also give some indication of the degree of anisotropy at various stress states. For the variations of the coefficient

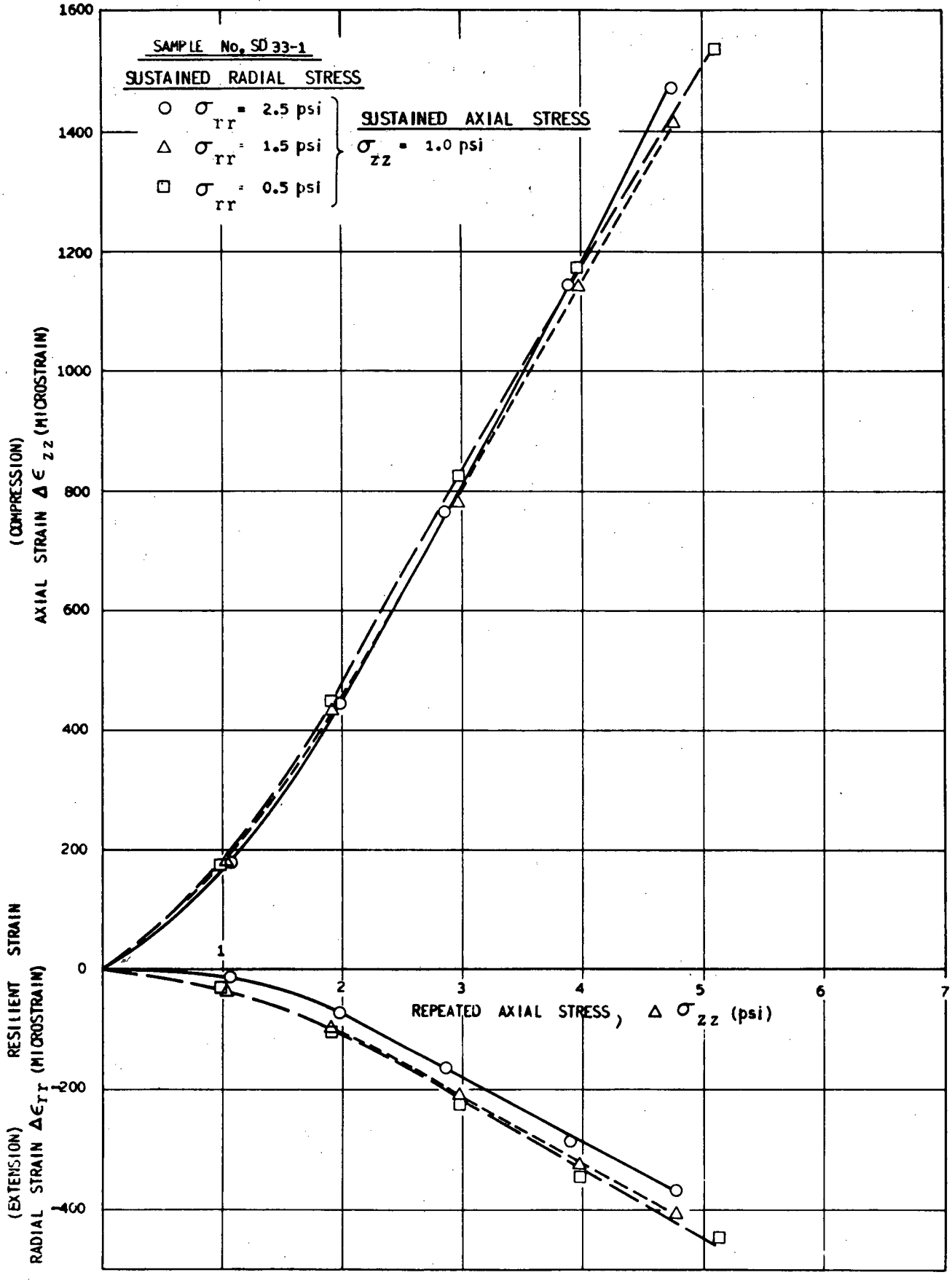

Figure 50. Variation of axial and radial strain with axial stress for laboratory-compacted San Diego subgrade.

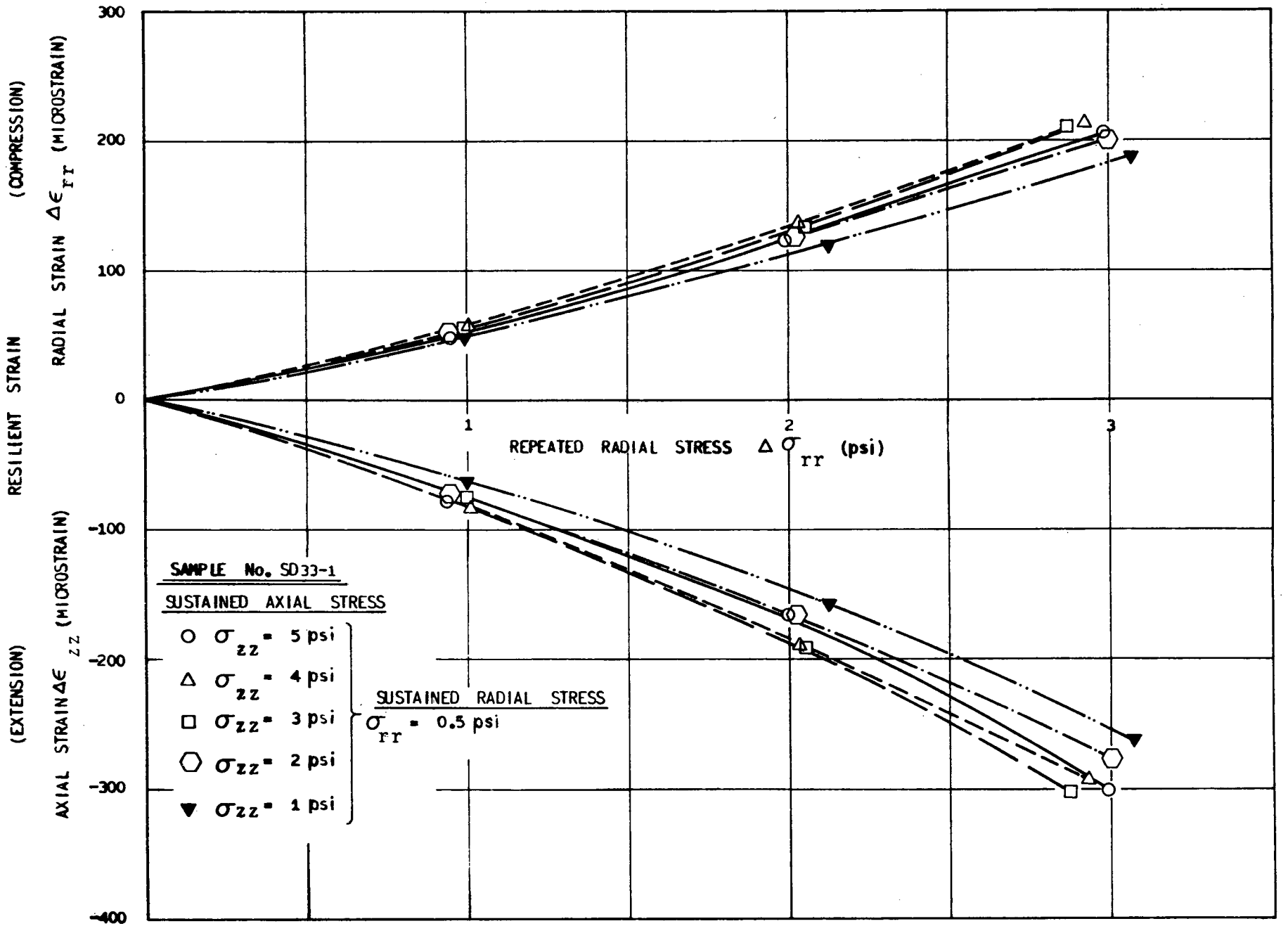

Figure 51. Variation of axial and radial strain with radial stress for laboratory-compacted San Diego subgrade.

ratio $(B_{11} + B_{12})/(B_{33} + B_{13})$ with the axial and radial reference stresses for two undisturbed subgrade samples, see Appendix D. In all cases, the ratio decreased with increasing radial reference stress, indicating that the degree of anisotropy varied with stress state.

Approximate Modulus of Elasticity and Poisson's Ratio

As with asphaltic concrete, approximate values of the modulus of elasticity and Poisson's ratio were calculated to permit use of the data for linear and "ad hoc" nonlinear analysis. These approximate values were calculated from the values of the incremental coefficients using the same procedures as for the asphaltic concrete.

The variations of the approximate modulus of elasticity and Poisson's ratio with the axial and radial reference stresses are shown in Figures 52 to 57. The values of the approximate modulus decrease with increasing axial reference stress. With the exception of Sample 40, the rate of decrease in modulus is greatest at the lower stress levels, between 0 and 2 to 3 psi, and diminishes as the stress level increases. At the stress levels higher than 5 to 6 psi, the modulus is nearly constant for constant radial reference stress. The modulus also decreased with increasing radial stress, but the effect was not as great as that of axial stress, especially at low levels of axial stress (below 2 psi). The variation of Poisson's ratio with the axial and radial reference stresses shows that the stress state does not significantly influence its value. This indicates that it is reasonable to assume a constant Poisson's ratio for the cohesive subgrade soil in the structural analysis of a pavement system.

Moisture Content

The effect of moisture content on the behavior of the San Diego subgrade soil was studied by testing samples at different moisture contents. Table 3 summarizes the range of values of the incremental coefficients, approximate modulus, and Poisson's ratio determined over the range of stress states studied for three samples of different moisture contents.

The variations of the range of values of the modulus and Poisson's ratio with moisture content are shown in Figures 58 and 59. The variation of the modulus with moisture content shown in Figure 58 indicates that the modulus decreases with increasing moisture content. The rate of change is greatest at moisture content varying from 19 to 21 percent. As Figure 59 shows, the values of Poisson's ratio increase with increasing moisture content.

Summary

The response of the San Diego subgrade soil to repeated stress applications of magnitudes comparable to those likely to occur under service conditions was essentially time-independent. Almost all the axial and radial strains induced due to repeated stress applications were recoverable. This suggests that the elastic time-independent model is suitable for characterizing subgrade soils.

A number of factors may affect the response of subgrade soils; these are moisture contents, density, stress state, and stress history. Some of these factors, such as moisture content and density, may be accounted for by testing undisturbed samples for evaluation purposes. For the San Diego subgrade soil, the moisture content and stress state exerted a significant influence on the soil response.

The stress-strain pairs, the stress-strain curves, and the incremental coefficients obtained from the repeated triaxial compression tests on the San Diego subgrade samples provided evidence of nonlinear behavior at all stress levels. The test results also showed that the strains resulting from a repeated stress were little affected by the magnitude of the transverse reference stress. Nonlinearity in the form of softening-type stress-strain relations was most apparent at lower stress levels between 0 and 2 to 3 psi. At higher stress levels, the stress-strain curves became nearly linear.

The approximate modulus and Poisson's ratio that may be incorporated in a linear or "ad hoc" nonlinear stress analysis of a pavement system were also found to vary with reference stress state. The value of the modulus decreased with increase in stress level, the change being greatest below 3 psi. At higher stress levels (above 5 psi) the modulus approached a constant value. The radial reference stress has a similar but relatively minor effect on the modulus. The variation of the approximate Poisson's ratio with stress state was so small that for practical purposes a constant value may be assumed in the structural analysis of a pavement system.

Moisture content had a significant effect on the response of the San Diego subgrade soil. The calculated value of the approximate modulus decreased with an increase in moisture content. The maximum decrease occurred between moisture contents from 19.1 to 21.7 percent. The nonlinear effects are far more significant at the lower moisture contents. The values of the Poisson's ratio increased slightly with increasing moisture content. The effect of moisture content on the response of a subgrade soil would depend on the particular subgrade soil being investigated.

GRANULAR MATERIALS

An examination of data summarized earlier indicates that the deformation of granular materials under loading conditions representative of those occurring in pavements is essentially time-independent and completely recoverable (after an initial conditioning period). In addition, the resilient response is nonlinear in that the confining pressure exerts a significant influence on the response of granular materials. This suggests that a nonlinear elastic constitutive law might be suitable in representing the behavior of granular materials. Techniques are described in previous sections to characterize paving materials using a nonlinear elastic model. Because of the limitations in time and funds for this study, no testing was performed on granular materials. The test results from a recent investigation conducted by Hicks (1970) at the University of California, Berkeley, to study factors influencing the resilient properties of granular materials, are analyzed using the techniques described earlier herein.

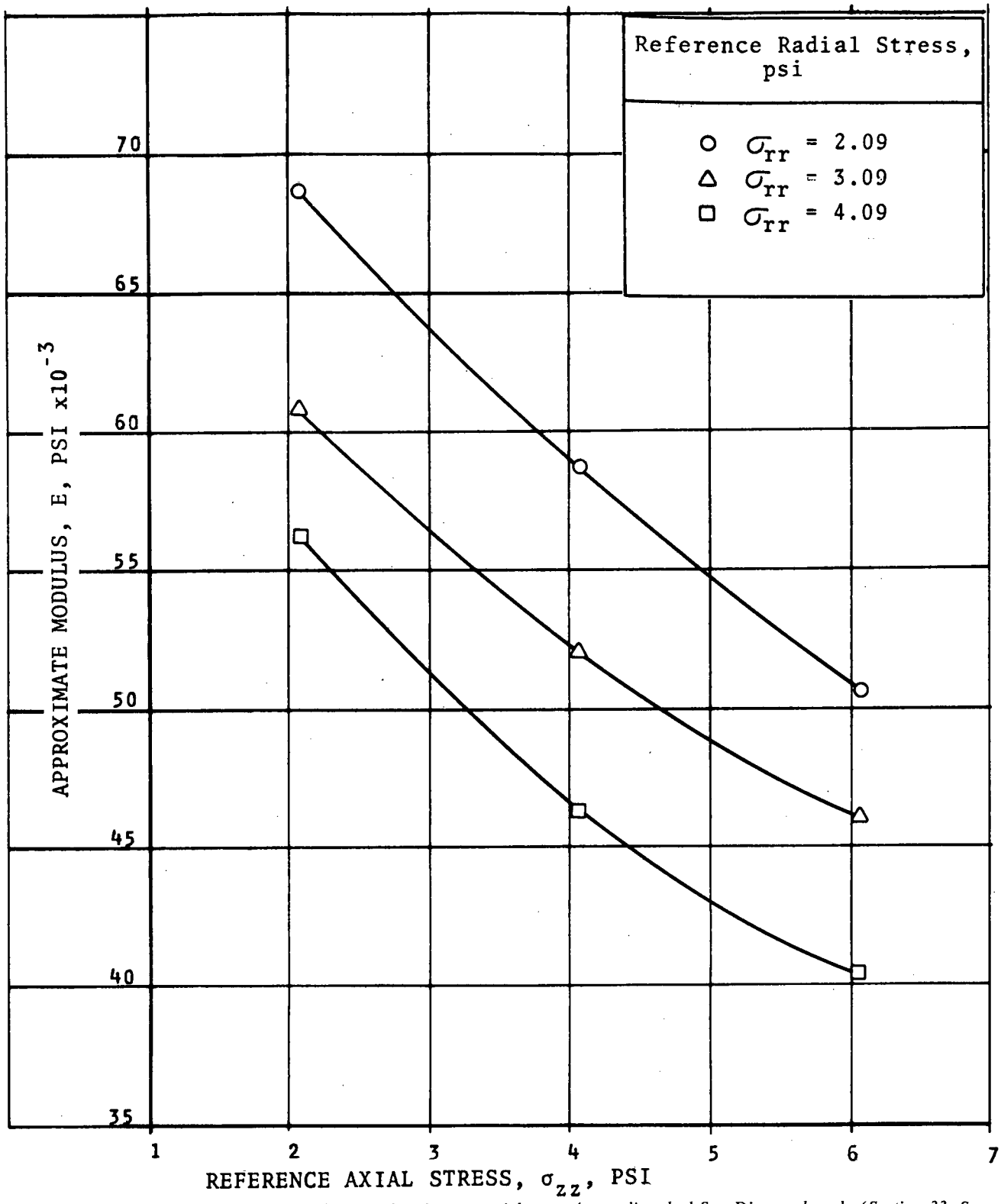

Figure 52. Variation of approximate modulus with reference axial stress for undisturbed San Diego subgrade (Section 33, Sample 40; Dehlen, 1969).

The incremental constitutive equation shown by Eq. 9 was selected to model nonlinear materials. However, all the available data (Hicks, 1970) were from tests in which only the axial stress was cycled above a static hydrostatic stress. Under these conditions, with measurements of axial and radial strains, only two of the incremental coefficients shown in Eq. 9 (namely, B_{13} and B_{33}) may be evaluated. These may be related to the elastic constants as follows:

$$E = 1/B_{33} \tag{14}$$

and

$$\nu = B_{13}/B_{33} \tag{15}$$

The testing procedures used for the characterization of

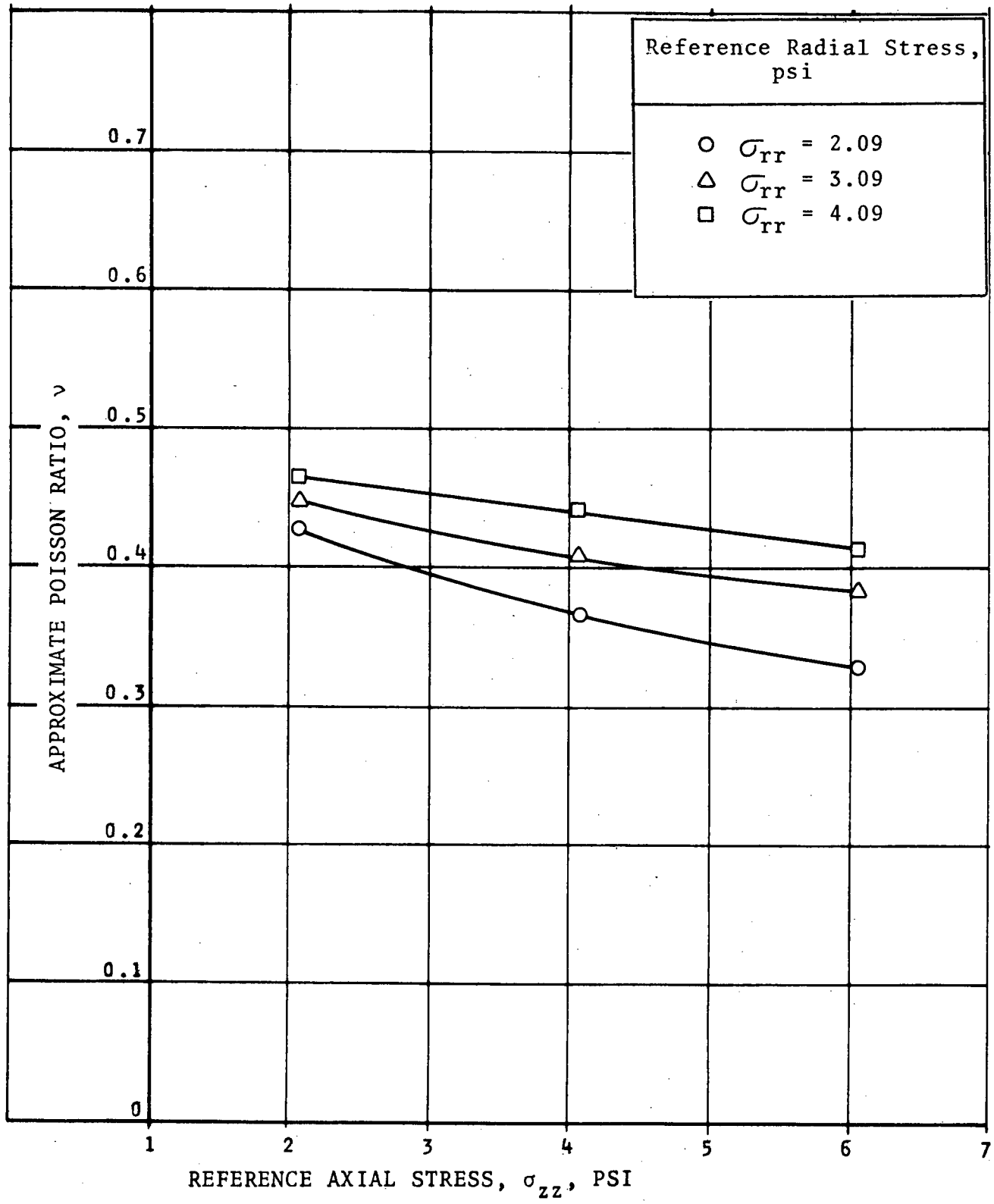

Figure 53. Variation of approximate Poisson's ratio with reference axial stress for undisturbed San Diego subgrade (Section 35, Sample 40; Dehlen, 1969).

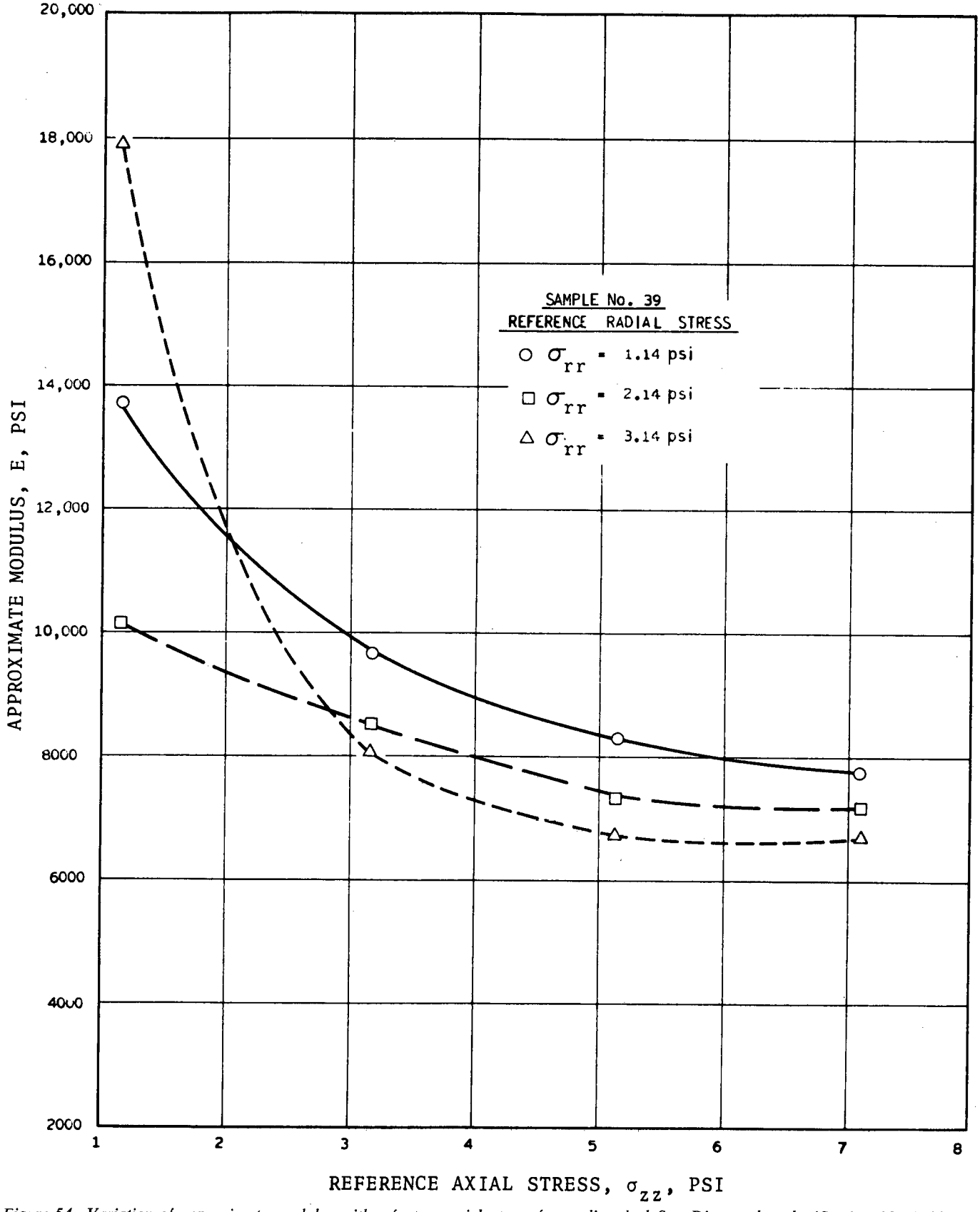

Figure 54. Variation of approximate modulus with reference axial stress for undisturbed San Diego subgrade (Section 35; Dehlen, 1969).

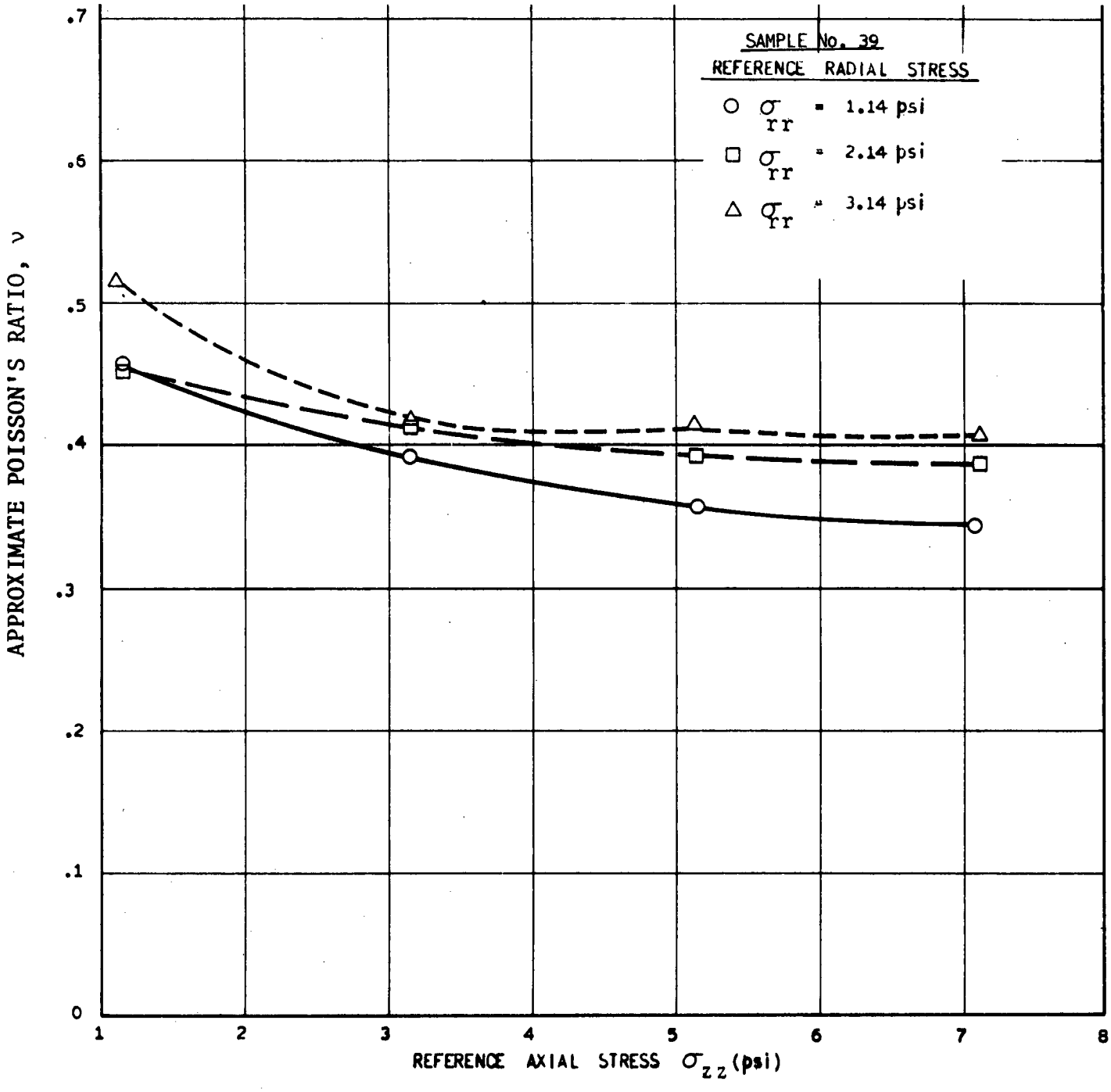

Figure 55. Variation of approximate Poisson's ratio with reference axial stress for undisturbed San Diego subgrade (Section 35; Dehlen, 1969).

granular materials adopted by Hicks (1970) were similar to those previously described for subgrade soils, except that the radial stress was not cycled. Specimens compacted to a desired density and moisture content were first conditioned with approximately 1,000 repetitions at a hydrostatic stress of 10 psi, and a repeated axial stress of 15 psi. After the application of the conditioning stresses, the axial stress was cycled and the axial and radial strains were measured after 50 to 100 repetitions. This procedure was repeated for different axial stress levels and hydrostatic stresses.

Stress-Strain Curves

Figures 60 and 61 show typical results of the repeated loading tests on a granular material in the form of stress-strain curves for dry and partially saturated, partially crushed aggregates. For tabulated values, see Appendix D. The nonlinear character of the stress-strain curves is evident in all cases. The effect of axial stress on the stress-strain curves increases with a decrease in hydrostatic stress. Furthermore, the magnitude of the hydrostatic stress in-

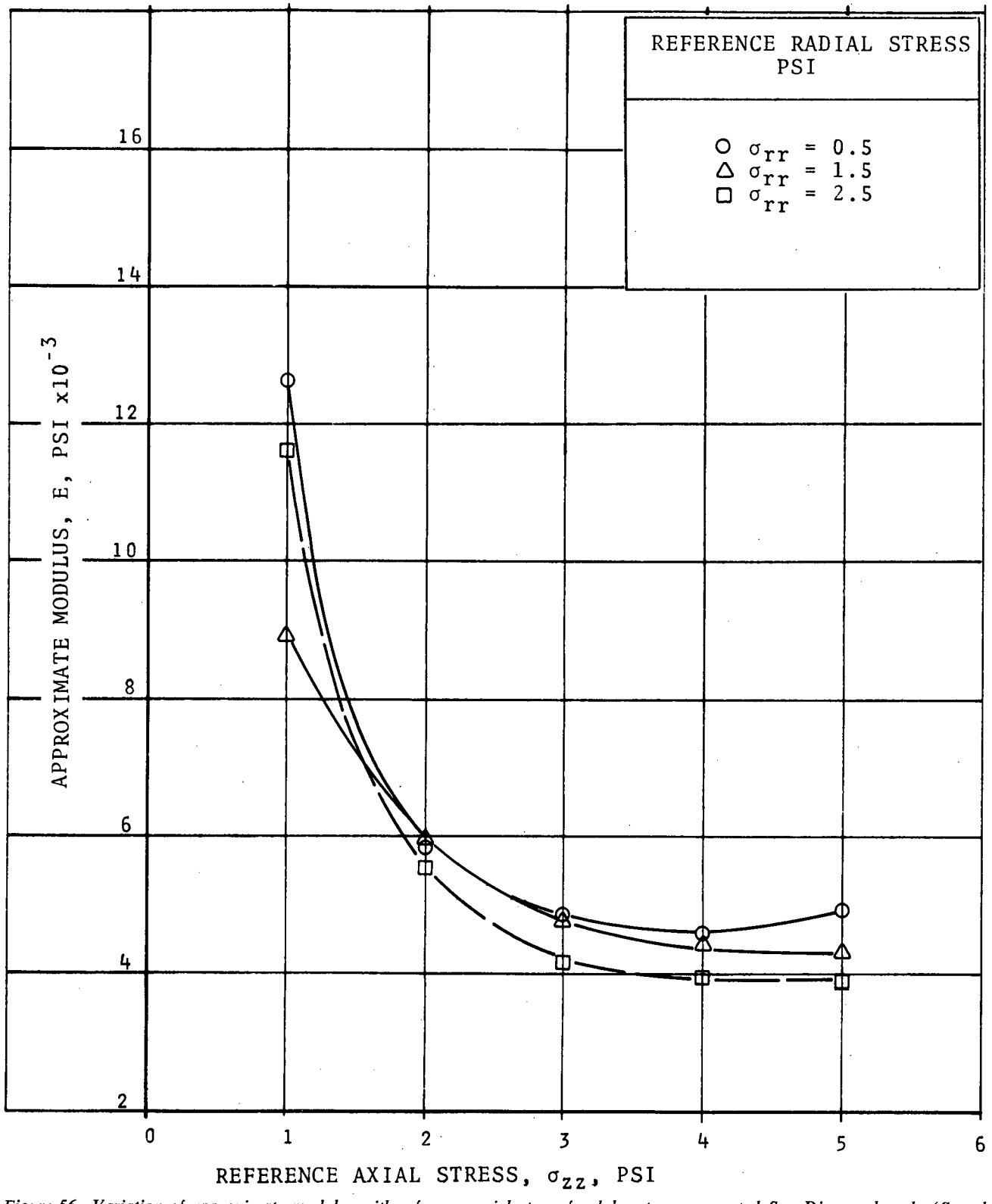

Figure 56. Variation of approximate modulus with reference axial stress for laboratory-compacted San Diego subgrade (Sample SD33-1).

fluences the slope of the axial stress-strain curve. For the axial strain, the specimens exhibited a stiffening-type response. For the radial strain, a softening pattern was observed.

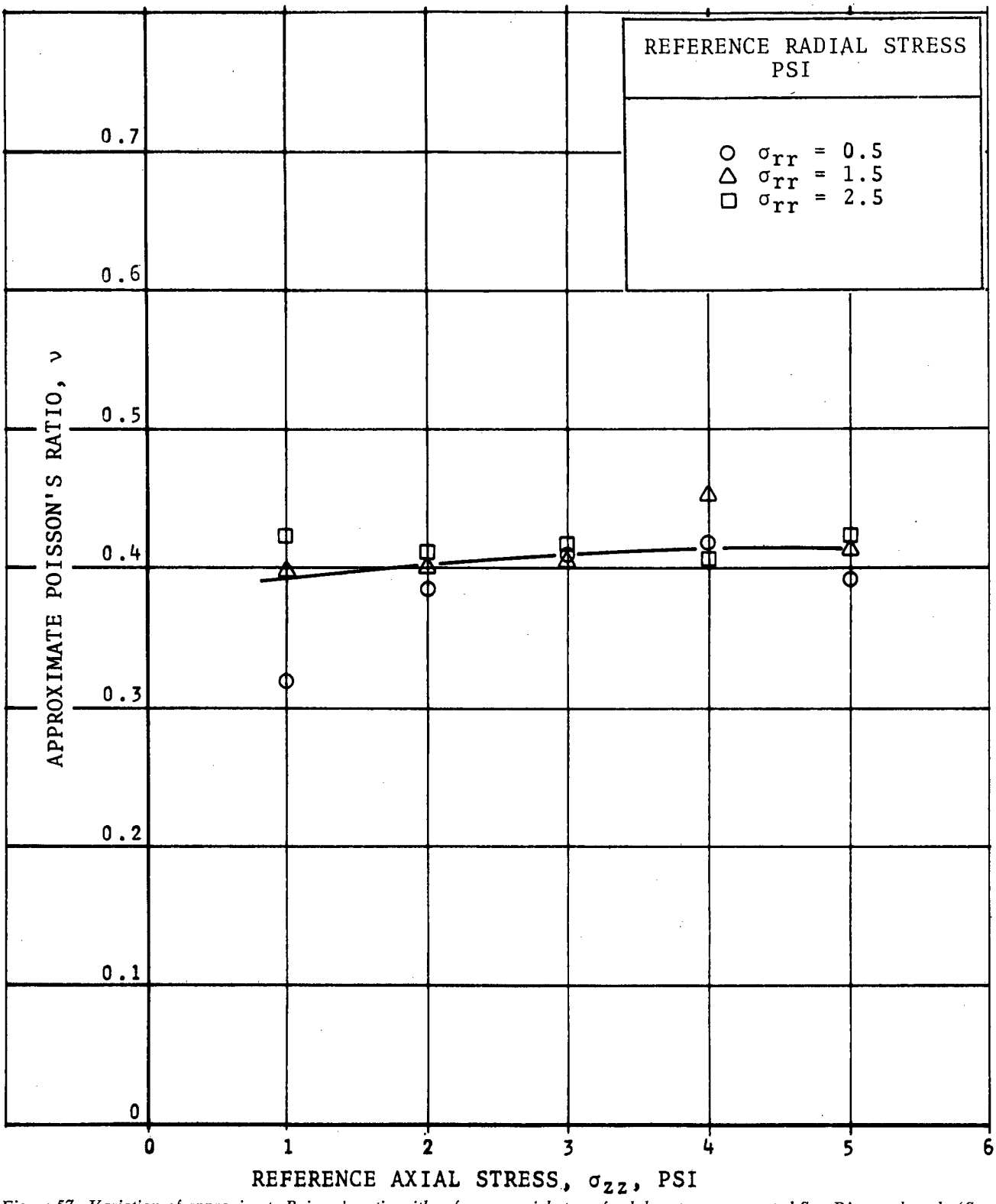

Figure 57. Variation of approximate Poisson's ratio with reference axial stress for laboratory-compacted San Diego subgrade (Sample SD33-1).

Incremental Coefficients and Approximate Modulus of Elasticity and Poisson's Ratio

Values of the incremental coefficients B_{33} and B_{13} at various stress states were calculated by a method used for subgrade soils. For the calculated values of the incremental coefficients, B_{33} and B_{13}, plotted against reference axial and radial stress, see Appendix D. In general, the value of B_{33} decreases with increasing axial stress for a fixed hydrostatic

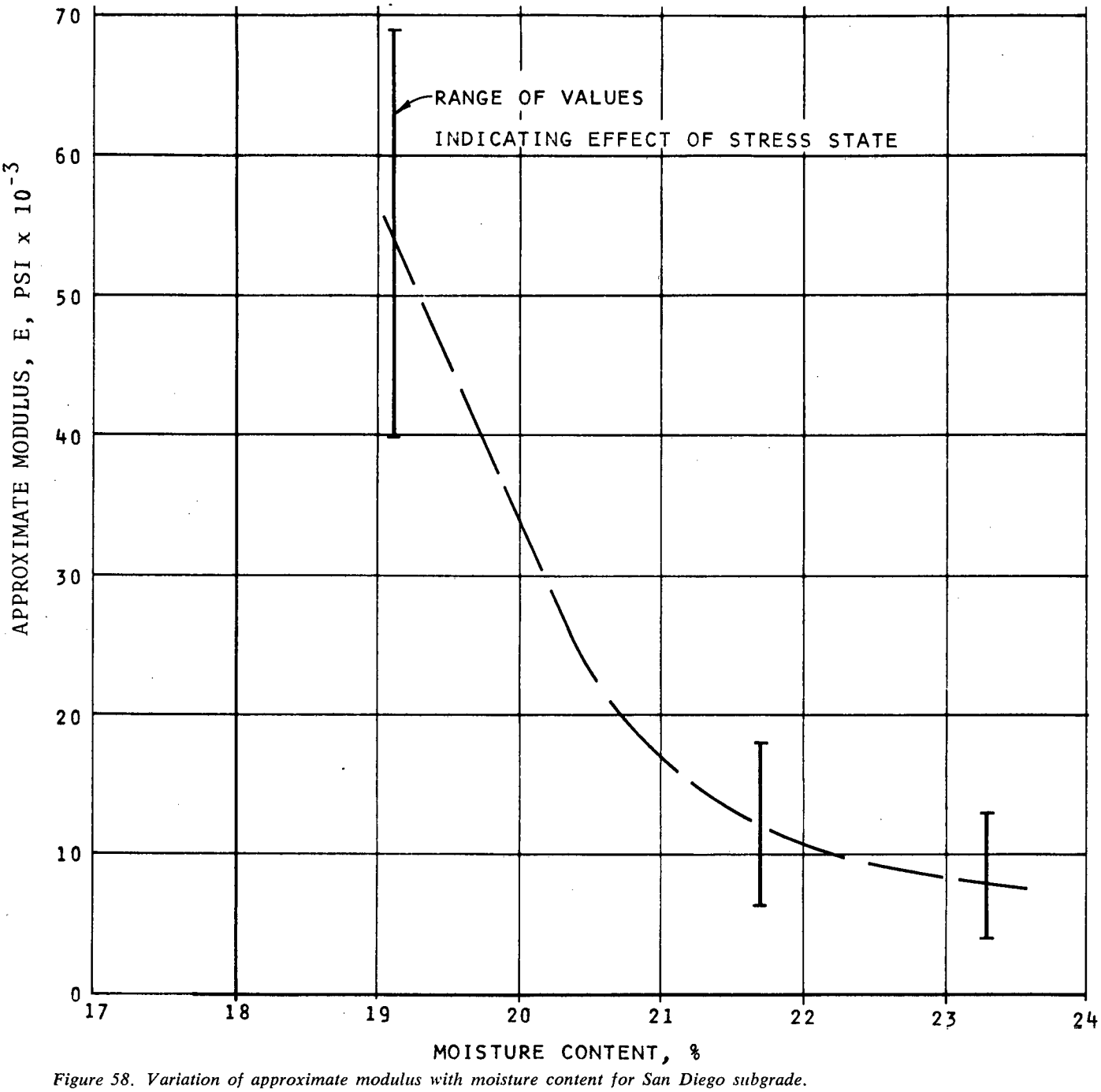

Figure 58. Variation of approximate modulus with moisture content for San Diego subgrade.

stress. The rate of decrease is greatest at the lower radial stress (or hydrostatic stress) and becomes smaller as the radial stress increases. This indicates that the value of the modulus increases with an increase in axial stress. The results show that B_{33} decreases with an increase in radial stress. The rate of decrease is greatest at the lower radial stress. B_{13} increases with increasing axial stress for a constant hydrostatic stress. The rate of increase becomes smaller as the radial stress increases. B_{13} decreases with an increase in radial stress. The values of the modulus and Poisson's ratio evaluated by Eqs. 14 and 15 are shown in Figures 62 to 65.

The variation of the modulus with radial stress (or hydrostatic stress) shown in Figures 62 and 64 indicates that for both dry and partially saturated granular materials the value of the approximate modulus increases with an increase in radial stress. An increase in axial stress also causes an increase in the modulus, as shown by the variation of B_{33} with axial stress. However, the effect of axial stress on the modulus is smaller than that of radial stress.

TABLE 3

SUMMARY OF RANGE OF INCREMENTAL COEFFICIENTS, APPROXIMATE MODULUS, AND POISSON'S RATIO FOR SAN DIEGO SUBGRADE SOIL

SAMPLE	MOISTURE CONTENT (%)	DRY DENSITY (PCF)	INCREMENTAL COEFFICIENTS $(1/PSI) \times 10^6$ $B_{11}+B_{12}$	$B_{31}+B_{32}$	B_{13}	B_{33}	APPROX. MODULUS (PSI)	APPROX. POISSON'S RATIO
Undisturbed No. 40	19.1	111	5.3 to 11.0	—7.3 to —19.0	—6.7 to —12.1	16.1 to 27.7	69,000 to 40,000	0.46 to 0.33
Undisturbed No. 39	21.7	107	30.0 to 58.0	—57.0 to —115.0	—23.0 to —75.0	80.0 to 189.0	18,000 to 6,600	0.50 to 0.34
Laboratory-compacted No. SD33-1	23.3	100	45.0 to 85.0	—52.0 to —120.0	—10.0 to —120.0	59.0 to 372.0	13,000 to 4,000	0.45 to 0.38

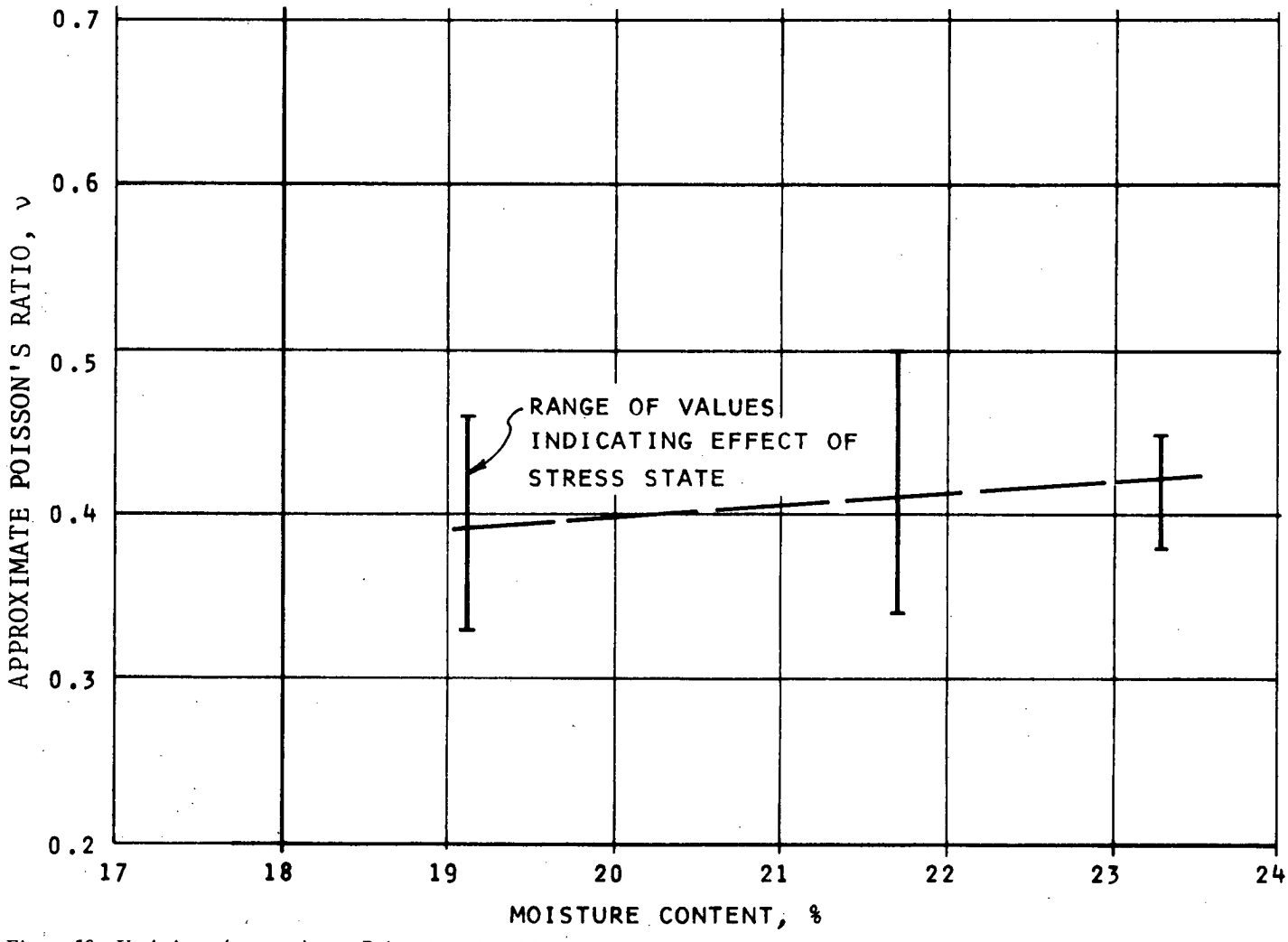

Figure 59. Variation of approximate Poisson's ratio with moisture content for San Diego subgrade.

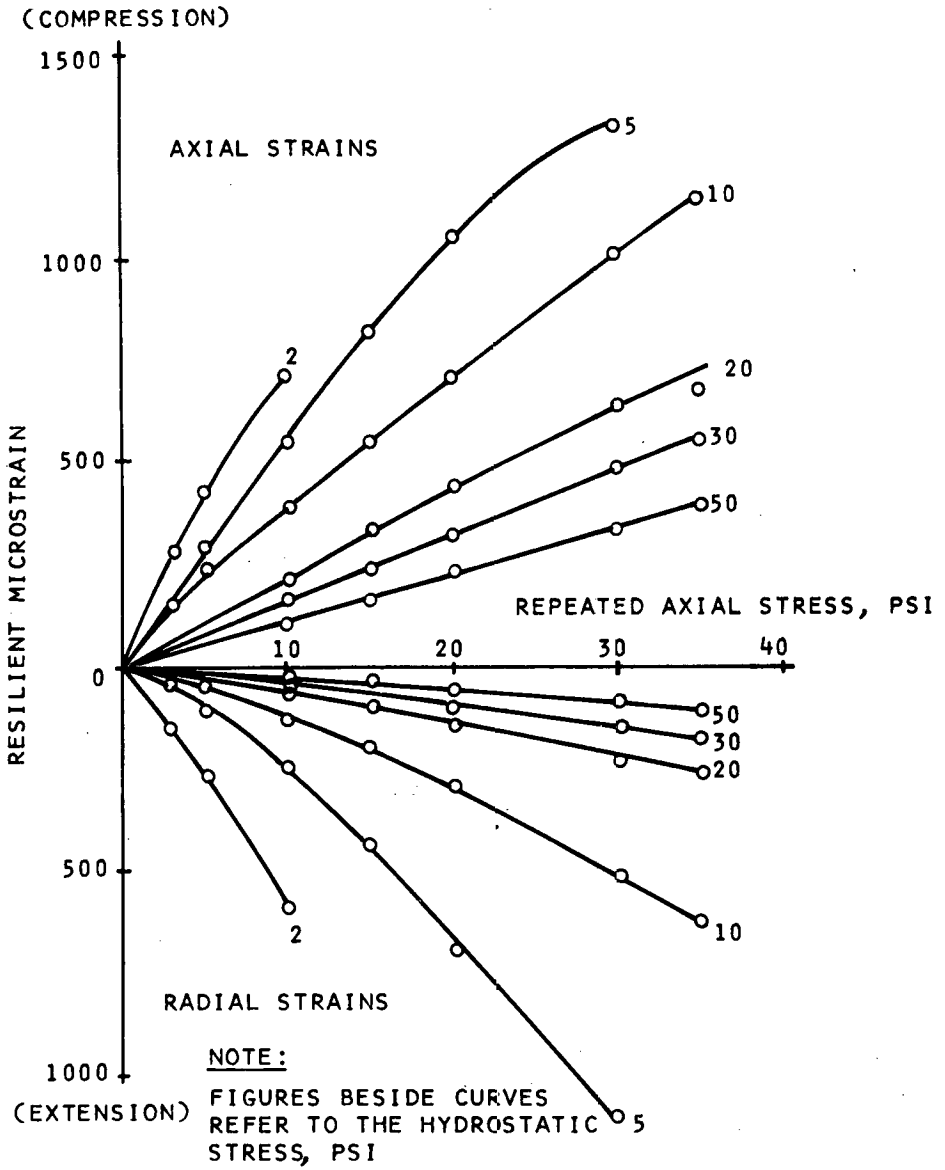

Figure 60. Variation in axial and radial strains with repeated axial stress. Aggregate base Sample No. K(0)-1D. (After Hicks, 1970.)

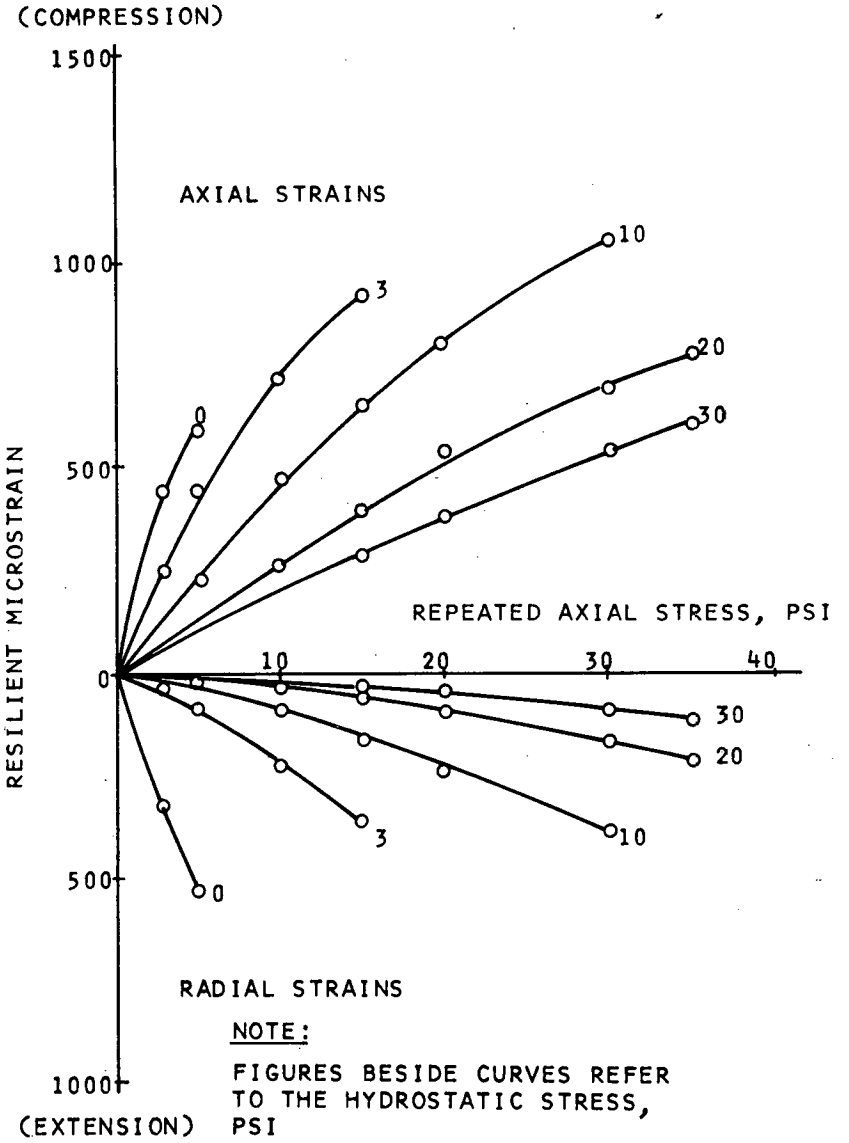

Figure 61. Variation in axial and radial strains with repeated axial stress. Aggregate base Sample No. K(0)-1P2. (After Hicks, 1970.)

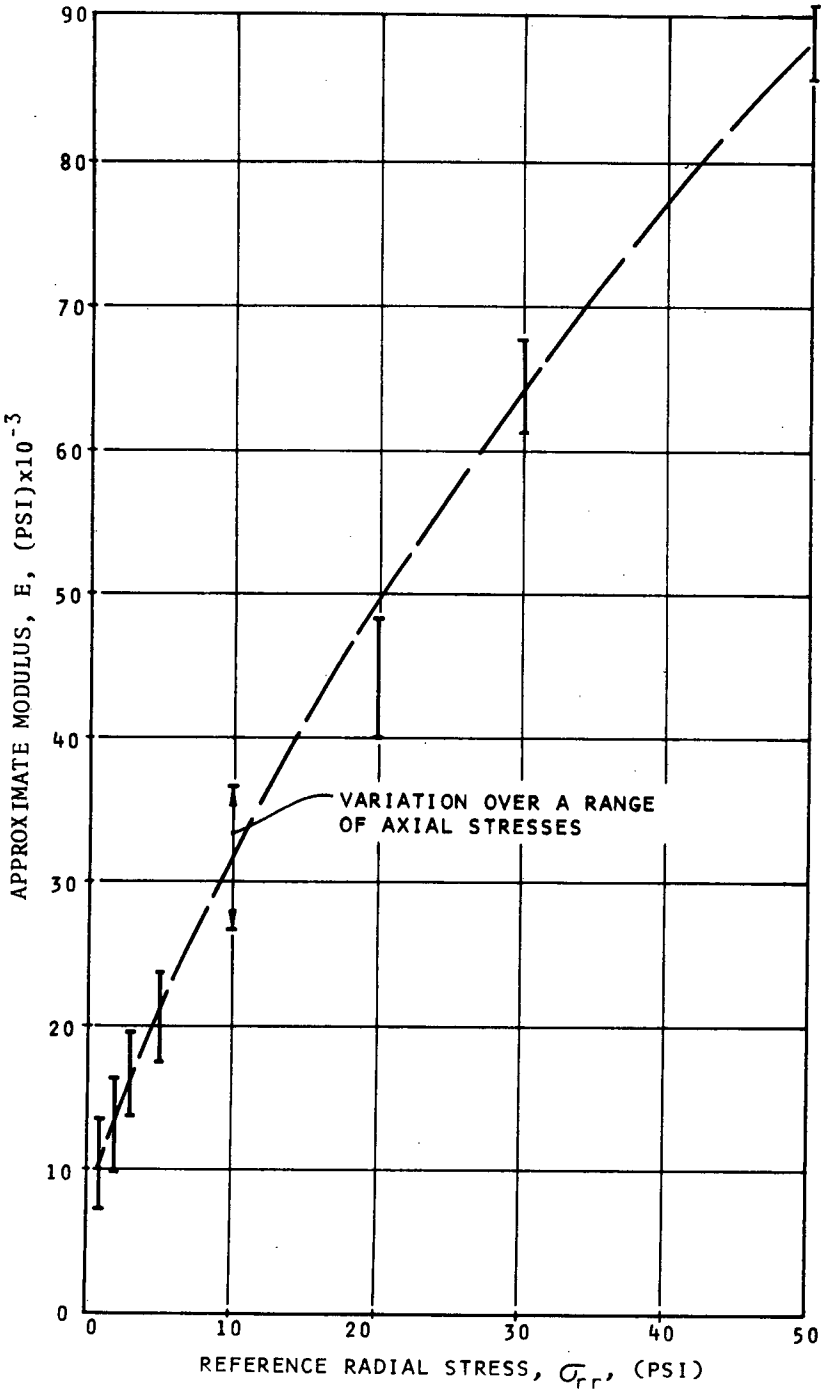

Figure 62. Variation of approximate modulus with radial stress for a dry granular material. Sample No. K(0)-1D.

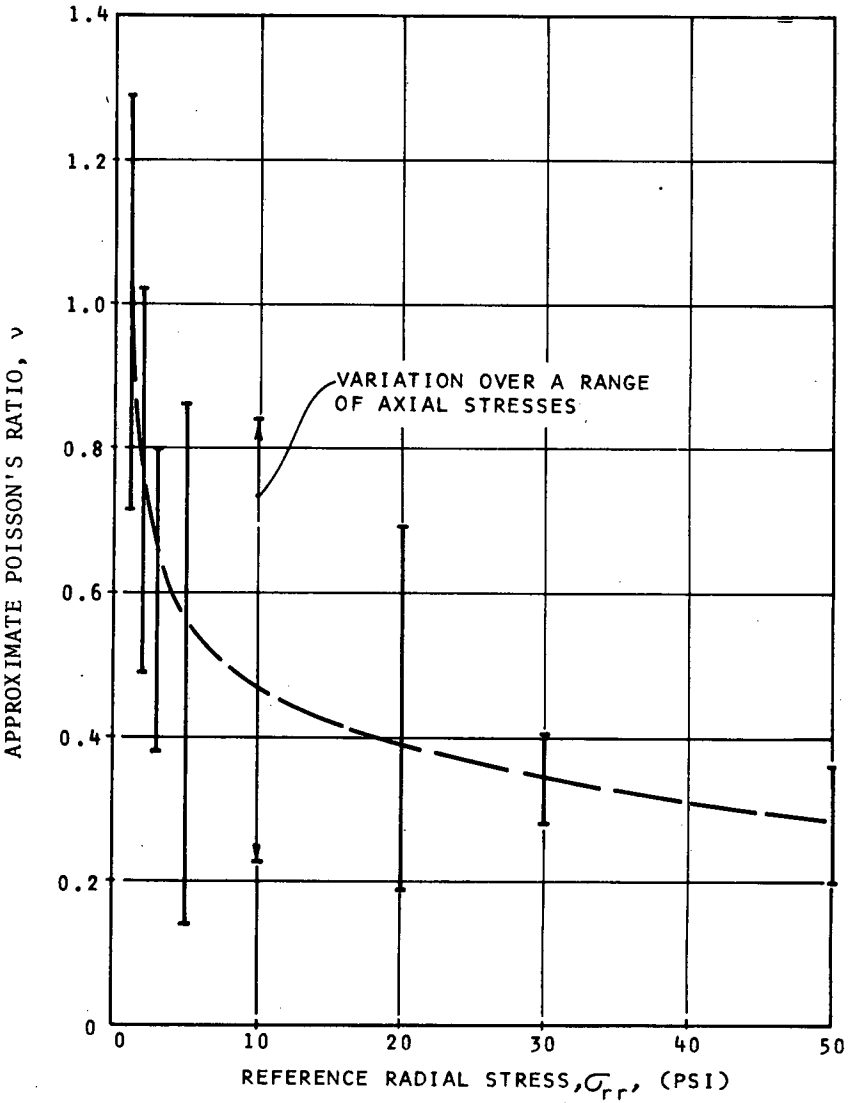

Figure 63. Variation of approximate Poisson's ratio with radial stress for a dry granular material. Sample No. K(0)-1D.

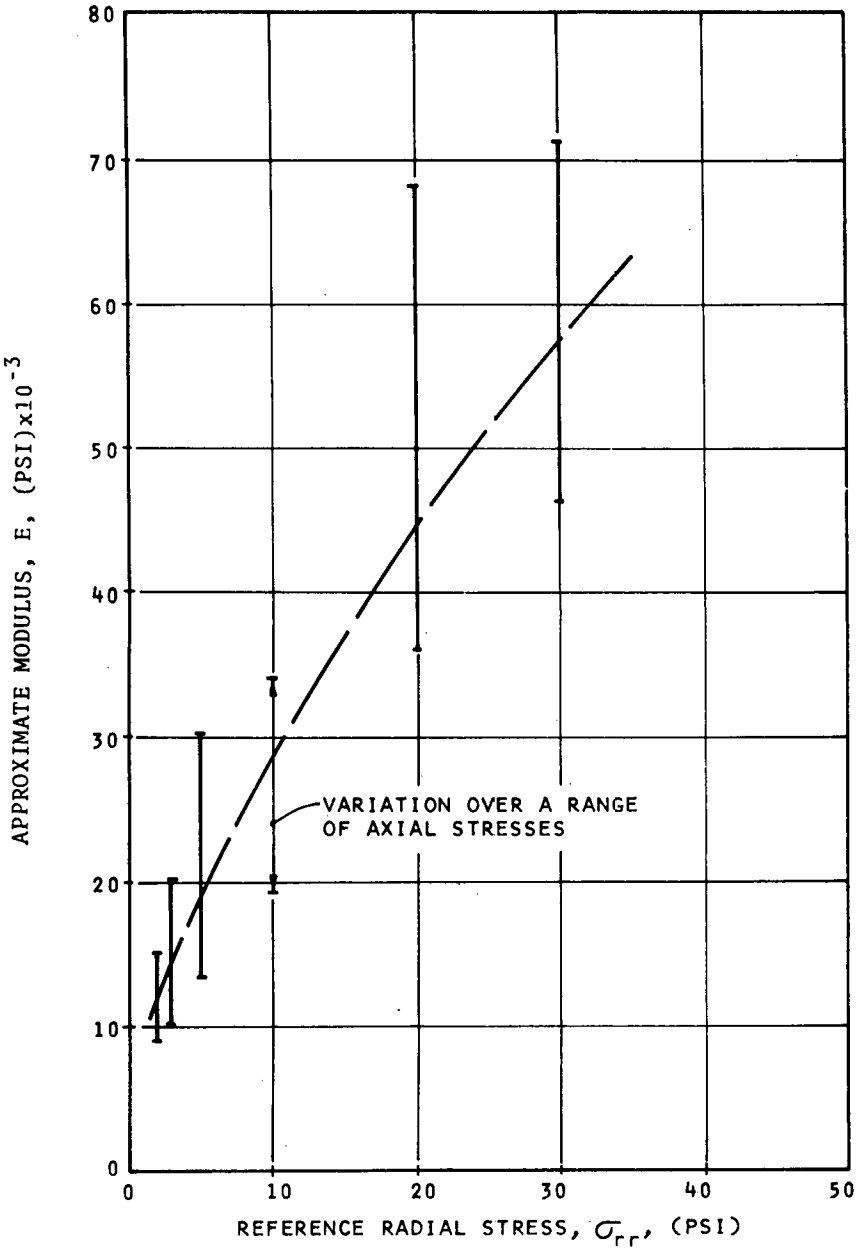

Figure 64. Variation of approximate modulus with radial stress for a partially saturated granular material. Sample No. K(0)-1P2.

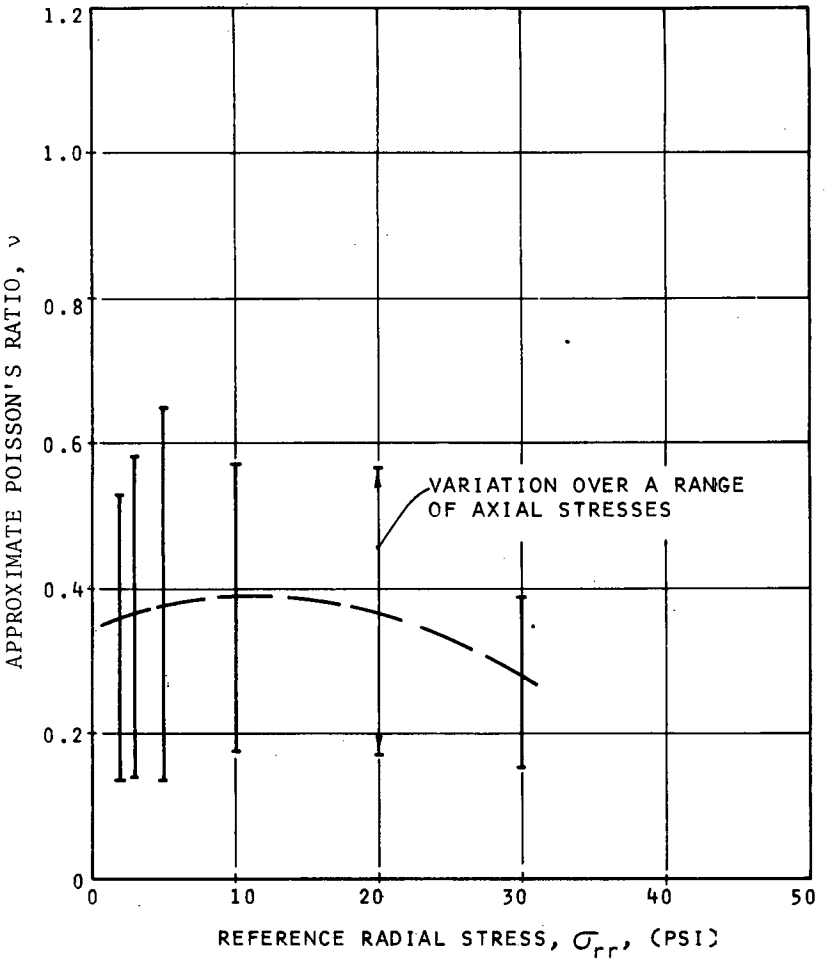

Figure 65. Variation of approximate Poisson's ratio with radial stress for a partially saturated granular material. Sample No. K(0)-1P2.

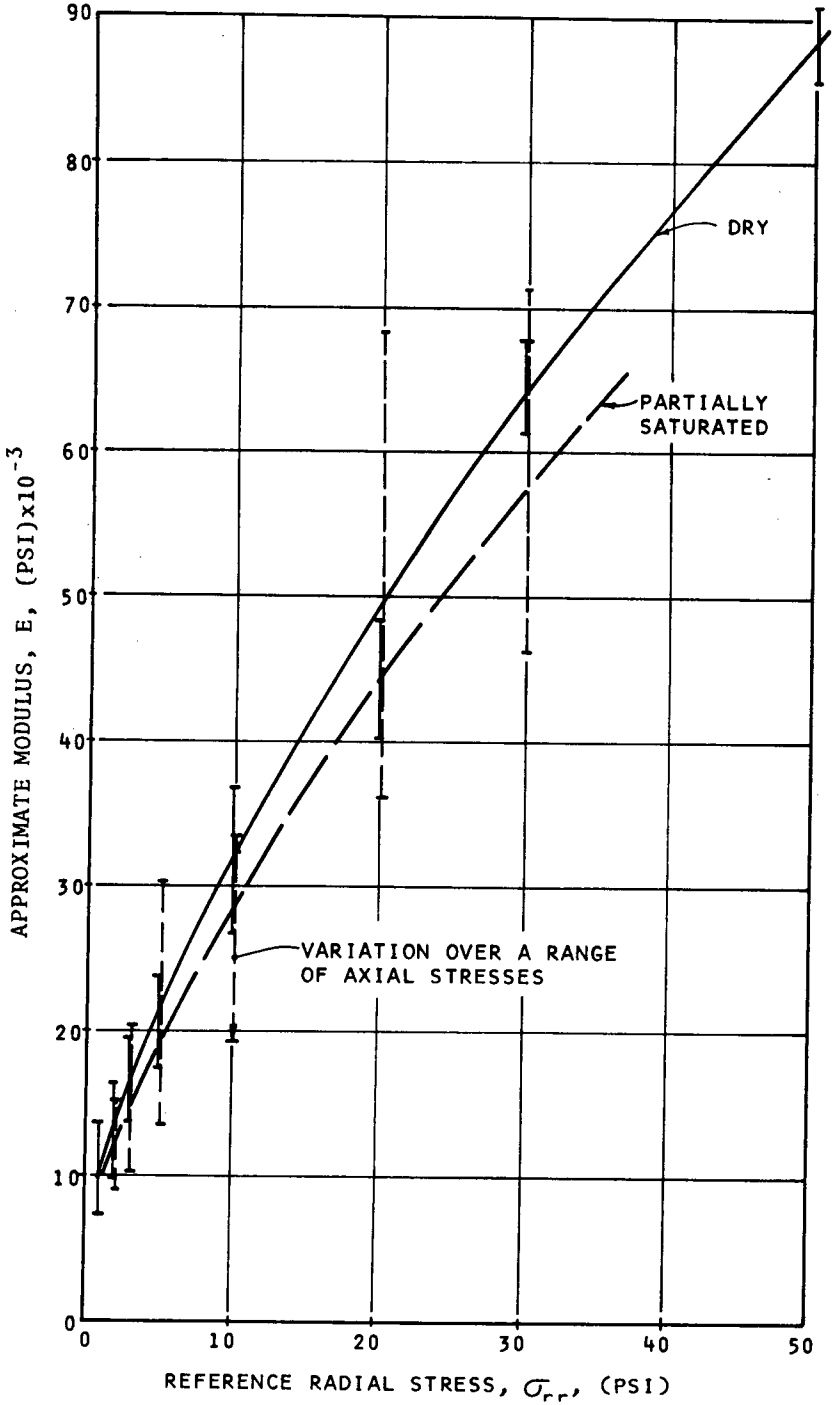

Figure 66. Variation of approximate modulus with radial stress for dry and partially saturated granular materials.

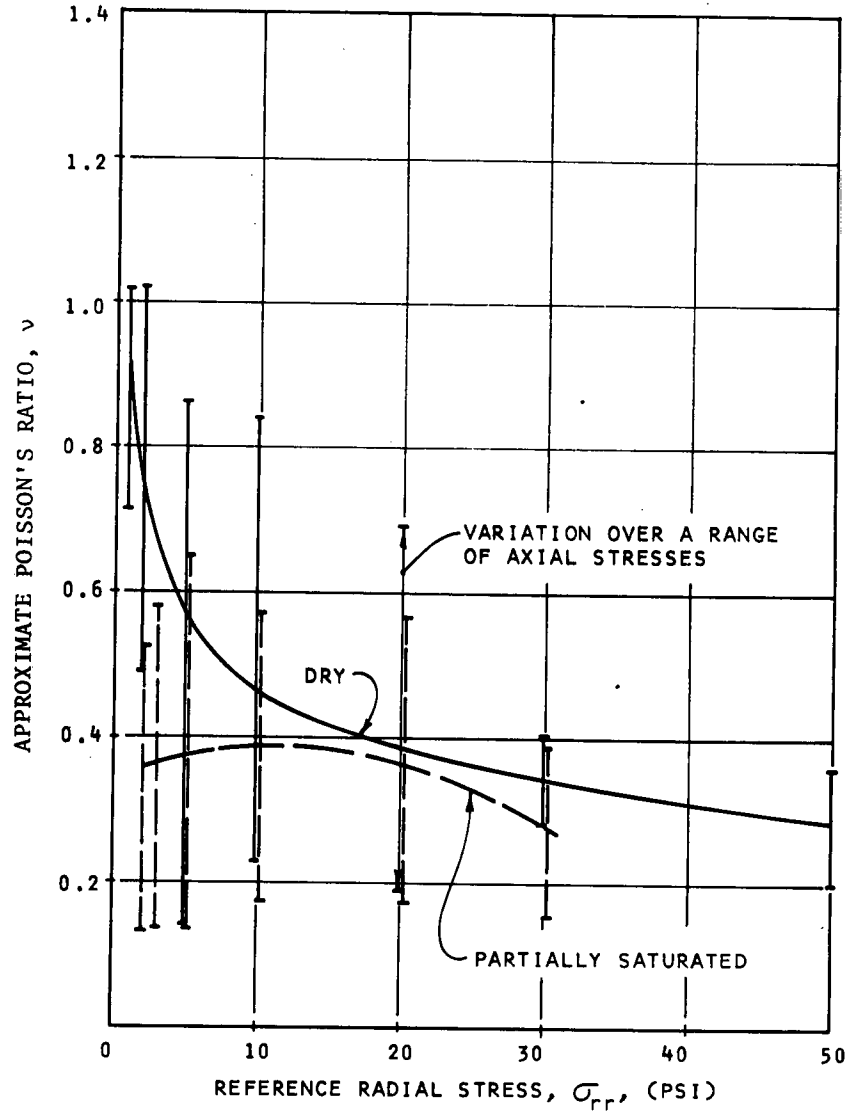

Figure 67. Variation of approximate Poisson's ratio with radial stress for dry and partially saturated granular materials.

The variation of the Poisson's ratio with reference stress state shown in Figures 63 and 65 indicates that both axial and radial stresses have a great effect on the value of the Poisson's ratio. The value of the Poisson's ratio varies from 0.2 to 1.3 for the dry sample and from 0.14 to 0.64 for the partially saturated sample. The higher values of Poisson's ratio were observed at stress states which included a combination of low radial stress and a relatively high axial stress. At the radial stress higher than 30 psi, the value of Poisson's ratio varies from 0.2 to 0.4. The high values of Poisson's ratio can be a result of the anisotropy of the material or the effect of a volume increase (dilation) under compressive stresses. The phenomena of dilatancy of granular materials are well documented in soil mechanics literature. Values of Poisson's ratio depend on the type of material, the relative density, and the stress state.

Comparison of the values of the modulus and Poisson's ratio for the dry and partially saturated samples on the basis of total stresses shown in Figures 66 and 67 indicates that both the approximate modulus and Poisson's ratio are reduced as the degree of saturation increases. Hicks (1970) indicates, however, that if compared on the basis of effective stresses, an increase in the degree of saturation causes a reduction in Poisson's ratio, but the effect on the modulus is not significant.

Summary

Previous investigators have shown that the response of granular materials is recoverable and time-independent, and is dependent on the stress state. This suggests that a nonlinear elastic model is suitable for characterizing granular materials.

The results of repeated loading tests on the granular materials performed by Hicks (1970) indicate that the radial stress (or hydrostatic stress) exerts a major influence on the stress-strain behavior of the material. Dilatancy effects can significantly influence the determination of any material functions.

The moisture content, as indicated by the degree of saturation, affected the response of the material. As the degree of saturation increased, both the approximate modulus and Poisson's ratio were reduced.

CHAPTER FOUR

CONCLUSIONS AND RECOMMENDATIONS

Characterization of materials (i.e., selection of constitutive equations) is an essential step in the determination of the mechanical state (i.e., stress and strain) that is induced in a pavement system under the loading and environmental conditions that are likely to exist in service. Consequently, material characterization is necessary to the development of a theoretically sound basis for the design and analysis of pavement systems.

The materials characterization phase of this project is considered to be the initial effort in a long-range endeavor to develop better methods for characterizing the materials that comprise a pavement system. During this project, significant effort was expended in developing an understanding of previous work relevant to materials characterization in the field of pavements and other related areas. This was done to provide a sound basis for future work in materials characterization as applied to the analysis and design of pavement systems.

CONCLUSIONS

From the results of this investigation, which considered both the general methodology of materials characterization and the application of the methodology to specific problems, the following general conclusions are drawn:

1. Characterization of materials for use in the analysis of pavement systems generally is an iterative process. It includes the selection of realistic constitutive equations to represent the materials and an evaluation and possible modification of the selection based on a study of field performance.

2. The selection of constitutive equations to represent material response is limited to those for which suitable testing techniques exist and for which pertinent boundary value problems can be solved.

3. Because it is not possible to select constitutive equations that are sufficiently general to be valid under all conditions, it is necessary to identify the conditions under which the pavement is expected to perform in service. The characterization of the materials should then be conducted for these "service conditions."

4. The materials in a pavement system are subject to general three-dimensional stress states. Therefore, conducting a complete characterization program would require the ability to apply arbitrary combinations of principal stresses, and also shear stress, in the presence of arbitrary normal stresses. The apparatus used in this study is a considerable improvement over that previously used in the characterization of materials for pavement systems;

however, it is deficient in that it does not completely meet the foregoing requirements.

5. From an examination of available experimental data of the response of asphaltic concrete and cohesive subgrade soils it was concluded that no single constitutive equations will be of sufficient generality to model all aspects of material response under the loading and environmental conditions that exist in a pavement system.

6. On the basis of conclusion (5), it is necessary to divide the problem of the determination of the mechanical state in order to reduce the number of aspects of material response that have to be modeled. This division is best done on the basis of loading conditions.

7. A standard procedure can be used for testing specimens in a triaxial configuration in order to determine a limited number of the material functions necessary to characterize a material according to a physically nonlinear elastic constitutive law. (In all further discussion it should be understood that when the term nonlinear is used, only physical nonlinearity is implied.)

The specific loading condition used in this investigation was a repeated load of short duration applied after an initial conditioning program. Based on a study of existing information, a nonlinear elastic model was selected as the first step in the iteration for developing suitable constitutive equations for asphaltic concrete, cohesive subgrade soil, and granular materials. Although an incremental formulation for the nonlinear law is used in this report, the data developed could be used in other methods of representing nonlinear behavior. Consequently, the experimental program was designed for verifying and quantifying the nonlinear elastic representation of the various materials. As an aid to understanding the following specific conclusions regarding material response which are based on the experimental information obtained in this investigation, the incremental form of the constitutive equation is restated.

The general form of the incremental formulation in the neighborhood of a reference state is

$$\epsilon_{ij} + \epsilon_{ij}' = G_{ij}(\sigma_{mn}) + B_{ijkl}\,\sigma_{kl}' \qquad (16)$$

in which ϵ_{ij} and σ_{mn} represent the reference stress and strain states; and ϵ_{ij}' and σ_{kl}' represent the increments of strain and stress. B_{ijkl} is the "incremental modulus tensor" that is, in general, anisotropic and depends explicitly on the stress state.

Under the stress conditions of a triaxial test, incremental stresses and strains are related as follows:

$$\begin{Bmatrix} \epsilon_{rr}' \\ \epsilon_{zz}' \end{Bmatrix} = \begin{bmatrix} B_{11} + B_{12} & B_{13} \\ B_{31} + B_{32} & B_{33} \end{bmatrix} \begin{Bmatrix} \sigma_{rr}' \\ \sigma_{zz}' \end{Bmatrix} \qquad (17)$$

An approximate modulus of elasticity and Poisson's ratio based on the following were also computed:

$$\nu/E = B_{12} = \tfrac{1}{3}(B_{13} + B_{31} + B_{32}) \qquad (18)$$

$$1/E = \tfrac{1}{2}(B_{11} + B_{33}) \qquad (19)$$

Specific conclusions for each of the three materials investigated follow.

Asphaltic Concrete

1. The response of asphaltic concrete is a function of stress state and temperature.

2. Temperature was the most important factor in determining the response of asphaltic concrete. This suggests that the characteristics of the asphalt cement are of major significance.

3. The assumption of no permanent deformation occurring under a single application of a load of short duration appears to be valid.

4. For temperatures in excess of 70°F, the magnitude of the time-dependent effects is such that the errors from using an elastic constitutive law could be significant.

5. At temperatures below 100°F, the major influence of the stress level was on B_{33}. However, at temperatures equal to and above 100°F, the stress level has considerable influence on all the coefficients.

6. A study of the ratios $2B_{13}/(B_{31} + B_{32})$ and $(B_{11} + B_{12})/(B_{33} + B_{13})$ indicates that the incremental modulus tensor is anisotropic. The degree of anisotropy is a function of temperature and stress state.

7. Temperature exerts a major influence on the approximate modulus of elasticity and Poisson's ratio. The average value of the approximate modulus decreased from 2.3×10^6 psi at 40°F, to 6.8×10^4 psi at 100°F, and to 8.5×10^3 psi at 140°F. The average value of Poisson's ratio increased from 0.27 at 40°F to 0.49 at 140°F.

8. The influence of the radial stress level at a constant temperature was less than that of the axial stress level. In general, the approximate modulus of elasticity increased with increasing axial compressive stress and decreased with increasing axial tensile stress. The influence of stress level increased with an increase in temperature.

Cohesive Subgrade Soils

1. Under the stress states used in this investigation, the response of the subgrade soil from the San Diego Test Road was essentially time-independent.

2. Water content and stress state significantly influenced the response of the subgrade soils.

3. Over the range of water contents used, a nonlinear elastic constitutive law provided a satisfactory means of representing the response of the subgrade soil.

4. The effect of water content was to change the magnitude of the parameters used in the representation of the nonlinear elastic formulation.

5. The incremental coefficients B_{33} and B_{13} increase with increasing axial stress, indicating nonlinear behavior. The influence of the radial stress is significant on $(B_{11} + B_{12})$ and $(B_{31} + B_{32})$.

6. An examination of the ratios $(B_{11} + B_{12})/(B_{33} + B_{13})$ and $2B_{13}/(B_{31} + B_{32})$ indicates that anisotropy in the incremental modulus of tensor is a function of the stress state.

7. The approximate modulus decreases with increasing axial reference stress at a constant radial stress; and the rate of decrease in modulus is greatest up to a stress level of 3 psi. The modulus decreased from 69,000 to 40,000 psi at water content of 19.1 percent and a dry density of 111 pcf; from 18,000 to 6,000 psi for a water content of

21.7 percent and a dry density of 107 pcf; and from 13,000 to 4,000 psi at a water content of 23.3 percent and a dry density of 100 pcf. At axial stress levels greater than 6 psi the modulus is approximately constant. The modulus also decreases with increasing radial reference stress, but the effect is minor compared to the effect of the axial stress.

8. The stress level has a minor influence on the approximate Poisson's ratio; the values range from 0.34 to 0.50.

9. An increase in water content and a decrease in density cause a decrease in the approximate modulus and an increase in Poisson's ratio. The modulus decreases from an average of 50,000 psi at 19.1 percent and a dry density of 111 pfc to 10,000 psi at a moisture content of 23.3 percent and a dry density of 100 pcf.

Granular Material

1. The response of granular materials is essentially time-independent and is dependent on the stress state. This is true for both dry and partially saturated granular materials.

2. The effect of axial stress on the axial stress-strain characteristics increases with a decrease in the hydrostatic (confining) stress. An increase in the hydrostatic stress causes the resistance to deformation in the axial direction to increase.

3. The influence of the stress state on the approximate modulus can be expressed as a function of the first stress invariant, indicating that the radial stress exerts the major influence on the modulus. The approximate modulus increased from about 10,000 to 90,000 psi for a hydrostatic stress increase from 5 to 90 psi. At any constant hydrostatic stress the increase in modulus due to a change in repeated axial stress did not exceed 10,000 psi.

4. Poisson's ratio was significantly influenced by the stress state. Values of Poisson's ratio greater than 0.5 were computed. These may result from neglecting stress-induced anisotropy or dilatation effects.

RECOMMENDATIONS

It is recommended that additional research be conducted along two phases that can and should be carried out concurrently.

1. *Phase I.* Characterization of soils and paving materials under representative service conditions. This involves continuing the research along present lines, but extending the characterization to include other constitutive laws and for other aspects of the pavement problem.

2. *Phase II.* Development and application of techniques for the solution of nonlinear boundary value problems.

Phase I would, in effect, be a continuation of the present work. Other aspects of the problem of determining the mechanical state (e.g., under stationary loads and at high temperature, where the time-dependent response is significant) should be studied. This would include the application of linear and nonlinear viscoelasticity to the characterization of paving materials. An important aspect of any continuing work in materials characterization is the development of new experimental techniques. Efforts should be directed toward developing methods for testing with independent control of the three principal stresses. In addition, new techniques for measuring the deformation of samples under dynamic loads should be investigated.

The work recommended in Phase II is essential in applying the improved characterization of paving materials to the analysis and design of pavement systems and in evaluating the degree of refinement necessary in the characterization of materials. At present, techniques for developing solutions to nonlinear boundary value problems representative of the pavement system are in a developmental stage. In nonlinear analysis, the solution techniques and the characterization procedures are interdependent. Therefore, it is necessary that Phase I and Phase II proceed concurrently.

REFERENCES

AVRAMESCO, A., "Dynamic Phenomena in Pavements Considered as Elastic Layered Structures." *Proc. 2d Internat. Conf., Structural Design of Asphalt Pavements,* Univ. of Mich. (1967) pp. 163-169.

BARDEN, L., "Stresses and Displacements in a Cross-Anisotropic Soil." *Geotechnique* (1963) p. 198.

BIAREZ, J., "Contribution à l'Étude des Properiétés Mecaniques des Sols et des Materiaux Pulverulents." D.Sc. thesis, Univ. of Grenoble (1962).

BROWN, S. F., and PELL, P. S., "An Experimental Investigation of the Stresses, Strains, and Deflections in a Layered Pavement Structure Subjected to Dynamic Loads." *Proc. 2d Internat. Conf., Structural Design of Asphalt Pavements,* Univ. of Mich. (1967) pp. 384-403.

BUSCHING, H. W., GOETZ, W. H., and HARR, M. E., "Stress-Deformation Behavior of Anisotropic Bituminous Mixtures." *Proc. AAPT* (1967) p. 632.

COFFMAN, B. S., "Pavement Deflections from Laboratory Tests and Layer Theory." *Proc. 2d Internat. Conf., Structural Design of Asphalt Pavements,* Univ. of Mich. (1967) pp. 664-708.

DEHLEN, G. L., "The Effect of Non-Linear Material Response on the Behavior of Pavements Subjected to Traffic Loads." Ph.D. dissertation, Univ. of Calif., Berkeley (1969).

EPPS, J. A., Influence of Mixture Variables on the Flexural Fatigue and Tensile Properties of Asphalt Concrete." Ph.D. thesis, Univ. of Calif., Berkeley (1968).

GERRARD, C. M., and MULHOLLAND, P., "Stress Strain and Displacement Distributions in Cross-Anisotropic and Two-Layer Isotropic Elastic Systems." *Proc. 3rd Conf. Australian Road Res. Board,* Part 2 (1966) p. 1123.

HICKS, R. G., "Factors Influencing the Resilient Properties of Granular Materials." Ph.D. thesis, Univ. of Calif., Berkeley (1970).

HOLDEN, J. C., "Stresses and Strains in a Sand Mass Subjected to a Uniform Circular Load." *Report No. 13,* Dept. of Civil Eng., Univ. of Melbourne (1967).

KROKOSKY, E. M., ANDREWS, R. D., JR., and TONS, E., "Rheological Properties of Asphalt/Aggregate Compositions." *Proc. ASTM,* Vol. 63 (1963).

LARA-THOMAS, M., "Time-Dependent Deformation of Clay Soils Under Shear Stress." *Proc. Internat. Conf., Structural Design of Asphalt Pavements,* Univ. of Mich. (1962) pp. 592-605.

MATERIALS RESEARCH AND DEVELOPMENT, INC., "Pavement Instrumentation Studies for San Diego County Experimental Base Project." (1966).

MATERIALS RESEARCH AND DEVELOPMENT, INC., "Pavement Instrumentation Studies for San Diego Experimental Base Project." *Rept. 10229-6* (1968).

MONISMITH, C. L., ALEXANDER, R. L., and SECOR, K. E., "Rheologic Behavior of Asphalt Concrete." *Proc. AAPT,* Vol. 35 (1966) pp. 400-450.

MORGAN, J. R., "The Response of Granular Materials to Repeated Loading." *Proc. 3rd Conf. Australian Road Res. Board,* Part 2 (1966) p. 1178.

PAGEN, C. A., "An Analysis of Thermorheological Response of Bituminous Concrete." Ph.D. thesis, Ohio State Univ. (1963).

PISTER, K. S., and WESTMANN, R. A., "Analysis of Viscoelastic Pavements Subjected to Moving Loads." *Proc. Internat. Conf., Structural Design of Asphalt Pavements,* Univ. of Mich. (1962) pp. 522-529.

RICHARDS, B. G., "Moisture Flow and Equilibria in Unsaturated Soils for Shallow Foundations." Symp. on Permeability and Capillarity of Soils, *ASTM STP 417* (1967).

SAUER, E. K., and MONISMITH, C. L., "Influence of Soil Suction on Behavior of Glacial Till Subjected to Repeated Loading." *Hwy. Res. Record No. 215* (1968) pp. 8-22.

SCHAUB, J. H., and GOETZ, W. H., "Strength and Volume Change Characteristics of Bituminous Mixtures." *Proc. HRB,* Vol. 40 (1961) pp. 371-405.

SEED, H. B., and CHAN, C. K., "Effect of Stress History and Frequency of Stress Application on Deformation on Clay Subgrades Under Repeated Loading." *Proc. HRB* (1958) p. 555.

SEED, H. B., CHAN, C. K., and LEE, C. E., "Resilience Characteristics of Subgrade Soils and Their Relation to Fatigue Failures in Asphalt Pavements." *Proc. Internat. Conf., Structural Design of Asphalt Pavements,* Univ. of Mich. (1962) pp. 611-636.

SEED, H. B., and FEAD, J. W. N., "Apparatus for Repeated Load Tests on Soils." *ASTM STP 254* (1959) pp. 78-87.

SEED, H. B., MITRY, F. G., MONISMITH, C. L., and CHAN, C. K., "Prediction of Flexible Pavement Deflections from Laboratory Repeated-Load Tests." *NCHRP Report 35* (1967).

SHIFLEY, L. H., "The Influence of Subgrade Characteristics on the Transient Deflections of Asphalt Concrete Pavements." D.Eng. thesis, Univ. of Calif., Berkeley (1967).

TERREL, R. L., "Factors Influencing the Resilient Characteristics of Asphalt Treated Aggregates." Ph.D. thesis, Univ. of Calif., Berkeley (1967).

TROLLOPE, D. H., LEE, I. K., and MORRIS, J., "Stresses and Deformations in Two-Layer Pavement Structures Under Slow Repeated Loading." *Proc. Australian Road Res. Board* (1962) p. 693.

APPENDIX A

THEORETICAL BACKGROUND FOR MATERIALS CHARACTERIZATION

The theoretical background for the characterization of materials can be grouped into three broad areas: constitutive equations, failure theories, and solution methods for boundary value problems. Available literature in these areas is extensive; however, much of it is in the context of general theories for workers in the field of solid mechanics. Therefore, it is necessary to review certain basic concepts in the three areas mentioned. The material consists of those topics that are considered significant for the development of pavement design techniques based on sound theoretical principles.

It is necessary to define briefly certain fundamental concepts that are used in further discussions.

MECHANICAL STATE—DEFINITIONS OF STRESS AND STRAIN

The determination of the mechanical state that exists in a pavement is an essential step in the structural design of a pavement system. The mechanical state is defined by the matrices of stress and strain that exist in a system. It is therefore appropriate to define stress and strain. The definitions and concepts that follow emphasize those aspects that apply in the design of pavements.

Stress—Concepts and Definitions

Consider a body under the action of various external forces. Take a closed surface, S, within this body and consider an elemental surface area, ΔS, on this surface (Fig. A-1). Draw a unit vector, η, normal to ΔS with its direction outward from the interior of S. Consider the material on the positive side of the normal. This material exerts a force, ΔF, which is a function of the area and orientation of the surface, on the material which is located on the negative side of the normal.

The following assumption is introduced: as $\Delta S \rightarrow 0$ the ratio $\Delta F/\Delta S \rightarrow dF/dS$ and further that the moment of the forces acting on the surface ΔS about any point within the area vanishes in the limit. The limiting vector dF/dS will be written as:

$$s = dF/dS \qquad \text{(A-1)}$$

This limiting vector, s, is called the stress vector * or traction, and represents the force per unit area acting on the surface. The stress vector can be resolved into components parallel and normal to the surface on which it acts; these components are known respectively as shear and normal stresses. The shear stress can be resolved into two perpendicular directions in the plane on which it acts.

It is first desirable to standardize the notation used for the representation of stress. Figure A-2 shows a parallelepiped made up of elemental surface areas, ΔS_x, ΔS_y, and ΔS_z, in a rectangular Cartesian coordinate system, x, y, z. On each of these surfaces consider a stress vector, S_x, S_y, and S_z. Figure A-2 shows the resolution of each of the three stress vectors, S_x, S_y, and S_z, into three components. Normal stresses are noted by σ; shear stress is noted by τ.

* This concept of stress was introduced by Cauchy and Euler.

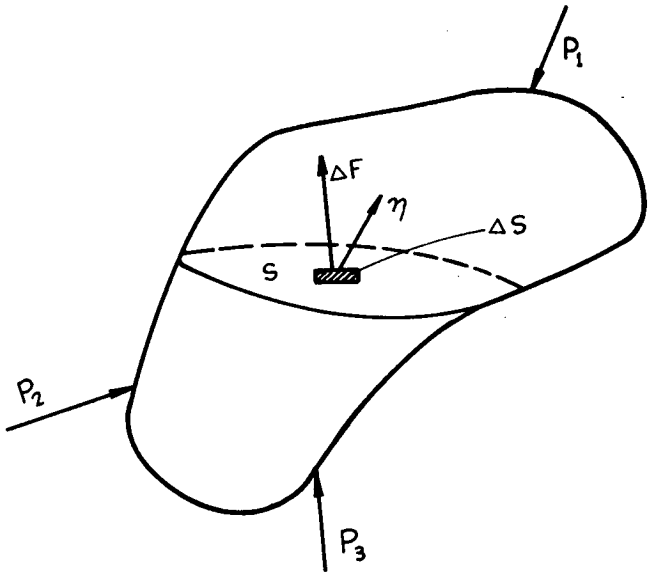

Figure A-1. Concept of stress.

To indicate the direction and the plane on which the stresses act, a system of subscripts is used in conjunction with σ and τ. The first subscript denotes the direction of the normal to the plane on which the stress acts; the second subscript denotes the direction in which the stress acts. For example, the stress σ_{xx} is the stress on the plane whose outer normal is parallel to the x axis and acts in the direction of the x axis. A stress with one subscript indicates only the plane on which it acts; the lack of a second subscript implies that it does not act in one of the coordinate directions. It may, therefore, be resolved into components in the three coordinate directions. With regard to signs, the following convention is adopted. On a plane whose outer normal is in the direction of a positive axis, stresses

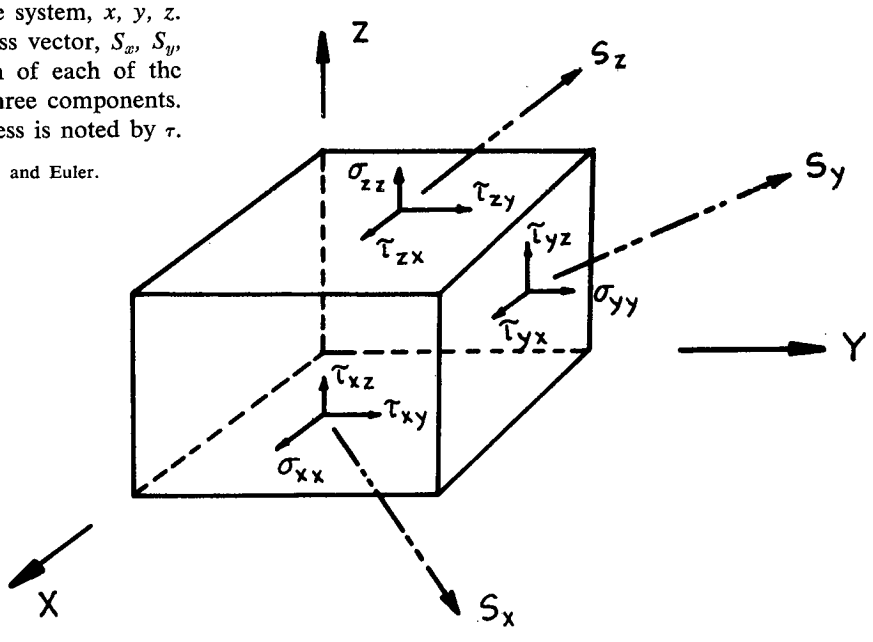

Figure A-2. Stress concepts—notation and definition in a Cartesian system.

will be positive when they are in the direction of a positive axis.

Through any point there passes an infinite system of planes, and the complete specification of the stresses at a point requires knowledge of the traction on all these planes. It can be shown (the original result is due to Cauchy) that if one knows the components of the stress vector on planes parallel to the three coordinate planes, the stress vector acting on any other surface, defined by its normal, can be obtained. More formally, this result gives the assurance that the nine components of stress

$$\begin{bmatrix} \sigma_{xx} & \tau_{xy} & \tau_{xz} \\ \tau_{yx} & \sigma_{yy} & \tau_{yz} \\ \tau_{zx} & \tau_{zy} & \sigma_{zz} \end{bmatrix}^{*}$$ are necessary and sufficient to define

the traction on any surface; hence, the state of stress in a body is completely characterized by these quantities.**

If a stress vector acts in a direction normal to a plane, its shear component is zero. A plane on which the stress vector acts in a normal direction is called a principal plane; the value of the normal stress is called the principal stress. On a principal plane there is no shear stress. It can be shown that there are three real valued principal stresses acting on a set of three mutually orthogonal planes. These stresses are sufficient to define the state of stress at any point.

There are a number of stress-states as defined by various particular combinations of the stress components that are of interest. These are discussed in the following.

Stress Invariants

There are certain algebraic scalar combinations of the stress components that do not change with a rotation of the coordinate axes. These combinations, known as stress invariants, are of considerable significance in defining stress for the purpose of formulating physical laws. This is because of their independence from the choice of a particular coordinate system.

In the Cartesian coordinate system these invariants are:

First invariant:

$$I_1 = \sigma_{xx} + \sigma_{yy} + \sigma_{zz} \qquad \text{(A-2)}$$

Second invariant:

$$I_2 = \begin{vmatrix} \sigma_{yy} & \tau_{yz} \\ \tau_{zy} & \sigma_{zz} \end{vmatrix} + \begin{vmatrix} \sigma_{xx} & \tau_{xz} \\ \tau_{zx} & \sigma_{zz} \end{vmatrix} + \begin{vmatrix} \sigma_{xx} & \tau_{xy} \\ \tau_{yx} & \sigma_{yy} \end{vmatrix} \qquad \text{(A-3)}$$

Third invariant:

$$I_3 = \begin{vmatrix} \sigma_{xx} & \tau_{xy} & \tau_{xz} \\ \tau_{yx} & \sigma_{yy} & \tau_{yz} \\ \tau_{zx} & \tau_{zy} & \sigma_{zz} \end{vmatrix} \qquad \text{(A-4)}$$

Expressed in terms of the principal stress, these invariants can be written as:

$$\begin{aligned} I_1 &= \sigma_1 + \sigma_2 + \sigma_3 \\ I_2 &= \sigma_2\sigma_3 + \sigma_1\sigma_3 + \sigma_1\sigma_2 \\ I_3 &= \sigma_1\sigma_2\sigma_3 \end{aligned} \qquad \text{(A-5)}$$

Hydrostatic and Deviator Stress States

The experimental study of materials showed that a large class of materials undergo changes in behavior that appear to be independent of the hydrostatic stress to which the material is subjected. The hydrostatic stress state is a special case of the first stress invariant, I_1, and is defined as:

$$\begin{bmatrix} \sigma & 0 & 0 \\ 0 & \sigma & 0 \\ 0 & 0 & \sigma \end{bmatrix} \qquad \text{(A-6)}$$

Because of this observed behavior, it is convenient to divide a general state of stress into two states of stress: (1) in which I_1 (the first stress invariant) $= 0$; and (2) in which I_1 (the first stress invariant) $\neq 0$.

Consider a general state of stress as represented by

$$\begin{bmatrix} \sigma_{zz} & \tau_{yz} & \tau_{xz} \\ \sigma_{xx} & \tau_{xz} & \tau_{xy} \\ \tau_{xy} & \tau_{zy} & \sigma_{yy} \end{bmatrix} \qquad \text{(A-7)}$$

Denote $\frac{1}{3}(\sigma_{xx} + \sigma_{yy} + \sigma_{zz})$ by p.

The general state of stress may be divided into two states of stress:

$$(1)\begin{bmatrix} \sigma_{xx} - p & \tau_{xy} & \tau_{xz} \\ \tau_{xy} & \sigma_{yy} - p & \tau_{yz} \\ \tau_{xz} & \tau_{yz} & \sigma_{zz} - p \end{bmatrix} \quad (2)\begin{bmatrix} p & 0 & 0 \\ 0 & p & 0 \\ 0 & 0 & p \end{bmatrix}$$

This division may be verified by adding the two stress states.

The first stress invariant for stress state (1) is:

$$I_1 = (\sigma_{xx} - p) + (\sigma_{yy} - p) + (\sigma_{zz} - p) \qquad \text{(A-8)}$$

which is zero, because of the definition of p.

For stress state (2):

$$I_1 = 3p \neq 0 \qquad \text{(A-9)}$$

A stress state z, where $I_1 = 0$, is called a deviatoric stress state,* and the components of stress defining a deviatoric stress state comprise the deviatoric stress tensor. The second stress state as defined by three normal stresses is termed a hydrostatic stress state.

Strain—Concepts and Definitions

When a body is subject to a stress field, it undergoes a displacement (Fig. A-3a). The three neighboring points, P_1, P_2, P_3, are displaced to positions Q_1, Q_2, Q_3. The displacement vector $\bar{u}$ defines the distance between corresponding points in the initial and displaced positions. This displacement has two results:

1. Points Q_1, Q_2, and Q_3 are at different locations than P_1, P_2, and P_3.
2. The relative positions of Q_1, Q_2, and Q_3 differ from those for P_1, P_2, and P_3; i.e., the shape of the triangle has changed.

* It can be shown that the collection of stress components is a tensor and hence is referred to as a stress tensor.

** Engineers are familiar with using the result; e.g., Mohrs Circle in three dimensions. It has been assumed that the stress can be defined everywhere in a body and that the stress field is continuous.

* This is the correct definition of a deviatoric stress state and is not identical to the one commonly used in pavement research.

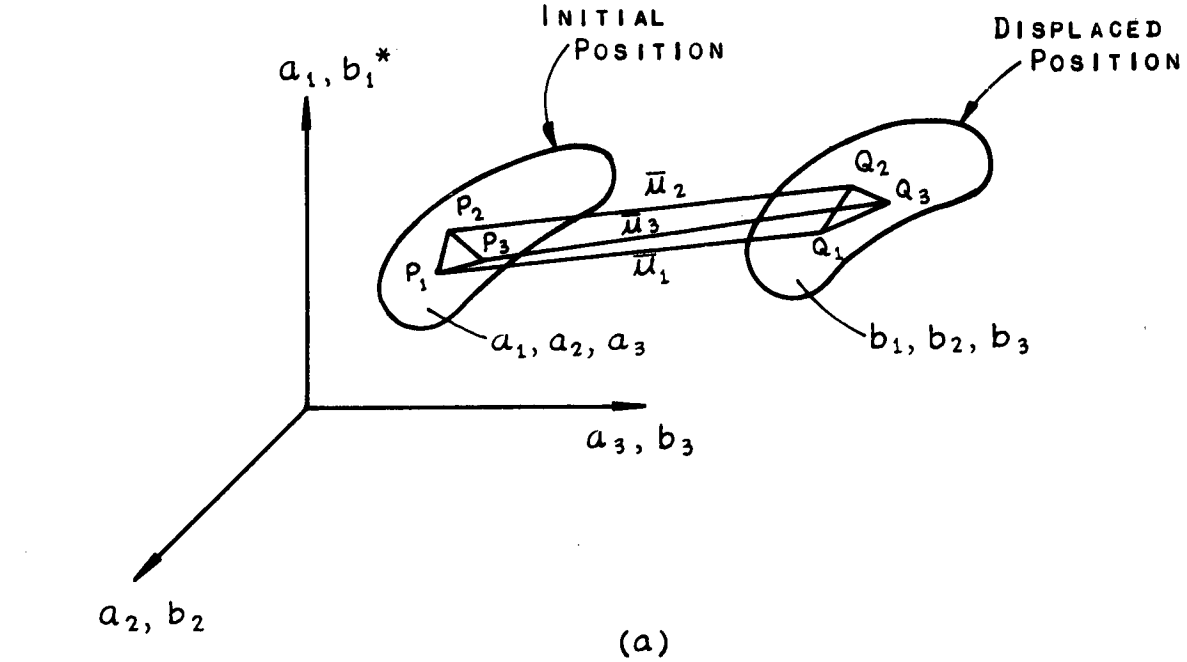

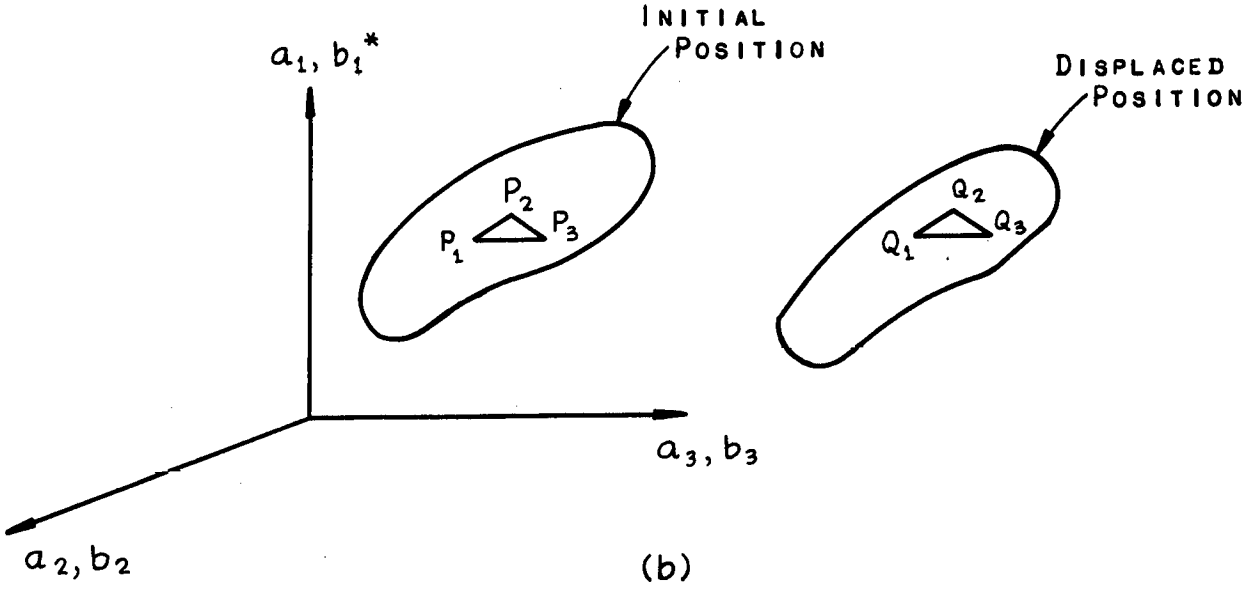

* THE COORDINATE SYSTEMS a_1, b_1, ARE USED TO DIFFERENTIATE BETWEEN THE INITIAL AND DISPLACED POSITIONS. a_1 REFERS TO THE INITIAL POSITION AND b_1 TO THE DISPLACED POSITION.

Figure A-3. Displacement pattern—relative and rigid body motion.

A special displacement pattern is shown in Figure A-3b. Points P_1, P_2, and P_3 have been displaced to Q_1, Q_2, and Q_3. However, there is no difference between the relative positions of Q_1, Q_2, and Q_3 when compared with P_1, P_2, and P_3; i.e., there is a change in location but no change in the shape of the triangle.

The latter case (Fig. A-3b) is called rigid body motion. Strain occurs only if the relative configuration of particles

in a body is altered. Displacement that consists of a pure rotation or translation (rigid body motion) will not cause any strain. The ensuing discussion deals with the concept of strain, because it is strain that is related to stress.

The analysis of strain is a geometrical study of the changes in the configuration of the particles; this involves the introduction of various quantities that serve as a measure of strain, and a discussion of how these quantities vary in the neighborhood of a point.

When a body deforms or flows, the motion of each point is expressed in terms of (1) its initial position, and (2) its instantaneous position.

These two methods for representing the deformed configuration of the body are termed the Lagrangian and Eulerian methods, respectively. If the motion (displacement) is small enough to neglect the difference between the original and deformed shapes, there is no difference between the Lagrangian and Eulerian descriptions.

The most logical measures of strain are the changes in length of a line, and the change in angle between planes and lines. The expressions for strains that follow were derived by considering these changes for infinitesimal line elements.

If the position of a point in the undeformed state is denoted by (a_1, a_2, a_3) and in the deformed state by (b_1, b_2, b_3), the strain components can be expressed as:

Lagrangian form (in terms of the initial position):

$$E_{a_1a_1} = \frac{\partial u}{\partial a_1} + \tfrac{1}{2}\left[\left(\frac{\partial u}{\partial a_1}\right)^2 + \left(\frac{\partial v}{\partial a_1}\right)^2 + \left(\frac{\partial w}{\partial a_1}\right)^2\right]$$

$$E_{a_2a_1} = \tfrac{1}{2}\left[\frac{\partial u}{\partial a_2} + \frac{\partial v}{\partial a_1} + \left(\frac{\partial u}{\partial a_1}\frac{\partial u}{\partial a_2} + \frac{\partial v}{\partial a_1}\frac{\partial v}{\partial a_2} + \frac{\partial w}{\partial a_1}\frac{\partial w}{\partial a_2}\right)\right] \tag{A-10}$$

Other terms may be obtained by a suitable permutation of a_1, a_2, and a_3.

Eulerian form (in terms of its instantaneous position):

$$e_{b_1b_1} = \frac{\partial u}{\partial b_1} - \tfrac{1}{2}\left[\left(\frac{\partial u}{\partial b_1}\right)^2 + \left(\frac{\partial v}{\partial b_1}\right)^2 + \left(\frac{\partial w}{\partial b_1}\right)^2\right]$$

$$e_{b_1b_2} = \tfrac{1}{2}\left[\frac{\partial u}{\partial b_2} + \frac{\partial v}{\partial b_1} - \left(\frac{\partial u}{\partial b_1}\frac{\partial u}{\partial b_2} + \frac{\partial v}{\partial b_1}\frac{\partial v}{\partial b_2} + \frac{\partial w}{\partial b_1}\frac{\partial w}{\partial b_2}\right)\right] \tag{A-11}$$

Other terms may be obtained by a suitable permutation of b_1, b_2, and b_3.

It can be shown that the collection of the nine components of strain is a symmetric tensor; i.e., $E_{a_1a_2} = E_{a_2a_1}$, $e_{b_1b_2} = e_{b_2b_1}$.

If one assumes that components of displacement are such that their first derivatives are small enough so that their squares and products can be neglected, and that the displacements are also small so that it is not necessary to differentiate between the Eulerian and Lagrangian systems:

$$E_{a_1a_1} = \frac{\partial u}{\partial a_1} = e_{b_1b_1} \quad E_{a_1a_2} = e_{b_1b_2} = \tfrac{1}{2}\left(\frac{\partial u}{\partial a_2} + \frac{\partial v}{\partial a_1}\right) \tag{A-12}$$

These strains are referred to as infinitesimal strains, to differentiate them from finite strains where displacement derivatives are not assumed small. In this work, unless explicitly stated, only infinitesimal strains and displacements (no distinction between Eulerian and Lagrangian methods) are considered.

In a Cartesian coordinate system, the position of an arbitrary point defined by (x, y, z), the strain components can be expressed as:

$$e_{xx} = \partial u/\partial x,\ e_{yy} = \partial v/\partial y,\ e_{zz} = \partial w/\partial z$$

$$e_{xy} = \tfrac{1}{2}\left[\frac{\partial u}{\partial y} + \frac{\partial v}{\partial x}\right],\ e_{xz} = \tfrac{1}{2}\left[\frac{\partial u}{\partial z} + \frac{\partial w}{\partial x}\right] \tag{A-13}$$

$$e_{yz} = \tfrac{1}{2}\left[\frac{\partial v}{\partial z} + \frac{\partial w}{\partial y}\right]$$

The physical significance of the quantities in Eq. A-13 is most readily understood by considering the two-dimensional case (Fig. A-4).

Consider the corner of the rectangle defined by ROQ which is deformed to the position R′O′Q′. The elongation of the line element OQ, when the partial derivatives are small, compared to unity, is:

$$\mathrm{O'Q'} - \mathrm{OQ} = \left(\delta x - u + u + \frac{\partial u}{\partial x}\delta x\right) - \delta x = \frac{\partial u}{\partial x}\delta x$$

$$\text{Strain (along the } x \text{ axis)} = \frac{\partial u}{\partial x} = \epsilon_{xx} = \frac{\text{change in length}}{\text{original length}} \tag{A-14}$$

Similarly,

$$\epsilon_{yy} = \text{strain in } y \text{ direction} = \partial v/\partial y \tag{A-15}$$

The only other component of strain that exists in two dimensions is the decrease in the right angle between the sides OQ and OR

$$\epsilon_{xy} = \alpha + \beta = \partial v/\partial x + \partial u/\partial y \tag{A-16}$$

This is known as a shear strain.

In three dimensions, one additional axial strain and two additional shear strains are given by:

$$\epsilon_{zz} = \partial w/\partial z,\ \epsilon_{yz} = \partial w/\partial y + \partial v/\partial z,\ \epsilon_{xz} = \partial w/\partial x + \partial u/\partial z \tag{A-17}$$

A comparison of these quantities with those in Eq. A-13 shows that e_{xx}, e_{yy}, and e_{zz} are the strains along the various coordinate axis and that e_{xy}, e_{xz}, and e_{yz} are one-half the shear strains. To differentiate between these strains, the quantities of Eq. A-13 are referred to as "tensor strains" and those in Eqs. A-14, A-15, and A-16 as "engineering strains." In engineering analysis one deals almost exclusively with the "matrix of engineering strains," which is:

$$\begin{bmatrix} \epsilon_{xx} & \epsilon_{xy} & \epsilon_{xz} \\ \epsilon_{yx} & \epsilon_{yy} & \epsilon_{yz} \\ \epsilon_{zx} & \epsilon_{zy} & \epsilon_{zz} \end{bmatrix} \tag{A-18}$$

This work deals with strains as represented in Eq. A-18 and which are related to the displacements by Eqs. A-14 to A-17. Note that the relationships between the strains and the displacement derivatives are linear. This is because displacements and displacement derivatives (and hence strains) are assumed to be small.

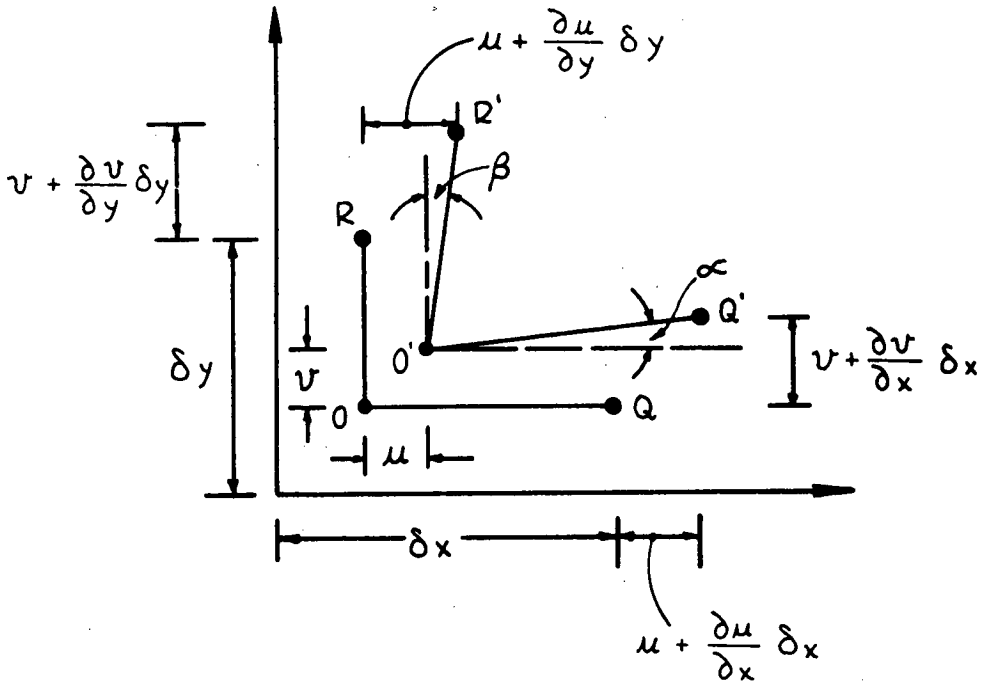

Figure A-4. Explanation of strain components in the two-dimensional case.

Compatibility of Strains

Consider the six strain displacement equations (Eqs. A-14 to A-17). If the strain components are given, there are six equations to determine the three unknowns, u, v, w. Therefore, one cannot expect that there will be, in general, a single-valued solution to the system of Eqs. A-14 to A-17 if the values of the strain components are assigned arbitrarily.

For a single-valued continuous solution to exist,* certain conditions have to be satisfied by the strain components. These are the compatibility conditions of St. Venant. These conditions can be derived by differentiating and manipulating the strain-displacement equations. In the rectangular Cartesian coordinates and for infinitesimal strain, the equations of compatibility are:

$$\frac{\partial^2 \epsilon_{xy}}{\partial x \partial y} = \frac{\partial^2 \epsilon_{xx}}{\partial y^2} + \frac{\partial^2 \epsilon_{yy}}{\partial x^2}$$

$$\frac{\partial^2 \epsilon_{yz}}{\partial y \partial z} = \frac{\partial^2 \epsilon_{yy}}{\partial z^2} + \frac{\partial^2 \epsilon_{zz}}{\partial y^2} \qquad \text{(A-19)}$$

$$\frac{\partial^2 \epsilon_{xz}}{\partial x \partial z} = \frac{\partial^2 \epsilon_{zz}}{\partial x^2} + \frac{\partial^2 \epsilon_{xx}}{\partial z^2}$$

$$2\frac{\partial^2 \epsilon_{xx}}{\partial y \partial z} = \frac{\partial}{\partial x}\left(\frac{-\partial \epsilon_{yz}}{\partial x} + \frac{\partial \epsilon_{xz}}{\partial y} + \frac{\partial \epsilon_{xy}}{\partial z}\right)$$

$$2\frac{\partial^2 \epsilon_{yy}}{\partial z \partial x} = \frac{\partial}{\partial y}\left(\frac{\partial \epsilon_{yz}}{\partial x} - \frac{\partial \epsilon_{xz}}{\partial y} + \frac{\partial \epsilon_{xy}}{\partial z}\right)$$

$$2\frac{\partial^2 \epsilon_{zz}}{\partial x \partial y} = \frac{\partial}{\partial z}\left(\frac{\partial \epsilon_{yz}}{\partial x} + \frac{\partial \epsilon_{xz}}{\partial y} - \frac{\partial \epsilon_{xy}}{\partial z}\right)$$

* Because rigid body motion does not introduce any strain, the solution is single-valued up to a rigid body motion.

Strain Invariants

The expressions for strain invariants can be developed in a manner analagous to that used for developing the stress invariants. The strain invariants in a Cartesian coordinate system are:

L_1 (first invariant) $= e_{xx} + e_{yy} + e_{zz}$

L_2 (second invariant) $=$

$$\begin{vmatrix} e_{yy} & e_{yz} \\ e_{zy} & e_{zz} \end{vmatrix} + \begin{vmatrix} e_{xx} & e_{xz} \\ e_{zx} & e_{zz} \end{vmatrix} + \begin{vmatrix} e_{xx} & e_{xy} \\ e_{yx} & e_{yy} \end{vmatrix} \qquad \text{(A-20)}$$

L_3 (third invariant) $= \begin{vmatrix} e_{xx} & e_{xy} & e_{xz} \\ e_{yx} & e_{yy} & e_{yz} \\ e_{zx} & e_{zy} & e_{zz} \end{vmatrix}$

Expressed in terms of principal strains, the stress invariants are:

$$\begin{aligned} L_1 &= e_1 + e_2 + e_3 \\ L_2 &= e_2 e_3 + e_1 e_3 + e_1 e_2 \\ L_3 &= e_1 e_2 e_3 \end{aligned} \qquad \text{(A-21)}$$

It is important to understand the physical significance of the first invariant. The change in length of the various sides of a parallelepiped of lengths l_1, l_2, and l_3 in the directions of the principal strains are $l_1(1 + e_1)$, $l_2(1 + e_2)$, $l_3(1 + e_3)$.* The sides remain orthogonal to each other; hence, the change in volume, ΔV, is given by

$$\begin{aligned} \Delta V &= l_1(1 + e_1) l_2(1 + e_2) l_3(1 + e_3) - l_1 l_2 l_3 \\ &= l_1 l_2 l_3 (e_1 + e_2 + e_3) ** \end{aligned} \qquad \text{(A-22)}$$

$$\Delta V / V = e_1 + e_2 + e_3 \qquad \text{(A-23)}$$

Thus, the first strain invariant represents the volumetric strain.

Hydrostatic and Deviator Strain States

By a method analagous to that used for decomposing the stress tensor, the strain tensor can be split in two by a hydrostatic strain tensor (where $L_1 \neq 0$) and a deviatoric strain tensor ($L_1 = 0$).

If $e = \frac{1}{3}(e_1 + e_2 + e_3)$, the hydrostatic state of strain (dilatation) is

$$\begin{bmatrix} e & 0 & 0 \\ 0 & e & 0 \\ 0 & 0 & e \end{bmatrix} \qquad \text{(A-24)}$$

and the deviatoric strain tensor is

$$\begin{bmatrix} e_{xx} - e & e_{xy} & e_{xz} \\ e_{yx} & e_{yy} - e & e_{yz} \\ e_{zx} & e_{zy} & e_{zz} - e \end{bmatrix} \qquad \text{(A-25)}$$

For the hydrostatic strain tensor:

$$L_1 = 3e \qquad \text{(A-26)}$$

For the deviatoric strain tensor the first strain invariant

$$L_1 = (e_{xx} - e) + (e_{yy} - e) + (e_{zz} - e) = 0 \qquad \text{(A-27)}$$

Because the first strain invariant is a measure of volume change, a deviatoric strain state implies no volume change.

MATHEMATICAL MODELS (CONSTITUTIVE EQUATIONS)

An essential step in determining the mechanical state, through the formulation and solution of the appropriate boundary value problems, is the selection of suitable mathematical models to represent the materials comprising the pavement system. An essential prerequisite to material characterization (selection of suitable mathematical models) is an understanding of the assumptions and idealizations that form the basis of various mathematical models. The following discussion explains the reasons for the choice of various models in this study, and provides a basis for the selection of mathematical models in future work. The discussion emphasizes basic concepts.

General Constitutive Equation

A constitutive equation reflects pertinent properties of the system through functional relations among the system variables. For definiteness, assume that certain materials have been prescribed and the method of construction has been established. The following postulates are introduced:

1. The mechanical state is defined by the stress and strain matrices.
2. The thermal and moisture states are defined by temperature and moisture content.
3. The stress at a point in the system at time t is a function of the histories of strain, temperature, and moisture content at that point and a function of the age of the system.

Postulate 3 forms the basis for the fundamental constitutive equation determining behavior of the pavement system. All mathematical models ("theories of pavement structural behavior") currently in use in the structural analysis of pavements appear as special cases of this postulate. Some notations are introduced here:

$\underset{\sim}{x}$ = position vector of a point, referred to as a coordinate system;
$\underset{\sim}{\sigma}(\underset{\sim}{x}, t)$ = stress, a matrix function of space and time;
$\underset{\sim}{\epsilon}(\underset{\sim}{x}, t)$ = strain, a matrix function of space and time;
$\underset{\sim}{T}(\underset{\sim}{x}, t)$ = temperature change above a reference state, a scalar function of space and time; and
$\underset{\sim}{M}(\underset{\sim}{x}, t)$ = moisture content, change above a reference state, a scalar function of space and time.

Postulate 3 is equivalent to

$$\underset{\sim}{\sigma}(\underset{\sim}{x}, t) = \underset{s=0}{\overset{t}{\underset{\sim}{F}}} [\underset{\sim}{\epsilon}(\underset{\sim}{x}, s), \underset{\sim}{T}(\underset{\sim}{x}, s), \underset{\sim}{M}(\underset{\sim}{x}, s); \underset{\sim}{x}, t] \qquad \text{(A-28)}$$

The notation implies that stress is a function of the histories of the variables shown, from time zero to current time t. Because stress is a function of arguments, which in turn are functions, it is customary to refer to this equation as a functional; i.e., stress is a functional of strain, temperature, and moisture content. In general, determination of the temperature and moisture content as functions of time cannot be carried out independently of the determination of mechanical variables; i.e., the variables are coupled. Because of the complexity of such theories, for the present it will be assumed that the temperature and moisture content variables are known functions of space and time. These functions can be found from the solution of separate diffusion boundary value problems (e.g., based on the heat equation).

It is not possible to proceed conceptually any farther, except to note that Eq. A-28 can be specialized further if the material is supposed to have symmetry in its behavior; i.e., whether the material is anisotropic or isotropic. It should be noted that the functional $\underset{\sim}{F}$ in Eq. A-28 depends on position $\underset{\sim}{x}$ and time t. The former reflects the possibility of a nonhomogeneous system (i.e., properties depend on position). If $\underset{\sim}{F}$ is independent of $\underset{\sim}{x}$, the system is homogeneous. When $\underset{\sim}{F}$ depends on $\underset{\sim}{t}$, the system is said to be an aging system—one whose properties depend on age. If $\underset{\sim}{F}$ is independent of age, or time-invariant, the time argument disappears, and only relative time $t - s$ appears in the histories. Thus, for a nonaging homogeneous pavement system:

$$\underset{\sim}{\sigma}(\underset{\sim}{x}, t) = \underset{s=0}{\overset{t}{\underset{\sim}{F}}} [\underset{\sim}{\epsilon}(\underset{\sim}{x}, t - s), T(\underset{\sim}{x}, t - s), M(\underset{\sim}{x}, t - s)] \qquad \text{(A-29)}$$

This equation forms the basis for further discussion.

Nonhereditary Models—Elastic Response

The constitutive Eq. A-29 is said to be hereditary in the sense that the current value of stress depends on the history of the argument functions. It may happen that a pavement system response is the same for all histories; i.e., the stress depends only on the current values of the arguments. In other words, the response of the system is not dependent on the history of the input variables but only on their current

* This is valid for small strains.
** Neglecting second order quantities.

value. This implies absence of hysteresis effects and permanent deformation; i.e., there is complete reversibility of effects. A material possessing these qualities is called elastic. It is not possible to specialize the very general form of Eq. A-29 until further restrictions on the response of the elastic material are introduced.

For example, if the response to mechanical, thermal, or moisture inputs is symmetric in some sense, the material is said to have that class of symmetry relative to a particular input variable. Complete symmetry is called isotropy. For example, if the material is isotropic relative to all inputs, then it is known that the most general representation of Eq. A-29 contains five unknown functions of temperature, moisture content, and the principal strain invariants (five functions of five variables). For constant temperature and moisture content, only three functions of three strain variables appear. For linear elastic behavior, only four constants appear. If moisture and temperature effects are not considered, only two constants are required. It should be recognized that elastic theory cannot, by definition, predict time dependent, rate dependent, or permanent deformation.

Linear Elastic Stress-Strain

Most current methods of pavement design use mathematical models that are based on linear elastic stress-strain laws.

The basis for linear elastic stress-strain relations is Cauchy's generalization of Hooke's Law: "Each of the six components of stress at any point of a body is a linear function of each of the six components of strain at that point."

The generalized Hooke's Law can be expressed in unabridged notation by:

$$\begin{aligned}
\sigma_{xx} &= a_{11}\epsilon_{xx} + a_{12}\epsilon_{yy} + a_{13}\epsilon_{zz} + a_{14}\epsilon_{xy} + a_{15}\epsilon_{xz} + a_{16}\epsilon_{yz} \\
\sigma_{yy} &= a_{21} + a_{22}\epsilon_{yy} + \\
\sigma_{zz} &= a_{31} + + a_{33}\epsilon_{zz} \\
\tau_{xy} &= a_{41} + + + a_{44}\epsilon_{xy} \\
\tau_{xz} &= a_{51} + + + + a_{55}\epsilon_{xz} \\
\tau_{yz} &= a_{61} + + + + + a_{66}\epsilon_{yz}
\end{aligned} \qquad \text{(A-30)}$$

These stress-strain relations (which are linear), when used with the equilibrium and strain-displacement relationship for infinitesimal displacements (which are also linear), form the basis for the classical linear theory of elasticity.*

The maximum number of constants under such an assumption is 36. Eq. A-30 refers to stresses at a point. To use these relationships in a continuum in addition to the assumption of continuity of the stress and displacement field, some assumption has to be made regarding the spatial variation of the elements a_{ij}. If the elements a_{ij} and the coefficient matrix are considered independent of position, the material is considered homogeneous; i.e., the stress-strain relationship is the same everywhere. If a_{ij} are functions of their position, the materials are considered nonhomogeneous; i.e., the stress-strain relationship varies from point to point in the material.

Because of the existence and positive definite character of the strain energy function,** it is now generally accepted that $a_{ij} = a_{ji}$ and that the maximum number of independent elastic constants for generalized Hooke's Law is 21 for the most general form of anistropy. If the elastic properties of a material possess symmetry in various directions, the number of independent elastic constants will be reduced further. If the material is elastically isotropic (i.e., the properties are independent of direction) the number of elastic constants is reduced to two (this assumes that moisture and temperature effects are not being considered). Most theoretical analyses in pavement design are based on the theory of linear isotropic elastic solids.

For this case, the stress-strain relations can be expressed in Cartesian coordinates:

$$\begin{aligned}
\epsilon_{xx} &= \frac{1}{E}[\sigma_{xx} - \nu(\sigma_{yy} + \sigma_{zz})] \\
\epsilon_{yy} &= \frac{1}{E}[\sigma_{yy} - \nu(\sigma_{xx} + \sigma_{zz})] \\
\epsilon_{zz} &= \frac{1}{E}[\sigma_{zz} - \nu(\sigma_{yy} + \sigma_{xx})] \\
\epsilon_{xy} &= \frac{2(1+\nu)}{E}\tau_{xy} \\
\epsilon_{yz} &= \frac{2(1+\nu)}{E}\tau_{yz} \\
\epsilon_{xz} &= \frac{2(1+\nu)}{E}\tau_{xz}
\end{aligned} \qquad \text{(A-31)}$$

The two independent elastic constants are known as E (modulus of elasticity) and (ν) Poisson's ratio. The quantity $[E/2(1+\nu)]$ that relates the shear stress to the shear strain is known as the shear modulus, G. E and ν are the only two constants needed to characterize an isotropic linear elastic material.

Adding the first three equations of Eq. A-31:

$$\epsilon_{xx} + \epsilon_{yy} + \epsilon_{zz} = \frac{1-2\nu}{E}(\sigma_{xx} + \sigma_{yy} + \sigma_{zz}) \qquad \text{(A-32)}$$

The first invariant of stress, I_1, has been defined as $(\sigma_{xx} + \sigma_{yy} + \sigma_{zz})$. The first invariant of strain, L_1, has been defined as $(\epsilon_{xx} + \epsilon_{yy} + \epsilon_{zz})$. It also has been shown that the first invariant of strain is a measure of the change in volume. Therefore, Eq. A-32 states that the change in volume is proportional to the first invariant of stress.

A deviatoric state of stress was defined as one in which the first invariant of stress is zero. Therefore, it can be concluded that for linear isotropic elastic solids, a deviatoric state of stress produces no volume change. An equivalent statement would be that a deviatoric state of stress produces only a deviatoric state of strain. This concept can be used as a basis for developing a critical experiment to determine if a material is both isotropic and linearly elastic.

Nonlinear Elastic Stress-Strain *

Many materials, even under small deformations, exhibit nonlinear effects; e.g., concrete exhibits different behavior under tension and compression, sands dilate under pure

* In tensor form these may be written as $\sigma_{ij}=\alpha_{ijkl}e_{kl}$, $(i, j, k, l=1,6$, summation implied over $k, l)$ $\alpha_{ijkl}=\alpha_{ijlk}$.

** Such materials are referred to as Green elastic or hyperelastic.

* Based on report by K. S. Pister, consultant to MR&D, Inc.

shear. In the analysis of many practical problems for pavement design, elastic deformations are sufficiently small to justify the use of linear strain-displacement equations. However, experimental evidence indicates that at low levels of stress and strain the materials comprising a pavement system exhibit significant amounts of nonlinear behavior. Because of this behavior, it is necessary to discuss nonlinear elastic stress-strain laws.

The most general constitutive equation for an isotropic nonlinear elastic material is:

$$\sigma_{ij} = F_{ij}(e_{mn}) \tag{A-33}$$

This states that stress is a function of the current state of strain, there being no restriction on the nature of this functional relationship.

Analytic representations of Eq. A-33 are discussed by Evans (1965) and Evans and Pister (1966).* For the isotropic case under the assumptions of kinematic linearity the most general form of Eq. A-33 is:

$$\sigma_{ij} = \Phi_1\delta_{ij} + \Phi_2 e_{ij} + \Phi_3 e_{ik}e_{kj} \tag{A-34}$$

in which Φ_1, Φ_2, and Φ_3 are dependent on the material and the current state of strain; i.e., the coefficients Φ_1, Φ_2, and Φ_3 are strain-dependent. For an elastic material under the assumption of the existence of a strain energy function $U(I_1, I_2, I_3)$, the following defines the Φ's:

$$\Phi_i = \frac{\partial U}{\partial I_i} \tag{A-35}$$

Assuming an expression for U in terms of the three strain invariants I_1, I_2, and I_3, various stress-strain laws may be derived. For example, if U is assumed to be a polynomial in I_i in which terms up to the fourth power in strain are retained, the resulting stress-strain law is cubic.

For stable materials, it can be shown (Evans, 1965) that Eq. A-33 has a unique inverse which can be written as:

$$e_{ij} = H_{ij}(\sigma_{mn}) \tag{A-36}$$

$$e_{ij} = \alpha_1\delta_{ij} + \alpha_2\sigma_{ij} + \alpha_3\sigma_{ik}\sigma_{kj} \tag{A-37}$$

The coefficients α_i are stress-dependent and are functions of the complimentary energy density, $C(\theta_1, \theta_2, \theta_3)$, in which θ_1, θ_2, and θ_3 are the three stress invariants. The relationship between α_i and C is given by:

$$\alpha_i = \frac{\partial C}{\partial \theta_i} \tag{A-38}$$

By assuming different variations of C with θ, it is possible to derive a variety of strain-stress laws.

The functional relationship for U or C is chosen on the basis of a study of appropriate experimental results obtained on the behavior of the material for which a constitutive law is required. Determination of the three material functions Φ_1, Φ_2, and Φ_3, or α_1, α_2, and α_3 for each stress or strain component is a formidable experimental task.

An alternate form of a nonlinear elastic stress-strain law can be formulated in incremental terms. Such a formulation might, in some cases, be more convenient to work with from an experimental or boundary value problem solution standpoint than the nonlinear law discussed here.

Consider the general nonlinear constitutive equation:

$$\sigma_{ij} = F_{ij}(e_{mn}) \tag{A-39}$$

In principle, it would be possible to determine satisfactorily the stress-strain relationship for a material by subjecting a volume element of that material to all strain states of interest and measuring the corresponding stress states. A strain state and its corresponding stress state is termed a stress-strain pair.

Obviously, a large number of stress-strain pairs would be required to satisfactorily define the behavior of a material. However, this number can be reduced substantially by determining the relation between small excursions of stress and strain superimposed on a stress-strain pair. If these stress and strain excursions are small, the relation between them will be linear. Therefore, one may interpolate between stress-strain pairs using the information on the relationship between small stress and strain excursions. In one dimension this is equivalent to defining a certain number of points (stress-strain pairs) and the slope at these points on a stress-strain curve. Using the defined slopes, one may interpolate between given stress-strain pairs to find the stress-strain pair at any point on the curve. A derivation of the incremental constitutive law for the three-dimensional case follows.

Define a stress-strain pair by σ_{ij} and e_{mn}. Superimpose on this a new strain state that differs from the old one by $\lambda_{mn}e_{mn}$* where $(\max|\lambda_{mn}|)^2 << 1$.

Using Eq. A-39:

$$(\sigma_{ij} + \lambda_{ij}\sigma_{ij}) = F_{ij}(e_{mn} + \lambda_{mn}e_{mn}) \tag{A-40}$$

Expanding the right-hand side:

$$(\sigma_{ij} + \lambda_{ij}\sigma_{ij}) = F_{ij}(e_{mn}) + \left(\frac{\partial F_{ij}}{\partial e_{kl}}\right)_{e_{mn}} \lambda_{kl}e_{kl} + \theta(\lambda^2) \tag{A-41}$$

Summation is implied over k, l. The derivative $(\partial F_{ij}/\partial e_{kl})$ is evaluated at the reference strain state, e_{mn}. Neglecting second order terms and using Eq. A-39:

$$\lambda_{ij}\sigma_{ij} = \left(\frac{\partial F_{ij}}{\partial e_{kl}}\right)_{e_{mn}} \lambda_{kl}e_{kl} \tag{A-42}$$

For convenience in notation, define

$$\sigma_{ij}\lambda_{ij} = \sigma_{ij}' \quad \text{(stress increment)} \tag{A-43}$$

$$e_{mn}\lambda_{mn} = e_{mn}' \quad \text{(strain increment)} \tag{A-44}$$

then

$$\sigma_{ij}' = \left(\frac{\partial F_{ij}}{\partial e_{kl}}\right)_{e_{mn}} e_{kl}' \tag{A-45}$$

Because $(\partial F_{ij}/\partial e_{kl})$ are derivatives evaluated at a particular strain state, they are constant for that strain state. For clarity, it is desirable to expand Eq. A-45 for one stress component:

* A more general representation which includes finite deformations is presented by Truesdell (1952).

* Summation not implied.

$$\sigma_{xx}' = \lambda_{xx}\sigma_{xx} = \left(\frac{\partial F_{xx}}{\partial e_{xx}}\right)_{e_{mn}} e_{xx}\lambda_{xx} + \left(\frac{\partial F_{xx}}{\partial e_{yy}}\right)_{e_{mn}} e_{yy}\lambda_{yy} + \left(\frac{\partial F_{xx}}{\partial e_{zz}}\right)_{e_{mn}} e_{zz}\lambda_{zz} + \left(\frac{\partial F_{xx}}{\partial e_{xy}}\right)_{e_{mn}} e_{xy}\lambda_{xy} + \left(\frac{\partial F_{xx}}{\partial e_{xz}}\right)_{e_{mn}} e_{xz}\lambda_{xz} + \left(\frac{\partial F_{xx}}{\partial e_{yz}}\right)_{e_{mn}} \lambda_{yz}e_{yz} \tag{A-46}$$

$$\sigma_{xx}' = \left(\frac{\partial F_{xx}}{\partial e_{xx}}\right)_{e_{mn}} e_{xx}' + \left(\frac{\partial F_{xx}}{\partial e_{yy}}\right)_{e_{mn}} e_{yy}' + \left(\frac{\partial F_{xx}}{\partial e_{zz}}\right)_{e_{mn}} e_{zz}' + \left(\frac{\partial F_{xx}}{\partial e_{xy}}\right)_{e_{mn}} e_{xy}' + \left(\frac{\partial F_{xx}}{\partial e_{xz}}\right)_{e_{mn}} e_{xz}' + \left(\frac{\partial F_{xx}}{\partial e_{yz}}\right)_{e_{mn}} e_{yz}' \tag{A-47}$$

or

$$\sigma_{xx}' = C_{xxxx}e_{xx}' + C_{xxyy}e_{yy}' + C_{xxzz}e_{zz}' + C_{xxxy}e_{xy}' + C_{xxxz}e_{xz}' + C_{xxyz}e_{yz}' \tag{A-48}$$

In general,

$$\sigma_{ij}' = C_{ijkl}e_{kl}' \tag{A-49}$$

Using an analogous derivation,

$$e_{ij}' = B_{ijkl}\sigma_{kl}' \tag{A-50}$$

Eqs. A-49 and A-50 indicate that the incremental stress is linearly related to the incremental strain, both being measured with reference to a reference stress-strain pair. Although the material was initially isotropic, the "incremental modulus tensor" B_{ijkl} or C_{ijkl} is anisotropic, and is dependent on the reference stress-strain state at which it has been defined.

Combining Eqs. A-39 and A-49, the state of stress for any strain state within a linear neighborhood of a reference state is given by:

$$\sigma_{ij} + \sigma_{ij}' = F_{ij}(e_{mn}) + [C_{ijkl}]e_{kl}' \tag{A-51}$$

Combining Eqs. A-36 and A-50, the state of strain for any stress state within a linear neighborhood of a reference state is given by:

$$e_{ij} + e_{ij}' = G_{ij}(\sigma_{mn}) + [B_{ijkl}]\sigma_{kl}' \tag{A-52}$$

Testing of pavement materials and the solution of boundary value problems applicable to the analysis of pavement systems is generally done for axisymmetric configurations. Because of this, it is appropriate to specialize the nonlinear constitutive law for cylindrical coordinates and axisymmetric conditions.

Under axisymmetric conditions, the matrices of stress and strain and the displacement vector are, respectively:

$$\underset{\sim}{\sigma}_{ij} = \begin{bmatrix} \sigma_{rr} & 0 & \tau_{rz} \\ 0 & \sigma_{\theta\theta} & 0 \\ \tau_{rz} & 0 & \sigma_{zz} \end{bmatrix}, \quad \underset{\sim}{e}_{ij} = \begin{bmatrix} e_{rr} & 0 & e_{rz} \\ 0 & e_{\theta\theta} & 0 \\ e_{rz} & 0 & e_{zz} \end{bmatrix} \tag{A-53}$$

$$\underset{\sim}{d} = \begin{bmatrix} u \\ \theta \\ w \end{bmatrix} \tag{A-54}$$

Consider a reference stress-strain pair σ_{ij}^{o} and e_{ij}^{o}:

$$\underset{\sim}{\sigma}_{ij}^{o} = \begin{bmatrix} \sigma_{rr}^{o} & 0 & \tau_{rz}^{o} \\ 0 & \sigma_{\theta\theta}^{o} & 0 \\ \tau_{rz}^{o} & 0 & \sigma_{zz}^{o} \end{bmatrix}, \underset{\sim}{e}_{ij}^{o} = \begin{bmatrix} e_{rr}^{o} & 0 & e_{rz}^{o} \\ 0 & e_{\theta\theta}^{o} & 0 \\ e_{rz}^{o} & 0 & e_{zz}^{o} \end{bmatrix} \tag{A-55}$$

In defining the general nonlinear constitutive law, it would be necessary to determine a number of stress-strain pairs and attempt to find a stress-strain law that would best "fit" the data.

For the formulation of the incremental constitutive law, it is necessary to impose a stress or strain increment on the reference stress-strain pair. It is more convenient to apply a stress increment than a strain increment.

Consider a small axisymmetric stress increment:

$$\underset{\sim}{\sigma}' = \begin{bmatrix} \sigma_{rr}' & 0 & \tau_{rz}' \\ 0 & \sigma_{\theta\theta}' & 0 \\ \tau_{rz}' & 0 & \sigma_{zz}' \end{bmatrix} \tag{A-56}$$

Using Eq. A-50, the strain increment is:

$$\begin{bmatrix} e_{rr}' \\ e_{\theta\theta}' \\ e_{zz}' \\ e_{rz}' \end{bmatrix} = \begin{bmatrix} B_{11} & B_{12} & B_{13} & B_{14} \\ B_{21} & B_{22} & B_{23} & B_{24} \\ B_{31} & B_{32} & B_{33} & B_{34} \\ B_{41} & B_{42} & B_{43} & B_{44} \end{bmatrix} \begin{bmatrix} \sigma_{rr}' \\ \sigma_{\theta\theta}' \\ \sigma_{zz}' \\ \tau_{rz}' \end{bmatrix} \tag{A-57}$$

The relation between B_{ij} in Eq. A-57 and B_{ijkl} in Eq. A-50 is obvious. The matrix B_{ij} is assumed to be symmetric.

If the principal axes coincide with r, θ, z (e.g., in the triaxial test), then $B_{41} = B_{42} = B_{43} = 0$. This is because of the initial isotropy of the material. If the principal axes do not coincide with r, θ, z, then B_{41}, B_{42}, and B_{43} have to be included. These coefficients can be determined from the other B's, if the rotation of the principal axes in the rz plane is known. Characterization of a nonlinear elastic material using an incremental constitutive law can be summarized as follows. Impose on the specimen a given reference stress state, record the corresponding strain state; these will be in terms of principal values. Perform small stress excursions from the reference state to determine the incremental coefficients B_{ij}. Repeat this procedure for a sequence of reference stress states. Because all stress and strains will be principal ones, all nonzero incremental coefficients, with the exception of B_{44}, can be determined.

The coefficient B_{44} could be found from a shear stress experiment:

$$B_{44}\tau_{rz}' = e_{rz}' \tag{A-58}$$

However, it is difficult to perform a shear test in the presence of arbitrary principal stresses. The following relation between the incremental shear strain and incremental shear stress can be used:

$$\tau_{rz}' = \left[\frac{\sigma_{zz} - \sigma_{rr}}{e_{zz} - e_{rr}}\right](1 + e_{rr} + e_{zz})e_{rz}' \tag{A-59}$$

This relation is given by Biot for the case of a material with "finite isotropy" and "incremental orthotropy." Biot defines finite isotropy as when the finite stress-strain relations are independent of the stress orientation, and incremental orthotropy as when there is elastic symmetry for incremental stresses.

Eq. A-59 shows that the incremental shear coefficients

may be expressed in terms of the initial stresses and strains. Note that if $e_{zz} = e_{rr}$ one must take appropriate limits to determine the relationship between τ_{rz}' and e_{rz}'. Biot has shown this expression to be:

$$\tau_{rz}' = \tfrac{1}{2}\left(\frac{\sigma_{zz}' - \sigma_{rr}'}{e_{zz}}\right) e_{rz}' \qquad \text{(A-60)}$$

Details of the characterization procedure for a nonlinear material with particular reference to the triaxial test apparatus are given elsewhere. The application of nonlinear elastic stress-strain relations to the solution of boundary value problems is discussed in subsequent sections.

Hereditary Models—Viscoelastic Response

It is pointed out in Eq. A-29, restated below:

$$\underset{\sim}{\sigma}(\underset{\sim}{x}, t) = \overset{t}{\underset{s=0}{F}}[\underset{\sim}{\epsilon}(\underset{\sim}{x}, t-s), T(\underset{\sim}{x}, t-s), M(\underset{\sim}{x}, t-s)] \qquad \text{(A-61)}$$

that the current value of stress depends on the history of the argument functions. For elastic materials, it was assumed that there were no history effects. To account for history effects, if it is assumed that the stress is dependent on the history of strain and the current value of temperature and moisture content, Eq. A-61 would become:

$$\underset{\sim}{\sigma}(\underset{\sim}{x}, t) = \overset{t}{\underset{s=0}{F}}[\underset{\sim}{\epsilon}(\underset{\sim}{x}, t-s), T(\underset{\sim}{x}, t), M(\underset{\sim}{x}, t)] \qquad \text{(A-62)}$$

A further simplification can be introduced if the temperature and moisture conditions are held fixed; i.e., the relationship between stress and strain is determined for particular temperature and moisture conditions:

$$\underset{\sim}{\sigma}(\underset{\sim}{x}, t) = \overset{t}{\underset{s=0}{F}}[\underset{\sim}{\epsilon}(\underset{\sim}{x}, t-s)] \qquad \text{(A-63)}$$

This represents a general nonlinear stress-strain-time relationship.

The term viscoelasticity results from an attempt to represent the behavior of real materials by combining time-dependent response, as represented by viscous models, and time-independent response, as represented by elastic models. Although the term viscoelasticity did not originally encompass all combinations of viscous and elastic effects, its use here includes all possible combinations. Linear viscoelasticity, the most widely used theory to date in pavement analysis, is discussed first. Some one-dimensional concepts are considered, to illustrate viscoelastic behavior. These concepts are then generalized to three dimensions.

One-Dimensional Linear Viscoelastic

Let a one-dimensional element (a prismatic bar) be subject to a force along its axis. Let the force at time t be $F(t)$ and the elongation be $u(t)$. If $F(t)$ is continuous and differentiable, considering small time interval $d\tau$ at time τ, the force applied in this interval is $\dfrac{dF(t)}{dt}\,d\tau$. At time t this increment has been acting for time $(t-\tau)$ and has a contribution $du(t)$ to $u(t)$; the relation between the incremental load and deflection is assumed to be given by a proportionality constant that is dependent on the time interval $(t-\tau)$ (Fig. A-5).

This may be expressed mathematically as:

$$du(t) = \Psi(t-\tau)\,(dF/dt)_\tau d\tau \qquad \text{(A-64)}$$

in which $(dF/dt)_\tau$ represents the rate of change of F evaluated at τ.

Consider the origin of time at the beginning of loading and deformation; the total deformation at any time can be obtained by integrating Eq. A-63.

$$u(t) = \int_0^t \Psi(t-\tau)\,(dF/dt)_\tau d\tau \qquad \text{(A-65)}$$

For a finite load applied suddenly at $t = 0$, with $F(t) = 0$ for $t < 0$ (Fig. A-5):

$$u(t) = F(x, 0^+)\Psi(t) + \int_0^t \Psi(t-\tau)\,(dF/dt)_\tau d\tau \qquad \text{(A-66)}$$

in which $F(x, 0^+)\Psi(t) =$ initial displacement.

The function $\Psi(t)$ is the creep function. From a physical standpoint, $\Psi(t)$ is the elongation produced by a sudden application of load of constant unit magnitude at time $t = 0$.

Using a similar argument, with the role of $F(t)$ and $u(t)$ interchanged:

$$F(t) = \int_0^t \phi(t-\tau)\,(du/dt)_\tau d\tau \qquad \text{(A-67)}$$

For a finite deflection applied suddenly at $t = 0$ and for $u(t) = 0, t < 0$.

$$F(t) = u(t, 0^+)\phi(t) + \int_0^t \phi(t-\tau)\,(du/dt)_\tau d\tau \qquad \text{(A-68)}$$

The function $\phi(t)$ is the relaxation function and is the force required to produce an elongation that changes from 0 to unity at $t = 0$ and then remains constant.*

The general linear theory of viscoelasticity can be developed by generalizing the one-dimensional stress-strain (force displacement) laws to three dimensions.** This situation is analogous to the situation in linear elasticity where Hooke's Law originally postulated in one dimension was generalized to three dimensions by Cauchy.

It is appropriate to consider certain special cases of the one-dimensional representations in Eqs. A-66 and A-68. It is convenient to represent these special cases by one-dimensional mechanical models. These models permit the formulation of physical concepts that assist in visualizing various types of behavior. They are not essential to the development of the theory.

The two basic models used in linear viscoelastic analyses are:

1. The linear elastic spring represented by the stress-strain equation:

---

* Eqs. A-65 and A-67 were introduced by Boltzman and the integral was called a hereditary integral by Voltera. Note that these laws are linear; integration being a limit of sums in the sense of Reimann-Steltjes.

** Force displacement relations can be converted to stress-strain relations by multiplying by a constant related to the ratio of the area of the bar to the length.

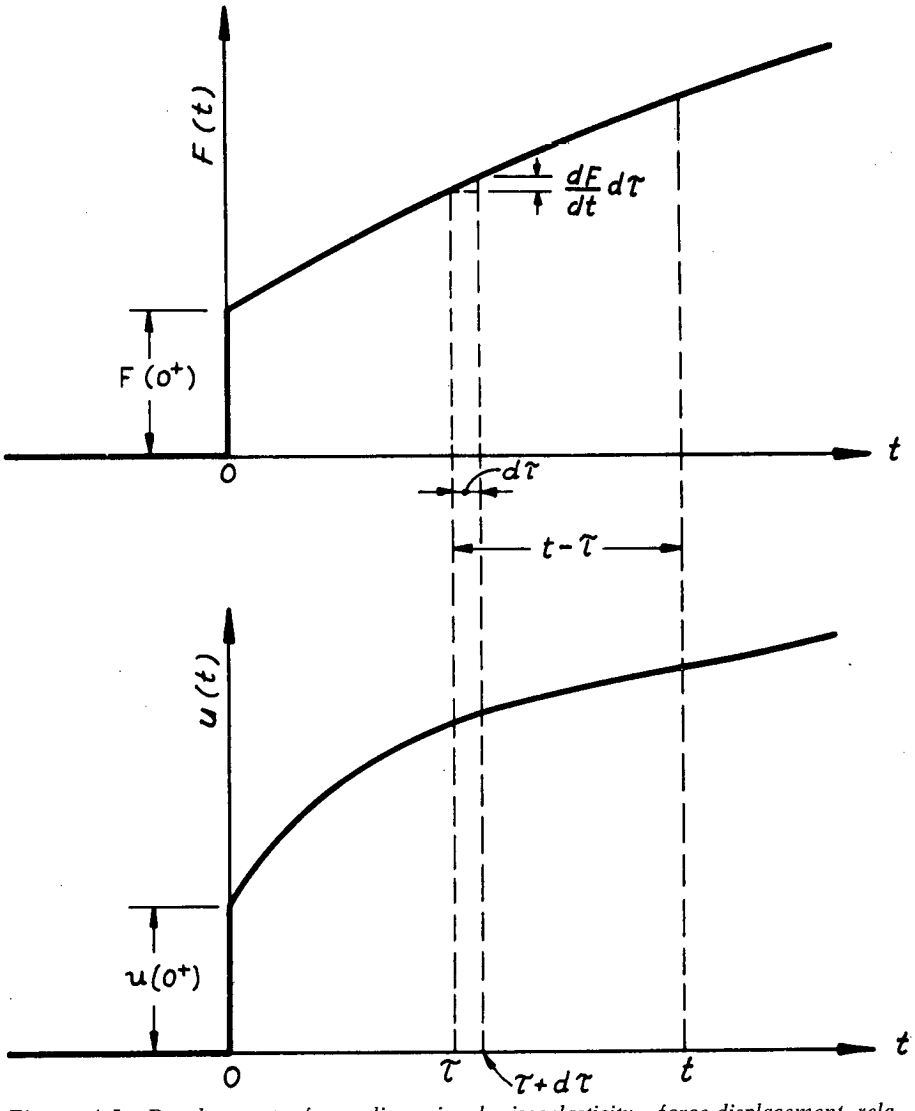

Figure A-5. Development of one-dimensional viscoelasticity—force-displacement relationship.

$$\sigma = k\epsilon \qquad \text{(A-69)}$$

(stress is proportional to strain)

2. A linear viscous model, represented by a dashpot where the stress is proportional to the rate of strain:

$$\sigma = \eta\dot{\epsilon}$$

The stress-strain law of any one-dimensional model composed of a one-dimensional network of these elements is formed from the following basic rule: *When two models are placed in series, the stress is the same in each model, but the total strain is the sum of the strain in each model. When two models are placed in parallel, the strain is the same in each model, but the total stress is the sum of the stresses in each model.*

Kelvin Model.—The stress-strain relationship of the Kelvin model (Fig. A-6) is:

$$\sigma = \eta D\epsilon + E\epsilon \qquad \text{(A-70)}$$

in which

$D = d/dt$, the differential operator;
η = viscosity of the dashpot; and
E = spring constant.

If the Kelvin model is subject to a constant stress σ_o,

$$\epsilon(t) = \frac{\sigma_o}{E}(1 - e^{-t/\tau_k}) \qquad \text{(A-71)}$$

where $\tau_k = \eta/E$ and has dimensions of time.

If σ_o is unity, $\epsilon(t)$ is the creep function.
$J_c(t)$, the creep compliance, is defined as:

$$\frac{\epsilon(t)}{\sigma_o} = \frac{1}{E}(1 - e^{-t/\tau_k}) \qquad \text{(A-72)}$$

If the stress is removed when $\epsilon = \epsilon_o$, the equation for the Kelvin model yields:

$$\epsilon = \epsilon_o e^{-t/\tau_k} \qquad \text{(A-73)}$$

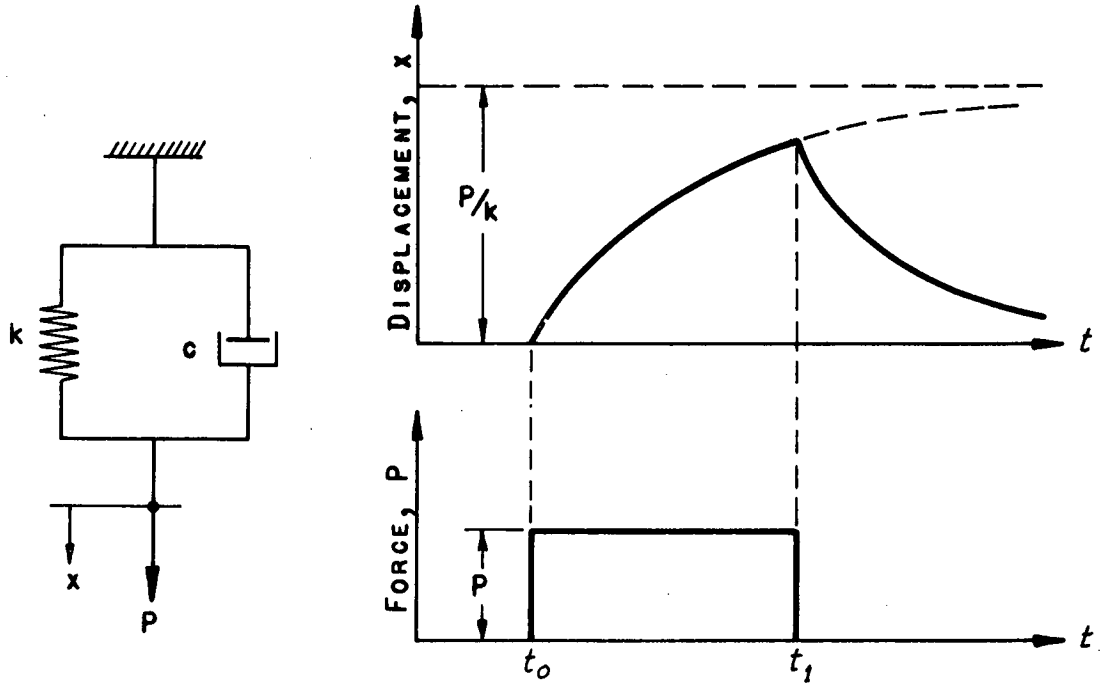

(a) KELVIN BODY AND ITS RESPONSE

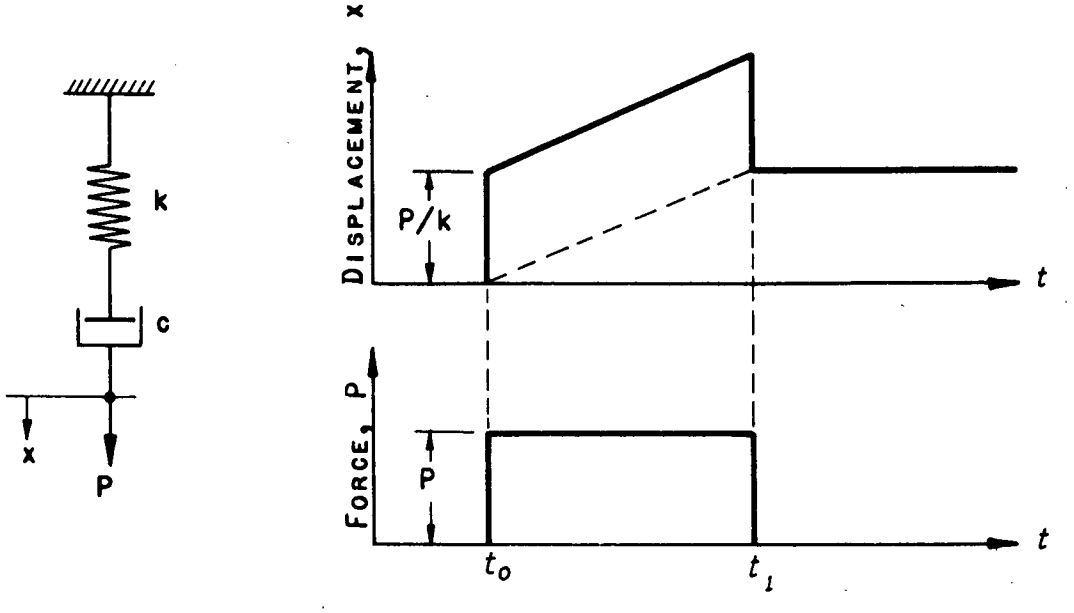

(b) MAXWELL BODY AND ITS RESPONSE

Figure A-6. Kelvin and Maxwell models.

This equation indicates that recovery progresses at an exponential rate; the quantity τ_k is characteristic of the rate of recovery and is called the retardation time. It may be defined as the time it takes for the strain to reach $1/e$ of its original value.

Maxwell Model.—The stress-strain relationship of the Maxwell model is:

$$D\epsilon = \frac{1}{E} D\sigma + \frac{1}{\eta}\sigma \qquad \text{(A-74)}$$

If the model is subject to a constant strain ϵ_0 (i.e., $D\epsilon = 0$), the stress relaxes according to

$$\sigma = \sigma_o e^{-t/\tau_m} \tag{A-75}$$

in which

σ_o = initial stress; and
$\tau_m = \eta/E$ (units of time).

Here τ_m is known as the relaxation time and represents the time for the stress to relax to $1/e$ of its initial value.

The quantity (Ee^{-t/τ_m}) is often defined as the relaxation modulus $E_r(t)$.

In cases where the material is represented by a number of connected Maxwell and Kelvin elements, the response for such a generalized model is characterized by retardation and relaxation spectra. This approach has been summarized by Ferry (1961).

Three-Dimensional Linear Viscoelastic

The previous section discusses one-dimensional representations; to conduct a meaningful stress analysis, these concepts must be extended to three dimensions. An analogous situation existed in the development of elasticity. Hooke's Law was originally stated for uniaxial stress and strain; the extension to three dimensions (generalized Hooke's Law) was performed by Cauchy.

Under one-dimensional considerations:

$$\sigma = \int_{-\infty}^{t} G(x, t-\tau)\frac{\partial e}{\partial \tau}(x, \tau)\, d\tau \tag{A-76}$$

This is the stress-strain form of the force extension relation derived in Eq. A-67.

It is assumed that e is continuous and differentiable in writing this integral. The lower limit of the integral is taken as $-\infty$ to indicate that the integration is taken from the very beginning of motion. Consider a motion of the type shown in Figure A-7. For $t < 0$, $\sigma = e = 0$. In this case Eq. A-76 reduces to

$$\sigma(x, t) = e(x, 0^+)G(x, t) + \int_0^t G(x, t-\tau)\frac{\partial e}{\partial \tau}(x, \tau)\, d\tau \tag{A-77}$$

The first term gives the effect of the initial disturbance, due to the finite value of $e(x, t)$ at $t = 0$, as shown in Figure A-7. Any other discontinuity in e will contribute a term similar to the first term in Eq. A-77. For the conditions in Figure A-8:

$$\begin{aligned}\sigma(x, t) = {} & e(x, 0^+)G(x, t) \\ & + \Delta e(x, \xi)G(x, t-\xi)H(t-\xi) \\ & + \int_0^t G(x, t-\tau)\frac{\partial e}{\partial \tau}\, d\tau\end{aligned} \tag{A-78}$$

in which $H(t)$ is the unit step function.

Because it will be necessary to write integrals of this type (convolution integrals) many times, it is convenient to use a shorthand notation. Define

$$\int_0^t \phi(t-\tau)\frac{\partial \Psi}{\partial \tau}\, d\tau + \phi(t)\Psi(0) = \phi * d\Psi \tag{A-79}$$

Hence, Eq. A-76 may be written as:

$$\sigma(x, t) = G(x, t) * de \tag{A-80}$$

Eq. A-80 represents a one-dimensional relation between stress and strain. An analogous situation existed in linear elasticity with Hooke's Law, which represented a one-dimensional stress-strain relationship. To generalize Eq. A-80 to three dimensions, it is assumed for the linear case that the six components of stress are linearly related to six components of strain: *

$$\begin{aligned}
\sigma_{xx} &= G_{11} * de_{xx} + G_{12} * de_{yy} + G_{13} * de_{zz} + G_{14} * de_{xy} + G_{15} * de_{yz} + G_{16} * de_{xz} \\
\sigma_{yy} &= G_{21} * de_{xx} + G_{22} * de_{yy} + \\
\sigma_{zz} &= G_{31} * de_{xx} + G_{32} + G_{33} * de_{zz} + \\
\tau_{xy} &= G_{41} * de_{xx} + G_{42} + + G_{44} * de_{xy} + \\
\tau_{yz} &= G_{51} * de_{xx} + G_{52} + + G_{55} * de_{yz} + \\
\tau_{xz} &= G_{61} * de_{xx} + G_{62} + + G_{66} * de_{xz}
\end{aligned} \tag{A-81}$$

Using tensor notation, Eq. A-81 can be written as

$$\sigma_{ij} = G_{ijkl} * de_{kl} \tag{A-82}$$

It may be necessary to consider the inverse stress-strain law:

$$e_{ij} = J_{ijkl} * d\sigma_{kl} \tag{A-83}$$

* This uses the shorthand notation of Eq. A-79.

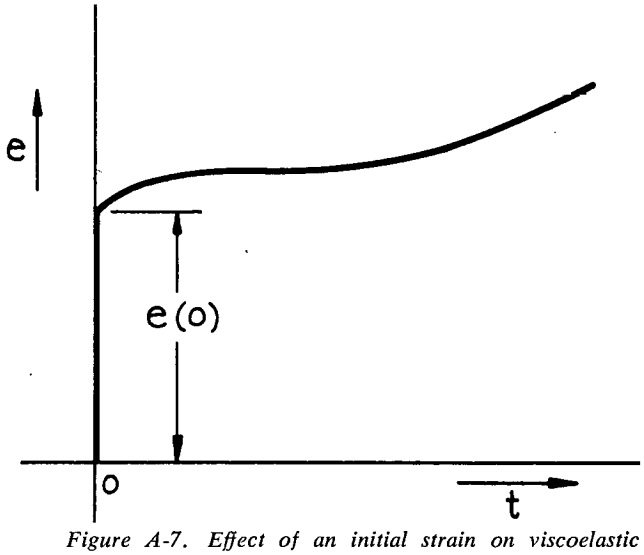

Figure A-7. Effect of an initial strain on viscoelastic response.

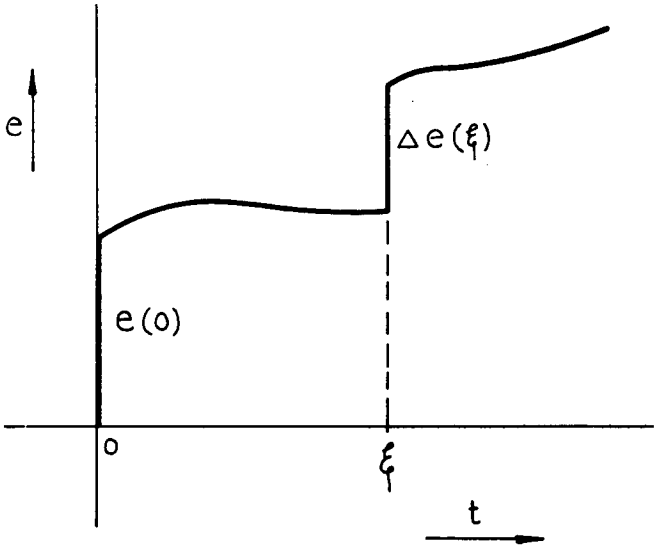

Figure A-8. Effect of a finite strain imposed at an arbitrary time.

Eqs. A-80 and A-82 represent a stress-strain law of the relaxation type; Eq. A-83 represents a strain-stress law of the creep type.

The symmetry of the stress and strain tensors requires that the number of functions G_{ijkl} or J_{ijkl} be 21.

Eqs. A-81 and A-83 deal with nonhomogeneous and anisotropic material. If the material is homogeneous, the functions G and J are independent of position. If the functions G and J are invariant with respect to rotations of the coordinate system, the material is considered isotropic. By arguments analogous to those in linear elasticity these equations can be reduced as follows for homogeneous, linear isotropic, viscoelastic solids:

$$\begin{aligned}
\sigma_{xx} &= G_{11} * de_{xx} + G_{12} * d(e_{yy} + e_{zz}) \\
\sigma_{yy} &= G_{12} * d(e_{xx} + e_{zz}) + G_{11} * de_{yy} \\
\sigma_{zz} &= G_{12} * d(e_{xx} + e_{yy}) + G_{11} * de_{zz} \\
\tau_{xy} &= G_{44} * de_{xy} \\
\tau_{yz} &= G_{44} * de_{yz} \\
\tau_{xz} &= G_{44} * de_{xz}
\end{aligned} \tag{A-84}$$

If one considers isotropic and deviatoric stresses, the following may be used. For deviatoric stress: *

$$\begin{aligned}
\tau_{xy} &= G_1 * de_{xy} \\
\tau_{xz} &= G_1 * de_{xz} \\
\tau_{yz} &= G_1 * de_{yz}
\end{aligned}$$

$$\begin{aligned}
\sigma_{xx} - \tfrac{1}{3}(\sigma_{xx} + \sigma_{yy} + \sigma_{zz}) &= G_1 * \\
&\quad d[e_{xx} - \tfrac{1}{3}(e_{xx} + e_{yy} + e_{zz})] \\
\sigma_{yy} - \tfrac{1}{3}(\sigma_{xx} + \sigma_{yy} + \sigma_{zz}) &= G_1 * \\
&\quad d[e_{yy} - \tfrac{1}{3}(e_{xx} + e_{yy} + e_{zz})] \\
\sigma_{zz} - \tfrac{1}{3}(\sigma_{xx} + \sigma_{yy} + \sigma_{zz}) &= G_1 * \\
&\quad d[e_{zz} - \tfrac{1}{3}(e_{xx} + e_{yy} + e_{zz})]
\end{aligned} \tag{A-85}$$

In summation notation these equations may be written as:

$$\sigma_{ij} - \tfrac{1}{3}\delta_{ij}\sigma_{kk} = G_1 * d(e_{ij} - \tfrac{1}{3}\delta_{ij}e_{kk}) \quad \text{or} \quad \sigma_{ij}' = G_1 * de_{ij}' \tag{A-86}$$

For dilational stress:

$$\sigma_{kk} = G_2 * de_{kk} \tag{A-87}$$

in which G_1 and G_2 are relaxation functions in shear and isotropic compression, respectively.

The corresponding stress-strain laws for an isotropic material using creep functions are:

$$(e_{ij} - \tfrac{1}{3}\delta_{ij}e_{kk}) = J_1 * d(\sigma_{ij} - \tfrac{1}{3}\delta_{ij}\sigma_{kk}) \tag{A-88}$$

$$e_{kk} = J_2 * d(\sigma_{kk}) \tag{A-89}$$

If J_1, J_2, G_1, and G_2 are step functions in time, the stress-strain laws represented by Eqs. A-86 to A-89 reduce to the stress-strain laws of isotropic elastic solids.

The representative of the stress-strain relation using differential operators has been approached from both thermodynamic and mechanical standpoints. The resulting equations are identical. The mechanical viewpoint is based on the hypothesis that the miscroscopic structure of the material is mechanically equivalent to a network of springs and dashpots without any restriction on their number or arrangement. This procedure is subject to the objection that one cannot assume a priori that the three-dimensional network will exhibit no features that are not shown in the one-dimensional model. However, this model is the one most commonly used and has given useful practical results.

The stress-strain relations of a linear viscoelastic material can be expressed as:

$$P_1(D)\sigma_{ij}' = Q_1(D)e_{ij}' \tag{A-90}$$

$$P_2(D)\sigma_{kk} = Q_2(D)e_{kk} \tag{A-91}$$

in which

$$D = d/dt,\ D^n = d^n/dt^n \tag{A-92}$$

$$P_1(D) = \sum_{k=0}^{n_1} a_k D^k,\ P_2(D) = \sum_{k=0}^{n_2} c_k D^k \tag{A-93}$$

$$Q_1(D) = \sum_{k=0}^{m_1} b_k D^k,\ Q_2(D) = \sum_{k=0}^{m_2} d_k D^k \tag{A-94}$$

in which a_k, b_k, c_k, and d_k are real valued functions of the spatial coordinates. If the material is homogeneous, these may be considered as constants.

The polynomials P_1, P_2, Q_1, and Q_2 define a linear viscoelastic material. The mechanical models introduced earlier are simple examples of these polynomial relationships for the one-dimensional case. In extending the model concept to three dimensions, one should realize that although a physical drawing of the model is in one dimension, it must be used to relate the three-dimensional stress system to the three-dimensional strain system. It is not enough to connect, say, the axial stress with the axial strain. For an isotropic medium, the relations between deviatoric and dilational stresses and strains are sufficient to define the material. As the foregoing expressions show, different models can be used to represent the relationships between stresses and strains. For example, a material may be considered as behaving as a Maxwell model under deviatoric stresses and as a Kelvin model under isotropic compression.

* The notations G_1 and G_2 are used for convenience. They are related to the coefficients in Eq. A-84.

Necessary and sufficient conditions for a linear viscoelastic material to be described by integral or differential operators have been derived by Gurtin and Sternberg (1962).

Nonlinear Viscoelasticity

Nonlinear viscoelastic theory has not been applied to the analysis of pavement structures. The reasons for this are the complexity of the theory; the difficulty in experimentally determining the material functions; and the problems associated with developing solutions to nonlinear boundary value problems. This section describes some of these difficulties.

A general form of a nonlinear viscoelastic constitutive law is:

$$\sigma_{ij}(\underset{\sim}{x}, t) = G_{ij}[E_{ij}(t)] + \overset{\tau=t}{\underset{\tau=0}{F_{ij}}}[E_{ij}(\underset{\sim}{x}, \tau); \underset{\sim}{x}, t] \qquad \text{(A-95)}$$

If it is assumed that the material is homogeneous and nonaging,

$$\sigma_{ij}(\underset{\sim}{x}, t) = G_{ij}[E_{ij}(t)] + \overset{\tau=t}{\underset{\tau=0}{F_{ij}}}[E_{ij}(\underset{\sim}{x}, t-\tau)] \qquad \text{(A-96)}$$

The first term on the right represents the instantaneous stress. If only physical nonlinearity is being considered, E_{ij} may be replaced by infinitesimal strain tensor e_{ij}.

The researchers' method of representing the nonlinear equation is an expansion into a series of integrals:

$$\begin{aligned}\sigma_{ij}(t) = G_{ij}[e_{ij}(t)] &+ \int_0^t K_{ijkl}(t-\tau_1)e_{kl}(\tau_1)d\tau_1 + \cdots \\ &+ \int_0^t\int_0^t \cdots \int_0^t K_{ijkl\ldots rs}(t-\tau_1, t-\tau_2 \ldots, t-\tau_p) \\ &e_{kl}(\tau_1)e_{mn}(\tau_2)\ldots e_{rs}(\tau_p)d\tau_1 d\tau_2 \ldots d\tau_p + \cdots\end{aligned} \qquad \text{(A-97)}$$

in which $K_{ijklmn\ldots rs}$ for $p = 1, 2 \ldots$ represent tensor relaxation functions that have to be determined experimentally. This implies subjecting samples to multiaxial stress states and measuring their multiaxial deformation history. Because each function requires a number of points for defining it, the complexity of the experimental task is evident.

An alternate formulation is to consider an incremental approach similar in concept to that outlined for nonlinear elastic materials by Dong et al. (1968). Assume that a reference history $\bar{\underset{\sim}{e}}(s)$ is specified, and that the stress corresponding to this history is

$$\bar{\underset{\sim}{\sigma}}(t) = \overset{s=t}{\underset{s=0}{\underset{\sim}{F}}}[\bar{\underset{\sim}{e}}(s)] \qquad \text{(A-98)}$$

Here, as before, multiaxial stress and strain states are being considered. Consider a small change in input strain history $\epsilon(s)$. The new strain history can be written as

$$\overset{s=t}{\underset{s=0}{\underset{\sim}{F}}}[\bar{\underset{\sim}{e}}(s) + \underset{\sim}{\epsilon}(s)] = \overset{s=t}{\underset{s=0}{\underset{\sim}{F}}}[\bar{\underset{\sim}{e}}(s)] + \int_0^t \overset{s=t}{\underset{s=0}{\underset{\sim}{G}}}[\bar{\underset{\sim}{e}}(s); t-\tau]: \frac{\partial \epsilon}{\partial \tau}\, d\tau \qquad \text{(A-99)}$$

The accuracy of the approximation depends on the magnitude $\underset{\sim}{\epsilon}(s)$. The following experimental program is suggested by Eq. A-99. First determine a reference state $\bar{\underset{\sim}{\sigma}}(t)$, $\bar{\underset{\sim}{e}}(s)$. Then repeat the experiment with a strain history input $\underset{\sim}{e} = \bar{\underset{\sim}{e}} + \underset{\sim}{\epsilon_0}H(t-\tau_k)$, in which $\underset{\sim}{\epsilon_0}$ is a constant tensor; and H is the Heaviside step function. From this input $\underset{\sim}{F}(\underset{\sim}{e})$ is determined. Because

$$\underset{\sim}{F}(\underset{\sim}{e}) = \underset{\sim}{F}(\bar{\underset{\sim}{e}}) + \overset{s=t}{\underset{s=0}{\underset{\sim}{G}}}[\bar{\underset{\sim}{e}}(s); t-\tau_k]: \underset{\sim}{\epsilon_0} \qquad \text{(A-100)}$$

and $\bar{\underset{\sim}{e}}(s)$ is a prescribed history, $\underset{\sim}{G}$ can be written as $\underset{\sim}{G}(t, t-\tau_k)$. Eq. A-100 therefore permits the determination of $\underset{\sim}{G}(t, t-\tau_k)$. This kernel defines the viscoelastic material in the neighborhood of the reference state. A detailed explanation of the incremental formulation is given in Dong et al. (1968). Note that the use of an incremental procedure is closely tied in with the technique of solution for the boundary value problem because the results of the solution guide the choice of reference states. The process is therefore an iterative one.

Simplified approaches to nonlinear laws can be applied to both differential and integral representations of linear viscoelasticity. In the differential representation (mechanical models), it is assumed that the constants of the springs and dashpots are no longer constants of the material but functions of the stress and strain and time. For example, a nonlinear Maxwell model can be represented as:

$$\frac{1}{E(\sigma, t)}\frac{d\sigma}{dt} + \frac{1}{\eta(\sigma, t)}\sigma = \frac{d\epsilon}{dt} \qquad \text{(A-101)}$$

The spring constant, E, and the viscosity coefficient, η, are functions of the stress, σ, and time, t.

In an integral representation, nonlinear behavior can be represented as:

$$\epsilon(t) = D(0)\sigma(t) + \int_0^t D(t-\tau)\frac{\partial}{\partial \tau} f[\sigma(\tau)]\, d\tau \qquad \text{(A-102)}$$

in which $D(t)$ is the creep function; and $f[\sigma(\tau)]$ is a function of σ. $D(t)$ and $f(\sigma)$ are to be determined from the experimental data. An alternate representation is

$$\epsilon(t) = D[0, \sigma(t)]\sigma(t) - \int_0^t \frac{\partial D[(t-\tau), \sigma(\tau)]}{\partial \tau}\sigma(\tau)d\tau \qquad \text{(A-103)}$$

In this case the kernel D is a function of t and σ. In general,

$$\epsilon(t) = k[\sigma(t)] + \int_0^t D[(t-\tau), \sigma(\tau)]\, d\tau \qquad \text{(A-104)}$$

in which $k[\sigma(\tau)]$ represent the instantaneous (not necessarily linear) strains, and the integrals represent the cumulative effect of the history of the stress and strains.

Extending these equations to the general three-dimensional case, where G, D, σ are considered as tensions as in the linear cases, raises questions of material frame indifference, as pointed out by Noll (1958) and Truesdell and Noll (1965).

Hereditary Models—Plastic Response

Basic Concepts and Constitutive Law of Plasticity *

The theories of plasticity can be divided into two categories: (1) physical, and (2) mathematical. The physical theories try to explain, from a microscopic viewpoint, why materials flow plastically. The mathematical theories are phenomenological in nature and are formalizations of the results of microscopic experiments. They are essential for the solution of stress analysis problems. This report is concerned with the mathematical theories of plasticity and their application in soil mechanics.

A distinction should be made between elasticity and plasticity. Both are time-independent theories. Plasticity is the behavior of materials that deform permanently under the action of external loads, whereas an elastic body returns to its original shape on removal of external forces. The assumption of elasticity is obviously an idealization, because all materials exhibit plastic behavior to a certain extent. However, in many cases the permanent deformations are sufficiently small to be negligible or otherwise practically insignificant. In these cases the use of elasticity theory is justified. Plasticity theory is used with situations in which loads are sufficiently large so that measurable amounts of permanent deformation occur.

The theory of plasticity can be divided into two ranges. For the types of problems that involve very large plastic strains and deformations the elastic strains usually can be neglected and the material can be assumed to be perfectly plastic. On the other hand, the elastoplastic problems refer to cases where the plastic strains are of the same order of magnitude as the elastic strains.

* By K. Sadigh, of Woodward-Lundgren & Associates.

In the elastic range the strains are assumed to be linearly related to the stresses by the generalized Hooke's Law. Consequently, in the elastic range the strains are uniquely determined by the stresses without any regard as to how this stress state was attained. The stress-strain relation in the plastic range generally will be nonlinear. Furthermore, the strains generally are not uniquely determined by the stresses but depend on the load history or how the stress state was reached.

Concept of Yielding.—To illustrate the concept of yielding, consider the stress-strain curve that is representative of the results of uniaxial tensile test.

Figure A-9 shows a typical stress-strain curve. Initially, the relation between stress and strain is essentially linear. This linear part of the curve extends up to point A, called the proportional limit. In this range the material would undergo complete recovery on unloading; the material is linearly elastic.

On further increase of the load the strain no longer increases linearly with stress, but the material still remains elastic. This range extends from A to point B, called the elastic limit, or yield point. Beyond the elastic limit, permanent deformation (called plastic deformation) takes place. The condition that governs the initiation of yield is termed the yield condition, or the yield surface, or the yield function. The term "yielding" has two interpretations when applied to real materials. That is, yielding can be caused either by "fracture," where separation of material takes place while the strains are still in essence elastic, or by "plastic yielding," where large permanent deformations follow elastic behavior with a more or less noticeable transition phase. The theories for yielding proposed about 1900 did not distinguish between the two phenomena.

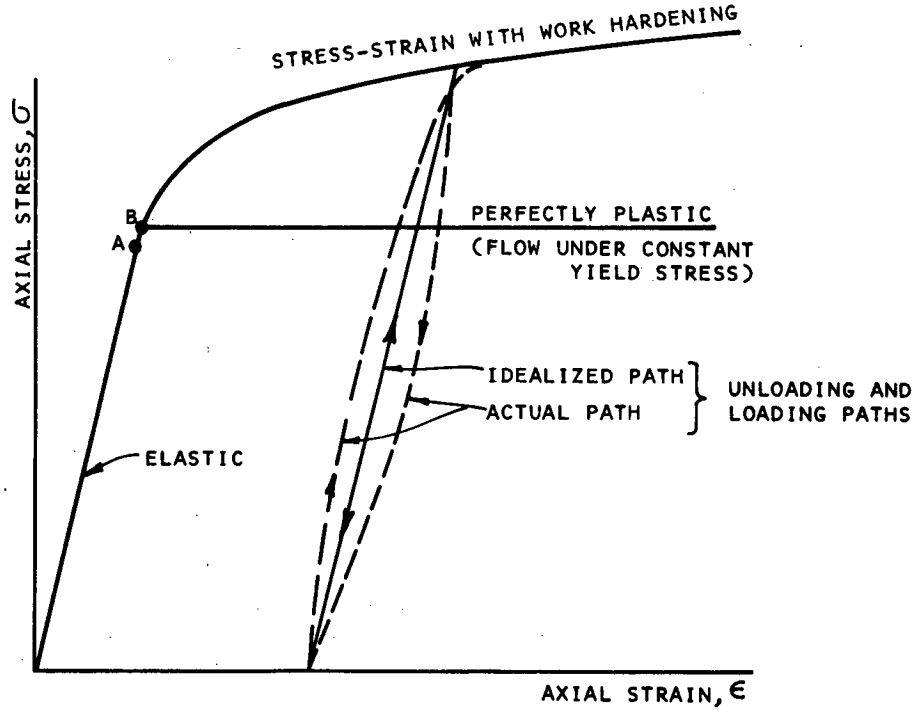

Figure A-9. Conventional stress-strain curve.

As the load is increased beyond the elastic limit, the strain increases at a greater rate. However, the specimen will not deform further unless the load is increased. This condition is called work hardening, or strain hardening. The stress required for further plastic flow is called flow stress.

The stress-strain curve described here is significant in that the concept of a yield criterion is a generalization of the yield limit in uniaxial tests. The term "yield" in plasticity is used to describe the onset of plastic deformation on the upper limit of elastic action. If the elastic deformation under stress is zero, the material is termed "rigid." Beyond yield, the plastic performance is termed "perfect" when flow continues under the constant (yield) stress. Normally an increasing stress is necessary to produce flow beyond the yield point (work-hardening).

At present, there is no theoretical basis for calculating the relation between the stress components for yielding in a three-dimensional state of stress from the information on yielding in the uniaxial tensile or compression test. Most theories proposed are empirical and attempt to be reasonably descriptive of experimental data. The various criteria that have been proposed are based on a concept of either stress, strain, or energy.

Some Early Failure Theories.—Numerous criteria have been proposed for the yielding of solids. Many of these were originally suggested as criteria for failure of brittle materials and were later adopted as yield criteria for ductile materials. The following theories are seldom used; however, they are of historic interest and demonstrate the type of approach used to develop yield criteria.

1. *Maximum Stress Theory:* Often referred to as Rankine's theory or Lamé-Navier theory; postulates that the maximum principal stress in the material determines failure, regardless of the magnitude and senses of the other two principal stresses. Thus, according to this theory, yielding begins when the absolute value of the maximum stress reaches the yield point of the material in simple tension or compression. Thus, the criterion becomes

$$\begin{aligned} \sigma_1 &= \sigma_{ot} \\ \sigma_2 &= \sigma_{oc} \end{aligned} \qquad \text{(A-105)}$$

in which σ_1 is the maximum principal stress; σ_2 is the minimum principal stress; σ_{ot} and σ_{oc} are, respectively, the yield stresses in simple tension and simple compression.

This theory is rarely used, because it disregards the influence of two of the three principal stresses and conflicts with the experimental information.

2. *Maximum Elastic Strain Theory:* Attributed to St. Venant; assumes that yielding will occur when the maximum value of the principal strain equals the value of the yield strain in simple tension (or compression). Thus, if ϵ_1 is the largest strain, yielding will occur when

$$\epsilon_1 = \frac{1}{E}[\sigma_1 - \nu(\sigma_2 + \sigma_3)] = \epsilon_y \qquad \text{(A-106)}$$

This maximum strain criterion is rarely used because it contradicts most experiments. For example, it is contradicted by material behavior under hydrostatic tensile or compressive stresses.

3. *Maximum Strain Energy Theory:* Also known as Beltrami's energy theory; assumes that yielding will occur when the total strain energy per unit volume equals the total strain energy per unit volume at yielding in uniaxial tension or compression. If one equates the energy stored at yield in simple tension to the strain energy for a given state of stress at failure the criterion may be written as:

$$\frac{(\sigma_y)^2}{2E} = \frac{1}{2E}[(\sigma_1^2 + \sigma_2^2 + \sigma_3^2) - 2\nu(\sigma_1\sigma_2 + \sigma_2\sigma_3 + \sigma_3\sigma_1)] \qquad \text{(A-107)}$$

or

$$\sigma_1^2 + \sigma_2^2 + \sigma_3^2 - 2\nu(\sigma_1\sigma_2 + \sigma_2\sigma_3 + \sigma_3\sigma_1) = \sigma_y^2$$

Yield Criteria Commonly Used.—The concept of a yield criterion is a generalization of the yield limit determined in a uniaxial test. In the most general case, the yield criterion will depend on the complete state of stress at the point under consideration and therefore will be a function of the nine components of stress at the point. However, the symmetry of the stress tensor indicates that its six independent components would be sufficient to define this function. The yield criterion for a material loaded to the initial yield can be expressed as

$$F(\sigma_{ij}) = K \qquad \text{(A-108)}$$

This function is called the yield function. This equation represents a hypersurface in the six-dimensional stress space, called an "initial yield surface," and any point on this surface represents a point at which yielding can begin. This hypersurface is thus enclosing a region of purely elastic behavior and is based on the idea of a yield point in the one-dimensional system.

For an initially isotropic material it is reasonable to assume that a yield function exists that would be a function of the stress invariants; i.e.,

$$F = F(I_1, I_2, I_3) \qquad \text{(A-109)}$$

in which I_1, I_2, and I_3 are the stress invariants defined as

$$\begin{aligned} I_1 &= \sigma_1 + \sigma_2 + \sigma_3 \\ I_2 &= \sigma_1\sigma_2 + \sigma_2\sigma_3 + \sigma_3\sigma_1 \\ I_3 &= \sigma_1\sigma_2\sigma_3 \end{aligned}$$

in which σ_1, σ_2, and σ_3 are the principal stresses. Because the material is assumed to be isotropic, the rotation of the axes does not affect the yielding, and the yield function can be expressed as

$$F(\sigma_1, \sigma_2, \sigma_3) = K \qquad \text{(A-110)}$$

On the basis of experimental results, it is generally assumed that (1) hydrostatic stress does not affect the initial yield condition, or the plastic deformation, and, consistent with this concept, that (2) plastic deformation takes place with no volume change. (However, many materials, such as cohesionless soils, exhibit relatively large volume changes during plastic deformation.)

Consequently, it is assumed that only the stress deviators enter into the yield function. Therefore, the initial yield function can be expressed as

$$f^o = f^o(S_1, S_2, S_3) = K \qquad \text{(A-111)}$$

in which

$S_{ij} = \sigma_{ij} - \sigma_m \delta_{ij}$

$\sigma_m = \frac{1}{3}(\sigma_1 + \sigma_2 + \sigma_3)$ represent the deviatoric stress and mean stress, respectively.

Alternatively, in terms of the invariants of the deviatoric stress, one can write (because J_1 vanishes)

$$f^o = f^o(J_2, J_3) = K \qquad \text{(A-112)}$$

in which

$J_1 = S_1 + S_2 + S_3 = 0$

$J_2 = \frac{1}{2}(S_1^2 + S_2^2 + S_3^2) = -(S_1S_2 + S_2S_3 + S_3S_1)$

$J_3 = \frac{1}{3}(S_1^3 + S_2^3 + S_2^3) = S_1S_2S_3$

If it is further assumed that the Bauschinger effect is absent, so that the yield stress in compression equals that in tension or more generally $f^o(\sigma_{ij}) = f^o(-\sigma_{ij})$ then $f^o(J_2, J_3)$ in Eq. A-112 must be an even function of J_3. The principal stress space (with coordinates σ_1, σ_2, and σ_3) is called the Haigh-Westergaard stress space. The line passing through the origin and making equal angles with the coordinate axes represents points where the stress state is such that $\sigma_1 = \sigma_2 = \sigma_3 = \sigma_m$. This line corresponds to a hydrostatic stress state and is referred to as the hydrostatic axis. The deviator stresses $S_1 = (2\sigma_1 - \sigma_2 - \sigma_3)/3$, etc., are equal to zero on this line. The plane ($\sigma_1 + \sigma_3 + \sigma_2 = 0$) passing through the origin and perpendicular to the hydrostatic axis is sometimes referred to as the π-plane.

In the principal stress space, the yield surface may be represented by a piecewise smooth uniform cylinder of infinite length (called the yield cylinder) whose elements are parallel to the hydrostatic axis. This is a consequence of the three assumptions of isotropy, the absence of Bauschinger effect, and no dependence of plastic deformation on mean normal stress. The yield cylinder is perpendicular to π-plane, and its intersection with π-plane or any plane parallel to it will produce a curve called a yield locus. Figure A-10 shows the π-plane as the plane of the paper and the projections on this plane of the coordinate axes σ_1, σ_2, and σ_3. It can be shown that the yield locus must have the same shape in each of the 12 30° sectors dividing the π-plane. This is a consequence of the assumptions of the isotropy and the absence of Bauschinger effect. The former implies symmetry with respect to the coordinate axes and the later requires symmetry with respect to coordinate planes.

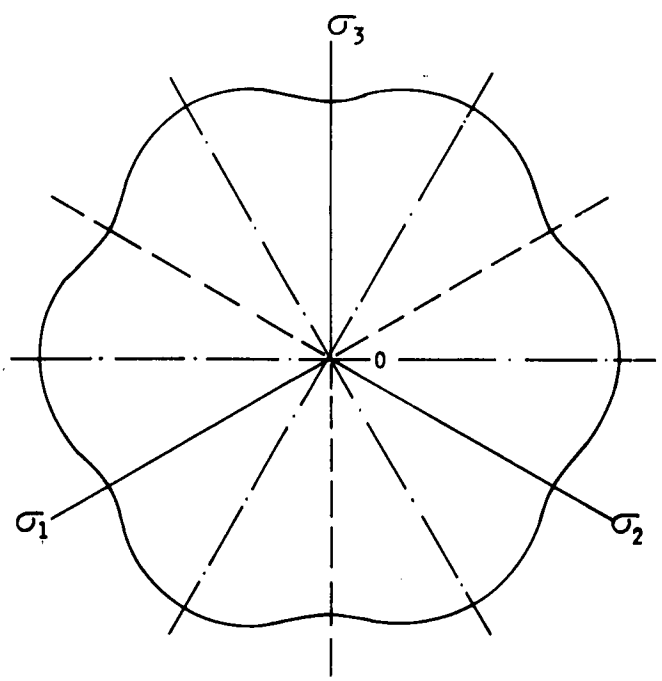

Figure A-10. π-plane.

At present, two basic theories are used to predict the incipience of plastic yielding in materials that behave in a ductile manner: (1) the Von Mises Criteria, and (2) the Tresca or Maximum Shear Stress Criteria. Both theories neglect the effect of the mean stress and require the knowledge of a single material constant, the yield stress, in uniaxial state of stress, to predict the behavior under any combination of principal stresses. Furthermore, the yield stress is assumed to be identical in tension and compression, and the material is assumed to be isotropic.

Von Mises Criteria.—The yield function can be expressed as

$$f^o = J_2 - k^2 \qquad \text{(A-113)}$$

This criterion is by far the simplest one that can be associated with Eq. A-112.

$$J_2 = \tfrac{1}{3}\sigma_y^2 = k^2 \qquad \text{(A-114)}$$

Therefore, this criterion states that yielding will occur when the second invariant of the stress deviator tensor reaches a critical value; i.e., the value of J_2 at yield in simple tension.

Von Mises originally proposed this criterion because of mathematical convenience. Hencky later reinterpreted it in terms of the distortion or shear strain energy; namely, yielding begins when the distortion energy equals the distortion energy at yield in simple tension. The distortion energy is given by

$$U_d = \frac{1}{12G}[(\sigma_1 - \sigma_2)^2 + (\sigma_2 - \sigma_3)^2 + (\sigma_3 - \sigma_1)^2] \qquad \text{(A-115)}$$

At the yield point in simple tension

$$U_d = \frac{\sigma_y^2}{6G}$$

Therefore, the yield condition becomes

$$(\sigma_1 - \sigma_2)^2 + (\sigma_2 - \sigma_3)^2 + (\sigma_3 - \sigma_1)^2 = 2\sigma_y^2 \qquad \text{(A-116)}$$

Also, because the octahedral shear stress is equal to

$$\tau_{oct} = \tfrac{1}{3}[(\sigma_1 - \sigma_2)^2 + (\sigma_2 - \sigma_3)^2 + (\sigma_3 - \sigma_1)^2]^{\frac{1}{2}} \qquad \text{(A-117)}$$

For the simple tension at yield

$$\tau_{oct,\,y} = \frac{\sqrt{2}}{3}\sigma_y$$

Therefore, Eq. A-116 can be written

$$\tau_{oct} = \tau_{oct,\,y} \qquad \text{(A-118)}$$

That is, yielding will occur when the octahedral shear stress reaches the octahedral shear stress at yield in simple tension.

All these expressions for yield stress differ from the uniaxial yield stress by a constant multiplying factor.

Tresca or Maximum Shear Stress Criteria.—The Tresca theory, also known as Coulomb-Tresca theory, assumes that yielding will occur when the maximum shear stress reaches the value of the maximum shear stress occurring under simple tension.

The Tresca criterion can be written in the more general form

$$f^o = 4J_2^3 - 27J_3^2 - 36k^2J_2^2 + 96k^4J_2 - 64k^6 = 0 \qquad \text{(A-119)}$$

This is a more complex relationship than the Von Mises criterion. Only in cases where the maximum and minimum principal stresses are known beforehand can it be put in the simple form

$$\sigma_1 - \sigma_3 = 2k \qquad \text{(A-120)}$$

The constant, k, is assigned on the basis of the results of simple experiments such as uniaxial tension or pure shear tests. The Von Mises criterion is easier to apply than the Tresca criterion because no prior knowledge of the relative magnitude of the principal stress is needed.

It can be shown that the yield locus for the Von Mises yield criterion is a circle of radius $r = \sqrt{\frac{2}{3}}\sigma_o$ (Fig. A-11). The yield surface in the principal stress space will be a circular cylinder whose axis is the hydrostatic axis (see Fig. A-12).

The yield locus for the Tresca maximum shear criterion is a regular hexagon inscribed in the Von Mises circle (Fig. A-11). In the stress space the Tresca yield surface is a regular hexagonal cylinder inscribed in the Von Mises cylinder (Fig. A-12).

It can also be shown that if the yield locus is assumed to be convex * and one circumscribes the Von Mises circle by a regular hexagon, all possible yield loci must lie between the two regular hexagons inscribed in, and circumscribing, the Von Mises circle.

Thus, all conceivable yield loci satisfying the conditions of isotropy, equal yield in tension and compression, independence of hydrostatic stress, and convexity must lie between two regular hexagons shown in Figure A-13; only convex curves are, of course, admissible. The usual Tresca yield locus is represented by the inner hexagon, and the Von Mises yield surface circumscribes the inner hexagon and is circumscribed by the outer one. If the Von Mises yield surface is taken as a reference, the maximum duration of any admissible yield surface is about 15.5 percent. From

* This implies that any straight line in the π-plane may pierce the locus in at most two points.

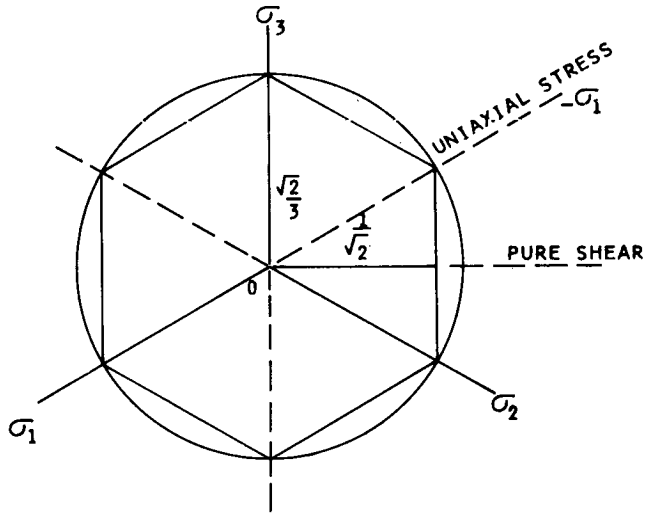

Figure A-11. Von Mises circle and Tresca hexagon.

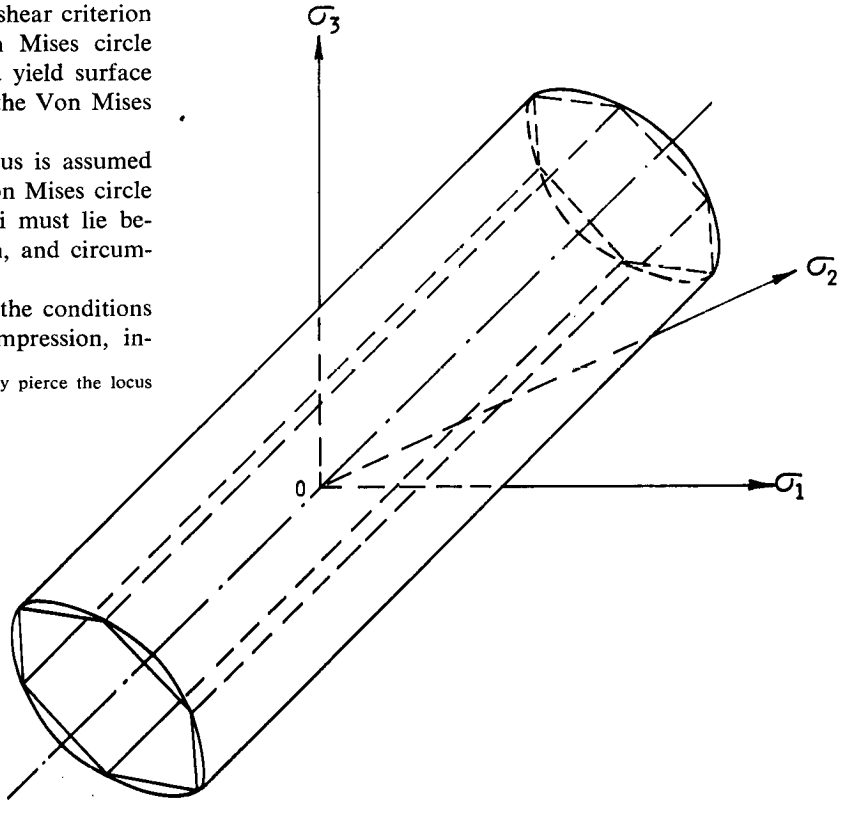

Figure A-12. Von Mises and Tresca yield surfaces in principal stress space.

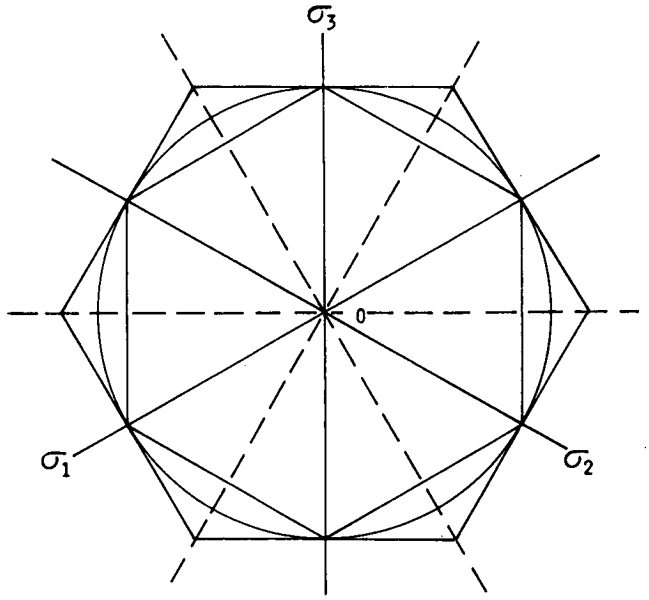

Figure A-13. Bonds on yield loci.

a practical standpoint, this implies that some general assumptions provide a simple failure criterion of considerable generality.

Subsequent Yield Surfaces, Loading and Unloading

The previous discussion deals with the initial yield surface at which a material first undergoes yielding. For a perfectly plastic material, the yield surface remains fixed. However, for a material that strain-hardens, the yield surface must change for continued straining beyond the initial yield.

In Eq. A-108 a yield function is defined by the relation

$$F(\sigma_{ij}) = K \qquad \text{(A-108)}$$

such that whenever the function F became equal to the constant K, yielding would begin. K then represented an initial yield surface in the stress space. This type of relation can now be generalized to subsequent yield surfaces. After yielding has occurred, K takes on a new value (or values), depending on the strain-hardening properties of the material. If the material is unloaded and then loaded again, additional yielding will not occur until the new value of K is reached. The function F can then be looked on as a loading function, or loading surface, which represents the load being applied; the function K is a yield function, or strain-hardening function, and will depend on the complete previous stress and strain history of the material and its strain-hardening properties.

Three cases can be distinguished for a strain-hardening material (see, for example, Naghdi, 1963):

1. Loading:

$$F = K \quad dF = \frac{\partial F}{\partial \sigma_{ij}} d\sigma_{ij} > 0$$

2. Neutral loading:

$$F = K \quad dF = \frac{\partial F}{\partial \sigma_{ij}} d\sigma_{ij} = 0 \qquad \text{(A-121)}$$

3. Unloading:

$$F = K \quad dF = \frac{\partial F}{\partial \sigma_{ij}} d\sigma_{ij} < 0$$

Geometrically, the conditions are readily visualized. $F = K$ means the stress state is on the yield surface. $dF > 0$ means the stress state is "moving out" from the yield surface and plastic flow is occurring. $dF < 0$ means the stress state is "moving in" from the yield surface and therefore unloading is taking place. $dF = 0$ corresponds to the case of the stress state moving on the yield surface and is called neutral loading. For a strain-hardening material no plastic flow occurs. If $F < K$, the stress state is an elastic one.

Hardening Rule.—Experiments show that during the occurrence of plastic deformation the yield surface is changing continuously in size and shape. A law governing this aspect of the problem (i.e., one that defines the manner of constructing yield surfaces) is called a hardening rule.

From a mathematical standpoint, the assumption of isotropic hardening is the simplest. For this type of hardening the yield cylinder will expand with the stress and strain history, but will retain the initial shape. For a Von Mises material, the subsequent yield loci will be a series of concentric circles; for a Tresca material they will be a series of concentric regular hexagons. The assumption of isotropic hardening does not, however, take into account a Bauschinger effect. The Bauschinger effect would tend to reduce the size of the locus on one side as that on the other side is increased. The yield surface would thus change shape as the yielding progresses.

To account for the Bauschinger effect, Prager (1955) introduced the kinematic models and hence the type of hardening called kinematic hardening. It takes into account a Bauschinger effect but, because it maintains the total elastic range constant, it probably overcorrects somewhat for this effect.

To determine the manner in which plastic deformation influences the yield surface, consider it first in the general form

$$f(\tau_{ij}, \epsilon_{ij}^p, \chi) = 0 \qquad \text{(A-122)}$$

in which χ is the work-hardening parameter through which the history effects enter. Although the correct form of χ is not yet known, it is generally assumed to be a function of the stresses and the plastic strains. Thus, one can write without loss of generality

$$f(\tau_{ij}, \epsilon_{ij}^p) = 0 \qquad \text{(A-123)}$$

The yield surface of a nonhardening plastic material remains unchanged during deformation.

Dibaj (1969) illustrates several of the proposed hardening rules by considering first the Tresca's initial yield surface which is a cylinder when expressed in terms of the principal stresses space $(\sigma_1, \sigma_2, \sigma_3)$. Its intersection with the so-called π-plane $(\sigma_1 + \sigma_2 + \sigma_3 = 0)$ is a regular hexagon. Consider the manner in which this hexagon changes as a result of strain hardening.

Figure A-14b shows the case of isotropic hardening which is characterized by a uniform expansion of the initial yield surface. Eq. A-123 may be written as

$$f = F(\tau_{ij}) - \chi = 0 \qquad \text{(A-124)}$$

in which χ depends on the plastic strain history.

Figure A-14c shows Prager's kinematic hardening, which assumes that the initial yield surface translates without rotation and without change in size. The general form of the yield surface under this assumption is

$$f = f^o(\tau_{ij} - \alpha_{ij}) = 0 \qquad \text{(A-125)}$$

in which α_{ij} is a tensor representing the translation of the center of the initial yield surface.

In addition to the isotropic and kinematic hardening rules, other hardening rules have been advanced; these include:

1. Ziegler's modified kinematic hardening (Fig. A-14d).
2. The concept of plastic deformation causing a linear segment to move (Fig. A-14e).
3. Plane yield surfaces changing with plastic loading in some independent manner.
4. Hodge's piecewise linear yielding which includes an

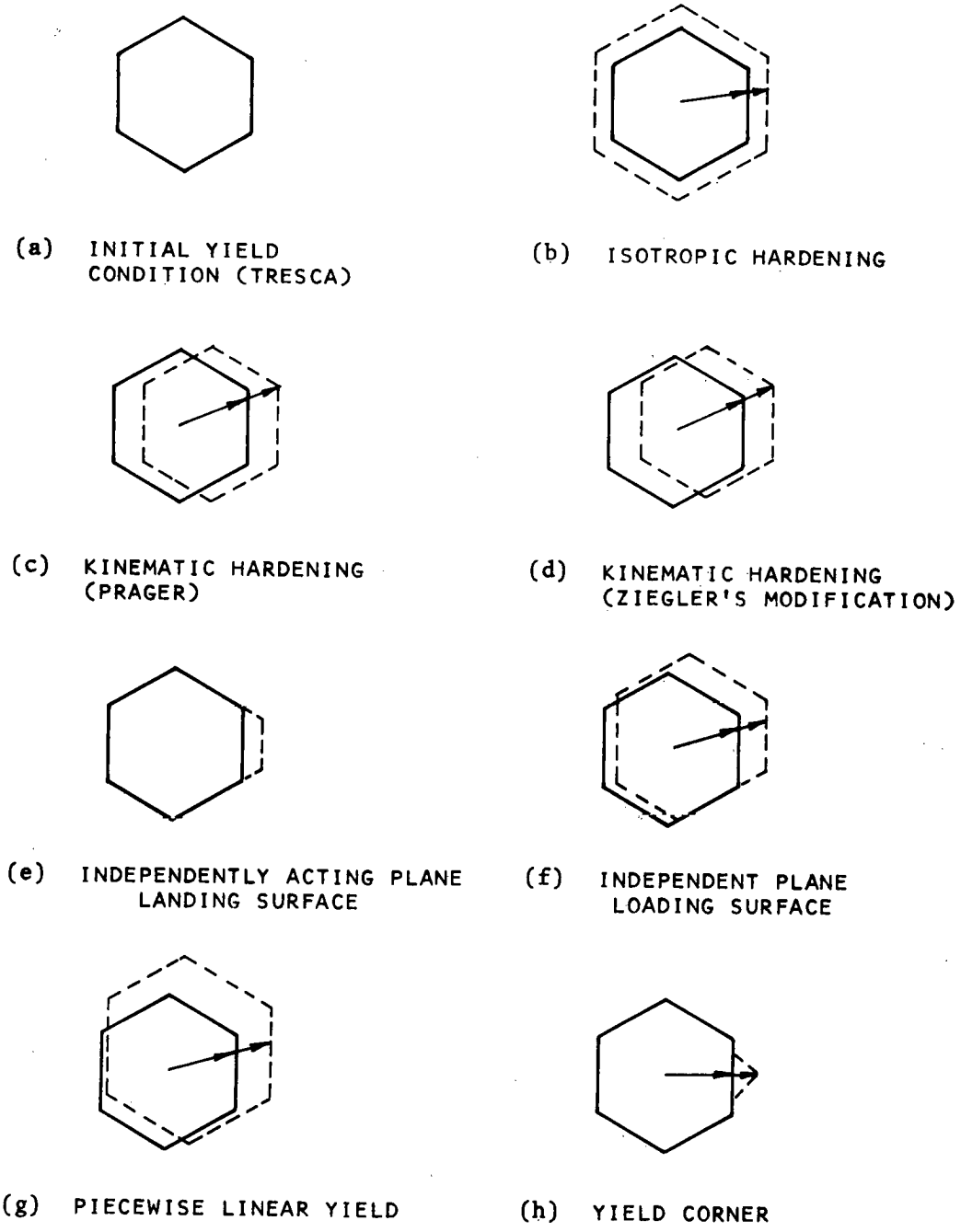

Figure A-14. Several hardening rules. (From Dibaj, 1969.)

expansion of the yield surface simultaneously with its translation in the kinematic hardening (Fig. A-14g).

5. The concept of yield corner stating that the yield surface changes only locally (Fig. A-14h).

Further details of these rules are given by Naghdi (1963), Drucker (1952), Fung (1965), and Ziegler (1959, 1963).

Elasto-Plastic Stress-Strain Relations.—There are two theories of plasticity: (1) the deformation theory, and (2) the flow (or incremental) theory. Both theories assume the material is elastic until the stress reaches a level that satisfies a yield criterion beyond which the material is plastic. In the deformation theory the total plastic strain components are related to the current stress; in the flow theory the plastic strain increments are related to strain increments, stress increments, and current stresses. The deformation theory results in simpler stress-strain relations; however, the plastic strains cannot, in general, be independent of loading path, and deformation theories cannot generally be correct. The tendency therefore has been to ignore the deformation theories as being of little value.* The flow theory, on the other hand, in general can account for history dependency by including the states of stress and strain as well as their increments.

The previous sections discussed the relations between stress and strain in the elastic range and considered the states at which plastic flow or yield would begin. In the following the flow theory is used to obtain relations between stress and strain when plastic flow is occurring.

It is a fundamental assumption in the theory of elasto-plastic solids that the strain tensor in the plastic range may be decomposed into elastic components and plastic components. Considering the increment of strain tensor,

$$\delta\epsilon_{ij} = \delta\epsilon_{ij}{}^{E} + \delta\epsilon_{ij}{}^{p}$$

the increment of stress tensor could be related to the increment of elastic strain tensor through the generalized Hooke's Law. The plastic strain increment however is expressed through the flow rule

$$\delta\epsilon_{ij}{}^{p} = \lambda \frac{\partial f}{\partial \sigma_{ij}} \qquad \text{(A-126)}$$

in which f is the yield function; and λ is a nonnegative scalar. (In the flow rule it is postulated that the plastic strain increment tensor is derivable from the plastic flow potential function; i.e.,

$$\delta\epsilon_{ij}{}^{p} = \lambda \frac{\partial g}{\partial \sigma_{ij}}$$

in which g is the plastic potential; and λ is a nonnegative scalar. Eq. A-126 is a consequence of the classical formulation of the theory of plasticity which considers a class material for which the yield function, f, can also serve as the plastic flow potential.)

Using Eq. A-126, the relations between the increments of plastic strain and the stresses at any instant can be determined for a given yield function. The fundamental problem in applying plasticity theory is to determine the total plastic strain as a function of the history of loading or history of stress. To calculate the plastic strains after the body is loaded along some specified load path to final load condition it is theoretically necessary to integrate the infinitesimal plastic strain increments over the actual loading path. However, it is more expeditious to assume the load applied in small finite increments and calculate the finite increments of plastic strain for each of the load increments. All these increments of plastic strain are then added to give the total plastic strain.

Let the total loading path be divided into N increments of load. Assume that the plastic strains have been computed for the first $i-1$ increments of load and it is now desired to compute them for the ith increment of load. The total strains at the end of the ith increment can be written as:

$$\begin{aligned}
\epsilon_x &= \frac{1}{E}[\sigma_x - \nu(\sigma_y + \sigma_z)] + \sum_{k=1}^{i-1} \Delta\epsilon^{p}{}_{x,k} + \Delta\epsilon^{p}{}_{x,i} \\
\epsilon_y &= \frac{1}{E}[\sigma_y - \nu(\sigma_x + \sigma_z)] + \sum_{k=1}^{i-1} \Delta\epsilon^{p}{}_{y,k} + \Delta\epsilon^{p}{}_{y,i} \\
\epsilon_z &= \frac{1}{E}[\sigma_z - \nu(\sigma_x + \sigma_y)] + \sum_{k=1}^{i-1} \Delta\epsilon^{p}{}_{z,k} + \Delta\epsilon^{p}{}_{z,i} \\
\epsilon_{xy} &= \frac{1+\nu}{E}\tau_{xy} + \sum_{k=1}^{i-1} \Delta\epsilon^{p}{}_{xy,k} + \Delta\epsilon^{p}{}_{xy,i} \qquad \text{(A-127)} \\
\epsilon_{yz} &= \frac{1+\nu}{E}\tau_{yz} + \sum_{k=1}^{i-1} \Delta\epsilon^{p}{}_{yz,k} + \Delta\epsilon^{p}{}_{yz,i} \\
\epsilon_{zx} &= \frac{1+\nu}{E}\tau_{zx} + \sum_{k=1}^{i-1} \Delta\epsilon^{p}{}_{zx,k} + \Delta\epsilon^{p}{}_{zx,i}
\end{aligned}$$

In these equations the sums are known and the problem is to calculate the plastic strain increments for the current ith increment of load, and the corresponding stresses. To do this it is necessary to choose a yield criterion and, using the associated flow rule, determine the plastic stress-strain relations. The most popular and the simplest self-consistent stress-strain relations are based on the octahedral shearing stress or second invariant of the stress deviator, J_2.

The following relations developed for the Von Mises criterion (see Mendelson, 1968) illustrate the method of analysis:

$$\begin{aligned}
\sigma_c = \sqrt{3J_2} &= \frac{3}{\sqrt{2}}\tau_{\text{oct}} \\
&= \frac{1}{\sqrt{2}}[(\sigma_x - \sigma_y)^2 + (\sigma_y - \sigma_z)^2 + (\sigma_z - \sigma_x)^2 \\
&\quad + 6(\tau_{xy}{}^2 + \tau_{yz}{}^2 + \tau_{zx}{}^2)]^{\frac{1}{2}} \qquad \text{(A-128)}
\end{aligned}$$

$$\begin{aligned}
\Delta\epsilon_p &= \sqrt{\tfrac{2}{3}\Delta\epsilon_{ij}{}^{p}\Delta\epsilon_{ij}{}^{p}} \\
&= \sqrt{\tfrac{2}{3}}[(\Delta\epsilon_x{}^{p})^2 + (\Delta\epsilon_y{}^{p})^2 + (\Delta\epsilon_z{}^{p})^2 \\
&\quad + 2(\Delta\epsilon_{xy}{}^{p})^2 + 2(\Delta\epsilon_{yz}{}^{p})^2 + 2(\Delta\epsilon_{zx}{}^{p})^2]^{\frac{1}{2}} \\
&= \frac{2}{\sqrt{3}}[(\Delta\epsilon_x{}^{p})^2 + (\Delta\epsilon_y{}^{p})^2 + (\Delta\epsilon_{xy}{}^{p})^2 \qquad \text{(A-129)} \\
&\quad + (\Delta\epsilon_{yz}{}^{p})^2 + (\Delta\epsilon_{zx}{}^{p})^2 + \Delta\epsilon_x{}^{p}\Delta\epsilon_y{}^{p}]^{\frac{1}{2}} \\
&= \frac{\sqrt{2}}{3}[(\Delta\epsilon_x{}^{p} - \Delta\epsilon_y{}^{p})^2 + (\Delta\epsilon_y{}^{p} - \Delta\epsilon_z{}^{p})^2 \\
&\quad + (\Delta\epsilon_z{}^{p} - \Delta\epsilon_x{}^{p})^2 + 6(\Delta\epsilon_{xy}{}^{p})^2 \\
&\quad + 6(\Delta\epsilon_{yz}{}^{p})^2 + 6(\Delta\epsilon_{zx}{}^{p})^2]^{\frac{1}{2}}
\end{aligned}$$

* Budianski (1959) has indicated that there are many problems where deformation theories may give acceptable results.

$$\Delta\epsilon_x^p = \frac{\Delta\epsilon_p}{2\sigma_e}(2\sigma_x - \sigma_y - \sigma_z)$$

$$\Delta\epsilon_y^p = \frac{\Delta\epsilon_p}{2\sigma_e}(2\sigma_y - \sigma_z - \sigma_x)$$

$$\Delta\epsilon_z^p = \frac{\Delta\epsilon_p}{2\sigma_e}(2\sigma_z - \sigma_x - \sigma_y) = -(\Delta\epsilon_x^p + \Delta\epsilon_y^p)$$

$$\Delta\epsilon_{xy}^p = \frac{3}{2}\frac{\Delta\epsilon_p}{\sigma_e}\tau_{xy} \qquad \text{(A-130)}$$

$$\Delta\epsilon_{yz}^p = \frac{3}{2}\frac{\Delta\epsilon_p}{\sigma_e}\tau_{yz}$$

$$\Delta\epsilon_{zx}^p = \frac{3}{2}\frac{\Delta\epsilon_p}{\sigma_e}\tau_{zx}$$

and $\Delta\epsilon_p$ is related to σ_e through the uniaxial tensile stress-strain curve shown in Figure A-15.

In addition to the previous stress-strain relation, the following sets of relations must be satisfied in the solution of a boundary value problem:

1. The equations of equilibrium of stresses.
2. The strain-displacement or compatibility relations.
3. The boundary conditions.

Application of Plasticity Theory in Pavement Analysis

Problems in pavements analysis that deal with failure or large pavement deformation have been treated as problems of plasticity. The major application of the theory of plasticity has been in considering failure problems in soils. In fact, the first law of yielding for soils suggested by Coulomb in 1773 is much older than the particular form of this law for metals that was used by Tresca in 1868.

Experiments show that the yield criteria for many plastic materials, such as metals, are essentially independent of isotropic pressure. Consequently, the yield criteria for such materials have been expressed in terms of stress deviatoric invariants only. The yield surfaces that are independent of the hydrostatic pressures are cylindrical surfaces, with their axes located along the hydrostatic axis ($\sigma_1 = \sigma_2 = \sigma_3$) in the principal stress space. The two well-known yield criteria in this group—those of Tresca and Von Mises—are discussed elsewhere. The yield surfaces are shown in Figure A-12.

For many soils, as for all porous materials, hydrostatic pressure influences the plastic deformation process of the material considered. Hydrostatic stress can either directly produce plastic deformation of the volume, or influence the process of plastic flow caused by the shearing stresses. Extensive tests carried out on soils and rock materials indicate that the Von Mises and Tresca criteria in their present form cannot be used to solve engineering problems. The influence of the first stress invariant, I_1, is very marked in many instances. Both criteria have been modified to include such effects for this purpose.

1. *Coulomb's Yield Condition.* The most widely used yield condition for soils was proposed by Coulomb (1773). This was the first yield function proposed that included the dependency of isotropic stress. The normal and shear stresses are related by

$$\tau = c - \sigma \tan\phi \qquad \text{(A-131)}$$

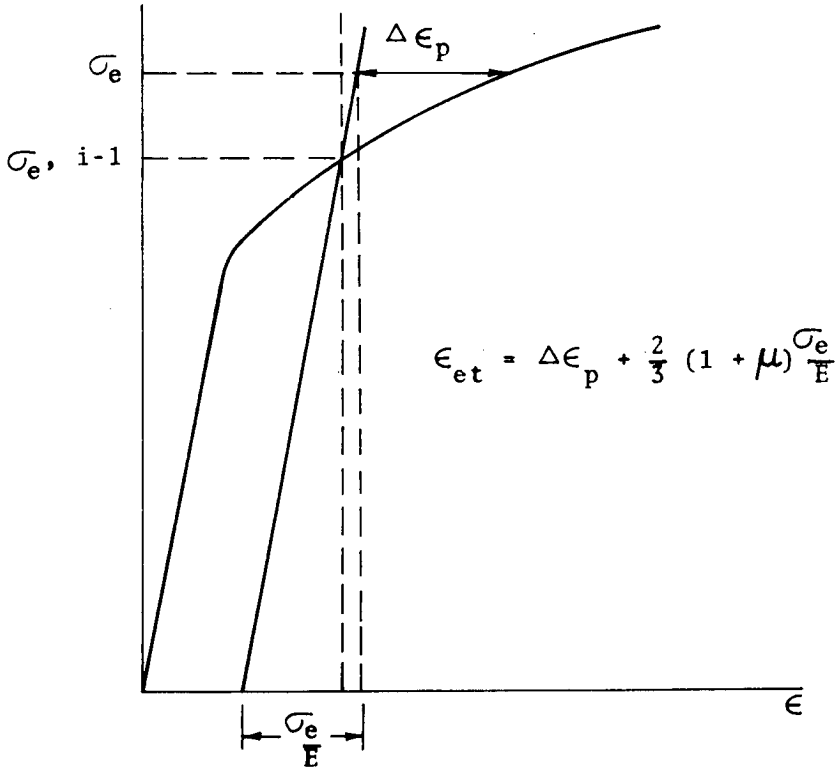

Figure A-15. Relation between ϵ_{et}, σ_e, and $\Delta\epsilon_p$. (After Mendelson, 1968.)

in which c is the cohesion; and ϕ is the angle of friction.

The Coulomb yield criterion (Fig. A-16) may be written in terms of the principal stresses, σ_1 and σ_3, as

$$\frac{\sigma_1 - \sigma_3}{2} = c \cos \phi - \frac{\sigma_1 + \sigma_3}{2} \sin \phi \qquad \text{(A-132)}$$

To be consistent with literature on the subject, tensile stresses are considered positive. The yield function $f = k$ is

$$f = \frac{\sigma_1 - \sigma_3}{2} + \frac{\sigma_1 + \sigma_3}{2} \sin \phi = c \cos \phi = k \qquad \text{(A-133)}$$

The implication of Coulomb's yield criterion is that the plastic deformation generally is accompanied by a volume increase, as shown in the following (after Finn, 1965). The principal plastic strain rates, ϵ_1, ϵ_3, are

$$\dot{\epsilon}_1 = \lambda \frac{\partial f}{\partial \sigma_1} = \frac{\lambda}{2}(1 + \sin \phi)$$

$$\dot{\epsilon}_3 = \lambda \frac{\partial f}{\partial \sigma_3} = -\frac{\lambda}{2}(1 - \sin \phi)$$

The rate of cubical dilatation, $\dot{\Delta}$ (rate of volumetric strain), is

$$\dot{\Delta} = \dot{\epsilon}_1 + \dot{\epsilon}_3 = \lambda \sin \phi$$

By invariance, the rate of dilatation with respect to any other set of orthogonal axes in the plans is

$$\dot{\Delta} = \dot{\epsilon}_x + \dot{\epsilon}_y = \lambda \sin \phi$$

Therefore, the plastic deformation is accompanied by an increase in volume when $\phi \neq 0$.

During plastic deformation soils may either expand, contract, or show no volume change at all. The application of the theory is restricted to soils that do not contract in volume during shear.

In the general form, the criterion can be expressed as

$$\{(\sigma_1 - \sigma_2)^2 - [2c \cos \phi + (\sigma_1 + \sigma_2) \sin \phi]^2\}$$
$$\{(\sigma_2 - \sigma_3)^2 - [2c \cos \phi + (\sigma_2 + \sigma_3) \sin \phi]^2\}$$
$$\{(\sigma_3 - \sigma_1)^2 - [2c \cos \phi + (\sigma_3 + \sigma_1) \sin \phi]^2\} = 0 \qquad \text{(A-134)}$$

The geometrical representation of this equation is a hexagonal pyramid with its vertex at the point

$$\sigma_1 = \sigma_2 = \sigma_3 = c \cot \phi \qquad \text{(A-135)}$$

(see Fig. A-17a). The pyramid is similar to that of Tresca, but does not have a regular hexagon in cross-section. For a cohesionless material $c = 0$, the vertex of the pyramid is at the origin.

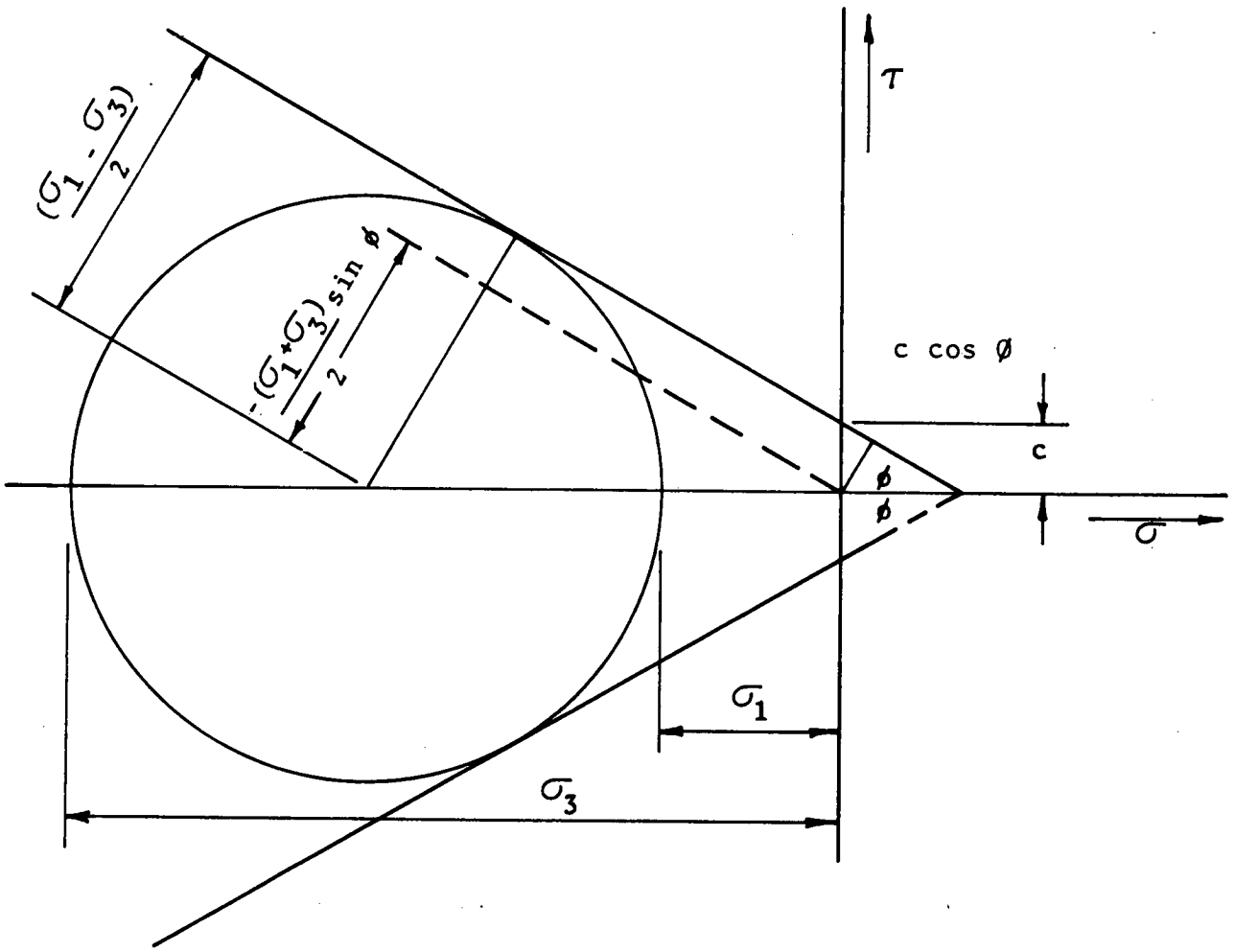

Figure A-16. Coulomb yield criterion.

2. *Modified Tresca's Yield Condition.* In this yield condition, the effect of isotropic pressure is included. This is similar to that which defines Coulomb's yield function, and is expressed in terms of the principal stresses:

$$\{(\sigma_1-\sigma_2)^2-r(p)\}\{(\sigma_2-\sigma_3)^2-r(p)\}\{(\sigma_3-\sigma_1)^2-r(p)\}=0 \qquad \text{(A-136)}$$

in which $r(p)$ is a function of p, which is defined as

$$p=\tfrac{1}{3}(\sigma_1+\sigma_2+\sigma_3)=\tfrac{1}{3}(I_1) \qquad \text{(A-137)}$$

The modified Tresca's yield surface is a right regular hexagon pyramid (Fig. A-17b).

3. A general modified Von Mises criterion in the form

$$f=J_2-r(p)=0 \qquad \text{(A-138)}$$

has also been proposed (Drucker and Prager, 1952) which is called the Von Mises-Schleicher condition. The yield surface for this case in terms of the principal stress space is a right circular cone (Fig. A-17c).

4. Drucker and Prager (1952) have proposed a generalization of the Mohr-Coulomb hypothesis in the form

$$f=\alpha I_1+J_2^{\frac{1}{2}}-k=0 \qquad \text{(A-139)}$$

in which $I_1=\tau_{ii}$ and $J_2=\frac{1}{2}S_{ij}S_{ij}$ are the first stress invariant and the second deviatoric stress invariant, respectively; and α and k are positive constants. The yield condition under this condition is a right circular cone for $\alpha>0$, and is identical to that of Von Mises for $\alpha=0$.

In addition to theoretical developments regarding yield conditions for soils, the results of a few experimental studies have been reported. Certain basic differences between the results obtained can easily be illustrated by considering the sections of the yield surfaces taken at right angles to the hydrostatic axis (space diagonal), as shown in Figure A-18. By adjusting the constant involved, these sections can be made to coincide with the Mohr-Coulomb surface at points A, B, and C. Kirkpatrick's experiment (1957), which was performed on sands under conditions of complete drainage, shows agreement with the Mohr-Coulomb yield surface. Bell's experiment (1965) shows that the yield surface for cohesionless soil is midway between that of Mohr-Coulomb and that of Von Mises.

These experiments indicate that all yield surfaces described in this section are more or less appropriate for certain types of soils. However, the extended Von Mises and Drucker-Prager yield surfaces have a mathematical advantage over the others presented because they can be expressed by a unique mathematical relation.

Work-Hardening Theories of Plasticity.—The inelastic behavior of a soil or rock material is extremely compli-

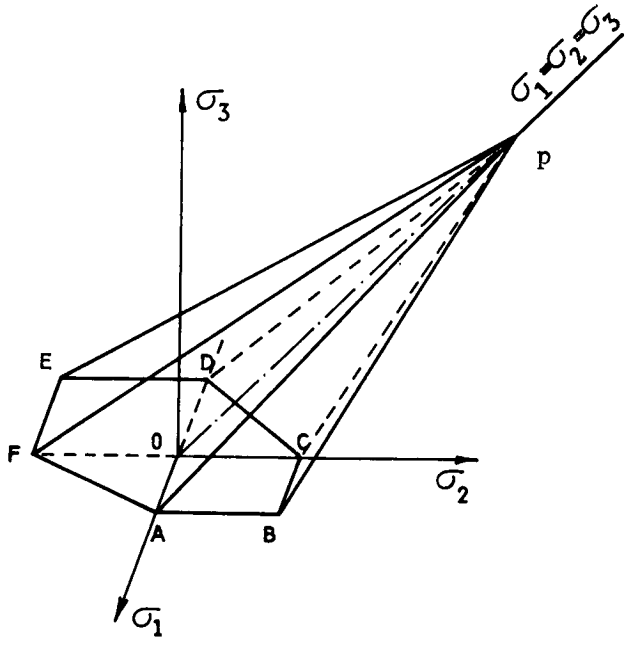

(a) COULOMB YIELD CONDITION

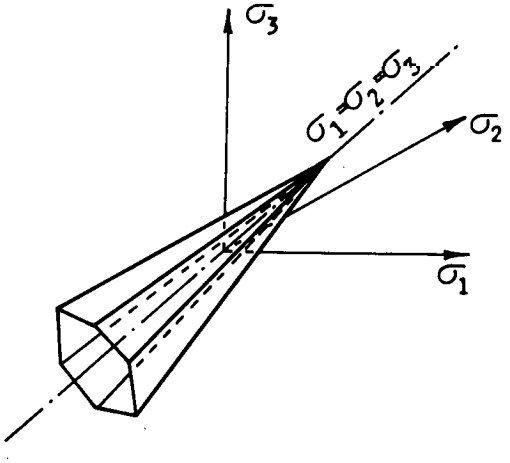

(b) MODIFIED TRESCA'S

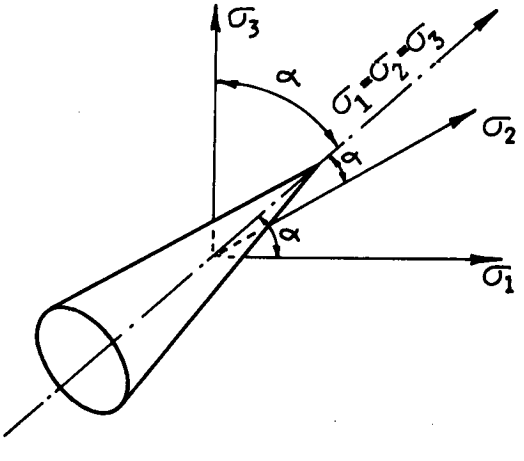

(c) MODIFIED VON MISES'S

Figure A-17. Yield surfaces in principal stresses space.

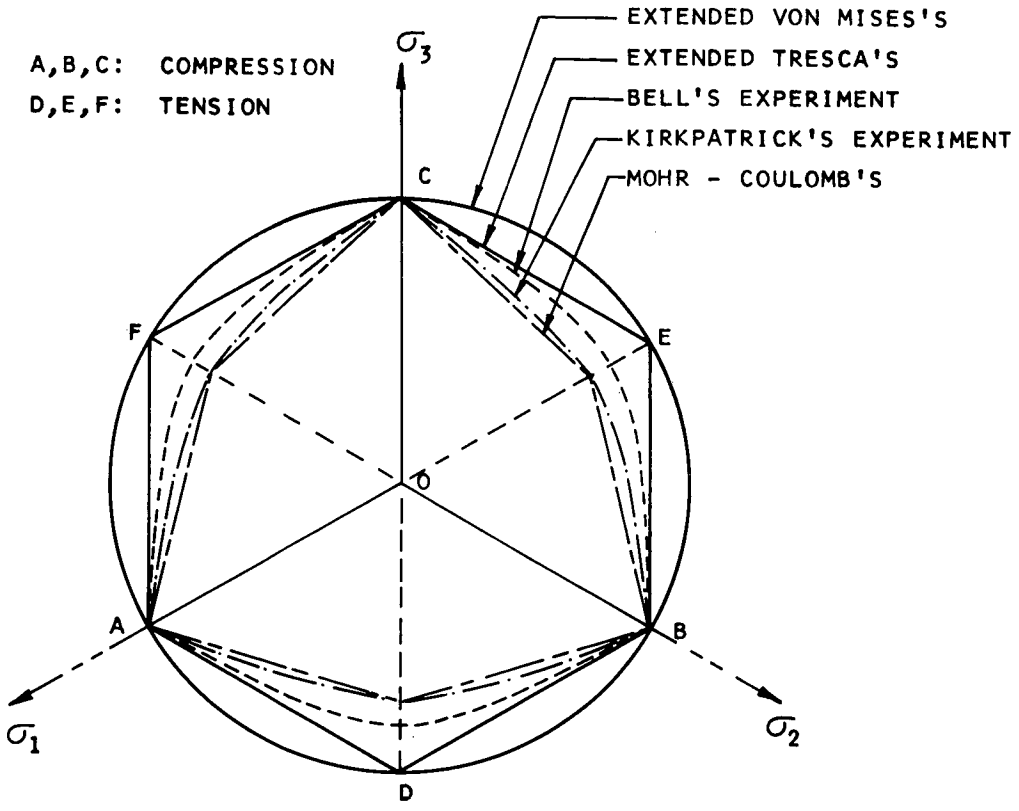

Figure A-18. Right sections of yield surfaces for soils.

cated, owing to the number of variables that can enter into any analysis. Any explicit description in phenomenological or mathematical terms is bound to be a drastic idealization of actual behavior and should not be expected to be valid over a wide range of conditions. Drastic idealizations are valuable not only theoretically but also in practical engineering design. This approach is well illustrated in the design of steel structures fabricated of a material that exhibits large plastic deformations at a lower yield point stress; aluminum structures composed of a material that work-hardens over its entire plastic range; and reinforced concrete structures formed of a composite of steel and a soil-like material. All of these can be, and in many cases are, designed on the basis of perfect plasticity. Usually an attempt to describe real behavior observed experimentally leads to an ever-increasing elaboration in detail of a mathematical or physical model as more types of tests are made on more materials (especially in the case of soil and rock mechanics).

The assumption of perfect plasticity is the simplest and strongest idealization at present. The assumption of the physical laws of perfect plasticity permits the application of the general theorems to problems of granular media; e.g., the theorem of limit analysis and uniqueness theorems. However, the application of perfect plasticity may not be nearly as appropriate for certain soils under certain conditions. Some of the disadvantages were discussed at the time of the idealization proposed by Drucker and Prager (1952) and were extended and improved on by Shield (1955). The strong difference between "frictional" and "plastic" behavior was brought out in a subsequent paper by Drucker (1954).

The concept of a loose-cohesionless medium exhibiting perfect plasticity gives rise to many objections in the light of experimental results. Thus, in many cases, instead of a volume increase, a volume decrease was observed in granular media during a deformation process. Furthermore, the assumptions of the theory of perfect plasticity do not take into consideration a number of complex phenomena; e.g., consolidation of the soil, and influence of variable water content. In addition, for certain soils, the hydrostatic type of loading results in permanent deformations (which indicates a closed form of yield surfaces).

The idea of considering a cohesive medium as a strain-hardening (or a work-hardening) plastic body was put forward by Drucker, Gibson, and Henkel in 1957. They emphasized the isotropic type of hardening more than any other. Since 1957, additional experimental data have been gathered and interpreted, and the significance of triaxial and shear tests and the importance of time effects are better understood (Drucker, 1964, 1967). Henkel (1958) found that most of the available information lay outside the scope of a useful theory of plasticity. Work done at Cambridge University by Roscoe and his associates sheds some light on the reliability of applying certain hardening rules for certain soils. Tests performed on "wet" clays indicate an isotropic type of work-hardening idealization. Jenike and

Shield (1959) also have considered isotropic type hardening in their studies.

Although Drucker (1964) in his study on the path-dependency and stability of soils proposed the consideration of isotropic hardening, he mentions that there is no difficulty in devising a perfectly reasonable test to demonstrate that any isotropic hardening form may be in error. Regardless of this possibility, isotropic hardening still seems to be reasonable.

Discrete Models

For this discussion, discrete models are defined as those where a continuum is represented by a system of independent or partially dependent mechanical models. The response at any point is either not dependent or only partially dependent on the response at any other point. These models have been used primarily in the design of rigid pavements. For the purposes of analysis, rigid pavements have been treated as thin elastic plates resting on a supporting medium. Because of the complexity of the boundary value problem, when the supporting medium is treated as a continuum, various simplified analytical models have been used to represent the supporting medium. The simplest of these models is the Winkler model, which is a series of independent linear springs. Many other models have been proposed to take into account some of the observed phenomena that could not be accounted for by the Winkler model. These models tend to bridge the gap between the Winkler model and the elastic continuum. In general, the analytical difficulties associated with these models depend on the closeness with which they approximate the elastic continuum. The characteristics of the various models are summarized briefly.

Winkler Model.—The Winkler model was introduced to applied mechanics by Winkler, and later formed the basis of a comprehensive study by Hetenyi (1946; see also 1966). The Winkler model consists of a series of independent linear elastic springs (Fig. A-19a). In the case of a two-dimensional problem like a plate, it is assumed that the springs are distributed in the plane at regular intervals. The functional relationship between the applied stress and the resulting displacement can be written as

$$\sigma(x_1, y_1) = k_o\, w(x_1, y_1) \qquad \text{(A-140)}$$

in which

x_1, y_1 = coordinates of arbitrary point; and
k_o = spring constant or modulus of subgrade reaction and has units of force per unit area per unit length, or force/length^3.

From analytic and computational standpoints, this model can be regarded as the simplest case. Much theoretical work has been done in applying this model to various problems in the design and analysis of concrete pavements. Various analyses have been presented by Biot (1937), Vesic (1961), and Gibson (1967) to determine the relationship between the modulus of elasticity and the modulus of subgrade reaction.

Hetenyi Foundation.—To achieve some measure of continuity in the model, Hetenyi (1950) suggested embedding a continuous elastic plate (in the case of a two-dimensional problem) or a beam (in the case of a one-dimensional problem) in a Winkler foundation (Fig. A-19b). The beam or plate is assumed to deform only as a result of bending (shear deflections are neglected). If the deflection of the surface is denoted by w_1, and the deflection of the

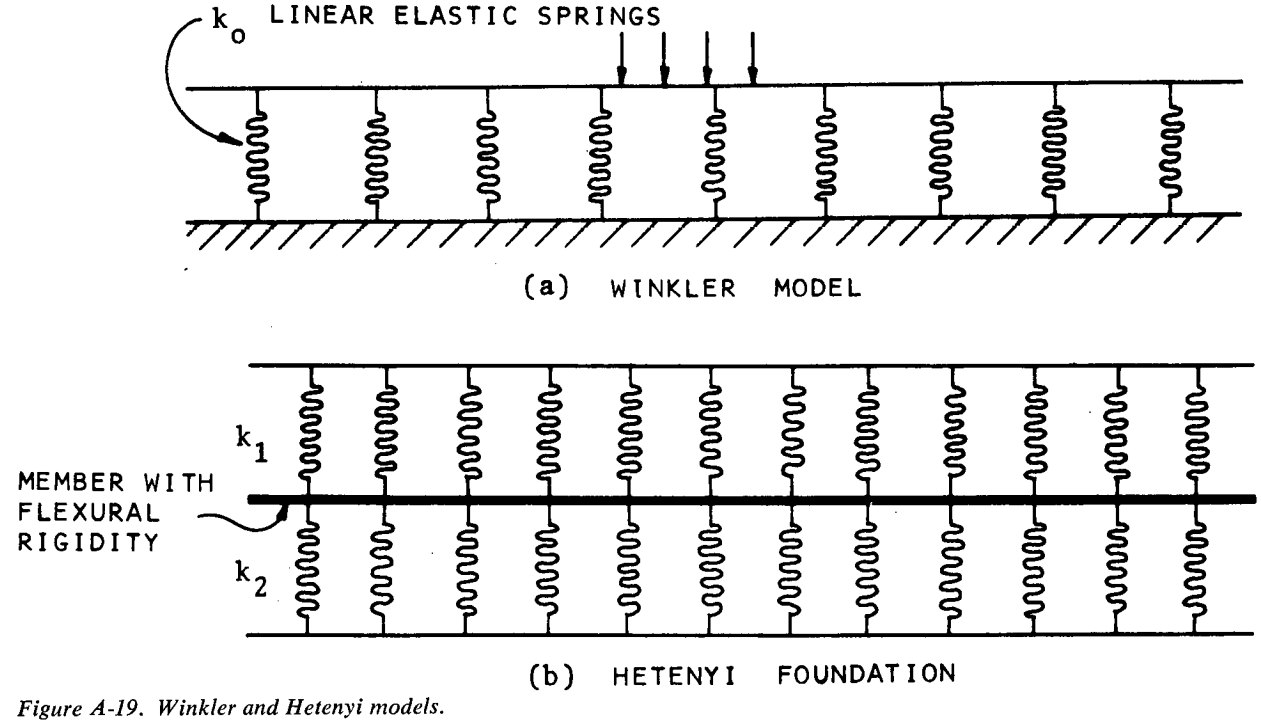

Figure A-19. Winkler and Hetenyi models.

embedded plate is denoted by w_2, the equation for the deflection of the lower plate would be

$$D_2\nabla^4 w_2 = k_1(w_1 - w_2) - k_2 w_2 \qquad \text{(A-141)}$$

The degree of continuity in the deflection can be controlled by the rigidity of the embedded plate; i.e., D_2. The extreme case of $D_2 = \infty$ implies a simple Winkler foundation of modulus k_1.

Filonenko-Borodich Foundation.—To obtain some continuity in the foundation, an elastic membrane in tension was used by Filonenko-Borodich (1940)* to provide the interaction between the spring elements of a Winkler foundation (Fig. A-20a). The membrane is subjected to a constant tension. To determine the stress-deflection relations it is necessary to consider the equilibrium of a membrane (Fig. A-20b). The summation of forces in the z-direction (assuming small deflections of the membrane) results in the following:

Forces acting along edges ab, bc, cd, da:

* See Kerr (1964).

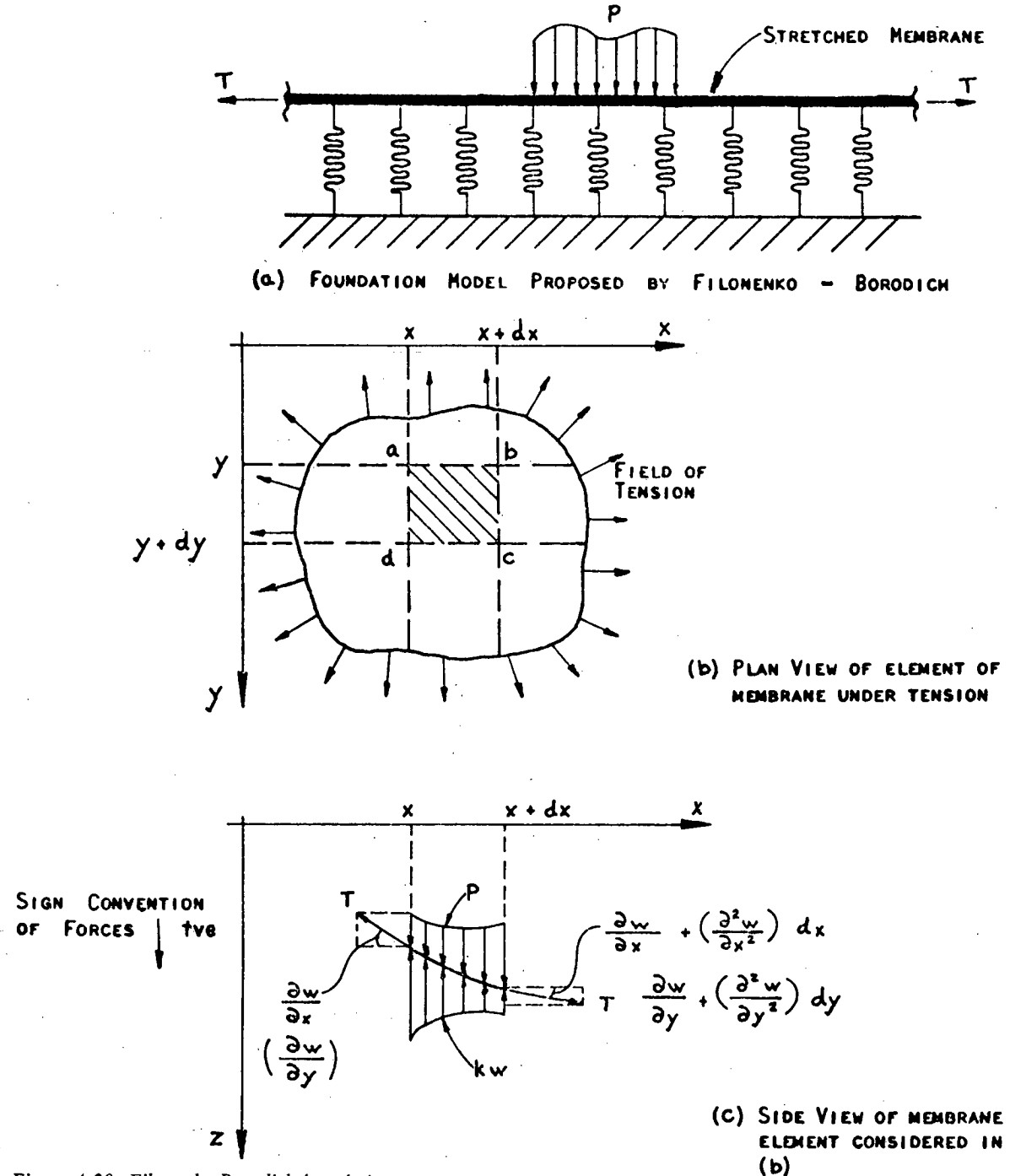

Figure A-20. Filonenko-Borodich foundation.

$$F_{z1} = T\,dx\,\frac{\partial w}{\partial y} - T\,dx\left\{\frac{\partial w}{\partial y} + \frac{\partial^2 w}{\partial y^2}\,dy\right\} + T\,dy\,\frac{\partial w}{\partial x} - T\,dy\left\{\frac{\partial w}{\partial x} + \frac{\partial^2 w}{\partial x^2}\,dx\right\} \tag{A-142}$$

Forces on area abcd:

$$F_{z2} = \sigma_z\,dxdy - k_o\,w\,dx\,dy \tag{A-143}$$

Summing the forces in the z direction:

$$T\left\{\frac{\partial^2 w}{\partial x^2} + \frac{\partial^2 w}{\partial y^2}\right\} dx\,dt - k_o\,wdxdy + \sigma_z\,dxdy = 0 \tag{A-144}$$

$$T\left\{\frac{\partial^2 w}{\partial x^2} + \frac{\partial^2 w}{\partial y^2}\right\} - k_o\,w + \sigma_z = 0 \tag{A-145}$$

$$\sigma_z = k_o w - T\nabla^2 w \tag{A-146}$$

This is the basic differential equation relating the stress and deflection of the model through the constants k_o and T, which characterize the model. When there is no tension in the membrane the foundation model is identical to the Winkler foundation. Variation in soil conditions can be incorporated in the analyses by varying the values of T and k_o.

Pasternak Foundation.—As the result of extensive investigations carried out on various kinds of soils, Pasternak (1954)* suggested a model to represent the soil that provided interaction between the elastic springs by an incompressible layer that could deform only as a result of shear forces (Fig. A-21).

* See Kerr (1964).

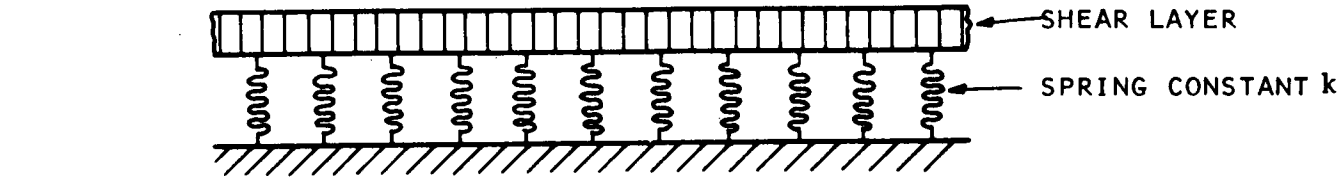

(a) PASTERNAK FOUNDATION MODEL

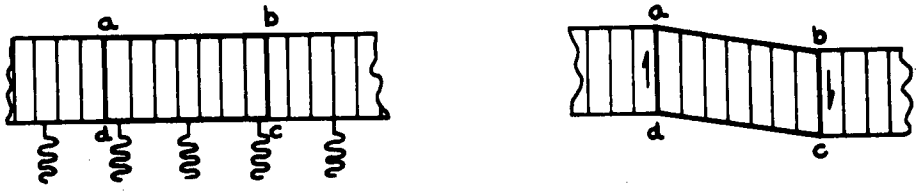

UNDISTORTED DISTORTED

(b) RELATIVE DISTORTION OF SHEAR LAYER DUE TO EXTERNAL FORCES

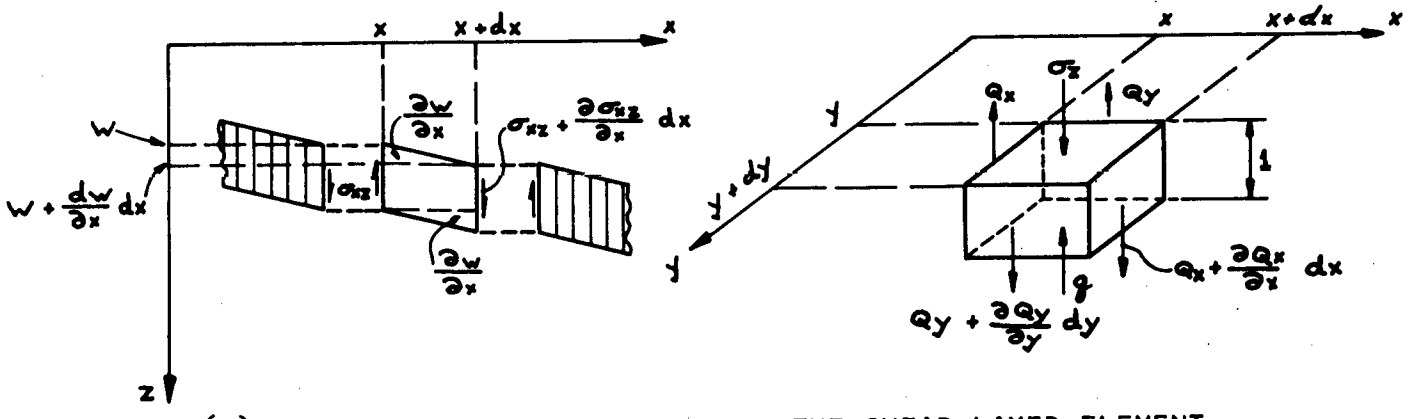

(c) FORCES AND DISPLACEMENTS OF THE SHEAR LAYER ELEMENT

Note:

If the displacements are small the equilibrium equations obtained for the undistorted body is approximately the same as for the deformed state.

Figure A-21. Pasternak foundation model.

To obtain the load deformation relation of this model, consider the equilibrium of an element of unit thickness with dimensions dx and dy.

The shear forces per unit length in the x direction are given by

$$Q_x = \int_0^1 \sigma_{xz}\, dz$$
$$Q_y = \int_0^1 \sigma_{yz}\, dz \qquad \text{(A-147)}$$

Assuming that the foundation is homogeneous and isotropic; i.e., $G_x = G_y = G$,

$$\sigma_{xz} = G_x \epsilon_{xz} = G\left\{\frac{\partial w}{\partial x} + \frac{\partial u}{\partial z}\right\}$$
$$\sigma_{yz} = G_y \epsilon_{yz} = G\left\{\frac{\partial w}{\partial y} + \frac{\partial v}{\partial z}\right\} \qquad \text{(A-148)}$$

Because no dilation or volume change occur in the shear layer, the displacements u and v are both zero. Hence, Eq. A-148 reduces to

$$\sigma_{xz} = G\frac{\partial w}{\partial x}$$
$$\sigma_{yz} = G\frac{\partial w}{\partial y} \qquad \text{(A-149)}$$

Substituting the above equations in Eq. A-147 and noting that $w = w(x, y)$ (not a function of z), $\partial w/\partial x$ and $\partial w/\partial y$ can be taken out of the integral signs in Eq. A-147. Therefore:

$$Q_x = G\frac{\partial w}{\partial x}$$
$$Q_y = G\frac{\partial w}{\partial y} \qquad \text{(A-150)}$$

Considering the equilibrium of element in Figure A-20c:

$$\frac{\partial Q_x}{\partial x} + \frac{\partial Q_y}{\partial y} + \sigma_{zz} - q = 0 \qquad \text{(A-151)}$$

Substituting the value Q_x and Q_y from Eq. A-150 in Eq. A-151 gives

$$\frac{\partial}{\partial x}\left\{G\frac{\partial w}{\partial x}\right\} + \frac{\partial}{\partial y}\left\{G\frac{\partial w}{\partial y}\right\} + \sigma_{zz} - q = 0 \qquad \text{(A-152)}$$

putting $q = k_o w(x, y)$

$$\sigma_{zz} = k_o w - G\nabla^2 w \qquad \text{(A-153)}$$

This foundation model is similar to the two previous foundation models. In this case, the additional variable parameter is the shear modulus of the layer.

Kerr Model.—The foundation model proposed by Kerr (1966) is a modification of the Pasternak foundation. This model was originally proposed for the analysis of the behavior of snow foundations but its application to soil foundation problems also has been suggested. The model consists of a layer of springs added to the existing Pasternak foundation (Fig. A-22).

The total deflection is made up of two parts: (1) the deflection of the upper spring, w_1, and (2) the deflection of the lower spring, w_2. Considering the upper spring alone,

$$\sigma_{zz} = cw_1 \qquad \text{(A-154)}$$

Considering the shear layer and the lower spring alone and using Eq. A-153,

$$\sigma_{zz} = kw_2 - G\nabla^2 w_2 \qquad \text{(A-155)}$$

For no compression in the shear layer, the total displacement in the z direction is given by

$$w = w_1 + w_2 \qquad \text{(A-156)}$$

From Eq. A-154:

$$\nabla^2\sigma_{zz} = c\nabla^2 w_1$$
$$G\nabla^2\sigma_{zz} = Gc\nabla^2 w_1 \qquad \text{(A-157)}$$
$$c\sigma_{zz} = kcw_2 - Gc\nabla^2 w_2 \qquad \text{(A-158)}$$

From Eqs. A-157 and A-158:

$$G\nabla^2\sigma_{zz} - c\sigma_{zz} = Gc\nabla^2(w_1 + w_2) - k\,cw_2 \qquad \text{(A-159)}$$

Substituting for w_2 in Eq. A-159:

$$G\nabla^2\sigma_{zz} - c\sigma_{zz} = Gc\nabla^2 w - kc\left\{w - \frac{\sigma_{zz}}{c}\right\}$$
$$(c + k)\sigma_{zz} - G\nabla^2\sigma_{zz} = ckw - Gc\nabla^2 w$$
$$\left\{1 + \frac{k}{c}\right\}\sigma_{zz} - \frac{G}{c}\nabla^2\sigma_{zz} = kw - G\nabla^2 w \qquad \text{(A-160)}$$

Eq. A-160 is the most general form of the load deflection relationship for the foundation, where the applied load varies throughout the whole area. However, for most cases occurring in engineering practice the applied load is either uniform over an area or concentrated at a point, in which case $\nabla^2\sigma_{zz} = 0$ or the equation reduces to

$$\left\{1 + \frac{k}{c}\right\}\sigma_{zz} = kw - G\nabla^2 w \qquad \text{(A-161)}$$

Tensionless Foundation (Tsai and Westmann, 1967).—This model has not been applied to design problems in foundation engineering. A major difficulty with this approach is that the resulting problem is nonlinear; hence, the principle of superposition is not valid. However, an iteration procedure using numerical techniques would overcome these difficulties.

Response of Discrete Models under Simple Loadings

To illustrate the important characteristics of the models discussed earlier, their response to a uniform load applied over the entire area of a perfectly flexible * circular plate is discussed. This is equivalent to applying the load directly to the foundation.

The theoretical approach would be to study the response of the various models to a concentrated load. Each model would then develop a characteristic deflected surface. However, such an approach leads to discontinuities at the point of load application, and may lead to difficulties in comparing model characteristics. It is therefore simpler to con-

* This is an idealized condition and implies that plate has no influence on the distribution of the load.

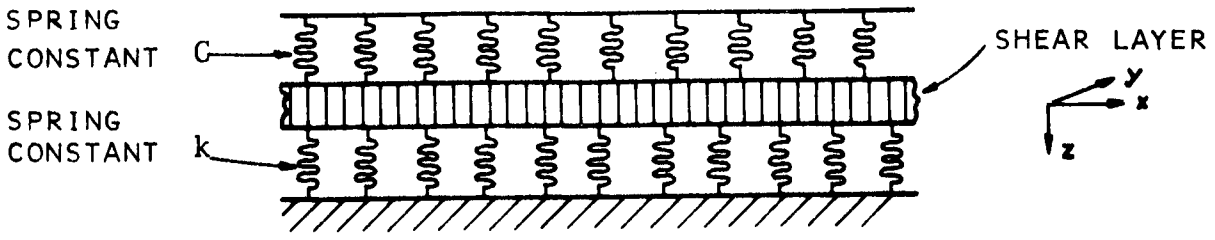

(a) FOUNDATION MODEL PROPOSED BY KERR (1966)

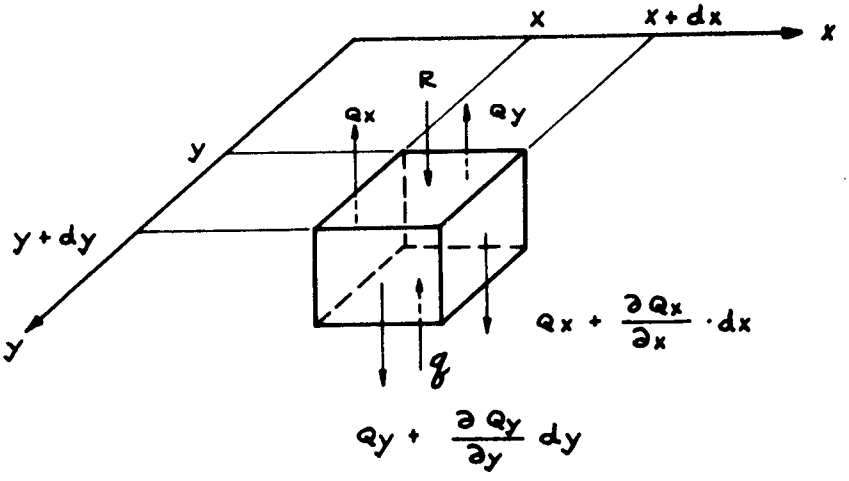

Figure A-22. Kerr foundation model.

sider the uniform load distributed over a circular area. Furthermore, the point load, although desirable mathematically, is not a practical problem. Note that, for a completely flexible plate, the reaction pressure from the foundation is identical to the applied pressure.

Winkler Model.—The deflected surface (Fig. A-23a) can be expressed as

$$\begin{aligned} w(r) &= p/k \qquad \text{for } r \leq a \\ w(r) &= 0 \qquad \text{for } r > a \end{aligned} \tag{A-162}$$

There is a discontinuity in the deflection at the edge of the loaded area, and there is no influence of the load on the foundation outside the loaded area. This is because the foundation is composed of independent springs.

Hetenyi Foundation.—The deflected surface (Fig. A-23b) can be expressed as

$$\begin{aligned} w(r) &= w_1 + w_2 \qquad r \leq a \\ w(r) &= w_1 \qquad\quad r > a \end{aligned} \tag{A-163}$$

in which

$$w_2(r) = p/k_2$$

The expression for $w_1(r)$ is obtained by solving the differential equation for the plate; i.e.,

$$D\nabla^4 w_1 - kw_1 = p \tag{A-164}$$

Although there is a discontinuity at the edge of the applied load, the influence of the applied load extends beyond its area of application.

Pasternak or Filonenko-Borodich Foundation.—To determine the deflected surface it is convenient to use the Kernel function for a concentrated load. This Kernel function is obtained by solving the governing differential equation for a Pasternak or Filonenko-Borodich foundation under the action of a concentrated load.

The differential equation governing the load displacement relationship for a Pasternak foundation is given by

$$P = kw - G\nabla^2 w \tag{A-165}$$

(The differential equation for the Filonenko-Borodich foundation is identical, with G replaced by T.)

The general solution of Eq. A-165 is

$$w(r) = AK_o(\beta r) + BI_o(\beta r) \tag{A-166}$$

in which

$\beta^2 = k/G$; and
$K_o(\beta r)$ and $I_o(\beta r)$ = modified Bessel functions.

Because the displacement has to vanish at $r \to \infty$, the final solution becomes

$$w(r) = \frac{p}{2\pi G} K_o(\beta r) \tag{A-167}$$

This expression for deflection is considered as the Kernel function.

By transferring the coordinate system to one shown in Figure A-24, the Kernel function can be written as

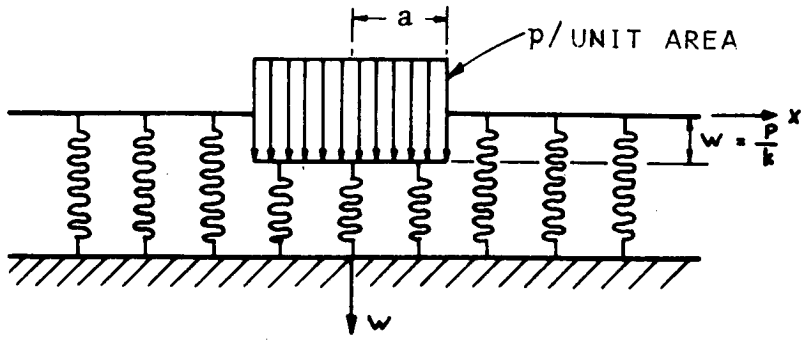

(a) WINKLER FOUNDATION

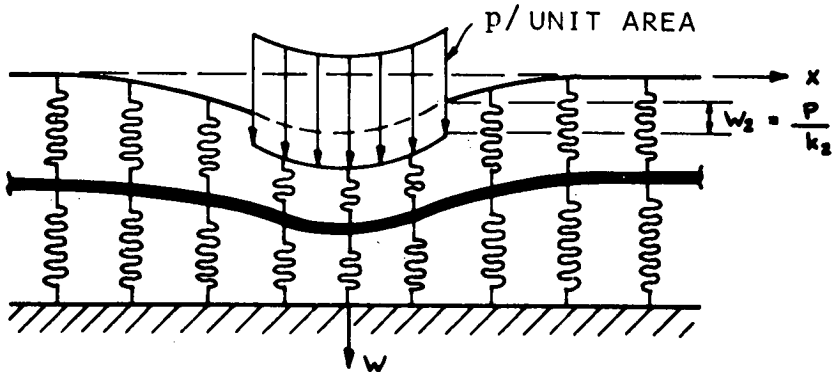

(b) HETENYI FOUNDATION

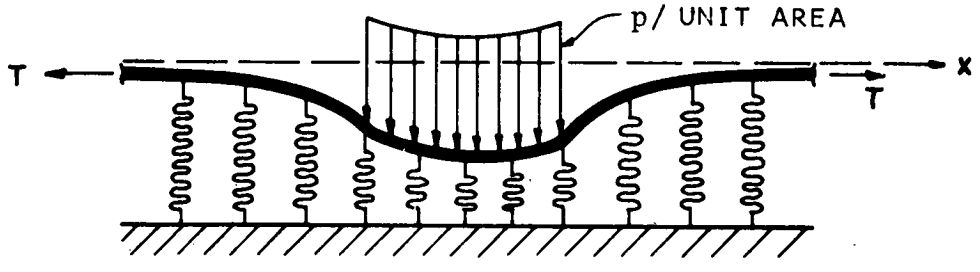

(c) FILONENKO - BORODICH / PASTERNAK FOUNDATION

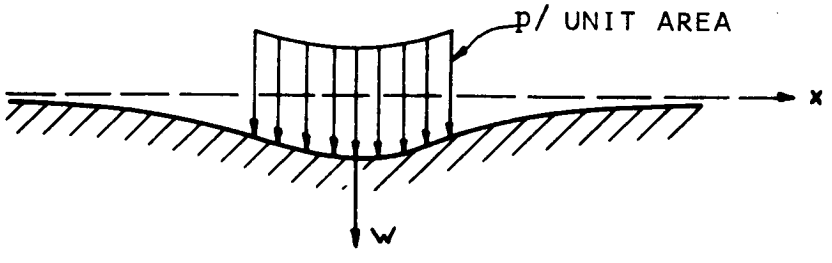

(d) ELASTIC HALFSPACE

Figure A-23. Response of foundation models to uniform circular load.

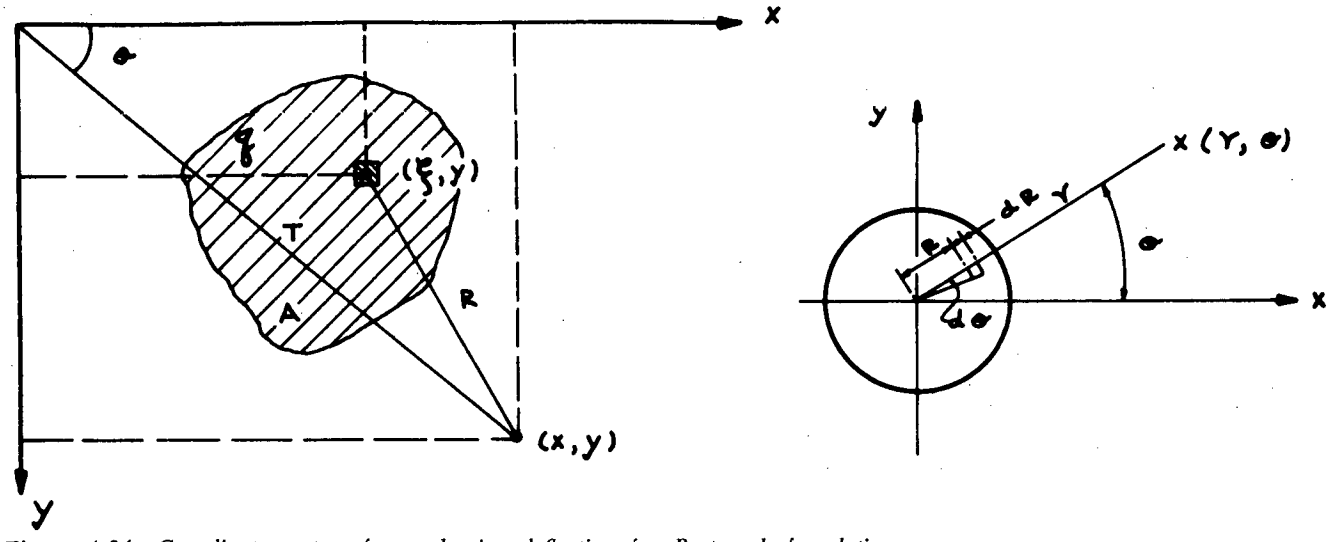

Figure A-24. Coordinate system for evaluating deflection for Pasternak foundation.

$$K(x-\xi, y-\eta) = \frac{1}{2\pi G} K_o(\beta R) \qquad \text{(A-168)}$$

in which

$$R^2 = (x-\xi)^2 + (y-\eta)^2 \qquad \text{(A-169)}$$

The deflection of any point on the foundation is obtained by integrating over the area

$$w(x, y) = \frac{1}{2\pi G}\iint_A p(\xi, \eta) K_o(\beta R)\, d\xi d\eta \qquad \text{(A-170)}$$

For a uniform circular area,

$$w(r, \theta) = \frac{p}{2\pi G}\int_0^{2\pi}\int_0^a K_o(\beta|R-r|) R d\theta dR \qquad \text{(A-171)}$$

Since

$$w = f(\theta) \qquad \text{(A-172)}$$

The deflection is given by

$$w(r) = p/G \int_0^a K_o(\beta|R-r|) R dR \qquad \text{(A-173)}$$

The maximum deflection is obtained by evaluating Eq. A-173 at $r = 0$. The absence of the discontinuity in deflection at the edge of the loaded area as different from the Winkler and Hetenyi foundation should be noted.

Of all the models discussed here, only the Winkler model has been used in the design of pavements. The discussion of the others is presented for completeness.

REFERENCES

BELL, J. M., "Stress-Strain Characteristics of Cohesionless Granular Materials Subjected to Statically Applied Homogeneous Loads in an Open System." Ph.D. thesis, Calif. Inst. of Tech., Pasadena (1965).

BIOT, M. A., "Bending of an Infinite Beam on an Elastic Foundation." *J. Appl. Mech.*, Vol. 4 (1937) pp. A1-A7.

BIOT, M. A., *Mechanics of Incremental Deformation.* Wiley (1965).

BLAND, D. R., "The Two Measures for Work-Hardening." *Proc. 9th Internat. Cong. Appl. Mech.*, Brussels, Vol. 8 (1957) pp. 45-50.

BUDIANSKI, B., "A Reassessment of Deformation Theories of Plasticity." *J. Appl. Mech.*, Vol. 26 (1959).

DIBAJ, M., "Non-Linear Seismic Response of Earth Structures." Ph.D. thesis, Univ. of Calif., Berkeley (1969).

DONG, R. G., PISTER, K. S., and DUNHAM, R. S., "Mechanical Characterization of Non-Linear Viscoelastic Solids for Iterative Solution of Boundary Value Problems." *Interior Tech. Rept.*, U.S. Army Research Office, Durham, N.C., Proj. No. 4547-E (1968).

DRUCKER, D. C., "A More Fundamental Approach in Plastic Stress-Strain Relations." *Proc. 1st U.S. Nat. Cong. Appl. Mech.* (Chicago, 1951), N.Y. (1952) pp. 487-491.

DRUCKER, D. C., and PRAGER, W., "Soil Mechanics and Plastic Analysis of Limit Design." *Quar. Appl. Math.*, Vol. 10, No. 2 (1952) pp. 157-165.

DRUCKER, D. C., "Limit Analysis of Two- and Three-Dimensional Soil Mechanics Problems." *J. Mech. and Phys. of Solids,* Vol. 1, No. 4 (July 1953) pp. 217-226.

DRUCKER, D. C., "Coulomb Friction, Plasticity and Limit Loads." *J. Appl. Mech.*, Vol. 21 (1954) pp. 71-74.

DRUCKER, D. C., GIBSON, R. E., and HENKLE, D. J., "Soil Mechanics and Work-Hardening Theories of Plasticity." *Trans. ASCE,* Vol. 122 (1957) pp. 338-346.

DRUCKER, D. C., "A Definition of Stable Inelastic Material." *J. Appl. Mech.* (1959) pp. 101-106.

DRUCKER, D. C., "Plasticity." *Proc. 1st Symp. Naval Structural Mech.* (1960) pp. 407-455.

DRUCKER, D. C., "Concept of Path Independence and Material Stability for Soils." *Proc. Internat. Symp. Rheology and Soil Mechanics,* Grenoble, Springer-Verlag (1966) pp. 23-46.

DRUCKER, D. C., "On Stress-Strain Relations for Soils and Load Carrying Capacity." Internat. Conf. on Mech. of Soil-Vehicle Systems, Torino, Italy (1967).

EVANS, R. J., "Physically Non-Linear Elastic Solids." Ph.D. thesis, Univ. of Calif., Berkeley (1965).

EVANS, R. J., and PISTER, K. S., "Constitutive Equations for a Class of Nonlinear Elastic Solids." *Internat. J. Solids Structures,* Vol. 2 (1966) pp. 427-445.

FERRY, J. D., *Viscoelastic Properties of Polymers.* Wiley (1961).

FILONENKO-BORODICH, M. M., "Some Approximate Theories of the Elastic Foundation" (in Russian). (1940). [See Vlasov and Leontiev (1960).]

FINN, W. D. L., "Application of Plasticity Theory in Soil Mechanics." Lecture series, Univ. of Calif., Berkeley (1965).

FUNG, Y. C., *Foundation of Solid Mechanics.* Prentice-Hall (1965).

GIBSON, R. E., "Some Results Concerning Displacements and Stresses in a Non-homogeneous Elastic Half Space." *Geotechnique,* Vol. 17, No. 1 (1967).

GURTIN, M. E., and STERNBERG, E., "On the Linear Theory of Viscoelasticity." *Archives Rational Mech. Analysis,* Vol. 11 (1962) pp. 291-356.

HENKEL, D. J., "The Correlation Between Deformation, Pore Water Pressure and Strength Characteristics of Saturated Clays." Ph.D. thesis, Imperial College Univ. of London (1958).

HETENYI, M., *Beams on Elastic Foundation.* Univ. of Mich. Press (1946).

HETENYI, M., "A General Solution for the Bending of Beams on an Elastic Foundation of Arbitrary Continuity." *J. Appl. Phys.,* Vol. 21 (1950) p. 55.

HETENYI, M., "Beams and Plates on Elastic Foundations and Related Problems." *Appl. Mech. Rev.,* Vol. 19 (1966) p. 95.

JENIKE, A. W., and SHIELD, R., "On the Plastic Flow of Coulomb Solids Beyond Original Failure." *J. Appl. Mech.* (1959) pp. 599-602.

KERR, A. D., "Elastic and Viscoelastic Foundation Models." *J. Appl. Mech.,* Vol. 31, *Trans. ASME, Series E* (1964) p. 491.

KERR, A. D., "A Study of a New Foundation Model." *Res. Rept. 186,* U.S. Army Materiel Command, Cold Regions Research and Eng. Lab., Hanover, N.H. (1966).

KIRKPATRICK, W. M., "The Condition of Failure for Sands." *Proc. ICSMFE,* Vol. 1, London (1957) pp. 172-178.

MENDELSON, A., *Plasticity: Theory and Application.* Macmillan (1968).

NAGHDI, P. M., "Stress-Strain Relations in Plasticity and Thermo-Plasticity." *Proc. 2nd Symp. Naval Structural Mech.,* Pergammon (1963) pp. 121-167.

NOLL, W., "A Mathematical Theory for the Mechanical Behavior of Continuous Media." *Archives Rational Mech. Analysis,* Vol. 2 (1958).

PASTERNAK, P. L., "Bases for New Methods of Calculations for Foundations on an Elastic Foundation by Means of Two Foundation Coefficients" (in Russian). (1954). [See Vlasov and Leontiev (1960).]

PRAGER, W., "The Theory of Plasticity: A Survey of Recent Achievements." *Proc. Inst. Mech. Eng.,* Vol. 169 (1955) pp. 41-52.

SHIELD, R. T., "On Coulomb's Law of Failure in Soils." *J. Mech. and Phys. of Solids,* Vol. 4 (1955) pp. 10-16.

TRUESDELL, C., "The Mechanical Foundations of Elasticity and Fluid Dynamics." *J. Ration. Mech. Anal.,* Vol. 1 (1952) p. 125.

TRUESDELL, C., and NOLL, W., "The Non-Linear Field Theories of Mechanics." *Handbuch der Physik,* Vol. III/3, Springer (1965).

TSAI, N. C., and WESTMANN, R. A., "Beam on a Tensionless Foundation." *J. Eng. Mech. Div., ASCE,* Vol. 93, No. EM5 (1967).

VESIC, A. S., "Bending of Beams Resting on Isotropic Elastic Solid." *J. ASCE,* Vol. 87, No. EM2 (1961).

VLASOV, V. Z., and LEONTIEV, N. N., "Beams, Plates, and Shells on Elastic Foundations." Trans. from Russian for NASA and NSF by Israel Program for Scientific Translations (1960).

ZIEGLER, H., "A Modification of Prager's Hardening Rule." *Quar. Appl. Math.,* Vol. 17 (1959) pp. 55-65.

ZIEGLER, H., "Some Extremum Principles in Irreversible Thermodynamics With Application to Continuum Mechanics." In *Progress in Solid Mechanics,* Sneddon and Hill (eds.), Vol. 4, Wiley (1963) pp. 91-193.

APPENDIX B

CONSTITUTIVE EQUATIONS AND FAILURE THEORIES: SUMMARY TABLES

Material properties enter into the design of a pavement system in two contexts: (1) the parameters that are necessary to quantify the constitutive equations selected to model material response, and (2) the parameters necessary to establish limiting criteria in terms of various failure theories.

Tables B-1 and B-2 provide the practicing engineer with an easy reference to the various parameters (basic properties) that have to be determined to quantify the more commonly used constitutive equations and failure theories. Failure criteria, fatigue, or other types of time-dependent failure are not considered.

TABLE B-1

CONSTITUTIVE EQUATION	MATERIAL FUNCTIONS (BASIC PROPERTIES)	MATERIALS REPRESENTED	COMMENTS
Linear elasticity	Isotropic modulus of elasticity (E). Poisson's ratio (ν). For orthotropic elasticity the parameters to be defined are: Modulus of elasticity (E_1, E_2, E_3) Poisson's ratio (ν_{12}, ν_{23}, ν_{31}) Shear modulus (G_{12}, G_{23}, G_{31})	1. Soil—cohesive and cohesionless (Refs.[a] 1 to 14). 2. Treated base courses (Refs. 1 to 14, 11 to 19). 3. Portland cement concrete (Refs. 20 to 24). 4. Asphaltic concrete (Refs. 1 to 4, 31, 25, 26, 27, 28).	If the material is nonhomogeneous, E and ν will vary with position. Linear homogeneous isotropic elasticity is the most widely used of all constitutive equations in the structural analysis of pavement systems. With the rapid development of numerical techniques, the ability to solve boundary value problems using nonhomogeneous and anisotropic material properties has increased.
Winkler model	Modulus of subgrade reaction (k).	1. Soil—cohesive and cohesionless (Refs. 20 to 24, 27, 28).	The Winkler model is used to determine the influence of the soil on the stresses and deflections in a slab resting on soil. It cannot be used to determine the stress in the soil below the surface. The Winkler model is used primarily in the analysis of portland cement concrete pavements.
Nonlinear isotropic elasticity	A. Incremental formulation: Incremental coefficient matrix B_{ijkl} and reference stress-strain pairs $\epsilon_{ij}' = B_{ijkl}\,\sigma_{kl}'$ in which ϵ'_{ij} = incremental strain; σ'_{kl} = incremental stress; and B_{ijkl} depends on the reference state. B. Polynomial formulation: The coefficient of the polynomial stress-strain relation.	A. 1. Cohesive subgrade soil (Refs. 30, 31). 2. Asphaltic concrete (Refs. 30, 31). B. 1. Cohesive subgrade soil (Refs. 30, 31). 2. Asphaltic concrete (Refs. 30, 31)	The choice of the incremental or polynomial formulation depends on the solution techniques available for solving boundary value problems and on the nature of the experimental data.
"Nonlinear" elasticity—approximate formulations[b]	Modulus of resilience (M_r) defined as a function of the stress level $M_r = M_r(\sigma)$. Poisson's ratio (ν).	1. Soil—cohesive and cohesionless (Refs. 11, 32, 34, 35, 36, 37). 2. Treated base courses (Refs. 17, 19, 38). 3. Asphaltic concrete (Ref. 30).	The modulus of resilience is determined from a repeated-load test and is defined as the resilient strain divided by the repeated stress.
	Secant modulus (E_s) defined as a function of the confining pressure. Poisson's ratio (ν).	1. Soil—cohesive and cohesionless (Refs. 39 to 42).	The secant modulus is determined from triaxial tests, the confining pressure being dependent on the anticipated stress level.
Linear isotropic viscoelasticity	Complex modulus (E^*). Complex Poisson's ratio (ν^*). Relaxation function. Creep function. Relaxation spectra. Retardation spectra. (All these functions are interrelated.)	1. Asphaltic concrete (Refs. 43 to 54). 2. Cohesive soil (Refs. 29, 33, 53, 54).	Sinusoidal, unconfined compression tests have been used to evaluate the complex modulus and complex Poisson's ratio. These constants, which are functions of frequency, are sufficient to characterize the response of isotropic homogeneous, linear viscoelastic materials. Relaxation and creep functions may be determined from relaxation, constant strain rate, or creep tests. For linear viscoelastic materials these two functions are interconvertible.

[a] It is not possible to list all the references that consider the application of various models to the analysis of pavement systems. Only a few selected references are included here. In addition, there are many references that are common to various categories, because of the treatment of the pavement problem as a layered system.

[b] There are many possibilities. Only a few selected models are indicated here.

TABLE B-2

FAILURE THEORY	GOVERNING CRITERIA (BASIC PROPERTIES)	MATERIALS REPRESENTED	COMMENTS
Maximum stress theory, Rankine's theory, or Lame-Navier theory	The maximum principal stress in the material determines failure regardless of the magnitude and senses of the other two principal stresses. Thus, yielding begins when the absolute values of the maximum stress reach the yield point of the material in simple tension or compression. 1. $\sigma_1=\sigma_{yp}$ (tensile) 2. $\sigma_2=\sigma_{yp}$ (compressive) The basic property is σ_{yp}.	Used for materials where there is a pronounced difference in strength properties in different directions or if the material cannot stand tensile stress (e.g., granular material).	The theory is contradicted in solid materials where three equal tensile or compressive stresses cannot produce a plastic, but only an elastic, deformation. For materials in which hydrostatic compressive stresses do cause plastic deformation, the theory is contradicted by the fact that failure in simple tension in an isotropic material would be along inclined planes on which neither the tensile nor the compressive stress is a maximum.
Maximum elastic strain theory, St. Venant's theory	Yielding begins when either the maximum (elongation) strain equals the yield point strain in simple tension or the minimum (shortening) strain equals the yield point in simple compression. $\frac{\sigma_1}{E}-\frac{\nu}{E}(\sigma_2+\sigma_3)=\frac{\sigma_{yp}}{E}$ (tensile) $\frac{\sigma_3}{E}-\frac{\nu}{E}(\sigma_1+\sigma_2)=\frac{\sigma_{yp}}{E}$ (compressive) The basic property is σ_{yp}.	—	This theory is also contradicted by material behavior under hydrostatic tensile or compressive stresses. It is rarely used.
Constant elastic strain energy theory, Beltrami energy theory	Yielding will occur when the total strain energy per unit volume equals the total strain energy per unit volume at yielding in uniaxial tension or compression. The criterion may be written $\sigma_1^2+\sigma_2^2+\sigma_3^2=2\Gamma(\sigma_1\sigma_2+\sigma_2\sigma_3+\sigma_3\sigma_1)=\sigma_y^2$ The basic property is σ_y.	—	Again, the performance of materials under hydrostatic stresses indicates that the elastic energy can have no significance as a limiting condition.
Maximum shear stress theory (Tresca, Coulomb)	1. *Original form:* The yielding begins when the maximum shear stress in the material equals the maximum shear stress at the yield point in simple tension. $(\sigma_1-\sigma_3)=\sigma_{yp}$ or $\tau_{max}=\frac{\sigma_1-\sigma_3}{2}=\text{const.}$ The basic property is σ_{yp}.	Has been used as a limiting criterion in pavement design. The shear stress was limited in the various components of the pavement section, especially the subgrade.	This criterion is in fair agreement with experiment and is used to a considerable extent by the designers. The yield locus for the Tresca maximum shear criterion is a regular hexagon shown in Fig. A-11. In the stress space the Tresca yield surface is a regular hexagonal prism, as shown in Fig. A-12.
	2. *Modified form, or "extended Tresca's yield criterion":* Here the effect of isotropic pressure, p, is included. In the most general form: $\{(\sigma_1-\sigma_2)^2-r(p)\}\{(\sigma_2-\sigma_3)^2-r(p)\}\{(\sigma_3-\sigma_1)^2-r(p)\}=0$		The yield locus for the extended Tresca criterion is a pyramid with a regular hexagon in cross-section (see Figs. A-18 and A-17b).

TABLE B-2 (Continued)

FAILURE THEORY	GOVERNING CRITERIA (BASIC PROPERTIES)	MATERIALS REPRESENTED	COMMENTS
Constant elastic energy of distortion theory; Huber, Hencky, Von Mises	1. Plastic yielding begins when the strain energy of distortion reaches a critical value $(\sigma_1-\sigma_2)^2+(\sigma_2-\sigma_3)^2+(\sigma_3-\sigma_1)^2=2(\sigma_{yp})^2$ An alternative statement of the theory would be $\tau_{oct}=\frac{\sqrt{2}}{3}\sigma_{yp}$ The basic property is σ_{yp}.	—	This criterion is in fairly good agreement with experiment. It is easier to apply than the Tresca criterion because no prior knowledge of the relative magnitude of the principal stresses is needed. The yield locus for the Von Mises yield criterion is a circle of radius $r=\frac{\sqrt{2}}{3}\sigma_{yp}$ (Fig. A-18).
	2. Modified form $(\sigma_1-\sigma_2)^2+(\sigma_2-\sigma_3)^2+(\sigma_3-\sigma_1)^2=r(p)$ The basic property is $r(p)$.	Used primarily for soils, but has found little application in pavement analysis.	The yield surface in the principal stress space will be then a circular cylinder whose axis is the hydrostatic axis (Fig. A-12). The yield locus for the extended Von Mises criterion is a cone, as shown in Fig. A-17c.
Mohr's failure theory	Failure depends on the stresses on the slip planes, and failure will take place when the obliquity of the resultant stress exceeds a certain maximum value. $\tau=f(\sigma)$ in which τ = shear stress along the failure plane; and σ = normal stress along the failure plane. A general form also proposed by Prandtl is $\frac{1}{2}(\sigma_3-\sigma_1)=f^*\frac{1}{2}(\sigma_3+\sigma_1)$ The basic property is $f\frac{1}{2}(\sigma_3+\sigma_1)$.	—	The curve defined by the functional relationship, $\tau=f(\sigma)$, is termed Mohr rupture envelope and represents the locus of all points defining the limiting values of both components of stress (τ and σ) in the slip planes under the different states of stress to which the material may be subjected.
Mohr-Coulomb theory	The normal and shear stresses are related by $\tau=s=c+\sigma\tan\phi$ or, in terms of principal stresses (Fig. A-16), $\frac{\sigma_1-\sigma_3}{2}=c\cos\phi+\left(\frac{\sigma_1+\sigma_3}{2}\right)\sin\phi$ And, in the most general form, $\{(\sigma_1-\sigma_2-[2c\cos\phi+(\sigma_1+\sigma_2)\sin\phi]^2\}\{(\sigma_2-\sigma_3)^2-[2c\cos\phi+(\sigma_2+\sigma_3)\sin\phi]^2\}\{(\sigma_3-\sigma_1)^2+[2c\cos\phi+(\sigma_3+\sigma_1)\sin\phi]^2\}=0$	The most widely used failure theory for soils.	In the $\tau-\sigma$ plane the criterion plots as shown in Fig. A-16. In the general form the geometrical representation of the criterion is a hexagonal pyramid with the vertex at the point $\sigma_1=\sigma_2=\sigma_3=c\cot\phi$ (see Fig. A-17a). This pyramid is similar to that of Tresca's in Fig. A-17b, but does not have a regular hexagon in cross-section (see Fig. A-18). For a cohesionless material, $c=0$, the vertex of the pyramid is at the origin.

* A special form of which results in Mohr-Coulomb criterion given here.

REFERENCES

1. BURMISTER, D. M., "Applications of Layered System Concepts and Principles to Interpretations and Evaluations of Asphalt Pavement Performances and to Design and Construction." *Proc. Internat. Conf., Structural Design of Asphalt Pavements,* Univ. of Mich. (1962) pp. 441-453.
2. BURMISTER, D. M., "The General Theory of Stresses and Displacements in Layered Systems." *J. Appl. Phys.,* Vol. 16, No. 2, pp. 89-96; No. 3, pp. 126-127; No. 5, pp. 296-302 (1945).
3. BURMISTER, D. M., "The Theory of Stresses and Displacements in Layered Systems and Applications to the Design of Airport Runways." *Proc. HRB,* Vol. 23, (1943) pp. 126-149.
4. WHIFFIN, A. C., and LISTER, N. W., "The Application of Elastic Theory to Flexible Pavements." *Proc. Internat. Conf., Structural Design of Asphalt Pavements,* Univ. of Mich. (1962) pp. 499-521.
5. ACUM, W. E. A., and FOX, L., "Computation of Load Stresses in a Three-Layer Elastic System." *Geotechnique,* Vol. II, No. 4 (1951) pp. 293-300.
6. JONES, A., "Tables of Stresses in Three-Layer Elastic Systems." *HRB Bull. 342* (1962) pp. 176-214.
7. PEATTIE, K. R., "Stress and Strain Factors for Three-Layer Elastic Systems." *HRB Bull. 342* (1962) pp. 215-253.
8. VESIC, A. S., and DOMASCHUK, L., "Theoretical Analysis of Structural Behavior of Road Test Flexible Pavements." *NCHRP Report 10* (1964).
9. ODEMARK, N., "Investigations as to the Elastic Properties of Soils and Design of Pavements According to the Theory of Elasticity." Meddelande 77, Statens Vaginstitut, Stockholm (1949).
10. TURNBULL, W. J., MAXWELL, A. A., and AHLVIN, R. G., "Stresses and Deflections in Homogeneous Soil Masses." *Proc. 5th Internat. Conf. on Soil Mechanics and Foundation Eng.,* Vol. 2 (1961) pp. 337-345.
11. SEED, H. B., MITRY, F. G., MONISMITH, C. L., and CHAN, C. K., "Prediction of Flexible Pavement Deflections from Laboratory Repeated-Load Tests." *NCHRP Report 35* (1967).
12. DORMON, G. M., and METCALF, C. T., "Design Curves for Flexible Pavements Based on Layered System Theory." *Hwy. Res. Record No. 71* (1965) pp. 69-84.
13. VERSTRAETEN, J., "Stresses and Displacements in Elastic Layered Systems." *Proc. 2d Internat. Conf., Structural Design of Asphalt Pavements,* Univ. of Mich. (1967) pp. 223-238.
14. SANBORN, J. L., and YODER, E. J., "Stress and Displacement in an Elastic Mass Under Semiellipsoidal Loads." *Proc. 2d Internat. Conf., Structural Design of Asphalt Pavements, Univ. of Mich.* (1967) pp. 239-250.
15. AHLVIN, R. G., and ULERY, H. H., "Tabulated Values for Determining the Complete Pattern of Stresses, Strains, and Deflections Beneath a Uniform Circular Load on a Homogeneous Half Space." *HRB Bull. 342* (1962) pp. 1-13.
16. VESIC, A. S., "The Validity of Layered Solid Theories for Flexible Pavements." *Proc. Internat. Conf., Structural Design of Asphalt Pavements,* Univ. of Mich. (1962) pp. 283-290.
17. MITCHELL, J. K., and SHEN, C.-K., "Soil-Cement Properties Determined by Repeated Loading in Relation to Bases for Flexible Pavements." *Proc. 2d Internat. Conf., Structural Design of Asphalt Pavements,* Univ. of Mich. (1967) pp. 348-364.
18. NUSSBAUM, P. J., and LARSEN, T. J., "Load-Deflection Characteristics of Soil-Cement Pavements." *Hwy. Res. Record No. 86* (1965) pp. 1-14.
19. MONISMITH, C. L., ET AL., "Load Transmission Characteristics of Asphalt-Treated Base Course." *Proc. 2d Internat. Conf., Structural Design of Asphalt Pavements,* Univ. of Mich. (1967) pp. 730-766.
20. WESTERGAARD, H. M., "Computation of Stresses in Concrete Roads." *Proc. HRB,* Part 1 (1925) pp. 90-112.
21. PORTLAND CEMENT ASSOCIATION, "Concrete Pavement Design." Chicago (1951).
22. SPANGLER, M. G., "Stresses in the Corner Region of Concrete Pavements." *Iowa Eng. Exper. Sta. Bull. 157* (1942).
23. PICKETT, G., and RAY, G. K., "Influence Charts for Rigid Pavements." *Trans. ASCE,* Vol. 116 (1951) pp. 49-73.
24. PICKETT, G., RAVILLE, M. E., JANES, W. C., and MCCORMICK, F. J., "Influence Charts for Concrete Pavements." Supplement to *Bull. No. 65,* Kansas State College Eng. Exper. Sta. (1951).
25. MONISMITH, C. L., "Asphalt Mixture Behavior in Repeated Flexure." *IER Rept. No. TE-63-2* (to Calif. Div. of Highways), Univ. of Calif. (1964).
26. SKOK, E. L., JR., and FINN, F. N., "Theoretical Concepts Applied to Asphalt Concrete Pavement Design." *Proc. Internat. Conf., Structural Design of Asphalt Pavements,* Univ. of Mich. (1962) pp. 412-440.
27. FINN, F. N., "Factors Involved in the Design of Asphaltic Pavement Surfaces." *NCHRP Report 39* (1967).
28. BUSCHING, H. W., GOETZ, W. H., and HARR, M. E., "Stress-Deformation Behavior of Anisotropic Bituminous Mixtures." *Proc. AAPT* (1967).
29. COFFMAN, B. S., "Pavement Deflections from Laboratory Tests and Layer Theory." *Proc. 2d Internat. Conf., Structural Design of Asphalt Pavements,* Univ. of Mich. (1967).
30. DEHLEN, G. L., "The Effect of Non-Linear Material Response on the Behavior of Pavements Subjected to Traffic Loads." Ph.D. dissertation, Univ. of Calif., Berkeley (1969).
31. DEHLEN, G. L., and MONISMITH, C. L., "Effect of Nonlinear Material Response on the Behavior of Pavements under Traffic." *Hwy. Res. Record No. 310* (1970) pp. 1-16.
32. SEED, H. B., CHAN, C. K., and LEE, C. E., "Resilience Characteristics of Subgrade Soils and Their Relation to Fatigue Failures in Asphalt Pavements." *Proc. Internat. Conf., Structural Design of Asphalt Pavements,* Univ. of Mich. (1962) pp. 611-636.

33. COFFMAN, B. S., KRAFT, D. C., and TAMAYO, J., "A Comparison of Calculated and Measured Deflections for the AASHO Road Test." *Proc. AAPT,* Vol. 33 (1964) pp. 54-91.
34. SEED, H. B., and CHAN, C. K., "Effect of Duration of Stress Application on Soil Deformation Under Repeated Loading." *Proc. 5th Internat. Conf. on Soil Mechanics and Foundation Eng.* (1961) Vol. 1, pp. 340-345.
35. HAYNES, J. H., and YODER, E. J., "Effects of Repeated Loading on Gravel and Crushed Stone Base Course Materials Used in the AASHO Road Test." *Hwy. Res. Record No. 39* (1963) pp. 82-96.
36. TROLLOPE, D. H., LEE, I. K., and MORRIS, J., "Stresses and Deformation in Two-Layer Pavement Structures Under Slow Repeated Loading." *Proc. Australian Road Res. Board,* Vol. 1, Part 2 (1963) pp. 693-721.
37. DUNLAP, W. A., "A Report on a Mathematical Model Describing the Deformation Characteristics of Granular Materials." *Tech. Rept. No. 1,* Texas Trans. Inst., Texas A&M (1963).
38. GREGG, J. A., ET AL., "On the Properties, Behaviour and Design of Bituminous Stabilized Sand Bases." *Proc. 2d Internat. Conf., Structural Design of Asphalt Pavements,* Univ. of Mich. (1967) pp. 709-729.
39. CASAGRANDE, A., and SHANNON, W. L., "Research on Stress-Deformation and Strength Characteristics of Soils and Soft Rocks Under Transient Loading." *Eng. Soil Mech. Ser. 31,* Harvard Grad. School (1948).
40. SEED, H. B., and LUNDGREN, R., "Investigation of the Effect of Transient Loading on the Strength and Deformation Characteristics of Saturated Sands."
41. CHEN, L. S., "An Investigation of Stress-Strain and Strength Characteristics of Cohesionless Soils by Triaxial Compression Tests," *Proc. 2d Internat. Conf. on Soil Mechanics and Foundation Eng.* (1948) Vol. 5, pp. 35-43.
42. JAKOBSON, B., "Some Fundamental Properties of Sand." *Proc. 4th Internat. Conf. on Soil Mechanics and Foundation Eng.,* London, Vol. 1 (1957) pp. 167-171.
43. ALEXANDER, R. L., "Limits of Linear Behavior of an Asphalt Concrete in Tension and Compression." D.Eng. thesis (Trans. Eng.), Univ. of Calif. (1964).
44. MONISMITH, C. L., and SECOR, K. E., "Viscoelastic Behavior of Asphalt Concrete Pavements." *Proc. Internat. Conf., Structural Design of Asphalt Pavements,* Univ. of Mich. (1962) pp. 476-498.
45. MONISMITH, C. L., ALEXANDER, R. L., and SECOR, K. E., "Rheologic Behavior of Asphalt Concrete." *Proc. AAPT,* Vol. 35 (1966) pp. 400-450.
46. PAGEN, C. A., and KU, B., "Effect of Asphalt Viscosity on Rheological Properties of Bituminous Concrete." *Hwy. Res. Record No. 104* (1965) pp. 124-140.
47. PAGEN, C. A., "A Study of the Temperature-Dependent Rheological Characteristics of Asphaltic Concrete." *Hwy. Res. Record No. 158* (1967) pp. 116-143.
48. PAGEN, C. A., "Rheological Response of Bituminous Concrete." *Hwy. Res. Record No. 67* (1965) pp. 1-26.
49. PAPAZIAN, H. S., "The Response of Linear Viscoelastic Materials in the Frequency Domain with Emphasis on Asphaltic Concrete." *Proc. Internat. Conf., Structural Design of Asphalt Pavements,* Univ. of Mich. (1962) pp. 454-463.
50. SECOR, K. E., and MONISMITH, C. L., "Analysis of Triaxial Test Data on Asphalt Concrete Using Viscoelastic Principles." *Proc. HRB,* Vol. 40 (1961) pp. 295-314.
51. SECOR, K. E., and MONISMITH, C. L., "Analysis and Interrelation of Stress-Strain-Time Data for Asphalt Concrete." *Trans. Soc. Rheology,* Vol. 8 (1964).
52. SECOR, K. E., and MONISMITH, C. L., "Viscoelastic Response of Asphalt Paving Slabs Under Creek Loading." *Hwy. Res. Record No. 67* (1965) pp. 84-97.
53. ASHTON, J. E., and MOAVENZADEH, F., "Analysis of Stresses and Displacements in a Three-Layered Viscoelastic System." *Proc. 2d Internat. Conf., Structural Design of Asphalt Pavements,* Univ. of Mich. (1967) pp. 149-162.
54. PERLOFF, W. H., and MOAVENZADEH, F., "Deflection of Viscoelastic Medium Due to a Moving Load." *Proc. 2d Internat. Conf., Structural Design of Asphalt Pavements,* Univ. of Mich. (1967) pp. 212-222.

APPENDIX C

DETERMINATION OF INCREMENTAL COEFFICIENTS

A polynomial approximation in a least squares sense was used to fit the test data. The incremental coefficients were obtained by differentiating the polynomial curve at each set of reference stress states. The least squares polynomial approximation used in this study is briefly described in the following.

LEAST SQUARES THEOREM

If the n measurements $Y_1, Y_2, \ldots Y_n$ are statistically independent with common variance σ^2 and have expected values $E(Y_i)$

$$\begin{aligned} E(Y_1) &= B_0 + B_1x_1 + B_2x_1^2 + \ldots + B_{k-1}x_1^{k-1} \\ E(Y_2) &= B_0 + B_1x_2 + B_2x_2^2 + \ldots + B_{k-1}x_2^{k-1} \\ &\ldots \\ E(Y_n) &= B_0 + B_1x_n + B_2x_n^2 + \ldots + B_{k-1}x_n^{k-1} \end{aligned} \qquad \text{(C-1)}$$

then the best linear unbiased estimates $\hat{B}_0, \hat{B}_1, \hat{B}_2, \ldots, \hat{B}_{k-1}$ of the unknown coefficients are given by the solution of k simultaneous equations, called the normal equations,

$$\begin{aligned} &nB_0 + \Sigma x_iB_1 + \Sigma x_i^2B_2 + \ldots + \Sigma x_i^{k-1}B_{k-1} = \Sigma Y_i \\ &\Sigma x_iB_0 + \Sigma x_i^2B_1 + \Sigma x_i^3B_2 + \ldots + \Sigma x_i^kB_{k-1} = \Sigma x_iY_i \\ &\ldots \\ &\Sigma x_i^{k-1}B_0 + \Sigma x_i^kB_1 + \Sigma x_i^{k+1}B_2 + \ldots \Sigma x_i^{2k-2}B_{k-1} = \Sigma x_i^{k-1}Y_i \end{aligned} \qquad \text{(C-2)}$$

and the estimate of σ^2 is given by

$$S^2 = \frac{1}{n-k}\sum_1^n Y_i - (\hat{B}_0 + \hat{B}_1x_i + \ldots + \hat{B}_{k-1}x_i^{k-1})^2$$

σ = the standard deviation.

Using matrix notation, Eq. C-2 can be restated:

$$[A]\{\hat{B}\} = \{Q\} \qquad \text{(C-3)}$$

in which

$$A = \begin{bmatrix} n & \Sigma x_i & \Sigma x_i^2 & \ldots & \Sigma x_i^{k-1} \\ \Sigma x_i & \Sigma x_i^2 & \Sigma x_i^3 & \ldots & \Sigma x_i^k \\ \ldots & & & & \\ \ldots & & & & \\ \ldots & & & & \\ \Sigma x_i^{k-1} & \Sigma x_i^k & \Sigma x_i^{k+1} & \ldots & \Sigma x_i^{2k-2} \end{bmatrix}$$

$$Q = \begin{Bmatrix} \Sigma Y_i \\ \Sigma x_iY_i \\ \ldots \\ \ldots \\ \ldots \\ \Sigma x_i^{k-1}Y_i \end{Bmatrix}$$

and

$$\hat{B} = \begin{Bmatrix} \hat{B}_0 \\ \hat{B}_1 \\ \hat{B}_2 \\ \ldots \\ \ldots \\ \hat{B}_{k-1} \end{Bmatrix}$$

The simultaneous equations described by Eq. C-3 may be solved by the Gauss elimination.

The incremental coefficients are obtained by differentiating

$$Y = \hat{B}_0 + \hat{B}_1x + \hat{B}_2x^2 + \hat{B}_3x^3 + \ldots + \hat{B}_{k-1}x^{k-1} \qquad \text{(C-4)}$$

i.e.,

$$\partial Y/\partial x = \hat{B}_1 + 2\hat{B}_2x + 3\hat{B}_3x^2 + \ldots + (k-1)\hat{B}_{k-1}x^{k-2} \qquad \text{(C-4)}$$

Substituting reference stress state for x in Eq. C-4 yields the incremental coefficients.

APPENDIX D

SUMMARY OF APPENDIX ITEMS NOT PUBLISHED

Data, stress levels, and stress states used in tests on asphaltic concrete and cohesive subgrade soils appeared in appendices to the agency's final report. These data are summarized in Chapter Three.

The complete data presentation, consisting of 235 tables and graphs, is not published in this report; however, this material may be obtained on a loan basis by contacting the Program Director, NCHRP.

Published reports of the

NATIONAL COOPERATIVE HIGHWAY RESEARCH PROGRAM

are available from:

Highway Research Board
National Academy of Sciences
2101 Constitution Avenue
Washington, D.C. 20418

Rep. No. *Title*

—* A Critical Review of Literature Treating Methods of Identifying Aggregates Subject to Destructive Volume Change When Frozen in Concrete and a Proposed Program of Research—Intermediate Report (Proj. 4-3(2)), 81 p., $1.80

1 Evaluation of Methods of Replacement of Deteriorated Concrete in Structures (Proj. 6-8), 56 p., $2.80

2 An Introduction to Guidelines for Satellite Studies of Pavement Performance (Proj. 1-1), 19 p., $1.80

2A Guidelines for Satellite Studies of Pavement Performance, 85 p.+9 figs., 26 tables, 4 app., $3.00

3 Improved Criteria for Traffic Signals at Individual Intersections—Interim Report (Proj. 3-5), 36 p., $1.60

4 Non-Chemical Methods of Snow and Ice Control on Highway Structures (Proj. 6-2), 74 p., $3.20

5 Effects of Different Methods of Stockpiling Aggregates—Interim Report (Proj. 10-3), 48 p., $2.00

6 Means of Locating and Communicating with Disabled Vehicles—Interim Report (Proj. 3-4), 56 p. $3.20

7 Comparison of Different Methods of Measuring Pavement Condition—Interim Report (Proj. 1-2), 29 p., $1.80

8 Synthetic Aggregates for Highway Construction (Proj. 4-4), 13 p., $1.00

9 Traffic Surveillance and Means of Communicating with Drivers—Interim Report (Proj. 3-2), 28 p., $1.60

10 Theoretical Analysis of Structural Behavior of Road Test Flexible Pavements (Proj. 1-4), 31 p., $2.80

11 Effect of Control Devices on Traffic Operations—Interim Report (Proj. 3-6), 107 p., $5.80

12 Identification of Aggregates Causing Poor Concrete Performance When Frozen—Interim Report (Proj. 4-3(1)), 47 p., $3.00

13 Running Cost of Motor Vehicles as Affected by Highway Design—Interim Report (Proj. 2-5), 43 p., $2.80

14 Density and Moisture Content Measurements by Nuclear Methods—Interim Report (Proj. 10-5), 32 p., $3.00

15 Identification of Concrete Aggregates Exhibiting Frost Susceptibility—Interim Report (Proj. 4-3(2)), 66 p., $4.00

16 Protective Coatings to Prevent Deterioration of Concrete by Deicing Chemicals (Proj. 6-3), 21 p., $1.60

17 Development of Guidelines for Practical and Realistic Construction Specifications (Proj. 10-1), 109 p., $6.00

18 Community Consequences of Highway Improvement (Proj. 2-2), 37 p., $2.80

19 Economical and Effective Deicing Agents for Use on Highway Structures (Proj. 6-1), 19 p., $1.20

20 Economic Study of Roadway Lighting (Proj. 5-4), 77 p., $3.20

21 Detecting Variations in Load-Carrying Capacity of Flexible Pavements (Proj. 1-5), 30 p., $1.40

22 Factors Influencing Flexible Pavement Performance (Proj. 1-3(2)), 69 p., $2.60

23 Methods for Reducing Corrosion of Reinforcing Steel (Proj. 6-4), 22 p., $1.40

24 Urban Travel Patterns for Airports, Shopping Centers, and Industrial Plants (Proj. 7-1), 116 p., $5.20

25 Potential Uses of Sonic and Ultrasonic Devices in Highway Construction (Proj. 10-7), 48 p., $2.00

26 Development of Uniform Procedures for Establishing Construction Equipment Rental Rates (Proj. 13-1), 33 p., $1.60

27 Physical Factors Influencing Resistance of Concrete to Deicing Agents (Proj. 6-5), 41 p., $2.00

28 Surveillance Methods and Ways and Means of Communicating with Drivers (Proj. 3-2), 66 p., $2.60

29 Digital-Computer-Controlled Traffic Signal System for a Small City (Proj. 3-2), 82 p., $4.00

30 Extension of AASHO Road Test Performance Concepts (Proj. 1-4(2)), 33 p., $1.60

31 A Review of Transportation Aspects of Land-Use Control (Proj. 8-5), 41 p., $2.00

32 Improved Criteria for Traffic Signals at Individual Intersections (Proj. 3-5), 134 p., $5.00

33 Values of Time Savings of Commercial Vehicles (Proj. 2-4), 74 p., $3.60

34 Evaluation of Construction Control Procedures—Interim Report (Proj. 10-2), 117 p., $5.00

35 Prediction of Flexible Pavement Deflections from Laboratory Repeated-Load Tests (Proj. 1-3(3)), 117 p., $5.00

36 Highway Guardrails—A Review of Current Practice (Proj. 15-1), 33 p., $1.60

37 Tentative Skid-Resistance Requirements for Main Rural Highways (Proj. 1-7), 80 p., $3.60

38 Evaluation of Pavement Joint and Crack Sealing Materials and Practices (Proj. 9-3), 40 p., $2.00

39 Factors Involved in the Design of Asphaltic Pavement Surfaces (Proj. 1-8), 112 p., $5.00

40 Means of Locating Disabled or Stopped Vehicles (Proj. 3-4(1)), 40 p., $2.00

41 Effect of Control Devices on Traffic Operations (Proj. 3-6), 83 p., $3.60

42 Interstate Highway Maintenance Requirements and Unit Maintenance Expenditure Index (Proj. 14-1), 144 p., $5.60

43 Density and Moisture Content Measurements by Nuclear Methods (Proj. 10-5), 38 p., $2.00

44 Traffic Attraction of Rural Outdoor Recreational Areas (Proj. 7-2), 28 p., $1.40

45 Development of Improved Pavement Marking Materials—Laboratory Phase (Proj. 5-5), 24 p., $1.40

46 Effects of Different Methods of Stockpiling and Handling Aggregates (Proj. 10-3), 102 p., $4.60

47 Accident Rates as Related to Design Elements of Rural Highways (Proj. 2-3), 173 p., $6.40

48 Factors and Trends in Trip Lengths (Proj. 7-4), 70 p., $3.20

49 National Survey of Transportation Attitudes and Behavior—Phase I Summary Report (Proj. 20-4), 71 p., $3.20

* Highway Research Board Special Report 80.

Rep. No.	Title
50	Factors Influencing Safety at Highway-Rail Grade Crossings (Proj. 3-8), 113 p., $5.20
51	Sensing and Communication Between Vehicles (Proj. 3-3), 105 p., $5.00
52	Measurement of Pavement Thickness by Rapid and Nondestructive Methods (Proj. 10-6), 82 p., $3.80
53	Multiple Use of Lands Within Highway Rights-of-Way (Proj. 7-6), 68 p., $3.20
54	Location, Selection, and Maintenance of Highway Guardrails and Median Barriers (Proj. 15-1(2)), 63 p., $2.60
55	Research Needs in Highway Transportation (Proj. 20-2), 66 p., $2.80
56	Scenic Easements—Legal, Administrative, and Valuation Problems and Procedures (Proj. 11-3), 174 p., $6.40
57	Factors Influencing Modal Trip Assignment (Proj. 8-2), 78 p., $3.20
58	Comparative Analysis of Traffic Assignment Techniques with Actual Highway Use (Proj. 7-5), 85 p., $3.60
59	Standard Measurements for Satellite Road Test Program (Proj. 1-6), 78 p., $3.20
60	Effects of Illumination on Operating Characteristics of Freeways (Proj. 5-2) 148 p., $6.00
61	Evaluation of Studded Tires—Performance Data and Pavement Wear Measurement (Proj. 1-9), 66 p., $3.00
62	Urban Travel Patterns for Hospitals, Universities, Office Buildings, and Capitols (Proj. 7-1), 144 p., $5.60
63	Economics of Design Standards for Low-Volume Rural Roads (Proj. 2-6), 93 p., $4.00
64	Motorists' Needs and Services on Interstate Highways (Proj. 7-7), 88 p., $3.60
65	One-Cycle Slow-Freeze Test for Evaluating Aggregate Performance in Frozen Concrete (Proj. 4-3(1)), 21 p., $1.40
66	Identification of Frost-Susceptible Particles in Concrete Aggregates (Proj. 4-3(2)), 62 p., $2.80
67	Relation of Asphalt Rheological Properties to Pavement Durability (Proj. 9-1), 45 p., $2.20
68	Application of Vehicle Operating Characteristics to Geometric Design and Traffic Operations (Proj. 3-10), 38 p., $2.00
69	Evaluation of Construction Control Procedures—Aggregate Gradation Variations and Effects (Proj. 10-2A), 58 p., $2.80
70	Social and Economic Factors Affecting Intercity Travel (Proj. 8-1), 68 p., $3.00
71	Analytical Study of Weighing Methods for Highway Vehicles in Motion (Proj. 7-3), 63 p., $2.80
72	Theory and Practice in Inverse Condemnation for Five Representative States (Proj. 11-2), 44 p., $2.20
73	Improved Criteria for Traffic Signal Systems on Urban Arterials (Proj. 3-5/1), 55 p., $2.80
74	Protective Coatings for Highway Structural Steel (Proj. 4-6), 64 p., $2.80
74A	Protective Coatings for Highway Structural Steel—Literature Survey (Proj. 4-6), 275 p., $8.00
74B	Protective Coatings for Highway Structural Steel—Current Highway Practices (Proj. 4-6), 102 p., $4.00
75	Effect of Highway Landscape Development on Nearby Property (Proj. 2-9), 82 p., $3.60
76	Detecting Seasonal Changes in Load-Carrying Capabilities of Flexible Pavements (Proj. 1-5(2)), 37 p., $2.00
77	Development of Design Criteria for Safer Luminaire Supports (Proj. 15-6), 82 p., $3.80
78	Highway Noise—Measurement, Simulation, and Mixed Reactions (Proj. 3-7), 78 p., $3.20
79	Development of Improved Methods for Reduction of Traffic Accidents (Proj. 17-1), 163 p., $6.40
80	Oversize-Overweight Permit Operation on State Highways (Proj. 2-10), 120 p., $5.20
81	Moving Behavior and Residential Choice—A National Survey (Proj. 8-6), 129 p., $5.60
82	National Survey of Transportation Attitudes and Behavior—Phase II Analysis Report (Proj. 20-4), 89 p., $4.00
83	Distribution of Wheel Loads on Highway Bridges (Proj. 12-2), 56 p., $2.80
84	Analysis and Projection of Research on Traffic Surveillance, Communication, and Control (Proj. 3-9), 48 p., $2.40
85	Development of Formed-in-Place Wet Reflective Markers (Proj. 5-5), 28 p., $1.80
86	Tentative Service Requirements for Bridge Rail Systems (Proj. 12-8), 62 p., $3.20
87	Rules of Discovery and Disclosure in Highway Condemnation Proceedings (Proj. 11-1(5)), 28 p., $2.00
88	Recognition of Benefits to Remainder Property in Highway Valuation Cases (Proj. 11-1(2)), 24 p., $2.00
89	Factors, Trends, and Guidelines Related to Trip Length (Proj. 7-4), 59 p., $3.20
90	Protection of Steel in Prestressed Concrete Bridges (Proj. 12-5), 86 p., $4.00
91	Effects of Deicing Salts on Water Quality and Biota—Literature Review and Recommended Research (Proj. 16-1), 70 p., $3.20
92	Valuation and Condemnation of Special Purpose Properties (Proj. 11-1(6)), 47 p., $2.60
93	Guidelines for Medial and Marginal Access Control on Major Roadways (Proj. 3-13), 147 p., $6.20
94	Valuation and Condemnation Problems Involving Trade Fixtures (Proj. 11-1(9)), 22 p., $1.80
95	Highway Fog (Proj. 5-6), 48 p., $2.40
96	Strategies for the Evaluation of Alternative Transportation Plans (Proj. 8-4), 111 p., $5.40
97	Analysis of Structural Behavior of AASHO Road Test Rigid Pavements (Proj. 1-4(1)A), 35 p., $2.60
98	Tests for Evaluating Degradation of Base Course Aggregates (Proj. 4-2), 98 p. $5.00
99	Visual Requirements in Night Driving (Proj. 5-3), 38 p., $2.60
100	Research Needs Relating to Performance of Aggregates in Highway Construction (Proj. 4-8), 68 p., $3.40
101	Effect of Stress on Freeze-Thaw Durability of Concrete Bridge Decks (Proj. 6-9), 70 p., $3.60
102	Effect of Weldments on the Fatigue Strength of Steel Beams (Proj. 12-7), 114 p., $5.40
103	Rapid Test Methods for Field Control of Highway Construction (Proj. 10-4), 89 p., $5.00
104	Rules of Compensability and Valuation Evidence for Highway Land Acquisition (Proj. 11-1), 77 p., $4.40

Rep. No. *Title*

105 Dynamic Pavement Loads of Heavy Highway Vehicles (Proj. 15-5), 94 p., $5.00
106 Revibration of Retarded Concrete for Continuous Bridge Decks (Proj. 18-1), 67 p., $3.40
107 New Approaches to Compensation for Residential Takings (Proj. 11-1(10)), 27 p., $2.40
108 Tentative Design Procedure for Riprap-Lined Channels (Proj. 15-2), 75 p., $4.00
109 Elastomeric Bearing Research (Proj. 12-9), 53 p., $3.00
110 Optimizing Street Operations Through Traffic Regulations and Control (Proj. 3-11), 100 p., $4.40
111 Running Costs of Motor Vehicles as Affected by Road Design and Traffic (Proj. 2-5a and 2-7), 97 p., $5.20
112 Junkyard Valuation—Salvage Industry Appraisal Principles Applicable to Highway Beautification (Proj. 11-3(2)), 41 p., $2.60
113 Optimizing Flow on Existing Street Networks (Proj. 3-14), 414 p., $15.60
114 Effects of Proposed Highway Improvements on Property Values (Proj. 11-1(1)), 42 p., $2.60
115 Guardrail Performance and Design (Proj. 15-1(2)), 70 p., $3.60
116 Structural Analysis and Design of Pipe Culverts (Proj. 15-3), 155 p., $6.40
117 Highway Noise—A Design Guide for Highway Engineers (Proj. 3-7), 79 p., $4.60
118 Location, Selection, and Maintenance of Highway Traffic Barriers (Proj. 15-1(2)), 96 p., $5.20
119 Control of Highway Advertising Signs—Some Legal Problems (Proj. 11-3(1)), 72 p., $3.60
120 Data Requirements for Metropolitan Transportation Planning (Proj. 8-7), 90 p., $4.80
121 Protection of Highway Utility (Proj. 8-5), 115 p., $5.60
122 Summary and Evaluation of Economic Consequences of Highway Improvements (Proj. 2-11), 324 p., $13.60
123 Development of Information Requirements and Transmission Techniques for Highway Users (Proj. 3-12) 239 p., $9.60
124 Improved Criteria for Traffic Signal Systems in Urban Networks (Proj. 3-5) 86 p., $4.80
125 Optimization of Density and Moisture Content Measurements by Nuclear Methods (Proj. 10-5A), 86 p., $4.40
126 Divergencies in Right-of-Way Valuation (Proj. 11-4), 57 p., $3.00
127 Snow Removal and Ice Control Techniques at Interchanges (Proj. 6-10), 90 p., $5.20
128 Evaluation of AASHO Interim Guides for Design of Pavement Structures (Proj. 1-11), 111 p., $5.60
129 Guardrail Crash Test Evaluation—New Concepts and End Designs (Proj. 15-1(2)), 89 p., $4.80
130 Roadway Delineation Systems (Proj. 5-7), 349 p., $14.00
131 Performance Budgeting System for Highway Maintenance Management (Proj. 19-2(4)), 213 p., $8.40
132 Relationships Between Physiographic Units and Highway Design Factors (Proj. 1-3(1)), 161 p., $7.20

Rep. No. *Title*

133 Procedures for Estimating Highway User Costs, Air Pollution, and Noise Effects (Proj. 7-8), 127 p., $5.60
134 Damages Due to Drainage, Runoff, Blasting, and Slides (Proj. 11-1(8)), 24 p., $2.80
135 Promising Replacements for Conventional Aggregates for Highway Use (Proj. 4-10), 53 p., $3.60
136 Estimating Peak Runoff Rates from Ungaged Small Rural Watersheds (Proj. 15-4), 85 p., $4.60
137 Roadside Development—Evaluation of Research (Proj. 16-2), 78 p., $4.20
138 Instrumentation for Measurement of Moisture—Literature Review and Recommended Research (Proj. 21-1), 60 p., $4.00
139 Flexible Pavement Design and Management—Systems Formulation (Proj. 1-10), 64 p., $4.40
140 Flexible Pavement Design and Management—Materials Characterization (Proj. 1-10), 118 p., $5.60

Synthesis of Highway Practice

No. *Title*

1 Traffic Control for Freeway Maintenance (Proj. 20-5, Topic 1), 47 p., $2.20
2 Bridge Approach Design and Construction Practices (Proj. 20-5, Topic 2), 30 p., $2.00
3 Traffic-Safe and Hydraulically Efficient Drainage Practice (Proj. 20-5, Topic 4), 38 p., $2.20
4 Concrete Bridge Deck Durability (Proj. 20-5, Topic 3), 28 p., $2.20
5 Scour at Bridge Waterways (Proj. 20-5, Topic 5), 37 p., $2.40
6 Principles of Project Scheduling and Monitoring (Proj. 20-5, Topic 6), 43 p., $2.40
7 Motorist Aid Systems (Proj. 20-5, Topic 3-01), 28 p., $2.40
8 Construction of Embankments (Proj. 20-5, Topic 9), 38 p., $2.40
9 Pavement Rehabilitation—Materials and Techniques (Proj. 20-5, Topic 8), 41 p., $2.80
10 Recruiting, Training, and Retaining Maintenance and Equipment Personnel (Proj. 20-5, Topic 10), 35 p., $2.80
11 Development of Management Capability (Proj. 20-5, Topic 12), 50 p., $3.20
12 Telecommunications Systems for Highway Administration and Operations (Proj. 20-5, Topic 3-03), 29 p., $2.80
13 Radio Spectrum Frequency Management (Proj. 20-5, Topic 3-03), 32 p., $2.80
14 Skid Resistance (Proj. 20-5, Topic 7), 66 p., $4.00
15 Statewide Transportation Planning—Needs and Requirements (Proj. 20-5, Topic 3-02), 41 p., $3.60
16 Continuously Reinforced Concrete Pavement (Proj. 20-5, Topic 3-08), 23 p., $2.80
17 Pavement Traffic Marking—Materials and Application Affecting Serviceability (Proj. 20-5, Topic 3-05), 44 p., $3.60
18 Erosion Control on Highway Construction (Proj. 20-5, Topic 4-01), 52 p., $4.00

THE NATIONAL ACADEMY OF SCIENCES is a private, honorary organization of more than 700 scientists and engineers elected on the basis of outstanding contributions to knowledge. Established by a Congressional Act of Incorporation signed by President Abraham Lincoln on March 3, 1863, and supported by private and public funds, the Academy works to further science and its use for the general welfare by bringing together the most qualified individuals to deal with scientific and technological problems of broad significance.

Under the terms of its Congressional charter, the Academy is also called upon to act as an official—yet independent—adviser to the Federal Government in any matter of science and technology. This provision accounts for the close ties that have always existed between the Academy and the Government, although the Academy is not a governmental agency and its activities are not limited to those on behalf of the Government.

THE NATIONAL ACADEMY OF ENGINEERING was established on December 5, 1964. On that date the Council of the National Academy of Sciences, under the authority of its Act of Incorporation, adopted Articles of Organization bringing the National Academy of Engineering into being, independent and autonomous in its organization and the election of its members, and closely coordinated with the National Academy of Sciences in its advisory activities. The two Academies join in the furtherance of science and engineering and share the responsibility of advising the Federal Government, upon request, on any subject of science or technology.

THE NATIONAL RESEARCH COUNCIL was organized as an agency of the National Academy of Sciences in 1916, at the request of President Wilson, to enable the broad community of U. S. scientists and engineers to associate their efforts with the limited membership of the Academy in service to science and the nation. Its members, who receive their appointments from the President of the National Academy of Sciences, are drawn from academic, industrial and government organizations throughout the country. The National Research Council serves both Academies in the discharge of their responsibilities.

Supported by private and public contributions, grants, and contracts, and voluntary contributions of time and effort by several thousand of the nation's leading scientists and engineers, the Academies and their Research Council thus work to serve the national interest, to foster the sound development of science and engineering, and to promote their effective application for the benefit of society.

THE DIVISION OF ENGINEERING is one of the eight major Divisions into which the National Research Council is organized for the conduct of its work. Its membership includes representatives of the nation's leading technical societies as well as a number of members-at-large. Its Chairman is appointed by the Council of the Academy of Sciences upon nomination by the Council of the Academy of Engineering.

THE HIGHWAY RESEARCH BOARD, organized November 11, 1920, as an agency of the Division of Engineering, is a cooperative organization of the highway technologists of America operating under the auspices of the National Research Council and with the support of the several highway departments, the Federal Highway Administration, and many other organizations interested in the development of transportation. The purpose of the Board is to advance knowledge concerning the nature and performance of transportation systems, through the stimulation of research and dissemination of information derived therefrom.

HIGHWAY RESEARCH BOARD
NATIONAL ACADEMY OF SCIENCES—NATIONAL RESEARCH COUNCIL
2101 Constitution Avenue Washington, D. C. 20418

ADDRESS CORRECTION REQUESTED